

Universiteit
Leiden
The Netherlands

# First-pass and systemic metabolism of cytochrome P450 3A substrates in neonates, infants, and children

Brussee, J.M.

**Citation**
Brussee, J. M. (2018, December 4). *First-pass and systemic metabolism of cytochrome P450 3A substrates in neonates, infants, and children*. Retrieved from https://hdl.handle.net/1887/67291

| | |
|---|---|
| Version: | Not Applicable (or Unknown) |
| License: | Licence agreement concerning inclusion of doctoral thesis in the Institutional Repository of the University of Leiden |
| Downloaded from: | https://hdl.handle.net/1887/67291 |

**Note:** To cite this publication please use the final published version (if applicable).

Cover Page



Universiteit Leiden




The handle http://hdl.handle.net/1887/67291 holds various files of this Leiden University dissertation.

**Author**: Brussee, J.M.
**Title**: First-pass and systemic metabolism of cytochrome P450 3A substrates in neonates, infants, and children
**Issue Date**: 2018-12-04

# First-pass and systemic metabolism of cytochrome P450 3A substrates in neonates, infants, and children

J.M. BRUSSEE

The research described in this thesis was performed at the division of Systems Biomedicine and Pharmacology of the Leiden Academic Centre for Drug Research (LACDR), Leiden University, the Netherlands. The research was financially supported by a Vidi grant (Vidi Knibbe 2013) of the Netherlands Organization for Scientific Research (NWO).
Printing of this thesis was financially supported by the Leiden Academic Centre for Drug Research.
Cover design: Dirk van Rijn, Paul Brussee, Jantine Brussee, and Proefschriften.nl
Printed by Proefschriften.nl
ISBN: 978-94-6332-426-7

© J.M. Brussee, 2018
All rights reserved. No parts of this thesis may be reproduced in any form or by any means without permission of the author.

# First-pass and systemic metabolism of cytochrome P450 3A substrates in neonates, infants, and children

PROEFSCHRIFT

ter verkrijging van
de graad van Doctor aan de Universiteit Leiden,
op gezag van Rector Magnificus prof. mr. C.J.J.M. Stolker,
volgens besluit van het College voor Promoties,
te verdedigen op dinsdag 4 december 2018
klokke 16.15 uur

door

**Janneke Maria Brussee**
geboren te Oegstgeest, Nederland
in 1989

| | |
|---|---|
| Promotoren: | prof. dr. C.A.J. Knibbe |
| | prof. dr. S.N. de Wildt (Radboud UMC) |
| Copromotor: | dr. E.H.J. Krekels |
| | |
| Promotiecommissie: | prof. dr. H. Irth (voorzitter) |
| | prof. dr. J.A. Bouwstra (secretaris) |
| | prof. dr. M. Danhof |
| | prof. dr. A.H.J. Mathijssen (Erasmus MC) |
| | prof. dr. R.A.A. Mathôt (AMC) |

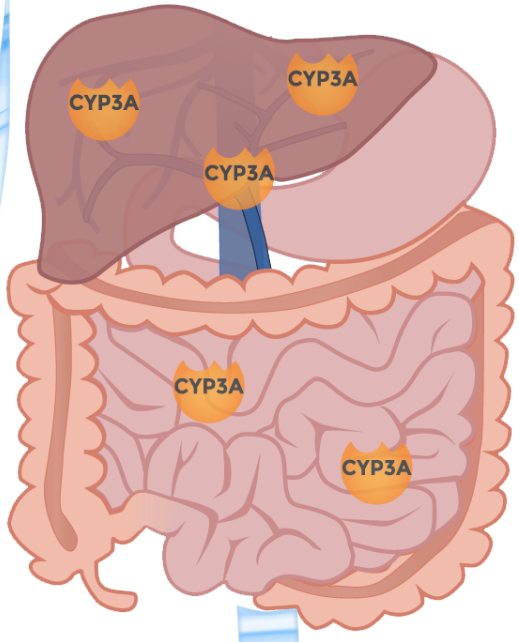
*Voor Sander*

# TABLE OF CONTENTS


| | | |
|---|---|---|
| **Section I** | **General introduction and background** | **9** |
| Chapter 1 | First-pass and systemic metabolism of cytochrome P450 3A substrates in neonates, infants, and children – General introduction, Scope, and Outline | 11 |
| Chapter 2 | Children in clinical trials: towards evidence-based pediatric pharmacotherapy using pharmacokinetic-pharmacodynamic modelling | 23 |
| **Section II** | **Systemic CYP3A-mediated metabolism in critically ill children** | **49** |
| Chapter 3 | Inflammation and organ failure severely affect midazolam clearance in critically ill children | 51 |
| Chapter 4 | Predicting CYP3A-mediated midazolam metabolism in critically ill neonates, infants, children and adults with inflammation and organ failure | 75 |
| **Section III** | **First-pass CYP3A-mediated metabolism in children after oral drug administration** | **97** |
| Chapter 5 | First-pass CYP3A-mediated metabolism of midazolam in the gut wall and liver in preterm neonates | 99 |
| Chapter 6 | Characterization of intestinal and hepatic CYP3A-mediated metabolism of midazolam in children using a physiological population pharmacokinetic modelling approach | 127 |
| **Section IV** | **Midazolam as probe drug for other CYP3A substrates** | **157** |
| Chapter 7 | A pediatric covariate function for CYP3A-mediated clearance can scale clearance of selected CYP3A substrates in children | 159 |
| **Section V** | **Summary, Conclusions, and Perspectives** | **187** |
| Chapter 8 | First-pass and systemic metabolism of cytochrome P450 3A substrates in neonates, infants, and children – Summary, Conclusions, and Perspectives | 189 |
| Chapter 9 | Nederlandse Samenvatting | 213 |
| **Appendices** | | **237** |
| Appendix I | Curriculum Vitae | 239 |
| Appendix II | List of publications | 241 |
| Appendix III | Nawoord/Acknowledgements | 243 |

# Section I

## General introduction and background



# Chapter 1

## First-pass and systemic metabolism of cytochrome P450 3A substrates in neonates, infants, and children – General Introduction, Scope, and Outline

## Pediatric pharmacology

"Children are not just small adults" (1) as, in addition to growth, many developmental physiological changes occur with increasing age. The physiological differences in children compared to adults and in children of different ages, are especially pronounced in neonates and young infants (2). The developmental changes, together with growth, may impact the pharmacokinetics (PK) of drugs administered to the pediatric population and increase the observed interindividual variability in absorption, distribution, metabolism, and excretion (ADME) in children (3).

Drug absorption after oral administration may differ between neonates, infants, and children due to differences in e.g. intestinal surface area, permeability, gastric emptying time and intestinal transit, gastric and intestinal pH, bile fluid, (pancreatic) enzyme production, membrane transporters, and drug metabolizing enzymes in gut and liver (4, 5). Distribution of the drug may differ because of the developmental changes in e.g. body composition, tissue/organ weight and size compared to total body weight (6), the cardiac output and tissue blood flows (7), plasma protein binding (8) and the tissue: plasma partitioning (7). Furthermore, kidney growth (7) and age-related changes in glomerular filtration rate and active tubular processes (3) impact renal excretion, and, finally, hepatic blood flow (7), plasma protein binding (8), liver growth (9), and maturation of enzyme expression and activity (3, 7) influence the rate of hepatic metabolic clearance of drugs (10).

## Cytochrome P450 3A enzymes

Cytochrome P450 (CYP) enzymes form an enzyme family involved in phase I metabolism of many drugs, of which the CYP3A subfamily, with its isoforms CYP3A4, CYP3A5, and CYP3A7, metabolizes many drugs. Profound changes occur in the activity of the CYP3A isoforms, with the CYP3A4 activity increasing with age, the CYP3A5 activity remaining relatively constant with age, while CYP3A7 is mostly expressed in fetal en neonatal tissue and decreases very fast in the first month after birth (11-13). For hepatic CYP3A4 enzymes, which are mainly responsible for the systemic metabolism of CYP3A substrates, the abundance is known to increase with age (12, 14), as well as the liver size (7), while the amount of microsomal protein in the liver is believed to remain constant with age (15). CYP3A enzyme activity per gram of liver has been studied *in vitro* and *in vivo* (11-13, 16), but many questions remain on the maturation of CYP3A-mediated drug clearance in children in a clinical setting, relevant to individualized dosing of CYP3A substrates in this population (17). For example, inflammation, sepsis, and organ failure, appear to impact CYP3A expression and activity (18-23), but what is the contribution of disease severity and inflammation, and is this consistent across the pediatric age range?

In addition to inflammation, age-related differences in clearance (24) and oral bioavailability of midazolam have been reported (25). Is this due to changes in intestinal and/or hepatic CYP3A activity with age? CYP3A enzymes reside in both the gut wall and the liver (16), for which different maturation profiles may be anticipated, leading to different activity in neonates, infants, and children compared to adults, but also to different maturation profiles for presystemic and systemic metabolism (26).

After oral administration of a CYP3A substrate, part of the initial dose does not enter the systemic blood circulation, as the total bioavailability ($F_{total}$) depends on the fraction of the drug that gets absorbed ($F_a$), and the fraction escaping gut wall ($F_g$) and hepatic ($F_h$) metabolism (Figure 1)(27). It is therefore of interest to distinguish between intestinal and hepatic CYP3A activity with respect to their roles in first-pass and systemic metabolism, as the fraction escaping gut wall and hepatic metabolism may differ with age, resulting in a different total bioavailability and total plasma clearance throughout the pediatric age range.

Furthermore, it has been assumed that clearance of drugs can be predicted from clearance of another drug sharing an elimination pathway, as shown for some drugs eliminated by glomerular filtration and drugs glucuronidated by UGT2B7 (28-30). But is this also the case for drugs that are mainly metabolized by CYP3A, and can this approach be used to predict clearance of CYP3A substrates in neonates, infants, and children?

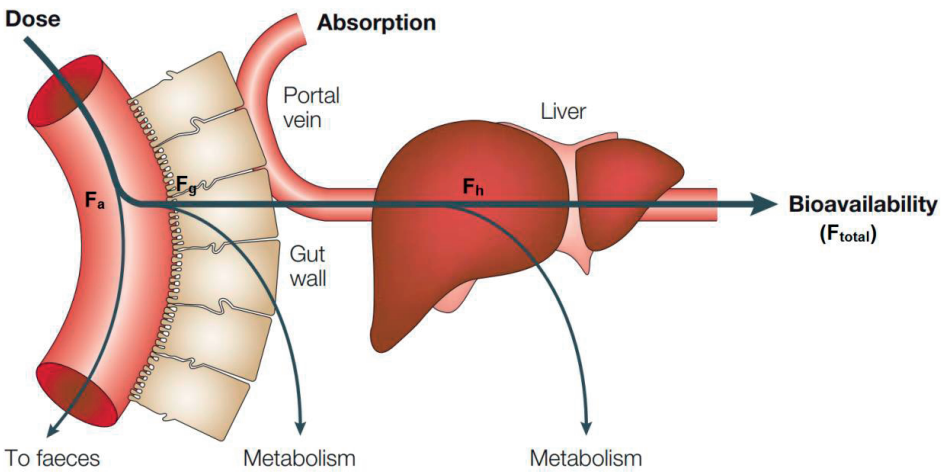



**Figure 1.** Presystemic metabolism upon oral drug administration. The total bioavailability ($F_{total}$) depends on the fraction absorbed of the initial dose ($F_a$), the fraction appearing in the portal vein escaping gut wall metabolism ($F_g$), and the fraction reaching the blood circulation after the first-pass through the liver ($F_h$) with $F_{total} = F_a \times F_g \times F_h$, adapted and modified from Waterbeemd et al. (27) with permission.

## CYP3A-mediated midazolam clearance in children

To predict plasma clearance of CYP3A substrates in children, the hydroxylation of drugs by CYP3A enzymes should be studied across a wide age range. Combining the knowledge of CYP3A-mediated drug clearance with the intended therapeutic window will enable the development of guidelines for dosing of CYP3A substrates in children. To describe CYP3A-mediated metabolism, midazolam is commonly used as probe drug, as its clearance is believed to reflect CYP3A activity (31, 32). Midazolam is a benzodiazepine, often used for sedation in the neonatal and pediatric intensive care unit (33, 34). Midazolam is considered a good probe drug for CYP3A4/5 activity (35), as midazolam is mainly metabolized by CYP3A4, with limited metabolism by CYP3A5 and CYP3A7 (36). Midazolam is an intermediate extraction ratio drug (37), and its metabolism depends mostly on intrinsic clearance by CYP3A enzymes rather than hepatic blood flow. That midazolam clearance is a good marker for (hepatic) CYP3A expression, was first proven by Thummel *et al.* who showed a significant *in vitro– in vivo* correlation ($p<0.01$) between CYP3A content in liver biopsy specimens and formation of 1-OH-midazolam *in vitro* with the measured midazolam clearance *in vivo* in patients who received a liver transplant (31). Furthermore, midazolam clearance adequately reflects the induction and inhibition of CYP3A4/5 activity by known CYP3A inducers and inhibitors (17), making midazolam a widely accepted probe drug for CYP3A activity.

Therefore, data on midazolam PK after intravenous administration from preterm neonates up to adolescents, would allow for the characterization of total systemic CYP3A activity at different stages of development. Moreover, midazolam PK data after oral administration will also allow for studying the proportional contribution of intestinal and hepatic CYP3A enzymes to the CYP3A-mediated first-pass metabolism in neonates, infants, and children, when added to results upon intravenous midazolam administration.

## Model-based approach to describe drug pharmacokinetics

To quantify CYP3A-mediated metabolism using clearance of midazolam or another CYP3A substrate as surrogate marker, a clinical trial may be performed to estimate PK parameters including clearance from densely sampled individual concentration-time profiles. Based on these PK profiles, the parameters can be estimated in each individual, after which summary statistics are used to describe the distribution of parameter values in the study population (the two-stage approach). However, this requires many samples per individual, and this is, especially in pediatric studies, not always feasible due to ethical and practical constraints (38). Therefore, a population approach is preferably applied, which requires less concentration measurements per individual and allows for simultaneous analysis of data from the

whole population, while taking into account the individual differences (39). This model-based approach, also known as non-linear mixed effects modeling, can be used to estimate PK parameters on the basis of a limited number of PK samples per child, and interindividual and residual variability can be described separately (39). This allows for a covariate analysis, in which covariates, e.g. body weight or age, can be identified within the studied pediatric population to (partly) explain the interindividual variability. These covariates can subsequently be used to guide dosing.

Several types of PK models can be developed, based on availability of data and the model's purpose (40), ranging from relatively simple empirical models to more complex (semi-) physiologically-based models. To describe clearance in a pediatric population, an empirical model may be sufficient, and after proper evaluation (41), these PK models can be used for the development of dosing guidelines in the studied population.

However, an empirical model might not be sufficient to obtain insight into drug independent systems information (42), for example to study what role intestinal and hepatic CYP3A play in the first-pass metabolism of CYP3A substrates like midazolam (43, 44). A combination of mechanistic and empirical models can be used to enable incorporation of physiological knowledge on the gastro-intestinal tract, while obtaining more insight into the system by parameter estimation of for example gut wall and hepatic intrinsic clearance based on reverse translation of the observed clinical data (42).

## Pediatric clearance of various CYP3A substrates

To obtain information on the pediatric clearance of different CYP3A substrates, dedicated PK studies in patients from all ages for all drugs should be performed. This requires a large burden and many resources. Therefore, other approaches have been proposed, including an approach in which a covariate relationship for clearance from one drug is extrapolated to another drug that shares the same elimination pathway (28). This has been shown to result in accurate pediatric clearance predictions for some drugs eliminated by glomerular filtration and drugs glucuronidated by UGT2B7 (28-30). In order to explore the potential use of this approach in a more general way, a framework was developed by Calvier *et al.* to identify the conditions in which clearance can accurately be scaled from adult clearance based on between-drug extrapolation of a pediatric covariate function for clearance from a model drug to a test drug (45). This framework can be applied to evaluate down to which age systemically accurate scaling of clearance is possible, based on drug properties including the fraction metabolized by the isoenzyme pathway for which plasma clearance is scaled, the hepatic extraction ratio of the drugs in adults, the type of

binding plasma protein, and the unbound fraction (45). This framework is useful to predict to which drugs a pediatric covariate function for CYP3A-mediated midazolam clearance can be extrapolated.

## Scope and intent of the investigations

A critical information gap exists with regard to the metabolism of CYP3A substrates in neonates, infants, and children, and CYP3A-mediated clearance of drugs cannot yet be predicted throughout the pediatric age range. Therefore, the aim of this thesis is to predict first-pass and systemic metabolism of CYP3A substrates in neonates, infants, and children, by development of pediatric (physiological) population PK models using the probe drug midazolam. For this purpose, the population approach is used to study systemic CYP3A-mediated midazolam clearance after intravenous administration, and a more physiological population approach is used to study the role of gut wall and hepatic CYP3A enzymes in presystemic metabolism when midazolam is administered orally. Lastly, we evaluate the application of a previously developed framework (45) to scale clearance of commonly used CYP3A substrates in children, using a pediatric covariate function for CYP3A-mediated midazolam clearance. This chapter provides an outline of the investigations that are described in this thesis.

**Section I** (**Chapter 2**) describes the general trend towards evidence-based pharmacotherapy in the pediatric population using pharmacokinetic-pharmacodynamic modeling. As many drugs, including many CYP3A substrates, are still used off-label in neonates, infants, and children, PK and PD studies are urgently needed in this population. We describe the different steps to take to come to an individualized dosing regimen, using PK and PKPD models, and how these models should be validated both internally and externally before a new dosing regimen can be proposed. Such new dosing regimens can be used to improve clinical practice, and guidelines can be updated accordingly. We foresee that properly designed clinical PKPD studies will remain the backbone of pediatric pharmacological research, and explaining the variability in PK is the first step towards individualized pharmacotherapy of CYP3A substrates and other drugs in children.

**Section II** focuses on the systemic metabolism by CYP3A enzymes in neonates, infants, and children, using intravenous midazolam clearance to reflect CYP3A-mediated metabolism, and aims to quantify the impact of maturation, critical illness, and inflammation on midazolam clearance in critically ill children. **Chapter 3** describes midazolam PK after intravenous administration in critically ill children aged between 1 day and 16.8 years of age. A PK model is developed to describe

clearance of midazolam in critically ill children and a covariate analysis is performed to explain the inter- and intra-individual variability within the population. The most important studied factors include body weight and age, reflecting the growth and maturation of the children, as well as critical illness and inflammation. Other pediatric studies suggested an important influence of these factors, but this has not been elucidated before. As it is important to evaluate the PK model both internally and externally before it is to be used to guide dosing in clinical practice or to derive dosing recommendations, in **Chapter 4** the predictive performance of the developed population PK model is evaluated in independent clinical datasets including data from similar populations (postoperative and critically ill term neonates, infants, and children) and other populations (including preterm neonates, healthy adults, and critically ill adults).

In **Section III** a novel physiological population PK modeling approach is used to delineate the contribution of enzymes in the gut wall and the liver to first-pass metabolism by CYP3A after oral administration of midazolam. The model includes physiological compartments representing the gastro-intestinal tract and the liver, and also empirical central and peripheral compartments for midazolam and 1-OH-midazolam distribution. Pediatric physiological information from literature is included to account for differences in relevant physiological parameters such as hematocrit, intestinal surface area, organ size, tissue blood flows, and plasma protein binding in neonates, infants, and children, compared to adults. Based on this physiological information and by using PK data from preterm neonates and children (25, 46, 47), the intrinsic intestinal and hepatic clearances are estimated to derive values for bioavailability and plasma clearance. **Chapter 5** focuses on intestinal and hepatic CYP3A activity in preterm neonates, while **Chapter 6** describes the characterization of intestinal and hepatic CYP3A-mediated metabolism in children from 1 – 18 years of age.

**Section IV** discusses how information on CYP3A-mediated clearance of the probe drug midazolam in children can be used for the scaling of plasma clearance of other commonly used CYP3A substrates in the pediatric population. Based on the developed framework by Calvier *et al.* which takes into account drug properties like hepatic extraction ratio and fraction unbound (45), **Chapter 7** describes the application of the between-drug extrapolation of a covariate relationship for clearance based on midazolam to scale clearance of other CYP3A substrates in children. Chapter 7 also evaluates whether a pediatric covariate function for CYP3A-mediated midazolam clearance can be used to scale clearance of various commonly used CYP3A substrates in children, by comparison of scaled clearance values with

reported pediatric clearance values. In addition, the pediatric covariate function for CYP3A-mediated clearance is applied to scale pediatric clearance of sildenafil, and these scaled clearance values are then compared with clearance values which are estimated based on sildenafil PK data in children 1-17 years of age.

Lastly, **Section V** (**Chapter 8**) summarizes the results presented in this thesis on the maturation of systemic and first-pass CYP3A-mediated metabolism reflected by midazolam clearance in neonates, infants, and children, and on the between-drug extrapolation of a pediatric covariate function for clearance from midazolam to other commonly used CYP3A substrates. Furthermore, it provides future perspectives on the translation of our results to the clinic, on the use of physiological modeling approaches, and on how information from midazolam PK models can be used to predict drug clearance of other CYP3A substrates in the pediatric population.

## REFERENCES


1. Kearns GL, Abdel-Rahman SM, Alander SW, Blowey DL, Leeder JS, Kauffman RE. Developmental pharmacology--drug disposition, action, and therapy in infants and children. N Engl J Med. 2003;349(12):1157-67.
2. Johnson PJ. Neonatal pharmacology--pharmacokinetics. Neonatal Netw. 2011;30(1):54-61.
3. Lu H, Rosenbaum S. Developmental pharmacokinetics in pediatric populations. J Pediatr Pharmacol Ther. 2014;19(4):262-76.
4. Debotton N, Dahan A. A mechanistic approach to understanding oral drug absorption in pediatrics: an overview of fundamentals. Drug Discov Today. 2014;19(9):1322-36.
5. Mooij MG, de Koning BA, Huijsman ML, de Wildt SN. Ontogeny of oral drug absorption processes in children. Expert Opin Drug Metab Toxicol. 2012;8(10):1293-303.
6. Haddad S, Restieri C, Krishnan K. Characterization of age-related changes in body weight and organ weights from birth to adolescence in humans. J Toxicol Environ Health A. 2001;64(6):453-64.
7. Bjorkman S. Prediction of drug disposition in infants and children by means of physiologically based pharmacokinetic (PBPK) modelling: theophylline and midazolam as model drugs. Br J Clin Pharmacol. 2005;59(6):691-704.
8. McNamara PJ, Alcorn J. Protein binding predictions in infants. AAPS PharmSci. 2002;4(1):E4.
9. Johnson TN, Tucker GT, Tanner MS, Rostami-Hodjegan A. Changes in liver volume from birth to adulthood: a meta-analysis. Liver Transpl. 2005;11(12):1481-93.
10. Alcorn J, McNamara PJ. Ontogeny of hepatic and renal systemic clearance pathways in infants: part II. Clin Pharmacokinet. 2002;41(13):1077-94.
11. de Wildt SN, Kearns GL, Leeder JS, van den Anker JN. Cytochrome P450 3A: ontogeny and drug disposition. Clin Pharmacokinet. 1999;37(6):485-505.

12. Hines RN, McCarver DG. The ontogeny of human drug-metabolizing enzymes: phase I oxidative enzymes. J Pharmacol Exp Ther. 2002;300(2):355-60.
13. Stevens JC, Hines RN, Gu C, Koukouritaki SB, Manro JR, Tandler PJ, et al. Developmental expression of the major human hepatic CYP3A enzymes. J Pharmacol Exp Ther. 2003;307(2):573-82.
14. Treluyer JM, Bowers G, Cazali N, Sonnier M, Rey E, Pons G, et al. Oxidative metabolism of amprenavir in the human liver. Effect of the CYP3A maturation. Drug Metab Dispos. 2003;31(3):275-81.
15. Barter ZE, Bayliss MK, Beaune PH, Boobis AR, Carlile DJ, Edwards RJ, et al. Scaling factors for the extrapolation of in vivo metabolic drug clearance from in vitro data: reaching a consensus on values of human microsomal protein and hepatocellularity per gram of liver. Curr Drug Metab. 2007;8(1):33-45.
16. Ince I, Knibbe CA, Danhof M, de Wildt SN. Developmental changes in the expression and function of cytochrome P450 3A isoforms: evidence from in vitro and in vivo investigations. Clin Pharmacokinet. 2013;52(5):333-45.
17. de Wildt SN, Ito S, Koren G. Challenges for drug studies in children: CYP3A phenotyping as example. Drug Discov Today. 2009;14(1-2):6-15.
18. Vet NJ, de Hoog M, Tibboel D, de Wildt SN. The effect of inflammation on drug metabolism: a focus on pediatrics. Drug Discov Today. 2011;16(9-10):435-42.
19. Carcillo JA, Doughty L, Kofos D, Frye RF, Kaplan SS, Sasser H, et al. Cytochrome P450 mediated-drug metabolism is reduced in children with sepsis-induced multiple organ failure. Intensive Care Med. 2003;29(6):980-4.
20. Aitken AE, Morgan ET. Gene-specific effects of inflammatory cytokines on cytochrome P450 2C, 2B6 and 3A4 mRNA levels in human hepatocytes. Drug Metab Dispos. 2007;35(9):1687-93.
21. Aitken AE, Richardson TA, Morgan ET. Regulation of drug-metabolizing enzymes and transporters in inflammation. Annu Rev Pharmacol Toxicol. 2006;46:123-49.
22. Kirwan CJ, MacPhee IA, Lee T, Holt DW, Philips BJ. Acute kidney injury reduces the hepatic metabolism of midazolam in critically ill patients. Intensive Care Med. 2012;38(1):76-84.
23. Pacifici GM. Clinical pharmacology of midazolam in neonates and children: effect of disease-a review. Int J Pediatr. 2014;2014:309342.
24. Anderson BJ, Larsson P. A maturation model for midazolam clearance. Paediatr Anaesth. 2011;21(3):302-8.
25. de Wildt SN, Kearns GL, Hop WC, Murry DJ, Abdel-Rahman SM, van den Anker JN. Pharmacokinetics and metabolism of oral midazolam in preterm infants. Br J Clin Pharmacol. 2002;53(4):390-2.
26. de Wildt SN. Profound changes in drug metabolism enzymes and possible effects on drug therapy in neonates and children. Expert Opin Drug Metab Toxicol. 2011;7(8):935-48.
27. van de Waterbeemd H, Gifford E. ADMET in silico modelling: towards prediction paradise? Nat Rev Drug Discov. 2003;2(3):192-204.
28. Krekels EH, Neely M, Panoilia E, Tibboel D, Capparelli E, Danhof M, et al. From pediatric covariate model to semiphysiological function for maturation: part I-extrapolation of a covariate model from morphine to Zidovudine. CPT Pharmacometrics Syst Pharmacol. 2012;1:e9.

29. Zhao W, Biran V, Jacqz-Aigrain E. Amikacin maturation model as a marker of renal maturation to predict glomerular filtration rate and vancomycin clearance in neonates. Clin Pharmacokinet. 2013;52(12):1127-34.
30. De Cock RF, Allegaert K, Sherwin CM, Nielsen EI, de Hoog M, van den Anker JN, et al. A neonatal amikacin covariate model can be used to predict ontogeny of other drugs eliminated through glomerular filtration in neonates. Pharmaceutical research. 2014;31(3):754-67.
31. Thummel KE, Shen DD, Podoll TD, Kunze KL, Trager WF, Hartwell PS, et al. Use of midazolam as a human cytochrome P450 3A probe: I. In vitro-in vivo correlations in liver transplant patients. J Pharmacol Exp Ther. 1994;271(1):549-56.
32. Gorski JC, Hall SD, Jones DR, VandenBranden M, Wrighton SA. Regioselective biotransformation of midazolam by members of the human cytochrome P450 3A (CYP3A) subfamily. Biochem Pharmacol. 1994;47(9):1643-53.
33. Hall RW, Shbarou RM. Drugs of choice for sedation and analgesia in the neonatal ICU. Clin Perinatol. 2009;36(1):15-26.
34. Vet NJ, Ista E, de Wildt SN, van Dijk M, Tibboel D, de Hoog M. Optimal sedation in pediatric intensive care patients: a systematic review. Intensive Care Med. 2013;39(9):1524-34.
35. Watkins PB. Noninvasive tests of CYP3A enzymes. Pharmacogenetics. 1994;4(4):171-84.
36. Williams JA, Ring BJ, Cantrell VE, Jones DR, Eckstein J, Ruterbories K, et al. Comparative metabolic capabilities of CYP3A4, CYP3A5, and CYP3A7. Drug Metab Dispos. 2002;30(8):883-91.
37. Dundee JW, Collier PS, Carlisle RJ, Harper KW. Prolonged midazolam elimination half-life. Br J Clin Pharmacol. 1986;21(4):425-9.
38. Shaddy RE, Denne SC, Committee on D, Committee on Pediatric R. Clinical report--guidelines for the ethical conduct of studies to evaluate drugs in pediatric populations. Pediatrics. 2010;125(4):850-60.
39. FDA. General Clinical Pharmacology Considerations for Pediatric Studies for Drugs and Biological Products, Guidance for Industry, December 2014. Available from: https://www.fda.gov/downloads/Drugs/GuidanceComplianceRegulatoryInformation/Guidances/UCM425885.pdf.
40. Tsamandouras N, Rostami-Hodjegan A, Aarons L. Combining the 'bottom up' and 'top down' approaches in pharmacokinetic modelling: fitting PBPK models to observed clinical data. Br J Clin Pharmacol. 2015;79(1):48-55.
41. Krekels EH, van Hasselt JG, Tibboel D, Danhof M, Knibbe CA. Systematic evaluation of the descriptive and predictive performance of paediatric morphine population models. Pharmaceutical research. 2011;28(4):797-811.
42. Rostami-Hodjegan A. Reverse Translation in PBPK and QSP: Going Backwards in Order to Go Forward With Confidence. Clin Pharmacol Ther. 2017.
43. Brill MJ, Valitalo PA, Darwich AS, van Ramshorst B, van Dongen HP, Rostami-Hodjegan A, et al. Semiphysiologically based pharmacokinetic model for midazolam and CYP3A mediated metabolite 1-OH-midazolam in morbidly obese and weight loss surgery patients. CPT Pharmacometrics Syst Pharmacol. 2016;5(1):20-30.
44. Frechen S, Junge L, Saari TI, Suleiman AA, Rokitta D, Neuvonen PJ, et al. A semiphysiological population pharmacokinetic model for dynamic inhibition of liver and gut wall cytochrome P450 3A by voriconazole. Clin Pharmacokinet. 2013;52(9):763-81.

45. Calvier EAM, Krekels EHJ, Yu H, Valitalo PAJ, Johnson TN, Rostami-Hodjegan A, et al. Drugs Being Eliminated via the Same Pathway Will Not Always Require Similar Pediatric Dose Adjustments. CPT Pharmacometrics Syst Pharmacol. 2018.
46. de Wildt SN, Kearns GL, Hop WC, Murry DJ, Abdel-Rahman SM, van den Anker JN. Pharmacokinetics and metabolism of intravenous midazolam in preterm infants. Clin Pharmacol Ther. 2001;70(6):525-31.
47. Gupta M EA, Willmann S, Adamson PC, Galinkin JL, Barrett JS. Model-based Approaches to Investigate Pharmacogenetic and Developmental Sources of Variation in the Pharmacokinetics of Midazolam after Oral administration in Children. 2006 [Available from: AAPS 2006. Abstract 003255. https://abstracts.aaps.org/Published/Browse.aspx.

# Chapter 2

## Children in clinical trials: towards evidence-based pediatric pharmacotherapy using pharmacokinetic-pharmacodynamic modeling

Janneke M Brussee[1], Elisa AM Calvier[1], Elke HJ Krekels[1], Pyry AJ Välitalo[1], Dick Tibboel[2], Karel Allegaert[2,3], Catherijne AJ Knibbe[1,4]

[1]Division of Pharmacology, Leiden Academic Centre for Drug Research, Leiden University, Leiden, The Netherlands; [2]Intensive Care and Department of Surgery, Erasmus MC-Sophia Children's Hospital, Rotterdam, the Netherlands; [3]Department of Development and Regeneration, KU Leuven, Belgium; [4]Department of Clinical Pharmacy, St. Antonius Hospital, Nieuwegein, The Netherlands

*Expert Rev Clin Pharmacol. 2016 Sep;9(9):1235-44*

## ABSTRACT

**Introduction**: In pediatric pharmacotherapy, many drugs are still used off-label, and their efficacy and safety is not well characterized. Different efficacy and safety profiles in children of varying ages may be anticipated, due to developmental changes occurring across pediatric life.

**Areas covered**: Beside pharmacokinetic (PK) studies, pharmacodynamic (PD) studies are urgently needed. Validated PKPD models can be used to derive optimal dosing regimens for children of different ages, which can be evaluated in a prospective study before implementation in clinical practice. Strategies should be developed to ensure that formularies update their drug dosing guidelines regularly according to the most recent advances in research, allowing for clinicians to integrate these guidelines in daily practice.

**Expert Commentary**: We anticipate a trend towards a systems-level approach in pediatric modeling to optimally use the information gained in pediatric trials. For this approach, properly designed clinical PKPD studies will remain the backbone of pediatric research.

**Keywords**

Pediatrics, clinical trial, off-label, maturation, PKPD, physiology, evidence-based dose recommendations, dose individualization, pharmacotherapy

**Key issues**

- In pediatric pharmacotherapy, many drugs are still used off-label, and their efficacy and safety is not well studied, even though developmental changes in children are known to lead to different pharmacokinetics (PK) and pharmacodynamics (PD) of drugs.
- Even though multiple PK(PD) studies have been performed particularly for many commonly used drugs, information obtained in these trials are not automatically translated into dosing regimens for clinical care.
- Proper study design can prevent structural and numerical identifiability of the PKPD model and clinical trial simulation and optimal design software provides a useful tool for optimizing the study design.
- As opportunities for plasma sampling in individual children are limited, the population approach is the preferred approach in PK and/or PD analyses to extract the greatest amount of PKPD information from the clinical data and perform covariate analyses.

- The optimal dosing regimen identified from a validated PKPD model should be preferably evaluated in a prospective clinical trial before implementation in clinical practice.
- Strategies should be developed to ensure that formularies update drug dosing guidelines regularly according to the most recent advances in research.
- More emphasis is needed to identify, quantify and validate biomarkers for disease and drug efficacy in the pediatric population.
- During the next few years, we anticipate a shift towards a systems-level approach in pediatric modeling in pediatric trials. For this approach, population PKPD studies will remain the backbone of pediatric research.

## 1. PHARMACOTHERAPY IN CLINICAL PRACTICE

A major problem in pediatric healthcare is that drugs are largely used in an unlicensed or off-label manner (1). For many drugs, the pharmacokinetic, efficacy and safety profile in children is not very well characterized (2), resulting in a much lower level of evidence of drug efficacy and safety in pediatric pharmacotherapy compared to adult pharmacotherapy. This review focuses more on current drugs used in clinical practice, rather than how to bring new drugs to the pediatric market.

In children, fewer and smaller studies on drug pharmacology are performed than in adults. This can be attributed to the ethical and practical limitations of pediatric trials (3, 4). As it is considered to be unethical to study drugs in healthy children, all pharmacological research in children involves diseased children of which the potential number of participants is limited while age may vary largely. Next, informed consent from the parents or legal guardians is needed and if children are old enough to understand, also informed assent is needed from the patients after informing them about the trial in such a manner they understand. Practical limitations of a trial include the limited number and volume of plasma samples that can be obtained per patient (e.g. the accepted rule that not more than 3% of circulating volume can be harvested during the course of the study), as well as the challenges related to obtain specimen at the extremes of childhood (e.g. extreme low birth weight infants). Furthermore, it is hard to find validated endpoints to measure efficacy in the pediatric population (5). Finally, both the dose that is used and sampling times are often limited to the patients' need in clinical care, which may not be optimal from a research point of view.

In absence of results of dedicated pediatric studies, pediatric doses have been scaled from adult pharmacokinetic (PK) and pharmacodynamic (PD) data using different methods (6, 7). These methods include empirical approaches (e.g. linear or allometric extrapolation on the basis of body weight or body surface area), or mechanistic modeling in which physiologically based pharmacokinetic (PBPK) models (8, 9) are used. Maturation functions that have been derived across the neonatal or pediatric age range, for instance for GFR in neonates (10) or for clearance in the youngest patients(11) , are largely data-driven and empirical. Mechanistic scaling methods have distinct advantages over empirical methods (12), however to date no single mechanistic method has been found suitable across the entire pediatric age range (13). Empirically determined dosages are typically expressed in mg/kg and have usually been adjusted based on clinical experience after which they are summarized in national formularies. It should be realized however, that this approach may not yield a dose with an optimal efficacy/safety profile, and that both during and after the process of optimizing a dose, the patients are at risk for over- and underdosing.

## 2. DEVELOPMENTAL CHANGES INFLUENCING DRUG PHARMACOLOGY

Inter-individual variability in pharmacokinetics (PK) and pharmacodynamics (PD) in the pediatric population is typically due to age and size, but can also for instance result from pharmacogenetic differences, disease or drug-drug interactions. Because developmental changes affect the pharmacology of administered compounds (14, 15), children who can vary in age between 0 and 18 years of age are an even more heterogeneous population than adults. As such, in children altered PK and/or PD and toxicity due to exaggerated PD effects or off-target effects may be expected (16). This is especially relevant in the youngest age groups such as (prematurely born) neonates, as this is where the changes are the largest (17, 18).

These developmental changes include maturation of enzyme expression activity influencing metabolic clearance of drugs, and age-related changes in glomerular filtration rate (GFR) and active tubular processes influencing renal excretion (19). Metabolizing enzymes such as P450 cytochromes (CYP) and UDP-glucuronosyltranferases (UGTs) may have different maturation profiles, as enzyme abundance increases or for some enzymes decreases with age (20, 21). Furthermore, depending on the drug properties, drug metabolism is also affected by hepatic blood flow and/or the unbound drug fraction (22), which also change throughout childhood. GFR is mostly influenced by renal blood flow (23) as has been described

by many empirical formulas and models (24). Total renal clearance is also affected by passive and active transporters in the tubular epithelium. Moreover, the drug-protein binding to albumin and α1-acid glycoprotein increases with increasing age, due to an increase in protein expression and binding capacity. This results in a decreased unbound drug fraction (25, 26), although for most drugs changes in protein binding have no clinical consequence.

In addition to the influence of age on elimination, age-related changes in body composition may also be of influence on the distribution of drugs. The body water to fat ratio is higher in neonates and young infants, as they have a larger amount of extracellular fluid and total-body water compared to adults (17). The exact implications of these changes for drug PK profiles are dependent on drug properties.

For drugs that are taken orally, the absorption process may also be subject to changes. The absorption rate of most drugs is slower in neonates and young infants than in older children, due to delayed gastric emptying and lower intestinal motility (17). Especially in early life, gastric emptying is delayed compared to older children and adults, potentially delaying absorption in this population as well (27). Also, the gastric pH in neonates may be increased after oral feeding (28), which may affect the bioavailability of some drugs (15, 17). Furthermore, it is assumed that intestinal surface area and age-associated blood flow in the intestinal mucosa is reduced in young infants (17). Unfortunately, developmental changes affecting drug absorption in infants and children have not been well-studied (17).

Drug response can be increased or decreased during maturation and growth of a child due to developmental changes in expression and function of receptors and post-receptor mechanisms involved in drug action, or population specific pathophysiology. This requires dedicated studies to quantify the effects of these changes. Additionally, risk for drug toxicity in children can be increased or decreased due to PK and/or PD ontogeny and the efficacy-toxicity trade-off could be different in children (29).

## 3. DEVELOPING EVIDENCE-BASED DOSING REGIMENS FOR CHILDREN

Due to anticipated drug dependent PK and PD changes among children of different ages and the current lack of knowledge on organ specific ontogeny processes (30), optimal drug efficacy and safety cannot be guaranteed when pediatric drug doses are

derived from adult data (31). Instead, pediatric PKPD models should be developed in order to propose dosing regimens, across the pediatric population. In order to get to evidence-based dosing regimens for children, a multi-step approach (Figure 1) (32) has been proposed. This multi-step approach is based on the learning-confirming principle (33) and it relies on the population approach (32).




**Figure 1.** Proposed multistep approach for the optimization of drug dosing in children. The four steps that are proposed are [1] optimization of clinical trial designs based on simulations using preliminary data; [2] development and internal validation of population PKPD models using sparse data; [3] external validation of the population PKPD models using independent data; and [4] prospective clinical evaluation of the PKPD model-based dosing regimen. PK, pharmacokinetics; PD, pharmacodynamics. Printed with permission from Ince I et al. (32).

Over the last decades, the population approach which is based on non-linear mixed effect modeling (34-36), has gained in popularity. Using this approach, models are developed to estimate population PK and/or PD parameters in an entire population of patients simultaneously, while still taking into account that different observations come from different patients. This approach allows for the characterization of general trends in the population and also for differentiation between inter-individual variability and residual or intra-individual variability within a single model (37). The latter is an advantage over the standard two-stage approach, in which first the PK or PD parameters are fit to observed data in each individual separately, requiring dense sampling, after which these individual parameters are presented using summary statistics like mean and standard error. Moreover, the population approach with its more statistically powerful description of inter-individual variability allows for a covariate analysis in which patient characteristics that can explain (part of) the inter-individual variability can be identified (38).

Particularly in children, the population approach as a tool in PK and/or PKPD analyses is preferred over the standard two-stage approach, because of limited sampling possibilities in individual children, known inter-individual variability that may or may not be related to age and advanced possibilities for so-called covariate analyses (39-41). This is particularly relevant for very young patients, such as term and preterm neonates, from whom only sparse samples can be collected. As a result, the population approach is the recommended approach by the EMA (42, 43) and FDA (44) for the analysis of pediatric PKPD data and the development of evidence-based

dosing regimens. Finally, this approach is found to be superior over the standard-two stage approach (40) and also allows, when deemed appropriate, for the use of adult data as priors to lower the sample size needed and/or increase the statistical power of the study (45).

The pharmacometric field develops mathematical models of physiology, pharmacology and/or disease to describe and quantify interactions between drugs and patients, including PK, PD and toxicity effects of both new and commonly used drugs. In pharmacometrics, most efforts have been focused on PK modeling, while in clinical care and drug development PK, PD and toxicity should be considered (42, 44, 46). As stated above, the concentration-effect relationship may change with age because of increased or decreased expression and function of receptors involved in drug action and response. For new drugs, the FDA and EMA developed a decision tree for the evaluation of the need for (the type of) pediatric trials (44, 47, 48). When it is reasonable to assume that children and adults have a similar disease progression and a similar response to intervention and it is also reasonable to assume similar concentration-response in both populations, then only PK studies to achieve plasma concentrations similar to adults and safety trials should be conducted. When only disease progression and response to intervention are assumed similar, PKPD studies to get concentration-response information are necessary in addition to the previously mentioned PK and safety studies. When disease progression and response to intervention are not assumed to be similar in pediatrics and adults, then both PK studies and safety/efficacy trials should be performed (48). For example, in infectious diseases, most model approaches are focused on development of a PK model to study PK maturation. These PK models are then used for simulations to give dose recommendations based on a target concentration pre-defined based on adult or in vitro data, rather than performing a PKPD trial (49).

For some drugs with a low PK variability and/or when it is not possible to collect all required PK information, the dose can be also directly related to the PD with K-PD models (50) which can be, with extra caution, then used to inform dosing. However, when PKPD models can be identified, they should be preferred over K-PD models (51). Below we describe the different steps of figure 1 in order to get to evidence-based dosing guidelines in children.

## 4. STUDY DESIGN AND DATA COLLECTION

Just as in any other research field, a proper study design is pivotal in answering the research questions of pharmacological studies. The study design should

be such that the parameters in the anticipated model are identifiable. Because practice and theory often do not match, the design of a study should be discussed within a multidisciplinary team including clinicians, pharmacists, nurses and pharmacometricians. Commonly, inter- and intra-individual variability in PKPD is higher in children and especially in neonates compared to adults, which is due to maturation aspects and inter-individual differences in weight (52). Moreover, patient numbers are typically lower and as a result both these aspects should be accounted for in the study design as it causes the statistical power of analysis to decrease.

## 4.1 Structural identifiability

Structural identifiability is concerned with whether the parameters of a postulated model can be identified from a specified experiment or experiments with perfect input-output data (53). For instance, identifiability issues can arise when plasma metabolite concentrations are included in the model. Metabolite concentrations are mostly studied in special populations when the metabolite is suspected to be active or when a certain elimination pathway is being studied. Trial design can solve structural parameter identifiability issues by, for example, the use of different routes of administration or sampling of different media (e.g. blood and urine samples). For example, , without urine sampling upon a single dose over a long time interval to estimate the fraction of the dose that is metabolized through the involved pathway, identifiability issues in quantifying the metabolism and excretion pathways of the parent compound may occur. An example of this problem including how to address this issue has been described elsewhere (54). In some cases, structural identifiability issues cannot be addressed by any method, which requires proper discussion of the specific limitations before starting the trial (54).

## 4.2 Numerical identifiability

Numerical identifiability relates to the informativeness of the data and can be improved by the optimization of study design and its execution (55). The impact of the study design on the precision and bias of the estimated parameters of a population model in adults is well established (56-60). In order to minimize the parameter uncertainty, two main clinical trial optimization methods exist, namely clinical trial simulation and optimal design (61). Clinical trial simulation allows for the investigation of a limited number of candidate study designs by simulating datasets with a given design and fitting the specified model to those simulated datasets. The mean and variance of the parameter estimates are then calculated, to come up with the bias and precision, respectively, of the design. Optimal design methods involve the direct calculation of the expected parameter standard errors, which could be compared to performing a clinical trial simulation with an infinite

number of simulated datasets. Several optimal design software programs exist and most of these have been evaluated by Nyberg *et al.* (62).

The optimization of all or specific PKPD parameters can be done over different clinical trial design parameters, like the number of samples, the number of patients included, the sampling times, the doses administered and patient characteristics (63, 64). The trial optimization can take into account practical and ethical (e.g. maximal number of samples per patients), as well as economic constraints (e.g. treatment costs). There is limited experience with all of these techniques in pediatric pharmacology research.

### *4.2.1 Sampling*

Increased numbers of blood samples per patient will increase the accuracy and precision of the estimated model parameters and the estimated inter-individual and residual variability (56, 58, 59). Depending on the practical constraints, specific sampling times or sampling windows can be optimized. A design allowing for variation in sampling time (design with multiple sampling windows) and dosages among subjects can be beneficial and protect against the ill-effects of model misspecification, as has been demonstrated before (57). Despite the use of clinical trial simulations, practical constraints might prevent the identifiability of some model parameters. For example, the impossibility to sample at early times would prevent the estimation of the absorption rate.

### *4.2.2 Data collection*

When designing a PK(PD) study, information on patient characteristics (potential model covariates) that can correlate to PK or PD parameters need to be collected. Body weight and age are the most commonly used covariates in the pediatric population, to describe the influence of growth and development. For children younger than 2 years of age, gestational age, postmenstrual age, post-conceptual age and postnatal age may be relevant covariates as well (65). Many other covariates which can influence the PK and /or PD of the drug studied, can be collected, such as disease state, co-medications or the treatment with artificial devices such as extracorporeal membrane oxygenation (ECMO), ventricular assist devices or renal replacement (66, 67). In general, correlations between potential covariates should be avoided whenever possible, as the combination of two correlated covariates in a population model may result in bias in parameter estimates (68).

### *4.2.3 Patient inclusion*

Several general design techniques allow to reduce bias, such as randomization and blinding. In general, potential confounders should be defined, such as co-treatment

(e.g. inotropics in cardiac surgery patients), as they might bias the results of the analysis. The distribution of covariates likely to be included in the model should guide, whenever possible, patient inclusion in the trial (69) or trial arms, to prevent unbalanced designs hindering accuracy and precision (70). In a research protocol, it could be useful to identify strata to assure a spread in the covariate (e.g. age) values over the strata in order to gain information across the required range. When patients with only a limited range in covariate values are included, prediction to other patients outside this covariate range would require extrapolation. As interpolations are generally more reliable, the correlations of the covariates to PK or PD parameters can be extended to other subjects more reliably when the covariate values are spread and balanced.

## 5. POPULATION PKPD MODELING AND COVARIATE ANALYSIS

When the data are available for analysis, model development including a covariate analysis is performed to identify which factors can explain (part of) the observed inter-individual variability in the study. Possible covariates include demographic factors like age, body weight and gender or clinical factors like pharmacogenetics, disease state or comorbidities, or co-medication. In a data-driven approach, covariate relationships are tested for their statistical significance and based on both statistical significance and possible clinical relevance they are retained in a model. Advantages of a data-driven approach in a covariate analysis, is that the covariate-parameter relationship is supported by the data. However, because it is a descriptive, empirical method, the extrapolation potential may be debatable. Mechanistic covariate models potentially have better extrapolation potential as they are supported by scientific theories and in vitro and/or in vivo data (71). On the other hand, strong physiological and pharmacological evidence is yet needed for these approaches, confirmed by trial data and its PK(PD) model. Therefore, to date data-driven covariate analysis is considered the most achievable in most settings.

Beside categorical influence of the covariates, the population approach also allows for continuous covariate functions to quantify maturation profiles in parameters across the pediatric age range. In order to develop a maturation function for e.g. drug clearance from for example 1-18 years of age, pediatric patients across this age range should be included. In general, when these maturation functions have been derived, it is typically not advised to extrapolate these functions to younger individuals < 1 year of age, including neonates, as extrapolations to neonates have

almost never been successful (31). To make PK and/or PD predictions within this younger age range, these patients should also be included as these patients are not only difficult to predict, but they are also part of a very heterogeneous group with respect to body weight (almost tenfold difference) and age (0-30 days of age) (10).

In the pediatric population, body weight is often identified as the most statistical significant covariate on clearance and volume of distribution (65). When such a covariate-parameter relationship has been identified, one should realize that it describes the correlation between body weight and a PK parameter, which does not necessarily imply a causal relationship. Therefore caution is needed when extrapolating these models to subpopulations at the extremes of the age-adjusted body weight range, e.g. underfed or obese children. For example, Van Rongen *et al.* found that midazolam clearance in adolescent patients with overweight or obesity seemed not very different from literature values of adolescents with a healthy body mass index (72). While this implies that dosing in adolescents with obesity should not be expressed in mg/kg, in another example, i.e. busulfan, a weight-based algorithm proved to lead to predictable concentrations both in underweight and overweight individuals (73). Furthermore, even in pediatrics there are also special populations like patients with renal and/or hepatic impairment. Due to high variability in PK parameters during childhood and usually few available plasma samples per individual over a prolonged time interval, functional impairment may become apparent only after the growth spurt in adolescence, when significant decrease in GFR and/or increase in metabolic load can be measured (74). Therefore it can be hard to distinguish between functional impairment and maturation of clearance pathways in children.

## 6. MODEL VALIDATION

When a trial is performed and a PKPD model has been developed, the model performance should be evaluated (75), which is a step that is often neglected (65). Marsot *et al.* have reviewed published population pharmacokinetic models developed in pediatric subjects from neonates to 2-year-old toddlers between 1985 and December 2010 (65). Disturbingly, the authors reported the use of model evaluation methods including bootstrap, cross-validation, Monte-Carlo simulations in only 37% of articles and the use of external validation methods in only 11% of articles. Without thorough model validation, predictions from simulations can however not be confirmed and therefore the level of certainty about the model-derived dosing recommendation is very low. Because it is essential to validate models if

clinical decisions are being based on a model, there is obviously an urgent need for higher standards in the methodologies used to develop and publish pediatric pharmacological studies, with a need to systematically implement advanced model validation methods and external model validation.

Validation techniques include goodness-of-fit plots (76), and simulation-based diagnostics by means of for instance visual predictive checks (VPC)(77, 78) or normalized prediction distribution errors (NPDE) (79). Furthermore, bootstrapping methods can be used to evaluate the precision of model predictions and to calculate imprecision in model parameter estimates (80). These validation and/or evaluation tools are available; however they may need adaptations for use in the pediatric population (75). For example, goodness-of-fit plots should be stratified for different age or weight categories, to check for misspecification in covariate-parameter correlations (75, 76).

This internal validation should be followed by an external validation by applying the model to data from other studies, whenever available (75). This external validation is important to make sure that the model reflects the target population, instead of a model that only reflects the patients studied during model development. For example, morphine pharmacokinetics have been described by a PK model for morphine in children younger than 3 years of age (81) and this model has been externally evaluated with six other datasets from literature (82). Krekels *et al.* proved that the predictive performance of the morphine PK model was good in the external datasets of neonates and infants up to 1 year of age. It is important to consider which criteria are used in the model evaluation, as not all validation techniques allow to separate predictive models from models descriptive to one dataset only (75). The good predictive performance of a model is proven only once it has been both internally and externally validated. We emphasize that an external validation does not always require a new trial, as for commonly used drugs literature data may be available that can be used to evaluate the model's performance. For new drugs, it might be beneficial to split the data and use one third of the data to externally validate the model. This validated model can then be used for simulations to individualize drug regimens using a predefined therapeutic endpoint, e.g. an AUC/MIC < plasma concentration threshold or a PD endpoint like a sedation score.

# 7. PROSPECTIVE CLINICAL TRIALS FOR INDIVIDUALIZED DOSING

Validated models are not a goal in itself, but these models can be used to individualize drug regimen, using the covariates included in the model such as bodyweight, or gestational age (83). Before these dosing recommendations can be implemented in the clinic, a prospective clinical evaluation study should preferable be performed to ascertain that the desired endpoints are obtained using the novel dosing regimen (32). This prospective study should be seen as a first stage of implementation of the new dosing recommendations into clinical practice. So far in the period from 1985-2010, Marsot *et al.* found that only 48 out of 98 population PK studies concluded with dosing recommendations and none of these dosing recommendations were followed by a new study devoted to their clinical evaluation (65), which displays a need for tailoring of model-based dosing regimen, and their clinical evaluation. Wilbaux *et al.* describe in their review of pharmacometric models for primarily renally eliminated antibiotics in neonates, that despite many models and prospective trials for most of the reviewed antibiotics in children there is still no consensus on the optimal dosing regimen for most antibiotics (84).

However, an example of a prospective study in which an individualized dosing regimen is evaluated that was proposed based on a previously developed model, is amikacin dosing in preterm and term neonates. In this study, scenario-based simulations were performed using the developed PK model that identified both body weight and the postnatal age of neonates as covariates. This amikacin neonatal PK model (85) was used to derive a novel amikacin dosing regimen in neonates that was prospectively studied (86). The results of the prospective study show that the measured plasma concentrations were accurately predicted by the model and using the model-based dose recommendations, 90.5% and 60.2% of the patients had optimized peak and trough concentrations respectively (86). In this case, correcting for PK was sufficient, as success of treatment is measured by concentration, probably because target concentrations and exposure are bacteria specific and not age-specific.

In another example, Krekels *et al.* performed a study in which a model-based dosing regimen correcting for developmental difference in morphine PK (81), was prospectively evaluated in children receiving morphine after a surgery procedure (87). Their study revealed that the plasma concentrations were as expected based on the model predictions, and confirmed that the PK model-based dosing regimen improved the exposure and led to clinical improvements. Moreover, it revealed that PK does not account for all inter-individual variability and that there is a need for

investigation in PD variability to further optimize the dosing guideline as older children proved less sensitive to morphine than neonates (87).

The described model-based approach to guide dosing in children is mainly applied to small molecular drugs, but its value has also been proven for biologics. Thymoglobulin® is an anti-thymocyte globulin (ATG) that is used as serotherapy in patients undergoing hematopoietic cell transplantations (HTC). It is assumed that individualizing the ATG dosing to prevent graft-versus-host disease and rejection of transplants, will improve survival in pediatric HCT (88). Admiraal *et al.* described the pharmacokinetics of ATG in children and concluded after internal and external validation that the developed PK model was able to predict thymoglobulin concentrations in children correctly (88). Model-based simulations proved the current dosing regimens to be suboptimal leading to varying exposures between individuals, especially in patients with a baseline lymphocyte count that was lower than average and/or a body weight that was higher than average (88). To improve dosing, the relation between ATG exposure and clinical outcomes were studied and a PKPD model was developed to describe this relation (89). It was found that the exposure before transplantation of at least 40 AU×day/mL correlated with a decrease the incidence of graft-versus-host-disease and a lower incidence of graft failure (89). Using this model-based approach, quantification of this PKPD relation resulted in a dosing regimen to achieve the optimal exposure to improve efficacy and safety of ATG treatment in children undergoing transplantation (89), which is currently prospectively evaluated in clinical practice.

## EXPERT COMMENTARY

Over the past decades, the field of pharmacology has been evolving and modeling and simulation has started to play a role in improving pharmacotherapy in the pediatric population (7, 29). In general, more efforts should be put in the design of pediatric studies, so that the obtained data are the most informative to answer the research question. Furthermore, the data should always be analyzed with advanced statistical tools like population modeling to enable extraction of all this information and to perform proper covariate analyses. In addition, research efforts should focus on previously unstudied drugs, instead of performing new (PK) studies on drugs that have already been extensively studied in children, such as aminoglycosides in neonates on which many publications are yet available. For the latter, there would however still be much to gain in terms of translation of the results on the PK of these drugs into clinical practice (90) for instance by identifying subgroups for which

these dosing guidelines may need further adaptation (e.g. neonates with asphyxia or renal insufficiency). However, before results of population models are used to guide dosing in clinical practice, it is imperative that these models are properly validated, both internally and externally, upon which the proposed model-based dosing regimen can be tested in a prospective trial. This next step, the translation of a model to novel dosing regimens, is often not taken (65), even though this is the most relevant step for improvement of pharmacotherapy in clinical care.

While more PK and PD information can be extracted from a trial on a specific drug in a specific age population when the population approach is used (90), it is not realistic to perform a trial and develop and validate a PK or PKPD model for each drug in each pediatric population. Therefore, further steps towards generating more generalizable, system-specific, information are also needed. In this respect, it has been hypothesized that pediatric PK models with covariate functions describing the ontogeny of drug clearance may contain drug-specific and physiological system-specific information (91). For example, the earlier mentioned neonatal model for GFR, originally developed to describe amikacin PK (10), was successfully used to predict ontogeny of clearance of other drugs eliminated by GFR (85, 92). However, more research on this type of extrapolation is needed, as it was reported that also drug properties may affect covariate relationships. For hepatically cleared drugs, it was for instance found that similarity in extraction ratio between the model drug and the drug the covariate relationship is extrapolated to, is important (93).

In addition, strategies should be developed to enable national formularies to adapt their dosing guidelines regularly based on the most recent advances in research published in literature, allowing clinicians to integrate guidelines in daily practice. For example, in gentamicin and tobramycin therapy in neonates, studies have shown that current dosing according to the Dutch National Formulary for Children (94), the British National Formulary for Children (95), Neofax (96) and the Red Book (97) leads to suboptimal exposure and inadequate target concentrations in neonates (98). Therefore, guidelines and national formularies should adapt to the most recent insights resulting in personalized medicine and improved clinical care. This is the case for gentamicin dosing in neonates, for which the Dutch National Formulary for Children (94) recently adjusted the dosing in premature neonates with a post-natal age of 0-7 days based on available literature.

## FIVE-YEAR VIEW

In the next years, we anticipate a stronger trend towards the generation and identification of more generalizable information from pediatric clinical trials that have been performed on specific drugs. The trend has already been initiated by increased focus on research fields like PBPK modeling and systems pharmacology. Both fields integrate information from multiple clinical and/or preclinical sources to derive drug-specific and system-specific information. Identifying developmental patterns in system-specific parameters can help to quantify and predict inter-individual variability in drug absorption and disposition, and receptor function and expression (99). The advantage of systems-based approaches in quantifying and predicting drug PK has for instance been illustrated for another special patient population. In morbidly obese and bariatric surgery patients, oral and intravenous midazolam PK was described by a semi-physiological PK model (100), taking into account both gut wall and liver processes. In this model, system-specific parameters (e.g. hepatic blood flow) and drug-specific parameters (e.g. extraction ratio) were combined, leading to the conclusion that in morbidly obese patients, hepatic CYP3A activity is reduced in comparison to healthy volunteers but normalizes one year after weight loss surgery (100). This approach does not require as much information as a full PBPK or systems pharmacology model, which is not always experimentally deducible. As some system-specific information is lacking, e.g. liver blood flow in special populations (100), different scenarios for this physiological parameter were tested for their influence on the conclusion. Ultimately, methods combining the population approach, based on outcome data, and the systems approach are being developed. In the near future we will see more of this approach in pediatric patients as well.

In order to describe the system and the maturation processes within the system, knowledge is required on disease mechanisms and drug action to be accounted for in the system models. Furthermore, to scale drug efficacy across a wide age range, the same endpoint to measure efficacy in children and adults is needed or scaling of endpoints between children and adults should be explored because PD endpoints used in adults cannot always be applied to children. For example, the gold standard for pain assessment in adults is based on self-report and in especially young children the same method cannot be applied. Therefore other validated and well-established scales like the COMFORT-B for pain after major surgery (101, 102) and PIPP pain scores for procedural pain in preterm neonates (103) have been used in preverbal children. It is important to validate these scores before use in clinical practice (101, 103), because even these pain scores give variable information about pain (104). The

lack of validated PD endpoints in children is one of the most important obstacles in the transition of mostly PK studies to the more clinical relevant PKPD studies. Often it is assumed that a certain drug exposure that is associated with desired drug action in adults will produce the same response in children (105). However, this assumption does not hold true in many cases and therefore biomarkers for disease and drug efficacy in the pediatric population are urgently needed to identify and quantify drug effects (105). To identify biomarkers for disease mechanisms and drug action in pediatrics, we foresee a trend in more interest in the metabolomics field (106, 107). Validated biomarkers and clear endpoints could also prevent pediatric trials to fail in answering the question addressed in the trial (108).

Predictive systems pharmacology models give novel insights in pediatric pharmacotherapy in relation to ontogeny and (patho)physiology, and advanced statistical techniques have been very instrumental in this field. As different types of data and multiple data analysis techniques are combined to integrate all information, pediatric pharmacological research will become even more multidisciplinary in nature. Not only in study design and data analysis, but also in implementation of novel dosing regimens in daily pharmacotherapy, professionals with different expertise are required to collaborate. There is an important urgency to actually use information that has been gathered on PK and/or PD of drugs in children into dosing recommendations through validated models and subsequent clinical trials. Ultimately all efforts should lead up to up-to-date formularies that can be used in clinical practice. To this end, approaches to accelerate the generation of dosing guidelines for drugs that have actually not yet been studied through PKPD modeling studies in children are needed for which physiologically based principles are promising. As such, in the next years, we anticipate a trend towards a systems-level approach in pediatric modeling to optimally use the information gained in pediatric trials. For this approach, properly designed clinical PKPD studies will remain the backbone of pediatric research. Ultimately, these efforts will lead to individualized drug treatment as standard pediatric care.

## REFERENCES


1. Balan S, Hassali MA, Mak VS. Awareness, knowledge and views of off-label prescribing in children: a systematic review. Br J Clin Pharmacol. 2015;80(6):1269-80.
2. Joseph PD, Craig JC, Caldwell PH. Clinical trials in children. Br J Clin Pharmacol. 2015;79(3):357-69.

3. Shaddy RE, Denne SC, Committee on D, Committee on Pediatric R. Clinical report--guidelines for the ethical conduct of studies to evaluate drugs in pediatric populations. Pediatrics. 2010;125(4):850-60.
4. Rosato J. The ethics of clinical trials: a child's view. J Law Med Ethics. 2000;28(4):362-78.
5. van Dijk M, Ceelie I, Tibboel D. Endpoints in pediatric pain studies. Eur J Clin Pharmacol. 2011;67 Suppl 1:61-6.
6. Mahmood I. Dosing in children: a critical review of the pharmacokinetic allometric scaling and modelling approaches in paediatric drug development and clinical settings. Clin Pharmacokinet. 2014;53(4):327-46.
7. Wang J, Avant D, Green D, Seo S, Fisher J, Mulberg AE, et al. A Survey of Neonatal Pharmacokinetic and Pharmacodynamic Studies in Pediatric Drug Development. Clin Pharmacol Ther. 2015;98(3):328-35.
8. Johnson TN, Rostami-Hodjegan A. Resurgence in the use of physiologically based pharmacokinetic models in pediatric clinical pharmacology: parallel shift in incorporating the knowledge of biological elements and increased applicability to drug development and clinical practice. Paediatr Anaesth. 2011;21(3):291-301.
9. Edginton AN, Schmitt W, Voith B, Willmann S. A mechanistic approach for the scaling of clearance in children. Clin Pharmacokinet. 2006;45(7):683-704.
10. De Cock RF, Allegaert K, Schreuder MF, Sherwin CM, de Hoog M, van den Anker JN, et al. Maturation of the glomerular filtration rate in neonates, as reflected by amikacin clearance. Clin Pharmacokinet. 2012;51(2):105-17.
11. Anderson BJ, Holford NH. Mechanistic basis of using body size and maturation to predict clearance in humans. Drug Metab Pharmacokinet. 2009;24(1):25-36.
12. Strougo A, Eissing T, Yassen A, Willmann S, Danhof M, Freijer J. First dose in children: physiological insights into pharmacokinetic scaling approaches and their implications in paediatric drug development. J Pharmacokinet Pharmacodyn. 2012;39(2):195-203.
13. Johnson TN. The problems in scaling adult drug doses to children. Arch Dis Child. 2008;93(3):207-11.
14. Janiaud P, Lajoinie A, Cour-Andlauer F, Cornu C, Cochat P, Cucherat M, et al. Different treatment benefits were estimated by clinical trials performed in adults compared with those performed in children. J Clin Epidemiol. 2015;68(10):1221-31.
15. Lu H, Rosenbaum S. Developmental pharmacokinetics in pediatric populations. J Pediatr Pharmacol Ther. 2014;19(4):262-76.
16. Johnson TN. The development of drug metabolising enzymes and their influence on the susceptibility to adverse drug reactions in children. Toxicology. 2003;192(1):37-48.
17. Kearns GL, Abdel-Rahman SM, Alander SW, Blowey DL, Leeder JS, Kauffman RE. Developmental pharmacology--drug disposition, action, and therapy in infants and children. N Engl J Med. 2003;349(12):1157-67.
18. Bjorkman S. Prediction of drug disposition in infants and children by means of physiologically based pharmacokinetic (PBPK) modelling: theophylline and midazolam as model drugs. Br J Clin Pharmacol. 2005;59(6):691-704.
19. Alcorn J, McNamara PJ. Ontogeny of hepatic and renal systemic clearance pathways in infants: part II. Clin Pharmacokinet. 2002;41(13):1077-94.
20. Hines RN. Developmental expression of drug metabolizing enzymes: impact on disposition in neonates and young children. Int J Pharm. 2013;452(1-2):3-7.

21. de Wildt SN, Kearns GL, Leeder JS, van den Anker JN. Cytochrome P450 3A: ontogeny and drug disposition. Clin Pharmacokinet. 1999;37(6):485-505.
22. Pang KS, Rowland M. Hepatic clearance of drugs. I. Theoretical considerations of a "well-stirred" model and a "parallel tube" model. Influence of hepatic blood flow, plasma and blood cell binding, and the hepatocellular enzymatic activity on hepatic drug clearance. J Pharmacokinet Biopharm. 1977;5(6):625-53.
23. Rhodin MM, Anderson BJ, Peters AM, Coulthard MG, Wilkins B, Cole M, et al. Human renal function maturation: a quantitative description using weight and postmenstrual age. Pediatr Nephrol. 2009;24(1):67-76.
24. Mahmood I, Staschen CM. Prediction of Human Glomerular Filtration Rate from Preterm Neonates to Adults: Evaluation of Predictive Performance of Several Empirical Models. AAPS J. 2016;18(2):445-54.
25. Sethi PK, White CA, Cummings BS, Hines RN, Muralidhara S, Bruckner JV. Ontogeny of plasma proteins, albumin and binding of diazepam, cyclosporine, and deltamethrin. Pediatr Res. 2016;79(3):409-15.
26. McNamara PJ, Alcorn J. Protein binding predictions in infants. AAPS PharmSci. 2002;4(1):E4.
27. Grand RJ, Watkins JB, Torti FM. Development of the human gastrointestinal tract. A review. Gastroenterology. 1976;70(5 PT.1):790-810.
28. Van Den Anker JN VU-DA, Woestenborghs R, Koster M and Sauer PJJ. The effect of gastric pH on the absorption of ketoconazole by very-low-birth-weight infants. Pediatric Research. 1994;36:4A-A.
29. Bellanti F, Della Pasqua O. Modelling and simulation as research tools in paediatric drug development. Eur J Clin Pharmacol. 2011;67 Suppl 1:75-86.
30. Abdel-Rahman SM, Amidon GL, Kaul A, Lukacova V, Vinks AA, Knipp GT, et al. Summary of the National Institute of Child Health and Human Development-best pharmaceuticals for Children Act Pediatric Formulation Initiatives Workshop-Pediatric Biopharmaceutics Classification System Working Group. Clin Ther. 2012;34(11):S11-24.
31. Cella M, Zhao W, Jacqz-Aigrain E, Burger D, Danhof M, Della Pasqua O. Paediatric drug development: are population models predictive of pharmacokinetics across paediatric populations? Br J Clin Pharmacol. 2011;72(3):454-64.
32. Ince I, de Wildt SN, Tibboel D, Danhof M, Knibbe CA. Tailor-made drug treatment for children: creation of an infrastructure for data-sharing and population PK-PD modeling. Drug Discov Today. 2009;14(5-6):316-20.
33. Sheiner LB. Learning versus confirming in clinical drug development. Clin Pharmacol Ther. 1997;61(3):275-91.
34. Ette EI, Williams PJ, Lane JR. Population pharmacokinetics III: design, analysis, and application of population pharmacokinetic Studies. Ann Pharmacother. 2004;38(12):2136-44.
35. Beal SL, Sheiner LB. Estimating population kinetics. Crit Rev Biomed Eng. 1982;8(3):195-222.
36. Sheiner LB, Beal SL. Evaluation of methods for estimating population pharmacokinetics parameters. I. Michaelis-Menten model: routine clinical pharmacokinetic data. J Pharmacokinet Biopharm. 1980;8(6):553-71.

37. Wade JR, Beal SL, Sambol NC. Interaction between structural, statistical, and covariate models in population pharmacokinetic analysis. J Pharmacokinet Biopharm. 1994;22(2):165-77.
38. De Cock RF, Piana C, Krekels EH, Danhof M, Allegaert K, Knibbe CA. The role of population PK-PD modelling in paediatric clinical research. European journal of clinical pharmacology. 2011;67 Suppl 1:5-16.
39. Jonsson EN, Wade JR, Karlsson MO. Nonlinearity detection: advantages of nonlinear mixed-effects modeling. AAPS PharmSci. 2000;2(3):E32.
40. Thomson AH, Elliott HL. Designing simple PK-PD studies in children. Paediatr Anaesth. 2011;21(3):190-6.
41. Bartelink IH, Rademaker CM, Schobben AF, van den Anker JN. Guidelines on paediatric dosing on the basis of developmental physiology and pharmacokinetic considerations. Clin Pharmacokinet. 2006;45(11):1077-97.
42. EMA. EMA (EMA/CHMP/EWP/147013/2004 Committee for Medicinal Products for Human Use [CHMP]). Guideline on the role of pharmacokinetics in the development of medicinal products in the paediatric population. 2007.
43. EMA. EMA (EMA/CHMP/QWP/805880/2012 Rev.2. Committe for medicinal Products for Human Use [CHMP] Paediatric Committee [PDCO]). Guideline on pharmaceutical development of medicines for paediatric use. 2014.
44. FDA. (U.S. Department of Health and Human Services Food and Drug Administration Center for Drug Evaluation and Research (CDER) Clinical Pharmacology) December 2014, General Clinical Pharmacology Considerations for Pediatric Studies for Drugs and Biological Products - Guidance for Industry. . 2014.
45. Goodman SN, Sladky JT. A Bayesian approach to randomized controlled trials in children utilizing information from adults: the case of Guillain-Barre syndrome. Clin Trials. 2005;2(4):305-10; discussion 64-78.
46. Milton MN, Horvath CJ. The EMEA guideline on first-in-human clinical trials and its impact on pharmaceutical development. Toxicol Pathol. 2009;37(3):363-71.
47. Manolis E, Pons G. Proposals for model-based paediatric medicinal development within the current European Union regulatory framework. Br J Clin Pharmacol. 2009;68(4):493-501.
48. Meibohm B, Laer S, Panetta JC, Barrett JS. Population pharmacokinetic studies in pediatrics: issues in design and analysis. AAPS J. 2005;7(2):E475-87.
49. Barker CI, Germovsek E, Hoare RL, Lestner JM, Lewis J, Standing JF. Pharmacokinetic/pharmacodynamic modelling approaches in paediatric infectious diseases and immunology. Adv Drug Deliv Rev. 2014;73:127-39.
50. Jacqmin P, Snoeck E, van Schaick EA, Gieschke R, Pillai P, Steimer JL, et al. Modelling response time profiles in the absence of drug concentrations: definition and performance evaluation of the K-PD model. J Pharmacokinet Pharmacodyn. 2007;34(1):57-85.
51. Barrett JS, Della Casa Alberighi O, Laer S, Meibohm B. Physiologically based pharmacokinetic (PBPK) modeling in children. Clin Pharmacol Ther. 2012;92(1):40-9.
52. Tayman C, Rayyan M, Allegaert K. Neonatal pharmacology: extensive interindividual variability despite limited size. J Pediatr Pharmacol Ther. 2011;16(3):170-84.
53. Evans ND, Godfrey KR, Chapman MJ, Chappell MJ, Aarons L, Duffull SB. An identifiability analysis of a parent-metabolite pharmacokinetic model for ivabradine. J Pharmacokinet Pharmacodyn. 2001;28(1):93-105.

54. Ahlers SJ, Valitalo PA, Peeters MY, Gulik L, van Dongen EP, Dahan A, et al. Morphine Glucuronidation and Elimination in Intensive Care Patients: A Comparison with Healthy Volunteers. Anesth Analg. 2015;121(5):1261-73.
55. Shivva V, Korell J, Tucker IG, Duffull SB. An approach for identifiability of population pharmacokinetic-pharmacodynamic models. CPT Pharmacometrics Syst Pharmacol. 2013;2:e49.
56. Sheiner LB, Beal SL. Evaluation of methods for estimating population pharmacokinetic parameters. III. Monoexponential model: routine clinical pharmacokinetic data. J Pharmacokinet Biopharm. 1983;11(3):303-19.
57. Hashimoto Y, Sheiner LB. Designs for population pharmacodynamics: value of pharmacokinetic data and population analysis. J Pharmacokinet Biopharm. 1991;19(3):333-53.
58. al-Banna MK, Kelman AW, Whiting B. Experimental design and efficient parameter estimation in population pharmacokinetics. J Pharmacokinet Biopharm. 1990;18(4):347-60.
59. Ette EI, Howie CA, Kelman AW, Whiting B. Experimental design and efficient parameter estimation in preclinical pharmacokinetic studies. Pharm Res. 1995;12(5):729-37.
60. Aarons L, Balant LP, Mentre F, Morselli PL, Rowland M, Steimer JL, et al. Practical experience and issues in designing and performing population pharmacokinetic/pharmacodynamic studies. Eur J Clin Pharmacol. 1996;49(4):251-4.
61. Ogungbenro K, Matthews I, Looby M, Kaiser G, Graham G, Aarons L. Population pharmacokinetics and optimal design of paediatric studies for famciclovir. Br J Clin Pharmacol. 2009;68(4):546-60.
62. Nyberg J, Bazzoli C, Ogungbenro K, Aliev A, Leonov S, Duffull S, et al. Methods and software tools for design evaluation in population pharmacokinetics-pharmacodynamics studies. Br J Clin Pharmacol. 2015;79(1):6-17.
63. Bouillon-Pichault M, Jullien V, Bazzoli C, Pons G, Tod M. Pharmacokinetic design optimization in children and estimation of maturation parameters: example of cytochrome P450 3A4. J Pharmacokinet Pharmacodyn. 2011;38(1):25-40.
64. Roberts JK, Stockmann C, Balch A, Yu T, Ward RM, Spigarelli MG, et al. Optimal design in pediatric pharmacokinetic and pharmacodynamic clinical studies. Paediatr Anaesth. 2015;25(3):222-30.
65. Marsot A, Boulamery A, Bruguerolle B, Simon N. Population pharmacokinetic analysis during the first 2 years of life: an overview. Clin Pharmacokinet. 2012;51(12):787-98.
66. Wildschut ED, de Wildt SN, Mathot RA, Reiss IK, Tibboel D, Van den Anker J. Effect of hypothermia and extracorporeal life support on drug disposition in neonates. Semin Fetal Neonatal Med. 2013;18(1):23-7.
67. Wildschut ED, Ahsman MJ, Houmes RJ, Pokorna P, de Wildt SN, Mathot RA, et al. Pharmacotherapy in neonatal and pediatric extracorporeal membrane oxygenation (ECMO). Curr Drug Metab. 2012;13(6):767-77.
68. Bonate PL. The effect of collinearity on parameter estimates in nonlinear mixed effect models. Pharm Res. 1999;16(5):709-17.
69. Bolton SaB, C. "Choosing samples," in Pharmaceutical Statistics Practical and Clinical Applications, Fifth edit., New York: Informa Healthcare USA, 2010, p. 76. 2010.

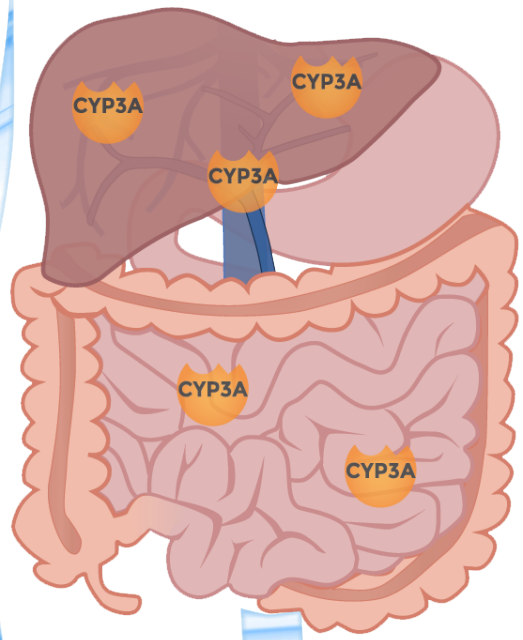
70. van Hasselt JG, Schellens JH, Beijnen JH, Huitema AD. Design of informative renal impairment studies: evaluation of the impact of design stratification on bias, precision and dose adjustment error. Invest New Drugs. 2014;32(5):913-27.
71. Jamei M, Dickinson GL, Rostami-Hodjegan A. A framework for assessing inter-individual variability in pharmacokinetics using virtual human populations and integrating general knowledge of physical chemistry, biology, anatomy, physiology and genetics: A tale of 'bottom-up' vs 'top-down' recognition of covariates. Drug Metab Pharmacokinet. 2009;24(1):53-75.
72. van Rongen A, Vaughns JD, Moorthy GS, Barrett JS, Knibbe CA, van den Anker JN. Population pharmacokinetics of midazolam and its metabolites in overweight and obese adolescents. Br J Clin Pharmacol. 2015;80(5):1185-96.
73. Bartelink IH, van Kesteren C, Boelens JJ, Egberts TC, Bierings MB, Cuvelier GD, et al. Predictive performance of a busulfan pharmacokinetic model in children and young adults. Ther Drug Monit. 2012;34(5):574-83.
74. Goldstein SL. Renal recovery at different ages. Nephron Clin Pract. 2014;127(1-4):21-4.
75. Krekels EH, van Hasselt JG, Tibboel D, Danhof M, Knibbe CA. Systematic evaluation of the descriptive and predictive performance of paediatric morphine population models. Pharmaceutical research. 2011;28(4):797-811.
76. Karlsson MO, Savic RM. Diagnosing model diagnostics. Clin Pharmacol Ther. 2007;82(1):17-20.
77. Karlsson M, Holford, N. A tutorial on visual predictive checks. PAGE 17 (2008)2008. p. Abstr 1434 [www.page-meeting.org/?abstract=].
78. Holford N. The visual predictive check—superiority to standard diagnostic (Rorschach) plots. PAGE 14 (2005)2005. p. Abstr 738 [www.page-meeting.org/?abstract=].
79. Brendel K, Comets E, Laffont C, Laveille C, Mentre F. Metrics for external model evaluation with an application to the population pharmacokinetics of gliclazide. Pharm Res. 2006;23(9):2036-49.
80. Lindbom L, Pihlgren P, Jonsson EN. PsN-Toolkit--a collection of computer intensive statistical methods for non-linear mixed effect modeling using NONMEM. Comput Methods Programs Biomed. 2005;79(3):241-57.
81. Knibbe CA, Krekels EH, van den Anker JN, DeJongh J, Santen GW, van Dijk M, et al. Morphine glucuronidation in preterm neonates, infants and children younger than 3 years. Clin Pharmacokinet. 2009;48(6):371-85.
82. Krekels EH, DeJongh J, van Lingen RA, van der Marel CD, Choonara I, Lynn AM, et al. Predictive performance of a recently developed population pharmacokinetic model for morphine and its metabolites in new datasets of (preterm) neonates, infants and children. Clin Pharmacokinet. 2011;50(1):51-63.
83. Zhao W, Zhang D, Storme T, Baruchel A, Decleves X, Jacqz-Aigrain E. Population pharmacokinetics and dosing optimization of teicoplanin in children with malignant haematological disease. Br J Clin Pharmacol. 2015;80(5):1197-207.
84. Wilbaux M, Fuchs A, Samardzic J, Rodieux F, Csajka C, Allegaert K, et al. Pharmacometric Approaches to Personalize Use of Primarily Renally Eliminated Antibiotics in Preterm and Term Neonates. J Clin Pharmacol. 2016.
85. De Cock RF, Allegaert K, Sherwin CM, Nielsen EI, de Hoog M, van den Anker JN, et al. A neonatal amikacin covariate model can be used to predict ontogeny of other

drugs eliminated through glomerular filtration in neonates. Pharmaceutical research. 2014;31(3):754-67.
86. Smits A, De Cock RF, Allegaert K, Vanhaesebrouck S, Danhof M, Knibbe CA. Prospective Evaluation of a Model-Based Dosing Regimen for Amikacin in Preterm and Term Neonates in Clinical Practice. Antimicrob Agents Chemother. 2015;59(10):6344-51.
87. Krekels EH, Tibboel D, de Wildt SN, Ceelie I, Dahan A, van Dijk M, et al. Evidence-based morphine dosing for postoperative neonates and infants. Clin Pharmacokinet. 2014;53(6):553-63.
88. Admiraal R, van Kesteren C, Jol-van der Zijde CM, van Tol MJ, Bartelink IH, Bredius RG, et al. Population pharmacokinetic modeling of Thymoglobulin((R)) in children receiving allogeneic-hematopoietic cell transplantation: towards improved survival through individualized dosing. Clin Pharmacokinet. 2015;54(4):435-46.
89. Admiraal R, van Kesteren C, Jol-van der Zijde CM, Lankester AC, Bierings MB, Egberts TC, et al. Association between anti-thymocyte globulin exposure and CD4+ immune reconstitution in paediatric haemopoietic cell transplantation: a multicentre, retrospective pharmacodynamic cohort analysis. Lancet Haematol. 2015;2(5):e194-203.
90. Admiraal R, van Kesteren C, Boelens JJ, Bredius RG, Tibboel D, Knibbe CA. Towards evidence-based dosing regimens in children on the basis of population pharmacokinetic pharmacodynamic modelling. Arch Dis Child. 2014;99(3):267-72.
91. Krekels EH, Tibboel D, Knibbe CA. Pediatric pharmacology: current efforts and future goals to improve clinical practice. Expert Opin Drug Metab Toxicol. 2015;11(11):1679-82.
92. Zhao W, Biran V, Jacqz-Aigrain E. Amikacin maturation model as a marker of renal maturation to predict glomerular filtration rate and vancomycin clearance in neonates. Clin Pharmacokinet. 2013;52(12):1127-34.
93. Calvier EAM KE, Knibbe CAJ. Extrapolation potential of semi-physiological covariate models to newborns: a simulation-based study. PAGE 24 (2015) Abstr 3595 [www.page-meeting.org/?abstract=3595]. 2015.
94. Kinderformularium. Dutch Knowledge Centre for Pharmacotherapy in Children. Dutch National Formulary for Children/Kinderformularium. http://www.kinderformularium.nl/.
95. BNFc. Paediatric Formulary Committee. British National Formulary for Children. London: BMJ Group, 2009.
96. Neofax. Young TE. Neofax. Montvale: Thomson Reuters, 2011.
97. Book R. Pickering LK, Baker CJ, Kimberlin DW. Red Book: 2012 Report of the Committee on Infectious Diseases. American Academy of Pediatrics, 2012.
98. Valitalo PA, van den Anker JN, Allegaert K, de Cock RF, de Hoog M, Simons SH, et al. Novel model-based dosing guidelines for gentamicin and tobramycin in preterm and term neonates. J Antimicrob Chemother. 2015;70(7):2074-7.
99. van der Graaf PH, Benson N. Systems pharmacology: bridging systems biology and pharmacokinetics-pharmacodynamics (PKPD) in drug discovery and development. Pharm Res. 2011;28(7):1460-4.
100. Brill MJ, Valitalo PA, Darwich AS, van Ramshorst B, van Dongen HP, Rostami-Hodjegan A, et al. Semiphysiologically based pharmacokinetic model for midazolam and CYP3A mediated metabolite 1-OH-midazolam in morbidly obese and weight loss surgery patients. CPT Pharmacometrics Syst Pharmacol. 2016;5(1):20-30.

101. Ista E, van Dijk M, Tibboel D, de Hoog M. Assessment of sedation levels in pediatric intensive care patients can be improved by using the COMFORT "behavior" scale. Pediatr Crit Care Med. 2005;6(1):58-63.
102. Carnevale FA, Razack S. An item analysis of the COMFORT scale in a pediatric intensive care unit. Pediatr Crit Care Med. 2002;3(2):177-80.
103. Stevens B, Johnston C, Petryshen P, Taddio A. Premature Infant Pain Profile: development and initial validation. Clin J Pain. 1996;12(1):13-22.
104. Valitalo PA, van Dijk M, Krekels EH, Gibbins S, Simons SH, Tibboel D, et al. Pain and distress caused by endotracheal suctioning in neonates is better quantified by behavioural than physiological items: A comparison based on Item Response Theory modelling. Pain. 2016.
105. Kearns GL, Artman M. Functional Biomarkers: an Approach to Bridge Pharmacokinetics and Pharmacodynamics in Pediatric Clinical Trials. Curr Pharm Des. 2015;21(39):5636-42.
106. Mussap M, Noto A, Cibecchini F, Fanos V. The importance of biomarkers in neonatology. Semin Fetal Neonatal Med. 2013;18(1):56-64.
107. Fanos V, Barberini L, Antonucci R, Atzori L. Metabolomics in neonatology and pediatrics. Clin Biochem. 2011;44(7):452-4.
108. Momper JD, Mulugeta Y, Burckart GJ. Failed Pediatric Drug Development Trials. Clin Pharmacol Ther. 2015;98(3):245-51.

# Section II

## Systemic CYP3A-mediated metabolism in critically ill children



# Chapter 3

## Inflammation and organ failure severely affect midazolam clearance in critically ill children

Nienke J Vet[1,2*], Janneke M Brussee[3*], Matthijs de Hoog[1,2], Miriam G Mooij[1,4], Carin WM Verlaat[5], Isabel S Jerchel[6], Ron HN van Schaik[7], Birgit CP Koch[8], Dick Tibboel[1,4], Catherijne AJ Knibbe[3,9], Saskia N de Wildt[1,4], On behalf of SKIC (Dutch collaborative PICU research network).

* These authors contributed equally to this work.

[1]Intensive Care, Erasmus MC - Sophia Children's Hospital, Rotterdam, The Netherlands; [2]Department of Pediatrics, Erasmus MC - Sophia Children's Hospital, Rotterdam, The Netherlands; [3]Division of Pharmacology, Leiden Academic Center for Drug Research, Leiden University, Leiden, The Netherlands; [4]Department of Pediatric Surgery, Erasmus MC - Sophia Children's Hospital, Rotterdam, The Netherlands; [5]Intensive Care, Radboud University Nijmegen Medical Center, Nijmegen, The Netherlands; [6]Department of Pediatric Oncology/Hematology, Erasmus MC - Sophia Children's Hospital, Rotterdam, The Netherlands; [7]Department of Clinical Chemistry, Erasmus MC, Rotterdam, The Netherlands; [8]Department of Hospital Pharmacy, Erasmus MC, Rotterdam, The Netherlands; [9]Department of Clinical Pharmacy, St Antonius Hospital, Nieuwegein, The Netherlands

*Am J Respir Crit Care Med. 2016 Jul 1;194(1):58-66*

## ABSTRACT

**Rationale:** Various in vitro, animal and limited human adult studies suggest a profound inhibitory effect of inflammation and disease on Cytochrome P450 3A (CYP3A)-mediated drug metabolism. Studies showing this relationship in critically ill patients are lacking, while clearance of many CYP3A drug substrates may be decreased, potentially leading to toxicity.

**Objectives:** To prospectively study the relationship between inflammation, organ failure and midazolam clearance, as validated marker of CYP3A mediated drug metabolism, in critically ill children.

**Methods**: From 83 critically ill children (median age 5.1 months (range 0.02-202 months)), midazolam plasma levels (n=532), cytokines (e.g. IL-6, TNF-α), C-reactive protein (CRP) and organ dysfunction scores (PRISM II, PIM2, PELOD), as well as number of failing organs were prospectively collected. A population pharmacokinetic model to study the impact of inflammation and organ failure on midazolam pharmacokinetics was developed using NONMEM 7.3.

**Main results**: In a two-compartmental pharmacokinetic model, body weight was the most significant covariate for clearance and volume of distribution. Both CRP and organ failure were significantly associated with clearance ($p<0.01$), explaining both inter-individual and inter-occasional variability. In simulations a CRP of 300 mg/L was associated with a 65% lower clearance compared to 10 mg/L and three failing organs were associated with a 35% lower clearance compared to 1 failing organ.

**Conclusions**: Inflammation and organ failure strongly reduce midazolam clearance, a surrogate marker of CYP3A-mediated drug metabolism, in critically ill children. Hence, critically ill patients receiving CYP3A substrate drugs may be at risk of increased drug levels and associated toxicity.



**Keywords**

Pediatrics; Critical illness; Midazolam; Pharmacokinetics; Inflammation; Cytochrome P450


**At a Glance Commentary**

*Scientific Knowledge on the Subject*: Various *in vitro*, animal and limited human adult studies suggest a profound inhibitory effect of inflammation and disease on Cytochrome P450 3A (CYP3A)-mediated drug metabolism. Studies showing this relationship in critically ill patients are lacking.

*What This Study Adds to the Field*: Inflammation and organ failure strongly reduce midazolam clearance, a surrogate marker of CYP3A-mediated drug metabolism, in critically ill children. Hence, critically ill patients receiving CYP3A substrate drugs may be at risk of increased drug levels and associated toxicity.

## INTRODUCTION

Critically ill patients often require life-saving polypharmacy including cardiotonics, antimicrobials and analgo-sedatives. Dependent on the underlying disease state, these patients show large variation in drug disposition and response (1). Understanding the underlying mechanisms contributing to this variation is of importance to ensure the safe and effective use of drugs in this vulnerable population.

Various in vitro, animal and limited human adult studies suggest a profound inhibitory effect of inflammation on drug metabolism by cytochrome P450 (CYP) enzymes. Drug-metabolizing enzymes are downregulated by cytokines released during inflammation (2). Inflammation-related changes in drug disposition have been described for disease states such as auto-immune disease and cancer (3). In addition, hepatic drug metabolism may be affected through a heavy loss of hepatocytes in liver failure or through a still unknown mechanism in renal failure (1, 4).

In children with sepsis and organ failure a two- and fourfold lower antipyrine clearance, respectively, was found compared to non-septic ICU children. In addition, IL-6 was negatively correlated with antipyrine clearance, suggesting inflammation as regulatory mechanism (5). Antipyrine is a global marker of CYP450 metabolism, and individual CYPs appear differentially regulated by inflammation (6). Individual enzymes need to be studied to better understand the substantial impact of drug metabolism on individual CYPs and to individualize drug therapy for individual drugs.

The most abundant CYP, CYP3A4/5, is involved in the metabolism of >50% of therapeutic drugs, of which many are prescribed daily to critically ill patients. Studies showing the relationship between inflammation and CYP3A mediated drug metabolism in critically ill patients are lacking, while clearance of many CYP3A drug substrates may be decreased, potentially leading to toxicity. The benzodiazepine midazolam is metabolized by CYP3A4/5 to a major hydroxylated active metabolite (1-OH midazolam), and subsequently metabolized to 1-OH-midazolam-glucuronide by UGTs and renally excreted (7). The clearance of midazolam to 1-OH-midazolam has been validated as surrogate measure of *in vivo* CYP3A4/5 activity (8). We therefore hypothesized that inflammation is inversely related to midazolam clearance in critically ill pediatric patients. A previous pilot study from our group, in 21 children supports this hypothesis (9). The aim of this study was to prospectively study the relationship between inflammation, organ failure, and midazolam clearance in critically ill children, as a model for CYP3A-mediated drug metabolism. Some of the results of this study have been previously reported in the form of an abstract (10).

## METHODS

### Subjects and setting

Patients were recruited in the context of a multicenter randomized controlled trial comparing daily sedation interruption plus protocolized sedation to protocolized sedation alone in critically ill children (11). For this pharmacokinetic study, patients from only two of the three participating PICUs in the Netherlands were enrolled: Erasmus MC-Sophia Children's Hospital and Radboud University Nijmegen Medical Center. Approval from each institutional review board and written informed consent from parents or legal representatives was obtained. Details on this study can be found elsewhere (11). A separate power analysis for this pharmacokinetic study was not performed. The sample size was calculated from the study's primary outcome, the number of ventilator-free days (11).

Patients were eligible for the study if they were between 0 and 18 years of age, born at least at 37 weeks of postconceptual age, required mechanical ventilation with an expected duration of at least 48 hours and received sedative drugs. The following exclusion criteria were applied: anticipated death or withdrawal of life support within 48 hours; impossibility of assessing level of sedation due to an underlying neurologic condition; neurological, respiratory or cardiac instability that may not tolerate inadequate sedation; therapeutic hypothermia after cardiopulmonary resuscitation; difficult airway; fixed duration of mechanical ventilation, admission for ECMO; already having been ventilated/sedated for >2 days in a transferring PICU. Midazolam was administered as an intravenous bolus (100 µg/kg) followed by intravenous infusion at a rate of 100 µg/kg/h. Sedation was titrated based on COMFORT-B scores. In the sedation interruption group sedative infusions were interrupted daily.

### Measurements

Blood for midazolam concentrations was sampled using an optimized sampling strategy for PK analysis, with 4 samples per day during the first 72 hours and 1 sample per day thereafter at different time points, for up to one week. Inflammatory markers (C-reactive protein (CRP), cytokines (IL-1a, IL-1b, IL-2, IL-4, IL-6, IL-10, TNF-$\alpha$, IFN-$\gamma$, MCP-1, MIP1a, MIP1b, RANTES, IL-8, FGF-b, G-CSF, GM-CSF)), liver and kidney function were determined once daily, CYP3A4*1G, *22 and CYP3A5*3 single nucleotide polymorphisms were also determined. Detailed description of the analytical methods can be found in the supplemental Methods.

Disease severity was scored using validated organ dysfunction scores: the Pediatric Risk of Mortality II (PRISM II) (range 0-100%)(12) and the Paediatric Index of Mortality (PIM2) (range 0-100%)(13) at admission and the Paediatric Logistic Organ Dysfunction (PELOD) score daily (range 0-71)(14). Since the PELOD score is a non-uniform ordered discrete scale, this score was also used to calculate the number of organs failing. If a patient scored the maximum score on an organ subscale (i.e. cardiovascular, renal, respiratory, hematological or hepatic), this was scored as organ failure 'yes'. The total number of organ failures was counted for each measurement (ranging from 0-5).

## Pharmacokinetic analysis

Midazolam concentration-time data were analyzed using non-linear mixed effects modelling version 7.3 (ICON, Globomax LLC, Ellicott, MD, USA), complying the latest FDA and EMA guidelines. Model development was in four steps: *1)* selection of a structural model, *2)* selection of an error model, *3)* covariate analysis and *4)* internal validation of the model. For model selection, we used the objective function value (a log-likelihood ratio test, assuming a Chi-squared distribution) to compare nested models. For the structural and error models, a decrease in objective function value (OFV) of 3.84 points was considered statistically significant ($p<0.05$). The optimal model was selected using standard methodology for population PK analysis with NONMEM. The details of model selection and validation can be found in the supplemental Methods.

Once the base model was selected, covariates were tested for their influence on pharmacokinetic parameters. The continuous covariates evaluated were age, weight, CRP, cytokines, PRISM II, PIM2, PELOD, number of organ failures, creatinine, ALAT and albumin. Since the concentration of IL-6 covered a large range, it was log-transformed and as such considered as covariate in the model. Categorical covariates included sex, diagnosis group, co-administration of CYP3A inhibitors (i.e. clarithromycin, voriconazole, fluconazole, erythromycin, haloperidole, metronidazole), study center and CYP3A genetic polymorphisms. Potential covariates were evaluated using forward inclusion and backward elimination with a level of significance of <0.005 (OFV -7.9 points) and <0.001 (OFV -10.8 points), respectively. In addition, inclusion of a covariate in the model had to result in a decline in unexplained inter-individual variability or unexplained inter-occasion variability before it was included in the final model (15, 16). Additional covariates had to reduce the objective function and unexplained variability further to be retained in the model. Next, the model was internally validated as described in the supplement.

## Dose simulations

To explore the quantitative impact of relevant covariates on midazolam clearance, identified from the population PK analysis, simulations were performed as follows. Using the currently recommended starting dose in children (a loading dose of 100 µg/kg and a maintenance dose of 100 µg/kg/h for 48 hours) concentration–time profiles were visualized for representative critically ill children with varying body weight, CRP concentrations and organ failure.

# RESULTS

## Patients and Data

Midazolam concentrations obtained from 83 children admitted to the intensive care unit were included between October 2009 and August 2014. A total of 523 plasma samples were available with a median of 6 (range 1-15) samples per patient. Patients were between 1 day and 17 years old (median age 5.1 months) and body weight ranged from 2.5 to 63 kg (median 5.6 kg). See further Table I.

**Table I.** Patient characteristics

| Characteristics | Total |
|---|---|
| Number of patients (n) | 83 |
| Number of samples (n) | 523 |
| Samples/patient* | 6 (1 – 15) |
| Sex (male/female,%) | 48/35 (58/42%) |
| Age (months)* | 5.1 (0.02 – 202) |
| Weight (kg)* | 5.6 (2.5 – 63) |
| Reason admission ICU | |
| - Respiratory disorder# | 58 (70.0%) |
| - Cardiac disorder## | 5 (6.0%) |
| - Sepsis | 8 (9.6%) |
| - Cardiac surgery | 9 (10.8%) |
| - Non-cardiac surgery | 3 (3.6%) |
| CRP (mg/L)* | 32 (0.3 – 385) |
| IL 6 (ng/L)* | 25 (0.55 – 43140) |
| PRISM II* | 17 (0 – 44) |
| Predicted mortality PIM 2 (%)* | 5.3 (0.25 – 33.2) |
| PELOD* | 11 (0 – 41) |
| Number of failing organs* | 2 (0 – 5) |

* Data are in median (range). PRISM II=Pediatric Risk of Mortality, PIM 2=Pediatric Index of Mortality, PELOD=Pediatric Logistic Organ Dysfunction, # viral/bacterial pneumonia, ARDS and asthma, ## congenital heart disease and cardiomyopathy.

## Model Development and Covariate Analysis

A two-compartmental model described the pharmacokinetics of midazolam well. Inter-individual variability (IIV) for clearance and volume of distribution of the central compartment could be estimated and adding these variability parameters improved the model. Then, the inclusion of inter-occasion variability (IOV) for clearance improved the model. A combined error model, combining a proportional and additive error, was superior over a proportional or additive error model. The inclusion of all these variances in the model resulted in lower residual unexplained errors and improved the model significantly (ΔOFV -119.6, $p<0.01$).

### *Body weight*

The covariate analysis showed that body weight was the most significant covariate resulting in a 76.5 reduction in objective function($p<0.005$). Using body weight as covariate, 32.9% and 43.9% of the IIV in clearance and volume, respectively, of the central compartment was explained (Table II). Therefore, body weight was incorporated in the model (Figure 1a,b and Figure 2a) and with this pediatric base model other covariates were tested to explain more interindividual and interoccasion variability.

**Table II.** Results of covariate analysis for the two-compartment pharmacokinetic model of miazolam

| Covariate | Model | Relationship of covariate | No. of structural parameters | ΔOFV |
|---|---|---|---|---|
| - | Simple model (without IOV) | - | 8 | +193.7 |
| Body weight | Pediatric base model (without IOV) | $CL_i=CL_{5kg}\cdot(WT/5)^{k1}$ $V1_i=V1_{5kg}\cdot(WT/5)^{k3}$ | 10 | +117.2 |
| Body weight | Pediatric base model | $CL_i=CL_{5kg}\cdot(WT/5)^{k1}$ $V1_i=V1_{5kg}\cdot(WT/5)^{k3}$ | 11 | - |
| Organ failure | Pediatric model with organ failure | $CL_i=CL_{5kg}\cdot(WT/5)^{k1}$ with varying $CL_{5kg}$ for varying number of organs failing | 14 | -34.7 |
| IL6 | Pediatric model with inflammatory marker* | $CL_i=CL_{5kg}\cdot(WT/5)^{k1}\cdot(1+l1\cdot(IL6/3.2))$ | 12 | -38.1 |
| CRP | Pediatric model with inflammation | $CL_i = CL_{5kg}\cdot(WT/5)^{k1}\cdot(CRP/32)^{k2}$ | 12 | -59.5 |
| CRP and organ failure | Pediatric model with inflammation and organ failure | $CL_i = CL_{5kg}\cdot(WT/5)^{k1}\cdot(CRP/32)^{k2}$ with varying $CL_{5kg}$ for varying number of organs failing | 15 | -75.3 |

*IL6: Interleukin-6 concentrations were log transformed.
ΔOFV: Difference in objective function value compared to Pediatric base model

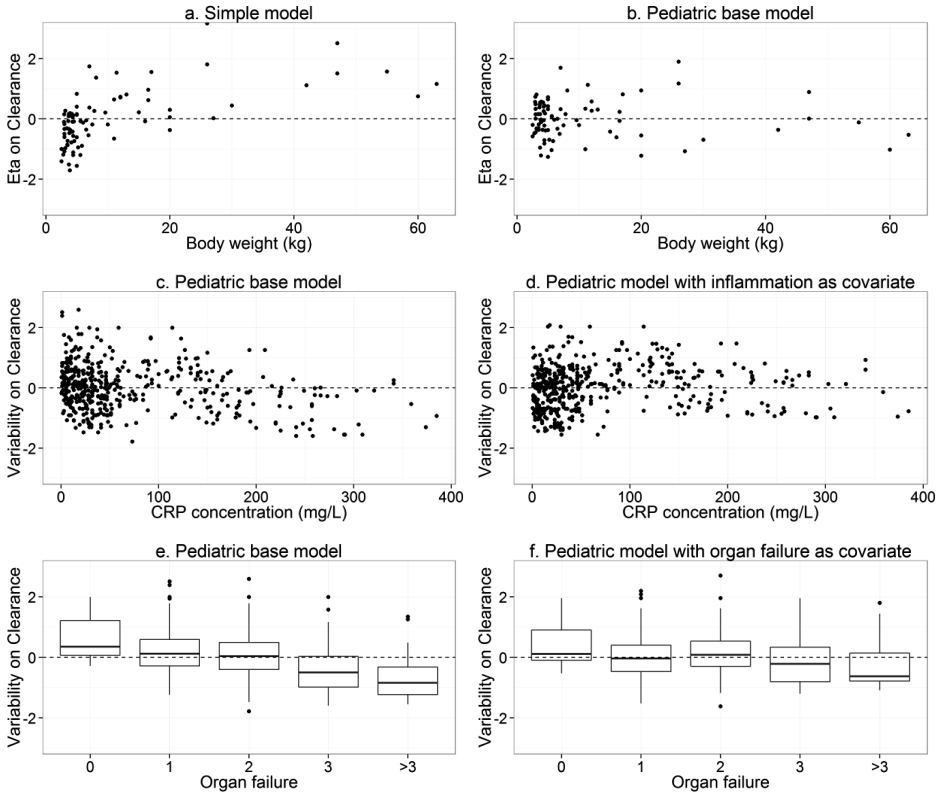



**Figure 1.** Variability in clearance versus the included covariates before (a,c,e) and after (b,d,f) inclusion of the different covariates. (a, b) Inter-individual variability on clearance versus body weight, before and after inclusion of body weight as covariate on clearance. (c, d) Variability on clearance before and after inclusion of CRP concentration as covariate on clearance. (e, f) Variability on clearance before and after inclusion of organ failure as covariate on clearance. Variability (c, d, e, f) includes inter-individual variability and inter-occasion variability.

### *Inflammation*

The inclusion of the inflammation markers IL-6 and CRP as covariate on clearance resulted in a decrease in the objective function by 38.1 and 59.5 points, respectively (Table II). Since IL-6 and CRP concentrations were highly correlated (Pearson, r=0.6, p<0.001), only CRP concentrations were included as covariate on clearance. Next to a decrease in OFV, incorporating CRP in the model resulted in better goodness-of-fit plots and a decrease in the IOV in clearance of 20.4% (Table II, Figure 1c,d). For higher concentrations of CRP, midazolam clearance was lower (Figure 2b). Figure 3a shows that a CRP of 300 mg/L is associated with a 65.4% lower clearance than a CRP of 10 mg/L. Incorporation of other cytokines (e.g. IL1a, IL1b, IL2, IL4, IL8, IL10 and TNF-α) did neither improve the model significantly, nor explained variability in clearance any further.

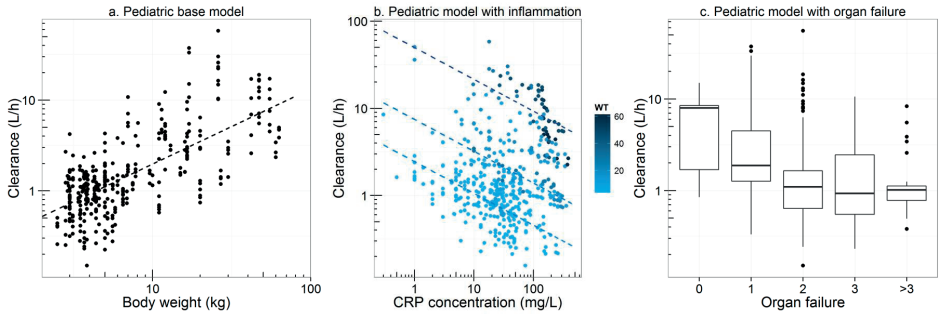



**Figure 2.** Post-hoc plots for clearance versus the included covariates body weight (a), inflammation marker CRP (b) and organ failure (c). a. Clearance versus body weight. • Individual estimated clearance value for each individual, – Population predicted clearance, predicted with the pediatric base model (table III). b. Clearance versus CRP concentration. • Individual estimated clearance value for each individual at each different CRP measurement in the study. Shaded blue colors indicate body weight (kg) with darker blue for increasing body weight. – Population predicted clearance for an individual of 3.5 (light blue), 10 (intermediate blue) and 60 kg (dark blue), predicted with the model with inflammation (Table III). c. Boxplot of the individual predicted clearance values for each individual on each day in the study versus number of organs failing. Of the 523 plasma samples, 10, 200, 209, 70 and 34 samples were taken from patients with 0, 1, 2, 3 and >3 organs failing respectively.

### *Organ failure*

There was no relation between clearance or volume of distribution and PRISM II or PIM2 scores. The PELOD score correlated negatively with clearance. Including the number of organ failures as covariate in the pediatric model (Figure 1e,f) significantly improved the model (OFV Δ-34.7 points, Table II) and resulted in better goodness-of-fit plots. It lowered the IIV and IOV with 8.6% and 7.8% respectively. The clearance of midazolam decreased with an increasing number of organ failures (Figure 2c). Three failing organs was associated with a 34.7% lower clearance compared to one failing organ (Figure 3b).

### *Other covariates*

Significant differences between study centers were not found. Fourteen patients received a CYP3A inhibitor; this had no effect on midazolam clearance. CYP3A polymorphisms, albumin, creatinine and ALAT concentrations were tested as covariates as well, but did neither improve the model nor explained variability in clearance or volume of distribution.

**Table III.** Parameter estimates of best models

| Parameter | Pediatric base model | Pediatric model with inflammation and organ failure included as covariates | |
|---|---|---|---|
| | Model fit (CV%) | Model fit (CV%) | Bootstrap median (5th-95th percentile) |
| **Clearance** | $CL_i = CL_{5kg} \cdot (WT/5)^{k1}$ | $CL_i = CL_{5kg} \cdot (WT/5)^{k1} \cdot (CRP/32)^{k2}$ with varying $CL_{5kg}$ for different number of organs failing | |
| $CL_{5kg}$ (L/h) | 1.11 (8%) | ORGF1: 1.29 (14%)<br>ORGF2: 0.96 (13%)<br>ORGF3: 0.84 (27%)<br>ORGF>3: 0.68 (25%) | ORGF1: 1.29 (1.05-1.70)<br>ORGF2: 0.96 (0.78-1.25)<br>ORGF3: 0.83 (0.54-1.30)<br>ORGF>3: 0.67 (0.43-0.99) |
| k1 | 0.828 (13%) | 1.02 (13%) | 1.03 (0.79-1.26) |
| k2 | – | -0.312 (21%) | -0.324 (-0.42- -0.21) |
| **Inter-compartmental clearance** | | | |
| Q (L/h) | 1.57 (43%) | 1.52 (34%) | 1.37 (0.09-3.43) |
| **Volume of distribution** | $V1_i = V1_{5kg} \cdot (WT/5)^{k3}$ | $V1_i = V1_{5kg} \cdot (WT/5)^{k3}$ | |
| $V1_{5kg}$ (L) | 3.58 (43%) | 3.28 (33%) | 3.45 (1.79-8.20) |
| k3 | 1.32 (19%) | 1.34 (17%) | 1.30 (0.93-1.74) |
| V2 (L) | 5.35 (21%) | 5.44 (16%) | 5.13 (0.94-6.71) |
| **Inter-individual variability** | | | |
| $\omega^2$ CL | 0.381 (25%) | 0.345 (21%) | 0.350 (0.226-0.513) |
| $\omega^2$ V1 | 1.14 (59%) | 1.19 (50%) | 1.07 (0.14-2.06) |
| **Inter-occasion variability** | | | |
| $\pi^2$ CL | 0.344 (24%) | 0.197 (24%) | 0.175 (0.103-0.265) |
| **Residual error** | | | |
| Proportional | 0.096 (15%) | 0.098 (15%) | 0.095 (0.074-0.121) |
| Additive (µg/L) | 0.121 (18%) | 0.138 (19%) | 0.139 (0.015-0.210) |

CL clearance (L/h), with $CL_i$ the individual predicted clearance of individual *i*, $CL_{5kg}$ the population predicted clearance for a median subject of 5kg, k1 exponent to relate body weight to clearance, k2 exponent to relate CRP concentrations to clearance, Q inter-compartmental clearance (L/h), V1 volume of distribution in the central compartment (L), with $V1_i$ the individual predicted volume of individual *i*, $V_{5\,kg}$ the population predicted volume for a median subject of 5 kg, k3 exponent to relate body weight to volume of distribution, V2 volume of distribution in the peripheral compartment, $\omega^2$ the variance for the inter-individual variability of the parameter mentioned, $\pi^2$ the variance for the inter-occasion variability of the parameter mentioned, WT body weight (kg), CRP C-reactive protein concentrations (mg/L), ORGF number of organs with organ failure, with failure defined by a maximum value on the PELOD score for that organ. A bootstrap was performed with 500 times of resampling the dataset.

## Final model

Incorporation of both inflammation and organ failure in the model resulted in a lower OFV (Table II) and better description of the data compared to models including

inflammation or organ failure only (goodness-of-fit plots, Suppl. Fig E1). Figure 3c shows that clearance is up to 77.4% lower when patients have both increased CRP and an increased number of organs failing.

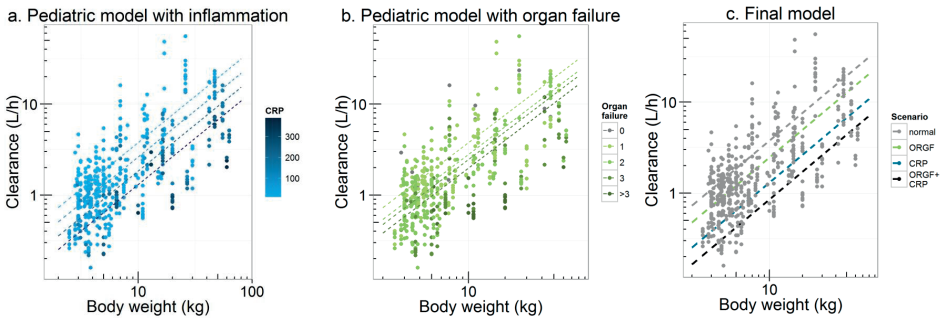



**Figure 3.** Post-hoc values for clearance versus body weight. Each point represents the posthoc clearance for an individual at a different time point in the study. a. Different colors reflect varying CRP concentrations while the four lines represent the model predictions for CRP concentrations of 10, 32, 100 and 300 mg/L respectively with darker blue lines for increasing CRP concentrations. b. Different colors reflect increasing organ failure while the four lines represent the model predictions for number of organs failing of 1, 2, 3 and >3 respectively with darker green lines for increasing number of organs failing. c. Different colors of the lines reflect different scenarios as predicted by the model. The grey line represents the scenario when the patient has a CRP concentration of 10 mg/L and 1 organ failure, the green line indicates 3 organ failures, the blue line indicates a CRP concentration of 300 mg/L and the black line indicates the scenario where both CRP and the level of organ failure are 300 mg/L and 3 respectively.
Abbrevations: *ORGF*, organ failure

## Model Evaluation

The final model was evaluated in a bootstrap analysis. Median parameter values as well as the 5$^{th}$ and the 95$^{th}$ percentiles were in agreement with the model estimations and standard errors (Table III). Normal distribution of errors was shown in the normalized prediction distribution errors (NPDE), with no significant trends in NPDE versus time and NPDE versus predictions (Suppl. Fig. E2).

## Dose simulations

Figure 4 shows simulated midazolam concentrations over time in the final PK model for patients with a body weight of 3.5, 10 and 60 kg. The simulations accounted for different clinical scenarios of increased CRP concentrations, increased organ failures or both increased CRP concentrations and organ failures. At a CRP level of 300 mg/L the plasma midazolam concentration is 2.7 fold higher than at a CRP level of 10 mg/L (Figure 4a-c). With three organ failures the plasma concentration is 1.5 fold higher than with one organ failure (Figure 4d-f). Plasma concentrations are

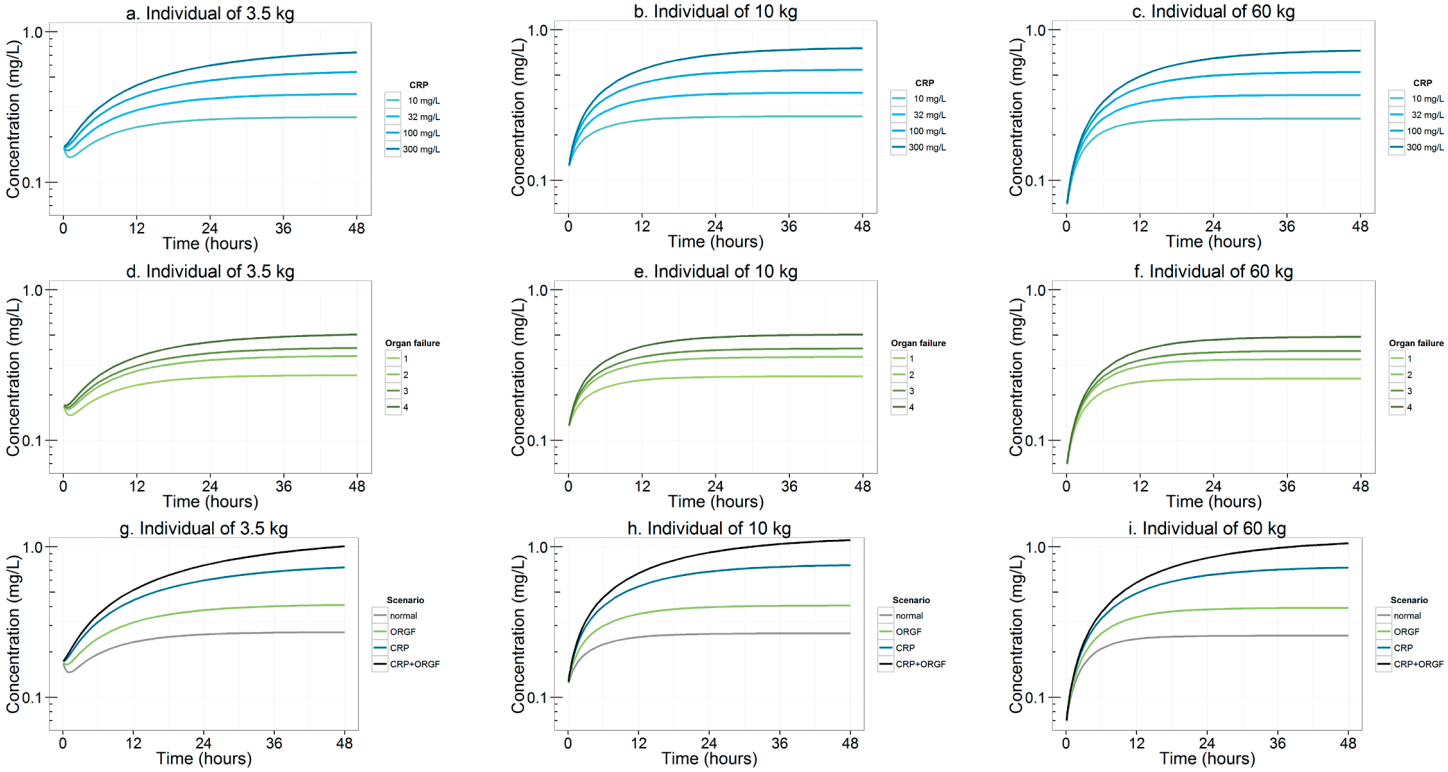



**Figure 4.** Simulations of midazolam concentration over time for three typical individuals in the study of 3.5, 10 and 60 kg, receiving a continuous infusion of 100 µg/kg/h for 48 hours and a loading dose of 100 µg/kg. (a-c) Concentration-time profiles for different CRP concentrations ranging from 10-300 mg/L. (d-f) Concentration-time profiles for different levels of organ failure. (g-i) Concentration-time profiles for the combined effect of different CRP concentrations and levels of organ failure (ORGF). The grey line represents the scenario when the patient has a CRP concentration of 10 mg/L and 1 organ failure, the green line indicates 3 organ failures, the blue line indicates CRP concentration of 300 mg/L and the black line indicates the scenario where both CRP and the level of organ failure are 300 mg/L and 3 respectively.

even higher in patients with both increased CRP concentration and higher number of organ failures (Figure 4g-l).

## DISCUSSION

This prospective population PK study shows that both inflammation, as reflected by CRP, and disease severity, as reflected by the number of organ failures, significantly affect midazolam clearance in critically ill children. These data suggest that critically ill patients may be at an increased risk of increased drug levels and associated toxicity when receiving CYP3A substrate drugs.

Our study importantly adds to existing data. In septic critically ill children, antipyrine clearance, as global marker of CYP450 metabolism was related to inflammation and severity of organ failure (5). By using midazolam as validated probe of CYP3A activity, our data may serve to predict more specifically the impact of inflammation and organ failure on CYP3A activity, and thereby the clearance of specific CYP3A substrates. A previous study found lower midazolam clearance on average in critically children than in children receiving midazolam for elective procedures (17). The reason for this lower clearance remained unclear, and they speculated that inflammation may contribute to decreased CYP activity.

Also, in a pilot study we showed that organ failure as reflected by PELOD score, but not CRP, was related to midazolam clearance (9). Most likely, the lack of correlation with CRP was due to the small sample size in this pilot study (n=17). Together, these studies suggest an important effect of inflammation and/or critical illness on CYP3A-mediated drug metabolism in children, but did not make clear to what extent inflammation and organ failure affect drug metabolism and consequent clearance. Furthermore, these studies were restricted by number and range of patients and data. The present study includes a much larger cohort of critically ill children, covering an extensive variation in age, bodyweight, degree of inflammation and disease severity. Therefore, we were able to demonstrate the effect of inflammation and organ failure within a pediatric ICU population.

To support our hypothesis that inflammation-mediated mechanisms are related to the observed lower midazolam clearance, we determined cytokines and CRP. IL-6 is a principal inhibitor of CYP3A mRNA expression (18). In adult patients after elective surgery and bone marrow transplant, and in patients with rheumatoid arthritis and cancer, elevated IL-6 levels correlated with reduced CYP3A4 activity (19-22).

Furthermore, inhibition of IL-6 by the IL-6 inhibitor tocilizumab seemed to reverse this IL-6 mediated CYP3A downregulation in adult rheumatoid arthritis patients (23).

Indeed, in line with these studies and as we hypothesized, higher IL-6 levels were related to lower midazolam clearance. Moreover, C-reactive protein levels were also negatively correlated with midazolam clearance. CRP is an acute phase protein whose production by the liver is triggered by pro-inflammatory cytokines such as IL-6(24). This is apparent by the strong correlation between the IL-6 and CRP serum levels. As CRP explained more of the variability within patients, is clinically easily available and measured frequently, CRP was chosen as final parameter in our pharmacokinetic model.

Next to inflammation, the number of organ failures was significantly related to midazolam clearance and adding this covariate further improved the model. As midazolam has a low to intermediate hepatic extraction ratio, changes in hepatic clearance are predominantly dependent on CYP enzymes, but some impact of liver flow cannot be excluded (8, 25). Variation in liver flow in critically ill patients may result from changes in cardiac output consequent to cardiac failure and/or mechanical ventilation. Also, kidney failure has been associated with decreased hepatic drug metabolism (4). In contrast, in our study, creatinine levels, as markers of kidney function, were not significantly associated with reduced midazolam clearance, while in an adult study midazolam clearance was significantly lower in critically ill patients with acute kidney failure (26).

Hence, in addition to inflammation-mediated CYP3A downregulation, organ failure in itself may add to a reduction in midazolam clearance. This is supported by the 20% higher concentrations in the simulations when organ failure was added to the effect of CRP.

Apart from age and disease, genetic variation in CYP3A4/5 activity may contribute to variation in midazolam clearance. We could, however, not identify a significant effect of genetic polymorphisms of CYP3A4 and CYP3A5 on midazolam clearance. There was a trend but not significant lower clearance in patients with CYP3A4*22, possibly due to the low prevalence of this SNP in our cohort. Patients who expressed the CYP3A5*1 allele, i.e. who express functional CYP3A5, did not have a higher midazolam clearance. We also could not confirm that functional CYP3A5 compensates for CYP3A4 suppression, as previously suggested (26).

Some possible limitations of our study should be acknowledged. First, all patients had at least one organ failure (the lung) as mechanical ventilation was an inclusion criterion of the original study. Only in a few patients we could collect data in

the absence of organ failure (i.e. after extubation).Second, we did not determine midazolam metabolite pharmacokinetics, the knowledge of which could have further supported our hypothesis that CYP3A metabolism is reduced in sicker patients. Lastly, our data show an association between inflammation and midazolam clearance but a definite causal relationship could not be established due to the nature of the study. A controlled study was considered not feasible in this ICU setting.

Despite these limitations, our results strongly indicate that critically ill patients are at an increased risk of drug toxicity or therapy failure due to important inflammation and organ failure mediated variation in clearance of CYP3A substrates. As CYP2D6, CYP1A2, CYP2C9 and CYP2C19 also appear downregulated in response to inflammation, our results may have an even wider impact and warrant further study for these enzymes and their substrates (27-30). In daily practice, our results may support more extensive therapeutic drug monitoring in patients with unexplained symptoms potentially related to drug toxicity. Finally, similar to drug metabolizing enzymes, drug receptors may also be subject to changes related to critical illness and in turn alter sensitivity to the drug's effect (21). Hence, further exploration of the pharmacokinetic-pharmacodynamic relationship in critical illness is recommended.

## ACKNOWLEDGEMENTS

The authors declare that they have no conflict of interest. We thank Ko Hagoort (Erasmus MC–Sophia Children's Hospital) for editorial assistance.

## REFERENCES

1. Zuppa AF, Barrett JS. Pharmacokinetics and pharmacodynamics in the critically ill child. *Pediatric clinics of North America* 2008; 55: 735-755, xii.
2. Aitken AE, Richardson TA, Morgan ET. Regulation of drug-metabolizing enzymes and transporters in inflammation. *Annual review of pharmacology and toxicology* 2006; 46: 123-149.
3. Vet NJ, de Hoog M, Tibboel D, de Wildt SN. The effect of inflammation on drug metabolism: a focus on pediatrics. *Drug Discov Today* 2011; 16: 435-442.
4. Lalande L, Charpiat B, Leboucher G, Tod M. Consequences of renal failure on non-renal clearance of drugs. *Clin Pharmacokinet* 2014; 53: 521-532.
5. Carcillo JA, Doughty L, Kofos D, Frye RF, Kaplan SS, Sasser H, Burckart GJ. Cytochrome P450 mediated-drug metabolism is reduced in children with sepsis-induced multiple organ failure. *Intensive Care Med* 2003; 29: 980-984.

6. Aitken AE, Morgan ET. Gene-specific effects of inflammatory cytokines on cytochrome P450 2C, 2B6 and 3A4 mRNA levels in human hepatocytes. *Drug Metab Dispos* 2007; 35: 1687-1693.
7. Gorski JC, Hall SD, Jones DR, VandenBranden M, Wrighton SA. Regioselective biotransformation of midazolam by members of the human cytochrome P450 3A (CYP3A) subfamily. *Biochem Pharmacol* 1994; 47: 1643-1653.
8. Thummel KE, Shen DD, Podoll TD, Kunze KL, Trager WF, Hartwell PS, Raisys VA, Marsh CL, McVicar JP, Barr DM, et al. Use of midazolam as a human cytochrome P450 3A probe: I. In vitro-in vivo correlations in liver transplant patients. *J Pharmacol Exp Ther* 1994; 271: 549-556.
9. Vet NJ, de Hoog M, Tibboel D, de Wildt SN. The effect of critical illness and inflammation on midazolam therapy in children. *Pediatr Crit Care Med* 2012; 13: e48-50.
10. Vet NJ BJ, de Hoog M, Mooij MG, Verlaat CW, Tibboel D, Knibbe CA, de Wildt SN. Organ failure and C-reactive protein both affect midazolam clearance in critically ill children: a population PK model. Presented at the Biannual meeting of the ESDPPP, Belgrade, June 2015. http://www.esdp2015.org/images/Abstract_book.pdf
11. Vet NJ, de Wildt SN, Verlaat CW, Knibbe CA, Mooij MG, Hop WC, van Rosmalen J, Tibboel D, de Hoog M, Skic. Daily interruption of sedation in critically ill children: study protocol for a randomized controlled trial. *Trials* 2014; 15: 55.
12. Pollack MM, Ruttimann UE, Getson PR. Pediatric risk of mortality (PRISM) score. *Crit Care Med* 1988; 16: 1110-1116.
13. Shann F, Pearson G, Slater A, Wilkinson K. Paediatric index of mortality (PIM): a mortality prediction model for children in intensive care. *Intensive Care Med* 1997; 23: 201-207.
14. Leteurtre S, Martinot A, Duhamel A, Proulx F, Grandbastien B, Cotting J, Gottesman R, Joffe A, Pfenninger J, Hubert P, Lacroix J, Leclerc F. Validation of the paediatric logistic organ dysfunction (PELOD) score: prospective, observational, multicentre study. *Lancet* 2003; 362: 192-197.
15. Krekels EH, Neely M, Panoilia E, Tibboel D, Capparelli E, Danhof M, Mirochnick M, Knibbe CA. From pediatric covariate model to semiphysiological function for maturation: part I-extrapolation of a covariate model from morphine to Zidovudine. *CPT Pharmacometrics Syst Pharmacol* 2012; 1: e9.
16. Krekels EH, Johnson TN, den Hoedt SM, Rostami-Hodjegan A, Danhof M, Tibboel D, Knibbe CA. From Pediatric Covariate Model to Semiphysiological Function for Maturation: Part II-Sensitivity to Physiological and Physicochemical Properties. *CPT Pharmacometrics Syst Pharmacol* 2012; 1: e10.
17. Ince I, Knibbe CA, Danhof M, de Wildt SN. Developmental changes in the expression and function of cytochrome P450 3A isoforms: evidence from in vitro and in vivo investigations. *Clin Pharmacokinet* 2013; 52: 333-345.
18. Morgan ET, Goralski KB, Piquette-Miller M, Renton KW, Robertson GR, Chaluvadi MR, Charles KA, Clarke SJ, Kacevska M, Liddle C, Richardson TA, Sharma R, Sinal CJ. Regulation of drug-metabolizing enzymes and transporters in infection, inflammation, and cancer. *Drug Metab Dispos* 2008; 36: 205-216.
19. Haas CE, Kaufman DC, Jones CE, Burstein AH, Reiss W. Cytochrome P450 3A4 activity after surgical stress. *Crit Care Med* 2003; 31: 1338-1346.

20. Chen YL, Le Vraux V, Leneveu A, Dreyfus F, Stheneur A, Florentin I, De Sousa M, Giroud JP, Flouvat B, Chauvelot-Moachon L. Acute-phase response, interleukin-6, and alteration of cyclosporine pharmacokinetics. *Clin Pharmacol Ther* 1994; 55: 649-660.
21. Mayo PR, Skeith K, Russell AS, Jamali F. Decreased dromotropic response to verapamil despite pronounced increased drug concentration in rheumatoid arthritis. *Br J Clin Pharmacol* 2000; 50: 605-613.
22. Rivory LP, Slaviero KA, Clarke SJ. Hepatic cytochrome P450 3A drug metabolism is reduced in cancer patients who have an acute-phase response. *Br J Cancer* 2002; 87: 277-280.
23. Schmitt C, Kuhn B, Zhang X, Kivitz AJ, Grange S. Disease-drug-drug interaction involving tocilizumab and simvastatin in patients with rheumatoid arthritis. *Clin Pharmacol Ther* 2011; 89: 735-740.
24. Fulop AK. Genetics and genomics of hepatic acute phase reactants: a mini-review. *Inflamm Allergy Drug Targets* 2007; 6: 109-115.
25. Thummel KE, Shen DD, Podoll TD, Kunze KL, Trager WF, Bacchi CE, Marsh CL, McVicar JP, Barr DM, Perkins JD, et al. Use of midazolam as a human cytochrome P450 3A probe: II. Characterization of inter- and intraindividual hepatic CYP3A variability after liver transplantation. *J Pharmacol Exp Ther* 1994; 271: 557-566.
26. Kirwan CJ, MacPhee IA, Lee T, Holt DW, Philips BJ. Acute kidney injury reduces the hepatic metabolism of midazolam in critically ill patients. *Intensive Care Med* 2012; 38: 76-84.
27. Jones AE, Brown KC, Werner RE, Gotzkowsky K, Gaedigk A, Blake M, Hein DW, van der Horst C, Kashuba AD. Variability in drug metabolizing enzyme activity in HIV-infected patients. *European journal of clinical pharmacology* 2010; 66: 475-485.
28. Frye RF, Schneider VM, Frye CS, Feldman AM. Plasma levels of TNF-alpha and IL-6 are inversely related to cytochrome P450-dependent drug metabolism in patients with congestive heart failure. *J Card Fail* 2002; 8: 315-319.
29. Williams ML, Bhargava P, Cherrouk I, Marshall JL, Flockhart DA, Wainer IW. A discordance of the cytochrome P450 2C19 genotype and phenotype in patients with advanced cancer. *Br J Clin Pharmacol* 2000; 49: 485-488.
30. Helsby NA, Lo WY, Sharples K, Riley G, Murray M, Spells K, Dzhelai M, Simpson A, Findlay M. CYP2C19 pharmacogenetics in advanced cancer: compromised function independent of genotype. *Br J Cancer* 2008; 99: 1251-1255.
31. Beal SL. Ways to fit a PK model with some data below the quantification limit. *J Pharmacokinet Pharmacodyn* 2001; 28: 481-504.
32. Wang C, Peeters MY, Allegaert K, Blusse van Oud-Alblas HJ, Krekels EH, Tibboel D, Danhof M, Knibbe CA. A bodyweight-dependent allometric exponent for scaling clearance across the human life-span. *Pharm Res* 2012; 29: 1570-1581.
33. Comets E, Brendel K, Mentre F. Computing normalised prediction distribution errors to evaluate nonlinear mixed-effect models: the npde add-on package for R. *Comput Methods Programs Biomed* 2008; 90: 154-166.

# SUPPLEMENTAL MATERIAL (CHAPTER 3)

## Supplemental methods

### Analytical methods

Midazolam plasma concentrations were measured using liquid chromatography-tandem mass spectrometry (LC-MS/MS), validated according to current ICH and FDA guidelines. The lower limit of quantification was 5.1 ng/ml. Serum cytokine levels were determined using a customized Luminex Performance Assay (R&D Systems) containing the following analytes: MCP-1, MIP1a, MIP1b, RANTES, IL-8, FGF-b, G-CSF, GM-CSF, IFN-γ, IL-1a, IL-1b, IL-2, IL-4, IL-6, IL-10, TNF-α. Samples were prepared according to the manufacturer's instructions, read on a BioPlex200 System, and analyzed in BioPlex Manager 6.0 software. CRP was measured using an immunoturbidimetric assay (Modular analytics <P> Roche diagnostics, Mannheim, Germany) and values <5 mg/L were considered normal. Genomic DNA was isolated from 200 Jl EDTA blood or saliva on the MagNA Pure Compact System with the use of MagNA Pure Compact Nucleic Acid Isolation Kit I (Roche®). The genetic variants CYP3A4*1G (rs2242480), *22 (rs35599367) and CYP3A5*3 (rs776746) were determined on the 7500 Real-Time PCR System (Applied Biosystems®) with the use of Taqman® SNP Genotyping Assay C__26201900_30, C__59013445_10 and C__26201809_30 (Applied Biosystems®), respectively.

### Analysis of Pharmacokinetic Data

Population pharmacokinetic (PK) data analysis was performed using first-order conditional estimation with interaction in NONMEM version 7.3 (ICON, Globomax LLC, Ellicott, MD, USA) with Pirana 2.9.0 and R version 3.1.1 for visualization of data. Of all measurements, 1.3% were below the limit of quantification (BLQ). BLQ observations were handled according to the M6 method(35), as other methods did not result in an improvement of the model.

### Model development

Model development was in four steps: (1) selection of a structural model, (2) selection of an error model, (3) covariate analysis and (4) internal validation of the model. For the structural and error models, a decrease in objective function value (OFV) of 3.84 points was considered statistically significant ($p<0.05$). Visual improvement of the goodness-of-fit plots (observed vs. individual and population predicted concentration, conditional weighted residuals (CWRES) vs. time and CWRES vs. population predicted concentration) was evaluated. In addition, the confidence interval for the estimated parameters, the correlation matrix, η-shrinkage and the

condition number (to find ill-conditioning or over-parameterization of the model) served to evaluate the models.

The individual pharmacokinetic parameters (post-hoc values) of the *i*th subject are modeled by use of Eq. 1:

(1) $P_i = P_{pop} \cdot e^{\eta_i}$

where $P^i$ is the individual value of the PK parameters of the *i*th individual, $P_{pop}$ the population prediction and $\eta_i$ the inter-individual variability, which is assumed to be a Gaussian random variable with a mean zero and variance of $\omega^2$ with a log-normal distribution. Inter-occasion variability on the different parameters was tested for the subsequent days to assess changes in pharmacokinetic parameters between days. This resulted in the identification of interoccasion variability (IOV) on clearance describing the changes in clearance within individuals during the study according to Eq. 2:

(2) $CL_{ij} = CL_{pop} \cdot e^{\eta_i + m_{ij}}$

where $CL_{ij}$ is the individual parameter estimate at the *j*th occasion, $CL_{pop}$ the population prediction of clearance, $\eta_i$ the inter-individual variability and $m_{ij}$ is a random variable for the *i*th individual at the *j*th occasion (IOV). Both ηi and mij were assumed to be independently normally distributed with a mean of zero and variances ω2 and π2, respectively. The IOV represents the variability between different occasions, where every 24 hours after the first dose was regarded as a new occasion. The residual unexplained variability was described with a combined error model (proportional and additive error model) for all data. The observations of the *j*th observation of the *i*th individual are described according to Eq. 3:

(3) $Y_{ij} = C_{pred,ij} \cdot (1 + \varepsilon_1) + \varepsilon_2$

where $Y_{ij}$ is the observed concentration, $C_{pred,ij}$ the predicted concentration for the *j*th observation in the *i*th individual and $\varepsilon_1$ and $\varepsilon_2$ the proportional and additive error samples respectively from a distribution with a mean of zero and variance of $\sigma^2$.

## Covariate Analysis

Tested covariates included patient characteristics (age, weight, sex, diagnosis group, coadministration of CYP3A inhibitors, study center, CYP3A polymorphisms), inflammation markers (CRP, cytokines) and disease severity (PRISM II, PIM2, PELOD, number of organ failures, creatinine, ALAT and albumin). Individual post-hoc parameters, inter-individual variability and conditionally weighted residuals (CWRES) were plotted against the covariates to evaluate possible relationships. Continuous covariates were tested in a linear or power function (Eqs. 4 and 5):

(4) $P_i = P_{pop} \cdot \left(1 + \left(\frac{Cov_i}{Cov_{median}}\right) \cdot l\right)$

$$P_i = P_{pop} \cdot \left(\frac{Cov_i}{Cov_{median}}\right)^k \quad (5)$$

where $P_i$ and $Cov_i$ are the values for the parameter and covariate, respectively, for the *i*th individual, $P_{pop}$ is the population mean for parameter P and $Cov_{median}$ is the standardized value of the covariate. In the linear function, the slope is depicted by *l*. For Eq. 5, *k* represents the scaling factor in the power function. For clearance, also a body weight dependent exponent *k* was tested(36). Since the concentration of IL-6 covered a large range, it was log-transformed and as such considered as covariate in the model. Categorical covariates such as co-administration of CYP3A inhibitors, sex and number of organs failing were tested as a fraction for each category or independently estimated for the different categories. When a CYP3A inhibitor (i.e. clarithromycin, voriconazole, fluconazole, erythromycin, haloperidole, metronidazole) was administered at the same day as midazolam, a factor affecting clearance was estimated for that day. Potential covariates were evaluated using forward inclusion and backward elimination with a level of significance of <0.005 (OFV -7.9 points) and <0.001 (OFV -10.8 points), respectively. In addition, inclusion of a covariate in the model had to result in a decline in unexplained inter-individual variability or unexplained inter-occasion variability before it was included in the final model(18, 19). Additional covariates had to reduce the objective function and unexplained variability further to be retained in the model.

## Model Evaluation

The model was internally validated using bootstrap analysis in Perl-speaks-NONMEM (PsN version 4.2.0). Five hundred datasets were resampled from the original datasets and refitted to the model. Normalized prediction distribution errors (NPDE) were calculated with the NPDE package in R(37). For this method, the dataset used for model development was simulated a thousand times with inclusion of inter-individual and inter-occasion variability and residual error.

## SUPPLEMENTAL FIGURES

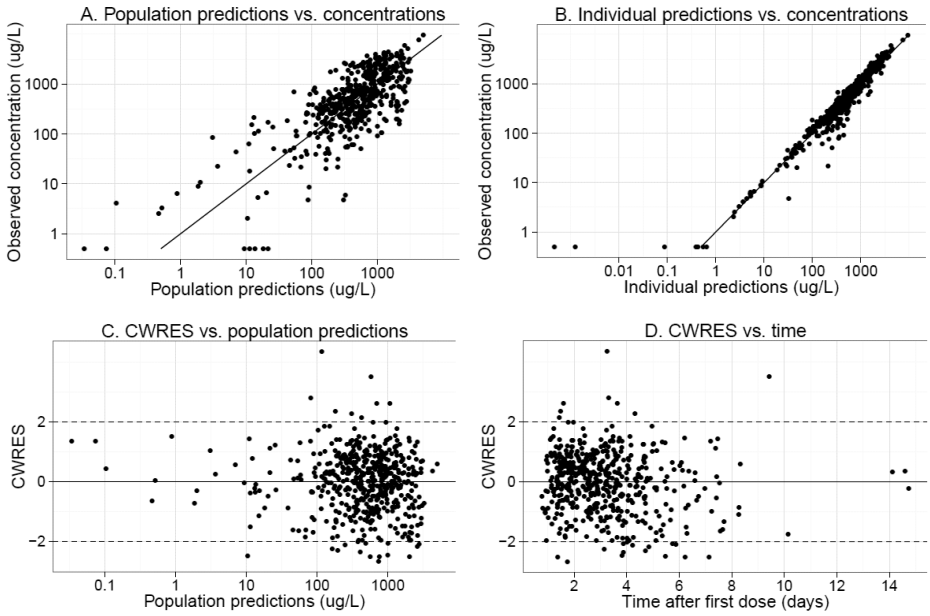



**Figure E1.** Goodness-of-fit plots for the final model with inflammation and organ failure included as covariates. A. Log observed plasma concentrations vs. log population predicted concentrations. B. Log observed plasma concentrations vs. log individual predicted concentrations on a log scale. C. Conditional weighted residuals (CWRES) versus log population predictions. D. CWRES versus time after first dose.

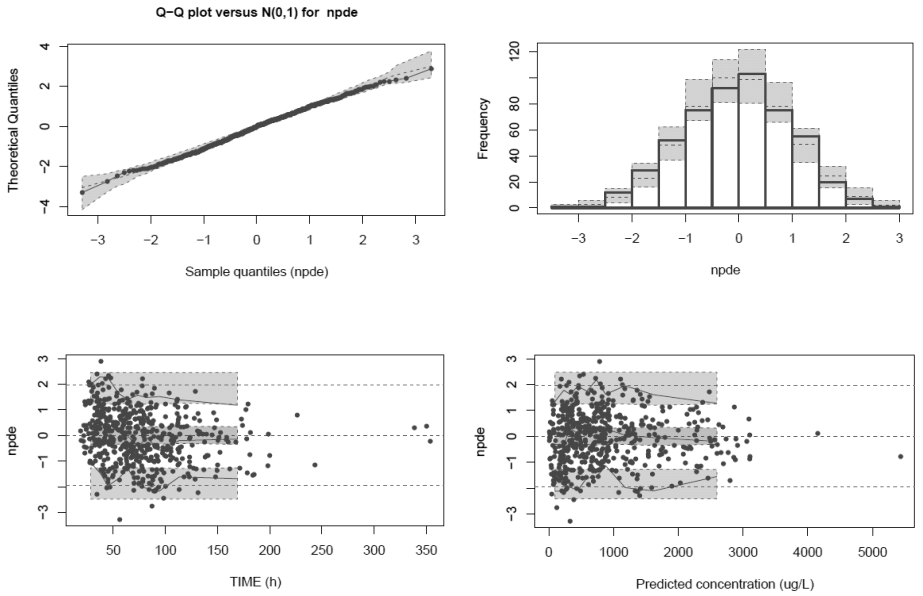



**Figure E2**. Normalized prediction distribution error (NPDE) results of the final model with inflammation and disease severity included as covariate plots. A. Q-Q plot. B. Histogram of the NPDE distribution. C. NPDE versus time after first dose in hours. D. NPDE versus predicted concentrations in µg/L.

## REFERENCES


1. Beal SL. Ways to fit a PK model with some data below the quantification limit. *J Pharmacokinet Pharmacodyn* 2001; 28: 481-504.
2. Wang C, Peeters MY, Allegaert K, Blusse van Oud-Alblas HJ, Krekels EH, Tibboel D, Danhof M, Knibbe CA. A bodyweight-dependent allometric exponent for scaling clearance across the human life-span. *Pharm Res* 2012; 29: 1570-1581.
3. Krekels EH, Neely M, Panoilia E, Tibboel D, Capparelli E, Danhof M, Mirochnick M, Knibbe CA. From pediatric covariate model to semiphysiological function for maturation: part I-extrapolation of a covariate model from morphine to Zidovudine. *CPT Pharmacometrics Syst Pharmacol* 2012; 1: e9.
4. Krekels EH, Johnson TN, den Hoedt SM, Rostami-Hodjegan A, Danhof M, Tibboel D, Knibbe CA. From Pediatric Covariate Model to Semiphysiological Function for Maturation: Part II-Sensitivity to Physiological and Physicochemical Properties. *CPT Pharmacometrics Syst Pharmacol* 2012; 1: e10.
5. Comets E, Brendel K, Mentre F. Computing normalised prediction distribution errors to evaluate nonlinear mixed-effect models: the npde add-on package for R. *Comput Methods Programs Biomed* 2008; 90: 154-166.

# Chapter 4

## Predicting CYP3A-mediated midazolam metabolism in critically ill neonates, infants, children, and adults with inflammation and organ failure

Janneke M Brussee[1], Nienke J Vet[2], Elke H J Krekels[1], Abraham J Valkenburg[3], Evelyne Jacqz-Aigrain[4], Joop M A van Gerven[5], Eleonora L Swart[6], Johannes N van den Anker[3,7,8], Dick Tibboel[2], Matthijs de Hoog[2], Saskia N de Wildt[3,9], Catherijne A J Knibbe[1,10]

[1]Division of Pharmacology, Leiden Academic Centre for Drug Research (LACDR), Leiden University, Leiden, the Netherlands; [2]Department of Pediatrics, Erasmus MC - Sophia Children's Hospital, Rotterdam, the Netherlands; [3]Intensive Care and Department of Pediatric Surgery, Erasmus MC - Sophia Children's Hospital, Rotterdam, the Netherlands; [4]Department of Pediatric Pharmacology and Pharmacogenetics, Hôpital Robert Debré, Paris, France; [5]Centre for Human Drug Research, Leiden, the Netherlands; [6]Department of Clinical Pharmacology and Pharmacy, VU University Medical Centre, Amsterdam, The Netherlands; [7]Division of Paediatric Pharmacology and Pharmacometrics, University of Basel Children's Hospital, Basel, Switzerland; [8]Division of Clinical Pharmacology, Children's National Health System, Washington, DC; [9]Department of Pharmacology and Toxicology, Radboud University Medical Centre, Nijmegen, the Netherlands; [10]Department of Clinical Pharmacy, St. Antonius Hospital, Nieuwegein, the Netherlands

*Br J Clin Pharmacol. 2018 Feb;84(2):358-368*

## ABSTRACT

Aims: Inflammation and organ failure have been reported to impact cytochrome P450 (CYP) 3A-mediated clearance of midazolam in critically ill children. Our aim was to evaluate a previously developed population pharmacokinetic model in both critically ill children and other populations in order to allow the model to be used to guide dosing in clinical practice.

Methods: The model was externally evaluated in 136 individuals, including (pre) term neonates, infants, children, and adults (body weight 0.77-90 kg, CRP 0.1-341 mg/L and 0-4 failing organs) using graphical and numerical diagnostics.

Results: The pharmacokinetic model predicted midazolam clearance and plasma concentrations without bias in post-operative or critically ill paediatric patients and term neonates (median prediction error (MPE) <30%). Using the model for extrapolation resulted in well-predicted clearance values in critically ill and healthy adults (MPE <30%), while clearance in preterm neonates was over predicted (MPE >180%).

Conclusion: The recently published pharmacokinetic model for midazolam, quantifying the influence of maturation, inflammation, and organ failure in children yields unbiased clearance predictions and can therefore be used for dosing instructions in term neonates, children, and adults with varying levels of critical illness including healthy adults, but not for extrapolation to preterm neonates.



**Key words**
Children, drug metabolism, cytochrome P450


**What is known about the subject**:
- Recently, the impact of inflammation and organ failure on cytochrome P450 (CYP) 3A-mediated midazolam metabolism has been quantified in critically ill children
- Before population pharmacokinetic models can be used for clinical decision making and deriving dosing recommendations, they should be thoroughly evaluated in external datasets

**What this study adds**:
- Metabolic midazolam clearance can be accurately predicted in critically ill term neonates, infants, and children using C-Reactive Protein and number of failing organs
- While extrapolation to preterm neonates on the basis of this model leads to considerable over-prediction of metabolic midazolam clearance, extrapolation to adults and patients beyond the studied disease severity levels yielded unbiased midazolam clearance predictions

## INTRODUCTION

Various studies suggest that cytochrome P450 3A (CYP3A)-mediated drug metabolism may be reduced by inflammation and disease (1-5). Decreases in CYP3A-mediated clearance may result in overdosing and side effects in certain patient populations. A previous study in critically ill children showed substantially reduced CYP3A-mediated clearance of midazolam in patients with inflammation and organ failure (6). A population pharmacokinetic (PK) model for midazolam was developed based on data from both critically ill term neonates and children between 0 and 17 years of age who were on mechanical ventilator support (6). Increased inflammation, reflected by a ten-fold increase in C-reactive protein (CRP) concentrations from 32 to 300 mg/L, was found to correlate with a 50% reduction in midazolam clearance in this population. Furthermore, an increase in disease severity, reflected by the number of failing organs (cardiovascular, renal, respiratory, haematological and/or hepatic failure) e.g. increasing from 1 to 3 or >3, correlates with 35 or 47% reduced midazolam clearance, respectively (figure 1).

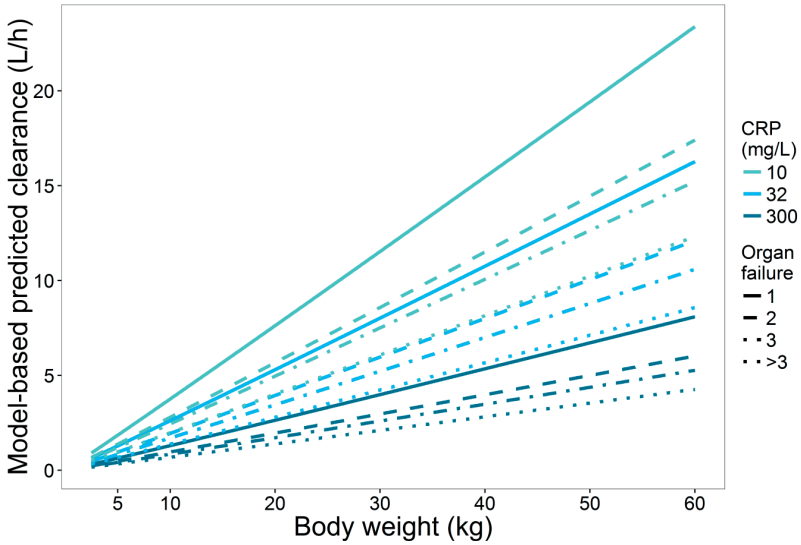



**Figure 1.** Model-predicted pediatric midazolam clearance for different levels of inflammation, as reflected by CRP concentrations of 10, 32, 300 mg/L (top to bottom), and disease severity scenarios, reflected by number of organ failures.

To allow population models to be used for clinical decision making, for instance for deriving dosing recommendations, they should be thoroughly evaluated (7-9). Without proper validation and evaluation, models can only be regarded as descriptive rather than predictive, thereby limiting their safe use for clinical and

**Table I.** Patient and study characteristics of datasets used for external validation (13, 14), and extrapolation (15-18), compared to model building data (6).

| | Model building | New data for external validation | | New data for extrapolation | | | |
|---|---|---|---|---|---|---|---|
| **Study** | **Vet et al (6)** | **De Wildt et al (13)** | **Valkenburg et al (14)** | **De Wildt et al (15)** | **Jacqz-Aigrain et al (16)** | **Van Gerven et al (17)** | **Swart et al (18)** |
| **Patient population** | Critically ill children | Critically ill children | Infants after cardiac bypass surgery | Preterm neonates | Preterm neonates | Healthy male adults | Critically ill adults |
| **Indication for midazolam** | Mechanical ventilation in intensive care | Conscious sedation in intensive care | Post-operative sedation | Sedation for invasive procedure | Mechanical ventilation in intensive care | Healthy volunteers | Sedation in intensive care |
| **Number of patients** | 83 | 18 | 26 | 31 | 24 | 20 | 17 |
| **Samples (n (median/ patient))** | 523 (6) | 262 (11) | 153 (6) | 231 (8) | 63 (3) | 336 (16) | 238 (13) |
| **Postnatal age (median (range))** | 5.1 months (1 d – 17 yr) | 30 months (1 d – 17 yr) | 6 months (3-31 mo) | 5 days (3-44 d) | 3 days (1-7 d) | 24 years (20-31 yr) | 56 years (21-84 yr) |
| **Body weight (kg) (median (range))** | 5.6 (2.5 – 63) | 13 (2.8 – 60) | 6.7 (3.6 – 12.9) | 1.1 (0.77 – 1.6) | 1.6 (0.96 – 3.7) | 72.5 (64 – 89) | 75 (63 – 90) |
| **C-reactive protein (mg/L) (median (range))** | 32.0 (0.3-385) | 40.2 (0.1-341) | 47.5 (0.1-259) | NA | NA | NA | NA |
| **Number of organ failure (median (range))** | 2 (0-5) | 2 (0-4) | 1 (1-2) | 1 (0-2) | 1 (1) | 0 (0) | 1 (1-3) |
| **Administered dose during study** | 0.15 (0.02-0.6) mg/kg /h infusion with 0.1 (0.02-0.6) mg/kg loading dose | 0.05-0.4 mg/kg/h infusion with 0.1 (0.05-0.35) mg/kg loading dose | 0.12 (0.02-0.3) mg/kg/h infusion with 0.05 (0.025-0.5) mg/kg loading dose titrated for effect | 0.1 mg/kg (0.05-0.25) 30-min infusion | 0.06 mg/kg/h infusion. If GA<33wk, after 24h 0.03 mg/kg/h | 0.1 mg/kg 20-min infusion | 0.2 (0.03-0.85) mg/kg/h infusion with 0.1 (0.04-0.4) mg/kg loading dose titrated for effect |

NA = not available

research applications (8). Three categories in model evaluation with increasing order of quality have been described (9-11): basic internal methods, advanced internal methods and external model evaluation. Marsot *et al.* found that only 10% of the population models in paediatric subjects from neonates to 2 years of age developed up to 2010 were externally evaluated (10), even though this step is essential if the model is to be used to predict adequate dosing regimens in routine clinical practice. An external validation is based on new data that were not used for model development. A valid population model should at least be able to accurately predict data from patients with a comparable distribution of characteristics (e.g. weight/age range or disease severity) as the patient population included in model development (8). When a model is applied to predict pharmacokinetics in individuals with characteristics outside the range of the population used in model development, this not an external validation, but a form of extrapolation and this may affect the model's predictions in the new population (12).

The previously developed PK model for midazolam quantifying CYP3A-mediated clearance in critically ill children (6) has the potential to define midazolam dosing regimens that reliably achieve target plasma concentrations. The aim of this study is to evaluate the predictive performance of the population pharmacokinetic model in external data from patients with the same patient characteristics as in the original model (i.e. critically ill children, infants and term neonates). Moreover, the extrapolation potential of the model was investigated by evaluating its predictive performance in populations beyond the studied age range (i.e. preterm neonates or adults) and disease severity (healthy state).

## METHODS

### Patients and Data

From the literature, data from six studies were available that could be used for this external validation and extrapolation study (13-18). These studies covered different patient populations, ranging largely in age from preterm neonates to adults with different disease severity levels. All studies had been approved by ethics committees and informed (parental) consent was obtained. Table I gives an overview of the patient and study characteristics of the available data for external validation (13, 14) and extrapolation (15-18) as well as of the internal data from the original model development (6) as comparison. The new data included 136 preterm neonates, infants, children, and adults, who all received intravenous midazolam. Organ failure, counted from 0-5, was defined based on a maximum sub score for cardiovascular,

renal, respiratory, haematological and hepatic failure on the paediatric logistic organ dysfunction (PELOD) score (19) for the paediatric subjects or on the Sequential Organ Failure Assessment (SOFA) score (20) for the adult subjects. For all study participants, information on respiratory function was known, while information on the other organ functions or CRP was not always reported. For missing CRP data in preterm neonates and healthy adult volunteers, values for an healthy individual were assumed, i.e. a CRP concentration of 10 mg/L. In case of missing sub scores on organ dysfunction, no organ failure was assumed. For missing CRP values in critically ill adults (18), a CRP concentration of 32 mg/L was assumed, which was the median CRP value in the previously reported model (6) (table I), see under Original model. In total ten observations from two individuals were discarded, because of a substantial increase in midazolam plasma concentration without a recorded prior dosing event, of which for at least one individual this was known to be due to flushing of the intravenous line in the contralateral arm before sampling.

## Original Model

The original population PK model consisted of a two compartment model in which the effect of body weight, inflammation, and organ failure on midazolam clearance in critically ill term neonates and children up to the age of 17 years was quantified (6). For a median patient of 5 kg with a concentration of the inflammation marker CRP of 32 mg/L and 1 failing organ, clearance was 1.29 L/h (6). Individual clearance was quantified as follows:

$$CL_i = CL_{5\ kg} \cdot (WT_i/5)^{1.02} \cdot (CRP_i/32)^{-0.312} \quad \text{(eq. 1)}$$

in which $CL_{5\ kg}$ varies for different number of organs failing with 1.29, 0.96, 0.83 or 0.67 L/h for 1, 2, 3 or >3 failing organs respectively, $WT_i$ is the body weight (in kg) of individual *i* and $CRP_i$ is the C-reactive protein concentration (in mg/L) of this individual. This corresponds with a clearance of 19.0 L/h for a 70 kg-individual with a CRP concentration of 32 mg/L and 1 failing organ. Volume of distribution in the central compartment for an individual *i* was

$$V1_i\,(L) = 3.28 \cdot (WT_i/5)^{1.34} \quad \text{(eq. 2)}$$

corresponding to 113 L for a 70 kg individual, and the peripheral distribution volume and the inter-compartmental clearance were 5.44 L and 1.52 L/h respectively.

## Model Evaluation

The predictive performance of the PK model was evaluated using several tools. First, we obtained population and individual concentration predictions using the model and its published model parameters in NONMEM (version 7.3, ICON, Ellicott City, MD, USA). Using R (version 3.2.2) and R-studio (version 0.98.1078), goodness-of-fit plots were constructed. Concentration predictions were visually compared to the

observed concentrations and the distribution of conditionally weighted residuals (CWRES) versus the population prediction of the plasma concentrations and versus time were visually assessed. When model predictions are unbiased, CWRES are randomly distributed around zero. Additionally, we plotted individual and population clearance predictions versus the most dominant covariate (i.e. body weight) to assess the accuracy of the covariate model. Furthermore, bias was calculated per dataset by taking the median of the prediction error (PE):

$$PE = \frac{(pred - obs) \times 100}{obs} \qquad \text{(eq. 3)}$$

in which *pred* are the predicted concentration and the individually predicted clearance, and *obs* the observed concentration and the population predicted clearance to evaluate PE in concentration and clearance respectively. An MPE of <30% was considered to be an accurate prediction. Moreover, a normalized prediction distribution error (NPDE) analysis was performed using the NPDE package in R (21). For each observed concentration in the external datasets, 1000 midazolam concentrations were simulated. The simulations were based on the dosing regimen, body weight, CRP concentrations and level of organ failure of the patients, and on the parameter values including inter-individual and residual variability that were obtained for the original model (table II). These 1000 predicted concentrations were compared with the observed concentrations in the external datasets. For accurate concentration predictions, the mean of the NPDE is expected to be 0 and an adequate description of the variability in the model is expected to yield a variance in the NPDE distribution of 1.

## RESULTS

Overall, 1045 plasma concentrations from 136 subjects, aged 1 day - 84 years with a body weight ranging from 0.77-90 kg, were available for the external validation and extrapolation (table I) (13-18). To compare, table I also shows the data used for development of the original model which were collected in 83 critically ill term neonates and children, ranging in age from 1 day up to 17 years (6). The subjects for the external validation included 18 critically ill children (13) and 26 children after cardiac bypass surgery (14), who were within the age and body weight range of the model building dataset and had comparable CRP concentrations and levels of organ failure. Furthermore, 55 preterm neonates ranging in age between 1-44 days (15, 16), 17 critically ill adults without alcohol abuse (18) and 20 healthy adults (17) were included to evaluate the extrapolation potential of the model predictions to patients outside the studied age and weight range and with different levels of disease severity.

| | | |
|---|---|---|
| **Model building data** | Critically ill children (6) | |
| **External validation data** | Critically ill children (13) | |
| | Patients after cardiac bypass surgery (14) | |
| **Extra-polation data** | Preterm neonates (15, 16) | |
| | Healthy adults (17) | |
| | Critically ill adults (18) | |

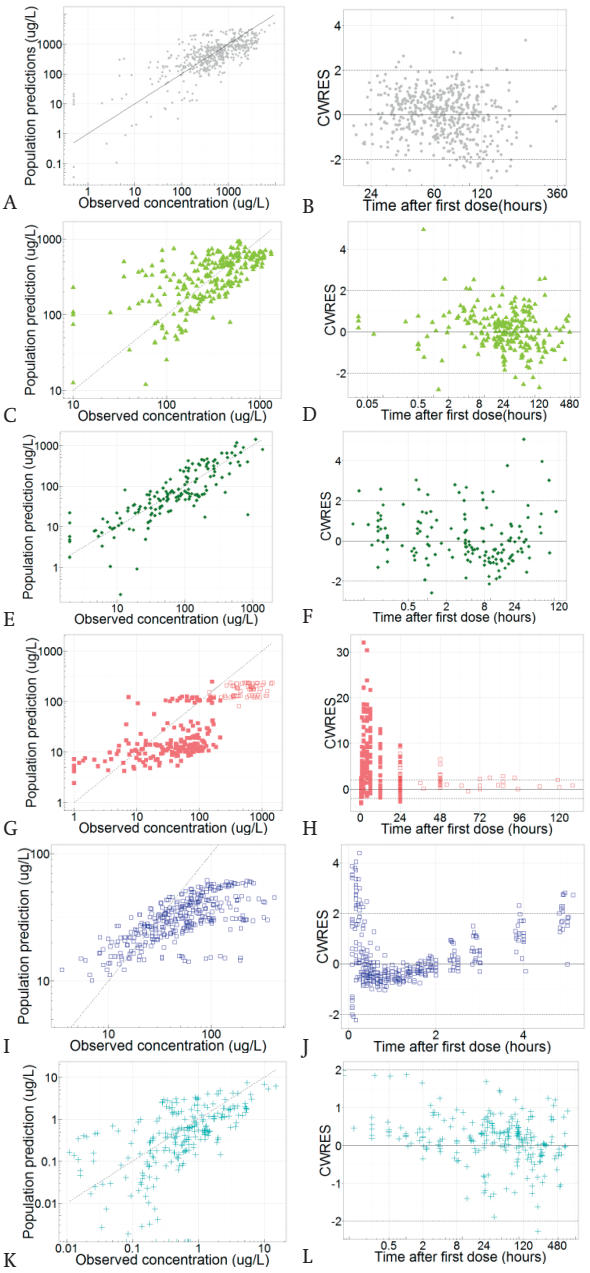



**Figure 2.** Goodness-of-fit plots, stratified per study. First column shows the population predicted concentrations versus the observed concentrations and the second column shows the conditionally weighted residuals (CWRES) over time for the different indicated patient populations. For panels G-H, closed squares (▪) represent predictions from preterm neonates from the study of De Wildt et al (15), while open squares (□) are data from preterm neonates from the study of Jacqz-Aigrain et al (16).

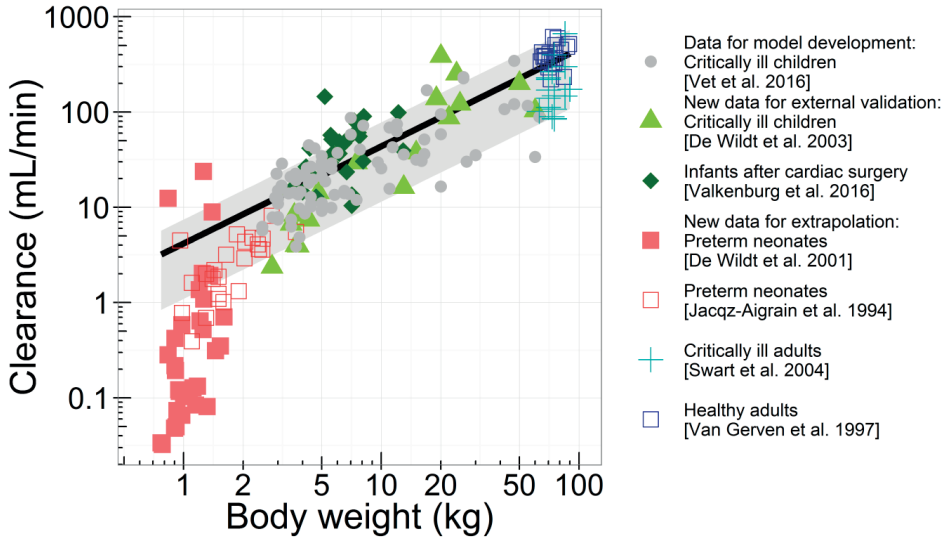



**Figure 3.** Population (line) and individual (symbols) predicted clearance versus the patient's body weight. The population prediction assumes an individual with a CRP concentration of 32 mg/L and 1 organ with organ failure. The grey shaded area indicates the range of population predicted clearance values from the healthiest patients (without inflammation [CRP 10mg/L] and without organ failure) (upper boundary) to the patient with most severe disease state (CRP 300 mg/L and >3 organ failures) (lower boundary).

The model described midazolam concentrations in the original dataset (figure 2, panels A-B) and was able to predict midazolam clearance and plasma concentrations without bias in critically ill children (13) and children after cardiac bypass surgery (14) (figure 2, panels C-F). Also, no trends were observed in the CWRES versus predicted plasma concentrations (plot not shown), confirming there was no bias in the peak and trough concentration predictions. In addition, the MPE was <30% for both concentrations and clearances (table II). The NPDE results indicated that model predictions are accurate without trends over time or concentration range (supplemental material). The mean of the NPDE for both populations was not significantly different from 0 (0.034 and -0.062 respectively), while the variance of the variability in the external data was statistically significantly larger than predicted by the model (2.24 and 1.95 respectively). This indicates that the concentrations in the population were accurately predicted, but that more variability is observed in the new data than is predicted by the model. Figure 3 shows that the individual clearance predictions (data points) which are based on the patient's level of inflammation and organ failure, are scattered around the population clearance predictions for patients with varying body weight and a CRP concentration of 32 mg/L and 1 organ with organ failure (black line).

**Table II.** Median Prediction Error (MPE) for predicted concentrations vs. observed concentrations and individual predicted clearance vs. population predicted clearance

| | Study | MPE (%)* | |
|---|---|---|---|
| | | Plasma concentrations | Clearance |
| **Model building** | Vet et al (6) | -13.7 | 5.27 |
| **New data for external validation** | De Wildt et al (13) | -14.1 | 25.4 |
| | Valkenburg et al (14) | 3.1 | 22.0 |
| **New data for extrapolation** | De Wildt et al (15) | -63.5 | 1746 |
| | Jacqz-Aigrain et al (16) | -68.3 | 186 |
| | Van Gerven et al (17) | -35.6 | 1.48 |
| | Swart et al (18) | -40.6 | -1.67 |

*The MPE is the median of the prediction error which reflects for plasma concentrations the difference in observed and predicted concentration (see Methods, eq. 3). For clearance, the difference in individual predicted and population predicted clearance is calculated.

The model building dataset included term neonates, but no preterm neonates (22). Extrapolation of model predictions to preterm neonates without inflammation or organ failure, resulted in under prediction of the high plasma concentrations at early time points (figure 2G, H) with an MPE > 60% for both datasets (table II). The NPDE results also indicated biased model predictions and an under prediction of the variability (figure S1, panels J-L). Figure 3 shows that clearance was generally over predicted for this population.

When the model was used for extrapolation to healthy adults without organ failure and an assumed CRP concentration of 10 mg/L, midazolam clearances were within the predicted range (MPE < 30%), albeit at the upper range, which may be expected given their normal CRP concentrations and lack of organ failure (figure 3). However, in the population predicted versus observed plot (figure 2I), in the CWRES over time plot (figure 2J) and the CWRES *versus* population predictions plot (not shown), a bi-phasic trend was observed, causing a large over prediction of peak and trough concentrations and under prediction for other plasma concentrations, which is suggestive of misspecification of drug distribution. The NPDE (figure S1M-O) also indicated this model misspecification for healthy adults. For critically ill adults with varying levels of organ failure and an assumed CRP concentration of 32 mg/L, midazolam clearances were also predicted within the range (MPE < 30%), although in the lower range (figure 3). Furthermore, the plasma concentrations were predicted with reasonable accuracy (figure 2 K,L). However, the NPDE also showed some model misspecification (mean distribution error is significantly different from 0,

see supplemental material), which may result from inappropriate information upon drug distribution.

## DISCUSSION

In this analysis, the predictive performance and extrapolation potential of a recently developed population PK model for midazolam, quantifying CYP3A-mediated clearance in critically ill children (6), was evaluated. According to the applied model evaluation methods, midazolam clearance and plasma concentrations are well-predicted in external data from critically ill children, infants and term neonates and children after cardiac bypass surgery who are in the same age range and have similar levels of inflammation and organ failure. Extrapolation to subjects outside the age range and with different levels of disease severity, resulted in biased clearance for preterm neonates and biased concentration predictions in healthy adults. Extrapolation to subjects outside the age range with similar levels of disease severity, e.g. critically ill adults, resulted in adequate clearance predictions (figure 3).

To our knowledge, the evaluated PK model (6) in this study is the first model to describe and quantify the relationship between inflammation and organ failure on midazolam clearance in children. As in the model, besides maturation, both inflammation and organ failure proved of relevance, these factors could be relevant for dosing of CYP3A substrates. Model evaluation is however essential before a model can be used for clinical decisions, like developing dosing recommendations (7-10). Ideally, a prospective study with more subjects for external evaluation would be undertaken, to ensure that patient characteristics and covariate information would be recorded in a standard way. However, with literature data available (13-18), it is unethical and unnecessary to put additional burden on these vulnerable paediatric critically ill patients by performing another PK study (49).

The external validation of this model in cohorts of critically ill paediatric patients and infants after cardiac bypass surgery confirms the accuracy of the obtained relationships also in patients not included in model building. The PK model predicts a 30% decrease in midazolam clearance when CRP concentrations reflecting inflammation increases 3-fold from 32 to 100 mg/L, irrespective of the cause of elevated CRP concentrations, which could be e.g. respiratory disorders, cardiac disorders, sepsis or (non-)cardiac surgery (6). Clearance decreases 26% when disease severity, expressed as number of organs failing, increases from 1 to 2 (figure 1). Cardiovascular, renal, respiratory, haematological and hepatic failure

each contributed to number of failing organs, in which e.g. cardiac failure and mechanical ventilation may cause changes in cardiac output, thereby impacting midazolam clearance. As during ICU stay, the number of organs failing and CRP concentrations may change over time thereby influencing midazolam clearance, so drug dosing in clinical practice may require adjustments over time, assuming the same effective concentration. In any case, it seems advisable to monitor drug effects of midazolam during ICU stay in patients with major inflammation and/or organ failure. This may especially be relevant in preterm neonates, as there are known risks for adverse neurological effects due to the immaturity of GABA receptors. By evaluation of the effects in both children and adults, also the fact that target plasma concentrations may be influenced by inflammation or organ failure is taken into account. Whether these results for midazolam also apply to other CYP3A substrates needs further study, and therapeutic drug monitoring may be required in case of a small therapeutic window of the CYP3A substrate involved.

Many PK studies on the CYP3A substrate drug midazolam (23-25) have been performed in children over the last two decades (26-36), ranging from critically ill children to relatively healthy children undergoing elective surgery, and we compared our clearance predictions to the reported clearance values in the literature from studies up to 25 years ago (figure 4). The clearance values predicted by our model are within the reported ranges, albeit in the lower range and with high variability. High inter-individual variability in clearance in children is partly due to maturation of CYP3A-mediated metabolism (37), but CYP3A activity is also known to be down-regulated by inflammatory cytokines *in vitro* (3). The reason for our model predictions being generally lower than the paediatric values reported in literature (figure 4) might have been due to differences in disease states, as the 'healthiest' children in our study still have 1 organ failure and are still admitted to the ICU, while reported values in the literature mainly originate from non-ICU children. This suggests that within a certain age and weight range, the disease state is relevant for drug dosing. For example, for paediatric oncology patients with acute-phase inflammatory disease, a decreased midazolam clearance has been reported (38), while for relatively healthy children undergoing elective craniofacial surgery, a much higher midazolam clearance has been reported (27).

A limitation of comparing results to literature values is that some studies only report summarized clearance data, which is less informative than individual data. Moreover, the clearance values described in literature are mostly reported per kg body weight (28-36), without reporting the individual body weight values or body weight ranges (31, 32, 34, 36). Furthermore, detailed information on inflammation and/or organ failure is missing in those studies.

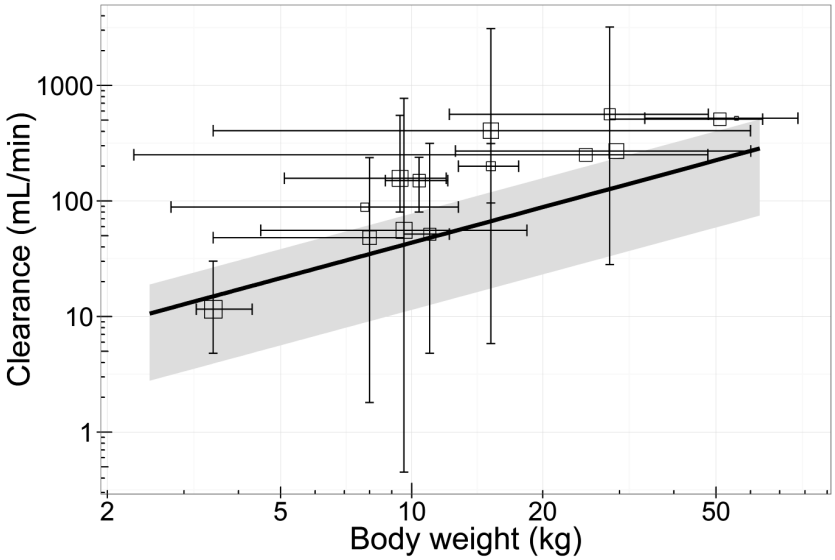



**Figure 4**. Population (line) predicted clearance versus the patient's body weight compared to literature reported clearance values (open squares with error bars) (27-36). The population prediction assumes an individual with a CRP concentration of 32 mg/L and 1 organ with organ failure. The grey shaded area indicates the range of population predicted clearance values from the healthiest patients (without inflammation [CRP 10mg/L] and without organ failure) (upper boundary) to the patient with most severe disease state (CRP 300 mg/L and >3 organ failures) (lower boundary). The squares represent the reported clearance for a mean body weight. The hortizontal error bars represent the included body weight range or the body weight range derived from the patient's age (40-42). Vertical errorbars represent the total range of reported clearances, or in case of 1 study the 95% confidence interval. Literature data was obtained after a literature search in PubMed with keywords including midzolam, clearance, pediatric, children and pharmacokinetics (PK) and additional studies were identified from reviews and summarizing studies (26, 43-48). Studies published up to 25 years ago were included if pediatric subjects in the study received intravenously administered midazolam. Studies with only preterm neonates, and patients receiving extracorporeal membrane oxygenation (ECMO) treatment were excluded.

The external validation of our model confirmed accurate predictions of the pharmacokinetics of midazolam in critically ill children. However, the results also show that the model should not be used for extrapolations to younger populations or populations with different levels of disease severity. Clearance was largely over predicted in preterm neonates with a body weight below 3.5 kg and a gestational age of less than 37 weeks, which is likely due to biased maturation predictions of CYP3A activity and/or abundance in these young patients, or possibly the lower level of inflammation and organ failure in this patient group. Due to rapid maturation after birth, which is not accounted for in our model, CYP3A capacity is likely over predicted in our model. Based on the current data, it is however not possible to discriminate between maturation and disease severity in this population. Disease state in the neonatal ICU population is known to be very diverse, and unfortunately,

information on CRP was not available from most of the preterm infants. Assuming lower CRP values than 10 mg/L would result in higher predictions of clearance, rather than lower clearance and with more failing organs (e.g. 1 to 4), the predicted clearance would be up to 47.3% lower, while the observed clearances in this population are even lower. Therefore, until the additional maturation processes in preterm neonates are accounted for in the model, it should not be used for extrapolation to this very young and critically ill population.

The extrapolation to adults included both healthy and critically ill subjects alike. In the healthy adult population, clearance was well predicted assuming normal CRP and the lack of organ failure that would be expected (figure 3); however the drug distribution was misspecified, resulting in a clear trend in the CWRES over time plot (figure 2J). This bi-phasic trend suggests that an additional peripheral compartment is required to describe the distribution after a single (semi-) bolus dose applied in adults. In the healthy volunteer study, more samples were taken directly after dosing, possibly allowing for the identification of relatively fast equilibrating peripheral compartments (figure 2J). In critically ill adults who were less densely sampled, this trend in CWRES was indeed not observed (figure 2L). Other possible explanations for these observations could be altered plasma protein binding in critically ill patients, which may alter drug distribution or capillary leaking in critically ill patients (39), which may result in ultra-fast equilibration of central and peripheral compartments. This ultra-fast equilibration in these patients prevents the identification of peripheral compartments that can be identified in healthy patients without capillary leaking.

In critically ill adults, midazolam clearance values were predicted in the lower range of the expected clearance values (figure 3). This indicates that despite the different age and weight range in the external validation data, the model was able to predict clearance in the critically ill adults with similar levels of inflammation and organ failure.

Some limitations of this extrapolation study should be acknowledged. As CRP concentrations were not available for all studies, the assumption was made that in healthy adults and preterm neonates, CRP was 10 mg/L and that in critically ill adults the inflammation marker had the median value of the internal dataset of 32 mg/L. To assess the impact of different CRP concentrations on clearance predictions, model-based simulations were performed with CRP values of 10 mg/L and 300 mg/L in figure 3 (outer boundaries of the grey area). For preterm neonates at the neonatal intensive care unit, assuming CRP values of 1 or 300 mg/L would both result in over prediction of midazolam clearance (likely due to immature CYP3A in this

population), while for critically ill adults, assuming a value of 10 mg/L or 300 mg/L yields an prediction of their clearance values within the predicted range (figure 3, grey area). The model should therefore not be extrapolated to preterm infants. In our study, we could not account for genetic variation in CYP3A4/5 activity, since in the original dataset the variability in genotype was too low to identify a statistically significant impact of CYP3A4/5 genotype on midazolam clearance and in the datasets of the current study information on genotype was not available. In literature, it has however been suggested that patients with expression of functional CYP3A5, metabolize midazolam faster and may compensate for the suppression of CYP3A4 activity due to inflammation or organ failure (50). These genotypes may also be of relevance in the different populations studied here, but, given the data obtained in this study, this could neither be confirmed nor rejected.

Finally, despite the adequate extrapolation potential of our model to the patient populations included in the current study, it should be noted that extrapolation to (special) populations not included in the current analysis (e.g. obese patients, pregnant women etc.) is not warranted without first formally evaluating the extrapolation potential to these populations.

## CONCLUSION

The recently published paediatric pharmacokinetic model for midazolam quantifying the influence of maturation, inflammation, and organ failure can be used for predictions of CYP3A-mediated midazolam clearance in term neonates, children, and adults with varying levels of critical illness, including infants after cardiac bypass surgery and healthy adults. Extrapolations with this model resulted in biased predictions of clearance in preterm neonates. The predictive performance of our model and its value for the development of paediatric dosing regimens for midazolam and potentially other CYP3A substrates is therefore confirmed for term neonates, infants, children, and adults with varying levels of critical illness.

## ACKNOWLEDGEMENTS AND DISCLOSURES

The authors would like to thank Dr. Cormac Breatnach for supervision of the study in infants after cardiac surgery and sharing the data for this external validation study. This study was supported by a NWO/Vidi grant to Catherijne A. J. Knibbe (2013), and project grants from the Netherlands Organization for Health Research and

Development, ZonMw Priority Medicines for Children (grant numbers 113202002 and 92003549), and Erasmus MC Cost-Effectiveness Research.

## REFERENCES

1. Vet NJ, de Hoog M, Tibboel D, de Wildt SN. The effect of inflammation on drug metabolism: a focus on pediatrics. Drug Discov Today. 2011;16(9-10):435-42.
2. Zuppa AF, Barrett JS. Pharmacokinetics and pharmacodynamics in the critically ill child. Pediatr Clin North Am. 2008;55(3):735-55, xii.
3. Aitken AE, Morgan ET. Gene-specific effects of inflammatory cytokines on cytochrome P450 2C, 2B6 and 3A4 mRNA levels in human hepatocytes. Drug Metab Dispos. 2007;35(9):1687-93.
4. Aitken AE, Richardson TA, Morgan ET. Regulation of drug-metabolizing enzymes and transporters in inflammation. Annu Rev Pharmacol Toxicol. 2006;46:123-49.
5. Carcillo JA, Doughty L, Kofos D, Frye RF, Kaplan SS, Sasser H, et al. Cytochrome P450 mediated-drug metabolism is reduced in children with sepsis-induced multiple organ failure. Intensive Care Med. 2003;29(6):980-4.
6. Vet NJ, Brussee JM, de Hoog M, Mooij MG, Verlaat CW, Jerchel IS, et al. Inflammation and Organ Failure Severely Affect Midazolam Clearance in Critically Ill Children. Am J Respir Crit Care Med. 2016;194(1):58-66.
7. Brussee JM, Calvier EA, Krekels EH, Valitalo PA, Tibboel D, Allegaert K, et al. Children in clinical trials: towards evidence-based pediatric pharmacotherapy using pharmacokinetic-pharmacodynamic modeling. Expert Rev Clin Pharmacol. 2016;9(9):1235-44.
8. Krekels EH, van Hasselt JG, Tibboel D, Danhof M, Knibbe CA. Systematic evaluation of the descriptive and predictive performance of paediatric morphine population models. Pharm Res. 2011;28(4):797-811.
9. Brendel K, Dartois C, Comets E, Lemenuel-Diot A, Laveille C, Tranchand B, et al. Are population pharmacokinetic and/or pharmacodynamic models adequately evaluated? A survey of the literature from 2002 to 2004. Clin Pharmacokinet. 2007;46(3):221-34.
10. Marsot A, Boulamery A, Bruguerolle B, Simon N. Population pharmacokinetic analysis during the first 2 years of life: an overview. Clin Pharmacokinet. 2012;51(12):787-98.
11. Tod M, Jullien V, Pons G. Facilitation of drug evaluation in children by population methods and modelling. Clin Pharmacokinet. 2008;47(4):231-43.
12. Collins GS, de Groot JA, Dutton S, Omar O, Shanyinde M, Tajar A, et al. External validation of multivariable prediction models: a systematic review of methodological conduct and reporting. BMC Med Res Methodol. 2014;14:40.
13. de Wildt SN, de Hoog M, Vinks AA, van der Giesen E, van den Anker JN. Population pharmacokinetics and metabolism of midazolam in pediatric intensive care patients. Crit Care Med. 2003;31(7):1952-8.
14. Valkenburg AJ, Calvier EA, van Dijk M, Krekels EH, O'Hare BP, Casey WF, et al. Pharmacodynamics and Pharmacokinetics of Morphine After Cardiac Surgery in Children With and Without Down Syndrome. Pediatr Crit Care Med. 2016;17(10):930-8.

15. de Wildt SN, Kearns GL, Hop WC, Murry DJ, Abdel-Rahman SM, van den Anker JN. Pharmacokinetics and metabolism of intravenous midazolam in preterm infants. Clin Pharmacol Ther. 2001;70(6):525-31.
16. Jacqz-Aigrain E, Daoud P, Burtin P, Desplanques L, Beaufils F. Placebo-controlled trial of midazolam sedation in mechanically ventilated newborn babies. Lancet. 1994;344(8923):646-50.
17. van Gerven JM, Roncari G, Schoemaker RC, Massarella J, Keesmaat P, Kooyman H, et al. Integrated pharmacokinetics and pharmacodynamics of Ro 48-8684, a new benzodiazepine, in comparison with midazolam during first administration to healthy male subjects. Br J Clin Pharmacol. 1997;44(5):487-93.
18. Swart EL, Zuideveld KP, de Jongh J, Danhof M, Thijs LG, Strack van Schijndel RM. Comparative population pharmacokinetics of lorazepam and midazolam during long-term continuous infusion in critically ill patients. Br J Clin Pharmacol. 2004;57(2):135-45.
19. Leteurtre S, Martinot A, Duhamel A, Proulx F, Grandbastien B, Cotting J, et al. Validation of the paediatric logistic organ dysfunction (PELOD) score: prospective, observational, multicentre study. Lancet. 2003;362(9379):192-7.
20. Vincent JL, Moreno R, Takala J, Willatts S, De Mendonca A, Bruining H, et al. The SOFA (Sepsis-related Organ Failure Assessment) score to describe organ dysfunction/failure. On behalf of the Working Group on Sepsis-Related Problems of the European Society of Intensive Care Medicine. Intensive Care Med. 1996;22(7):707-10.
21. Comets E, Brendel K, Mentre F. Computing normalised prediction distribution errors to evaluate nonlinear mixed-effect models: the npde add-on package for R. Comput Methods Programs Biomed. 2008;90(2):154-66.
22. Vet NJ, de Wildt SN, Verlaat CW, Knibbe CA, Mooij MG, Hop WC, et al. Daily interruption of sedation in critically ill children: study protocol for a randomized controlled trial. Trials. 2014;15:55.
23. Gorski JC, Hall SD, Jones DR, VandenBranden M, Wrighton SA. Regioselective biotransformation of midazolam by members of the human cytochrome P450 3A (CYP3A) subfamily. Biochem Pharmacol. 1994;47(9):1643-53.
24. Thummel KE, Shen DD, Podoll TD, Kunze KL, Trager WF, Bacchi CE, et al. Use of midazolam as a human cytochrome P450 3A probe: II. Characterization of inter- and intraindividual hepatic CYP3A variability after liver transplantation. J Pharmacol Exp Ther. 1994;271(1):557-66.
25. Thummel KE, Shen DD, Podoll TD, Kunze KL, Trager WF, Hartwell PS, et al. Use of midazolam as a human cytochrome P450 3A probe: I. In vitro-in vivo correlations in liver transplant patients. J Pharmacol Exp Ther. 1994;271(1):549-56.
26. Anderson BJ, Larsson P. A maturation model for midazolam clearance. Paediatr Anaesth. 2011;21(3):302-8.
27. Peeters MY, Prins SA, Knibbe CA, Dejongh J, Mathot RA, Warris C, et al. Pharmacokinetics and pharmacodynamics of midazolam and metabolites in nonventilated infants after craniofacial surgery. Anesthesiology. 2006;105(6):1135-46.
28. Muchohi SN, Kokwaro GO, Ogutu BR, Edwards G, Ward SA, Newton CR. Pharmacokinetics and clinical efficacy of midazolam in children with severe malaria and convulsions. Br J Clin Pharmacol. 2008;66(4):529-38.

29. Reed MD, Rodarte A, Blumer JL, Khoo KC, Akbari B, Pou S, et al. The single-dose pharmacokinetics of midazolam and its primary metabolite in pediatric patients after oral and intravenous administration. J Clin Pharmacol. 2001;41(12):1359-69.
30. De Wildt SN RL, van den Anker JN, Murray DJ. Does age alter the pharmacokinetics of midazolam and I-OH-midazolam in paediatric patients? Clin Pharmacol Ther. 2000;67:104.
31. Nahara MC, McMorrow J, Jones PR, Anglin D, Rosenberg R. Pharmacokinetics of midazolam in critically ill pediatric patients. Eur J Drug Metab Pharmacokinet. 2000;25(3-4):219-21.
32. Hughes J, Gill AM, Mulhearn H, Powell E, Choonara I. Steady-state plasma concentrations of midazolam in critically ill infants and children. Ann Pharmacother. 1996;30(1):27-30.
33. Burtin P, Jacqz-Aigrain E, Girard P, Lenclen R, Magny JF, Betremieux P, et al. Population pharmacokinetics of midazolam in neonates. Clin Pharmacol Ther. 1994;56(6 Pt 1):615-25.
34. Tolia V, Brennan S, Aravind MK, Kauffman RE. Pharmacokinetic and pharmacodynamic study of midazolam in children during esophagogastroduodenoscopy. J Pediatr. 1991;119(3):467-71.
35. Rey E, Delaunay L, Pons G, Murat I, Richard MO, Saint-Maurice C, et al. Pharmacokinetics of midazolam in children: comparative study of intranasal and intravenous administration. Eur J Clin Pharmacol. 1991;41(4):355-7.
36. Hartwig S, Roth B, Theisohn M. Clinical experience with continuous intravenous sedation using midazolam and fentanyl in the paediatric intensive care unit. Eur J Pediatr. 1991;150(11):784-8.
37. Ince I, Knibbe CA, Danhof M, de Wildt SN. Developmental changes in the expression and function of cytochrome P450 3A isoforms: evidence from in vitro and in vivo investigations. Clin Pharmacokinet. 2013;52(5):333-45.
38. Rivory LP, Slaviero KA, Clarke SJ. Hepatic cytochrome P450 3A drug metabolism is reduced in cancer patients who have an acute-phase response. Br J Cancer. 2002;87(3):277-80.
39. Cordemans C, De Laet I, Van Regenmortel N, Schoonheydt K, Dits H, Huber W, et al. Fluid management in critically ill patients: the role of extravascular lung water, abdominal hypertension, capillary leak, and fluid balance. Ann Intensive Care. 2012;2(Suppl 1 Diagnosis and management of intra-abdominal hyperten):S1.
40. World Health Organization (WHO). Child Growth Standards, Weight-for-age: Boys 2-5 years; 2016 October 20. Available from: http://www.who.int/childgrowth/standards/cht_wfa_boys _z_2_5.pdf [Website]
41. World Health Organization (WHO). Child Growth Standards, Weight-for-age: Boys birth-2 years; 2016 October 20. Available form: http://www.who.int/childgrowth/standards/cht_wfa_boys_z_0_2.pdf [Website]
42. Royal College of Paediatrics and Child Health (RCPCH) and Department of Health. UK Growth chart Boys 2-18 years. 2nd Edition; 2016 October 20. Available from: http://www.rcpch.ac.uk/child-health/research-projects/uk-who-growth-charts/uk-growth-chart-resources-2-18-years/school-age2013 [Website]
43. Altamimi MI, Sammons H, Choonara I. Inter-individual variation in midazolam clearance in children. Arch Dis Child. 2015;100(1):95-100.
44. Pacifici GM. Clinical pharmacology of midazolam in neonates and children: effect of disease-a review. Int J Pediatr. 2014;2014:309342.

45. Ng E, Taddio A, Ohlsson A. Intravenous midazolam infusion for sedation of infants in the neonatal intensive care unit. Cochrane Database Syst Rev. 2012(6):CD002052.
46. Swart EL, Slort PR, Plotz FB. Growing up with midazolam in the neonatal and pediatric intensive care. Curr Drug Metab. 2012;13(6):760-6.
47. Bjorkman S. Prediction of drug disposition in infants and children by means of physiologically based pharmacokinetic (PBPK) modelling: theophylline and midazolam as model drugs. Br J Clin Pharmacol. 2005;59(6):691-704.
48. Blumer JL. Clinical pharmacology of midazolam in infants and children. Clin Pharmacokinet. 1998;35(1):37-47.
49. Knibbe CAJ, Krekels EH, Danhof M. Advances in paediatric pharmacokinetics. Expert Opin Drug Metab Toxicol. 2011 Jan;7(1):1-8.
50. Kirwan CJ, MacPhee IA, Lee T, Holt DW, Philips BJ. Acute kidney injury reduces the hepatic metabolism of midazolam in critically ill patients. Intensive Care Med 2012;38:76–84.

# SUPPLEMENTAL MATERIAL (CHAPTER 4)

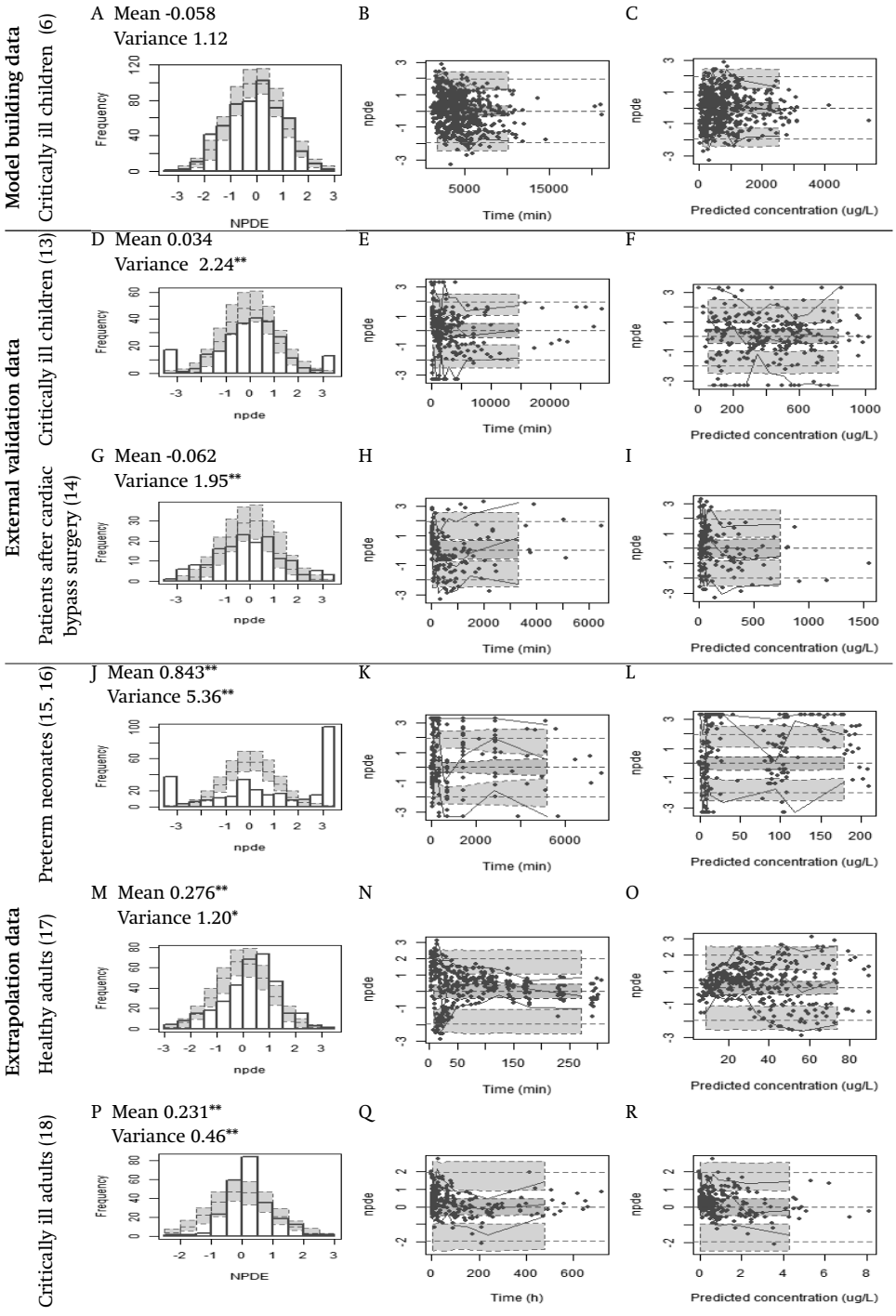


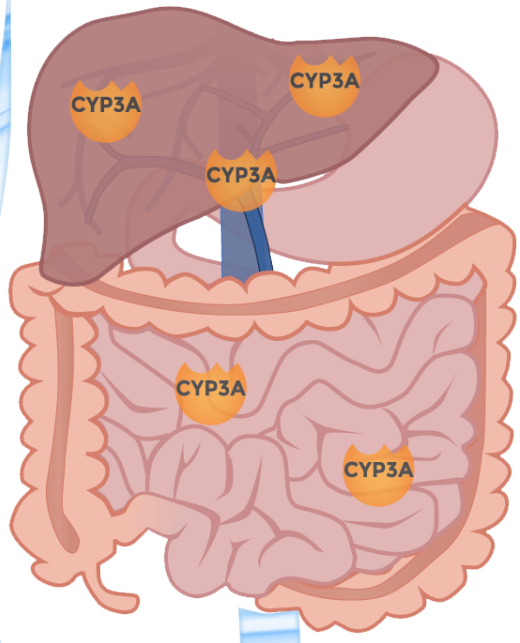
**Figure S1.** NPDE results, stratified per subpopulation. The histograms in the first column show the overall distribution of the normalized prediction distribution error (NPDE), and the second and third column show the NPDE versus time and the population predicted plasma concentrations respectively. Mean and variance are tested for signifcant difference from 0 and 1 respectively (** $p<0.001$, * $p<0.05$).

# REFERENCES


6. Vet NJ, Brussee JM, de Hoog M, Mooij MG, Verlaat CW, Jerchel IS, et al. Inflammation and Organ Failure Severely Affect Midazolam Clearance in Critically Ill Children. Am J Respir Crit Care Med. 2016;194(1):58-66.
13. de Wildt SN, de Hoog M, Vinks AA, van der Giesen E, van den Anker JN. Population pharmacokinetics and metabolism of midazolam in pediatric intensive care patients. Crit Care Med. 2003;31(7):1952-8.
14. Valkenburg AJ, Calvier EA, van Dijk M, Krekels EH, O'Hare BP, Casey WF, et al. Pharmacodynamics and Pharmacokinetics of Morphine After Cardiac Surgery in Children With and Without Down Syndrome. Pediatr Crit Care Med. 2016;17(10):930-8.
15. de Wildt SN, Kearns GL, Hop WC, Murry DJ, Abdel-Rahman SM, van den Anker JN. Pharmacokinetics and metabolism of intravenous midazolam in preterm infants. Clin Pharmacol Ther. 2001;70(6):525-31.
16. Jacqz-Aigrain E, Daoud P, Burtin P, Desplanques L, Beaufils F. Placebo-controlled trial of midazolam sedation in mechanically ventilated newborn babies. Lancet. 1994;344(8923):646-50.
17. van Gerven JM, Roncari G, Schoemaker RC, Massarella J, Keesmaat P, Kooyman H, et al. Integrated pharmacokinetics and pharmacodynamics of Ro 48-8684, a new benzodiazepine, in comparison with midazolam during first administration to healthy male subjects. Br J Clin Pharmacol. 1997;44(5):487-93.
18. Swart EL, Zuideveld KP, de Jongh J, Danhof M, Thijs LG, Strack van Schijndel RM. Comparative population pharmacokinetics of lorazepam and midazolam during long-term continuous infusion in critically ill patients. Br J Clin Pharmacol. 2004;57(2):135-45.

# Section III

## First-pass CYP3A-mediated metabolism in children after oral drug administration



# Chapter 5

## First-pass CYP3A-mediated metabolism of midazolam in the gut wall and liver in preterm neonates

Janneke M Brussee[1], Huixin Yu[1], Elke HJ Krekels[1], Berend de Roos[1], Margreke JE Brill[2], Johannes N van den Anker[3,4,5], Amin Rostami-Hodjegan[6,7], Saskia N de Wildt[3,8], Catherijne AJ Knibbe[1,9]

[1]Division of Systems Biomedicine and Pharmacology, Leiden Academic Centre for Drug Research (LACDR), Leiden University, Leiden, the Netherlands; [2]Department of Pharmaceutical Biosciences, Uppsala University, Uppsala, Sweden; [3]Intensive Care and Department of Pediatric Surgery, Erasmus MC - Sophia Children's Hospital, Rotterdam, the Netherlands; [4]Division of Paediatric Pharmacology and Pharmacometrics, University of Basel Children's Hospital, Basel, Switzerland; [5]Division of Clinical Pharmacology, Children's National Health System, Washington, DC; [6]Centre for Applied Pharmacokinetic Research, University of Manchester, Manchester, UK; [7]Simcyp Limited (A Certara Company), Sheffield, UK; [8]Department of Pharmacology and Toxicology, Radboud University Medical Centre, Nijmegen, the Netherlands; [9]Department of Clinical Pharmacy, St. Antonius Hospital, Nieuwegein, the Netherlands.

*CPT Pharmacometrics Syst Pharmacol. 2018 Jun;7(6):374-383*

## ABSTRACT

To predict first-pass and systemic cytochrome P450 (CYP) 3A-mediated metabolism of midazolam in preterm neonates, a physiological population pharmacokinetic model was developed describing intestinal and hepatic midazolam clearance in preterm infants. On the basis of midazolam and 1-OH-midazolam concentrations from 37 preterm neonates (gestational age 26 - 34 weeks) receiving midazolam orally and/or via a 30 minute intravenous infusion, intrinsic clearance in the gut wall and liver were found to be very low, with lower values in the gut wall (0.0196 and 6.7 L/h, respectively). This results in a highly variable and high total oral bioavailability of 92.1% (range 67-95%) in preterm neonates, while this is around 30% in adults. This approach in which intestinal and hepatic clearance were separately estimated, shows that the high bioavailability in preterm neonates is explained by, likely age-related, low CYP3A activity in the liver and even lower CYP3A activity in the gut wall.



**Keywords**

CYP3A ontogeny, extraction ratio, first-pass, absorption, preterm neonates


### Study highlights

*What is the current knowledge on the topic?*

Cytochrome P450 (CYP) enzymes are present in the gut wall and liver, but a different contribution of the gut and the liver to the first-pass effect may be anticipated in children as compared to adults, due to different rates of maturation of intestinal and hepatic enzymes in infants and children.

*What question did this study address?*

Can first-pass metabolism in the gut wall and liver be predicted for the CYP3A substrate midazolam using a state-of-the-art physiological population PK modelling approach?

*What this study adds to our knowledge?*

A very low first-pass effect by intestinal and hepatic CYP3A-mediated metabolism was found for midazolam in preterm neonates, yielding much higher bioavailability of midazolam in preterm neonates compared to adults. Furthermore, intestinal CYP3A activity, represented by intrinsic clearance in the gut wall, was much lower than hepatic CYP3A activity, represented by the intrinsic clearance in the liver.

*How might this change drug discovery, development, and/or therapeutics?*

Characterization of gut wall and hepatic CYP3A activity enables quantitative predictions of first-pass and systemic metabolism of midazolam and potentially other CYP3A substrates in preterm neonates.

## INTRODUCTION

The neonatal body is undergoing many dynamic changes in the first months of life (1), with preterm neonates showing delayed maturation of many organs as compared to term neonates. This results amongst others in an altered and highly variable capacity to deal with xenobiotics, including drugs (2, 3). Metabolic capacity is an important determinant for the bioavailability and systemic clearance of drugs that are subject to metabolic clearance. Bioavailability, impacted by intestinal and hepatic metabolism, and systemic clearance, impacted by hepatic metabolism, are the two main drivers of drug exposure. Inter-individual differences in these two parameters are therefore two of the main drivers of differences in drug dose requirements between patients.

Physiological parameters that affect drug metabolism include protein binding, blood flow and intrinsic clearance, the latter of which represents metabolic capacity (3, 4). Developmental changes in albumin concentrations (5) and drug protein binding (6), have been reported in neonates, as well as changes in cardiac output (5) which influence the intestinal and hepatic blood flow (7). However, there is limited knowledge on the development of intrinsic clearance of many drugs, especially with respect to the intestinal and hepatic enzyme activity in preterm infants.

Cytochrome P450 (CYP) is an enzyme family involved in drug metabolism and its ontogeny in children has been studied both *in vitro* and *in vivo* (8). The CYP3A subfamily (i.e. CYP3A4, CYP3A5 and CYP3A7) is involved in metabolism of many clinical important drugs with midazolam commonly used as probe drug to reflect combined CYP3A activity (9, 10). Midazolam is a benzodiazepine, often used for sedation in the neonatal intensive care unit (11) and its CYP3A-mediated clearance has been reported to be lower in neonates, infants and children, compared to adults (12). As CYP3A resides in both the gut wall and the liver (13), it is of interest to distinguish between intestinal and hepatic CYP3A activity with respect to their roles in first-pass metabolism, particularly because intestinal and hepatic enzymes may mature at different rates. Beside CYP3A activity in the gut wall and liver, important factors that may affect the absorption and metabolism of drugs in the gut wall are amongst others the intestinal surface area and the permeability of the endothelium (14). Preterm infants have a smaller surface area, and are known to have an underdeveloped intestinal barrier (15), resulting in a higher intestinal permeability in neonates with gestational ages (GA) of less than 34 weeks (16).

To describe and predict pharmacokinetic (PK) profiles and drug exposure in patients, different types of models have been used based on availability of data and their

purpose. These models range from relatively simple, empirical models, to more complex (semi-)physiologically based PK models (17). Empirical models often lack predictive value outside the studied population, while large PBPK models are not always identifiable and may depend on systems parameters that are difficult to determine experimentally in children. Therefore, a hybrid of these models is useful not only to determine PK of a single drug, but also to obtain insight into drug independent systems information when the models are used for several drugs simultaneously (18). In this analysis we used a physiological population PK modelling approach, in which we account for the attributes of the gastrointestinal tract, and use available systems data together with PK information from the preterm population, to describe intestinal and hepatic midazolam clearance and ultimately predict first-pass and systemic metabolism by CYP3A of midazolam in preterm neonates.

# METHODS

## Data

Thirty-seven preterm neonates (gestational ages ranging from 26 to 34 weeks, birth weights 745-2135 grams) of a previously published data set from the neonatal intensive care unit of the Sophia's Children Hospital in Rotterdam were included (19, 20). At the time of the clinical investigation their postnatal ages ranged from 3 to 11 days and their body weights between 770 and 2030 grams. These infants were randomly assigned to receive 0.1 mg/kg midazolam orally via a nasogastric tube (n=13) or intravenously via a 30-minute infusion (n=25). If, after 72 hours, the participating infants still met the inclusion criteria, they received another dose of midazolam but this time via the other route. Midazolam and its primary metabolite 1-OH-midazolam were measured in plasma 0.5, 1, 2, 4, 6, 12 and 24 hours post-dose (19, 20) and measurements below the lower limit of quantification were discarded (<1% and <2% of 329 and 153 midazolam and 1-OH-midazolam measurements, respectively).

## Model development

### *Structural physiological pharmacokinetic model*

Physiological population pharmacokinetic (PK) modelling was performed using first-order conditional estimation with interaction in NONMEM version 7.3 (ICON, Globomax LLC, Ellicott, MD, USA) with Pirana 2.9.0 and R (version 3.3.1) and R-studio (version 0.98.1078) for processing of the runs and visualization of data.

**Table I.** Parameter values for physiological and drug specific parameters in the model

| Parameter definition (unit) | Para-meter | Formula for calculation | Value | References |
|---|---|---|---|---|
| **Tissue volumes (L)** | | | | |
| Liver | $V_h$ | $V_{h,3.55kg\ neonate} \times (WT/3.55)$<br>$V_{h,3.55kg\ neonate} = 0.120$ | | (7) |
| Portal vein | $V_{pv}$ | $V_{pv} = 0.778 \times V_h$ | | (24) |
| Gut | $V_{gw}$ | $V_{gw,3.55kg\ neonate} \times (WT/3.55)$<br>$V_{gw,3.55kg\ neonate} = 0.050$ | | (7) |
| **Tissue blood flows (L/h)** | | | | |
| Hepatic blood flow | $Q_h$ | $Q_{h,3.55kg\ neonate} \times (WT/3.55)^{0.75}$<br>$Q_{h,3.55kg\ neonate} = 13.2$ | | (7) |
| Portal vein | $Q_{pv}$ | $0.75 \times Q_h$ | | (5,48) |
| Hepatic artery | $Q_{ha}$ | $0.25 \times Q_h$ | | (5,48) |
| Small intestine | $Q_{in}$ | $0.4 \times Q_h$ | | (25) |
| Mucosa | $Q_{muc}$ | $0.8 \times Q_{in}$ | | (25) |
| Microvilli | $Q_{villi}$ | $0.6 \times Q_{muc}$ | | (25) |
| **Plasma proteins** | | | | |
| Plasma albumin concentration (g/L) | $[P]_{pediatric}$<br>$[P]_{adult}$ | $1.1287 \times \ln(Age[yr]) + 33.746$ | 27.1<br>37.0 | (5) |
| Hematocrit (%) | Hem | - | 0.45 | (31) |
| **Intestinal surface area and permeability** | | | | |
| Intestinal surface area ($dm^2$) | A | $2\pi \times r \times h$<br>With radius r = 1 cm and length $h=2.736\times(WT[g])^{0.512}$ cm | 5.97 | r: (26)<br>h: (27) |
| Permeability through the enterocyte (L/h)# | $CL_{perm}$ | $CL_{perm} = P_{eff,man}$ [dm/h] × A [$dm^2$] | 0.95 | (25) |
| **Midazolam** | | | | |
| Fraction absorbed | $F_a$ | - | 1 | (10) |
| Absorption rate constant | $K_a$ ($h^{-1}$) | - | 10 | - |
| Blood:plasma ratio | B:P ratio | $1+ [Hem \times (f_{u,m} \times K_p - 1)]$<br>$K_p = 1$ | 0.568 | (30) |
| Fraction unbound in gut | $F_{u,G}$ | - | 1 | (25) |
| Fraction unbound in blood | $F_{u,B}$<br>$F_{u,adult}$ | $\frac{1}{1 + \frac{(1 - f_{u,adult}) \times [P]_{pediatric}}{[P]_{adult} \times f_{u,adult}}}$ | 0.04094<br>0.0303 | (6)<br>(28) |
| Effective intestinal permeability per unit surface area (cm/s) | $P_{eff,man}$ | - | $4.4\times10^{-4}$ | (25) |

**Table I.** Parameter values for physiological and drug specific parameters in the model (*continued*)

| Parameter definition (unit) | Parameter | Formula for calculation | Value | References |
|---|---|---|---|---|
| **1-OH-midazolam** | | | | |
| Fraction midazolam metabolized into 1-OH-midazolam | $f_M$ | - | 1 | - |
| Blood:plasma ratio | B:P ratio | $1+[Hem \times (f_{u,M} \times K_p - 1)]$<br>$K_p = 1$ | 0.613 | (30) |
| Fraction unbound in blood | $F_{u,M}$ | $\frac{1}{1+\frac{(1-f_{u,M,adult}) \times [P]_{pediatric}}{[P]_{adult} \times f_{u,M,adult}}}$ | 0.1394 | (6) |
| | $f_{u,M,adult}$ | | 0.106 | (29) |

A physiological population PK model, earlier described by Yang *et al.*(21), Frechen *et al.* (22) and Brill *et al.* (23), was applied to describe the data (figure 1). For this, using the blood:plasma ratio and the measured molar concentrations in plasma, drug and metabolite molar concentrations in blood were calculated to be able to be used in the well-stirred model. The model describes physiological compartments representing the gut wall, the portal vein and the liver, and an empirical central compartment for midazolam and 1-OH-midazolam, representing the blood circulation and equilibrating tissue (21, 22). For midazolam and 1-OH-midazolam, also the addition of empirical peripheral compartments was evaluated. The fraction of midazolam metabolized into 1-OH-midazolam was assumed to be 1.

Tissue volumes for the physiological compartments in the preterm neonatal population were allometrically scaled from tissue volumes of a term neonate (7) with a fixed exponent of 1 (table I). Volume of the portal vein was assumed to be 77.8% of hepatic volume (24). The hepatic blood flow was assumed to allometrically scale from a term neonate (7) with a fixed exponent of 0.75. Blood flows in the other tissues were assumed to be proportional to the hepatic blood flow (table I).

The well-stirred model was used to quantify the hepatic extraction of midazolam ($E_H$) and 1-OH-midazolam ($E_{H,M}$):

$$E_H = \frac{CL_{int,H} \times f_{u,B}}{Q_h + (CL_{int,H} \times f_{u,B})} \qquad \text{(Eq. 1)}$$

where $CL_{int,H}$ is the estimated intrinsic clearance in the liver based on unbound blood concentrations, $f_{u,B}$ is the fraction unbound drug concentration in blood and $Q_h$ the hepatic blood flow.

For gut wall metabolism into 1-OH-midazolam ($E_G$), the $Q_{gut}$ model was applied (25):

$$E_G = \frac{CL_{int,G} \times f_{u,G}}{Q_{gut} + (CL_{int,G} \times f_{u,G})} \qquad \text{(Eq. 2)}$$

where $CL_{int,G}$ is the estimated intrinsic clearance in the gut wall based on unbound concentrations, $f_{u,G}$ is the fraction unbound drug concentration in the gut wall and $Q_{gut}$ is the local blood flow, which is defined by (25):

$$Q_{gut} = \frac{Q_{villi} \times CL_{perm}}{Q_{villi} + CL_{perm}} \qquad \text{(Eq. 3)}$$

where $Q_{villi}$ is the villous blood flow and $CL_{perm}$ is the permeability of the drug through the enterocytes in the gut wall, which depends on the effective intestinal permeability per unit surface area (25) and the intestinal surface area. The intestinal surface area (A) was calculated based on the net cylindrical surface area of the small intestine using equation 4.

$$A = 2\pi \times r \times h \qquad \text{(Eq. 4)}$$

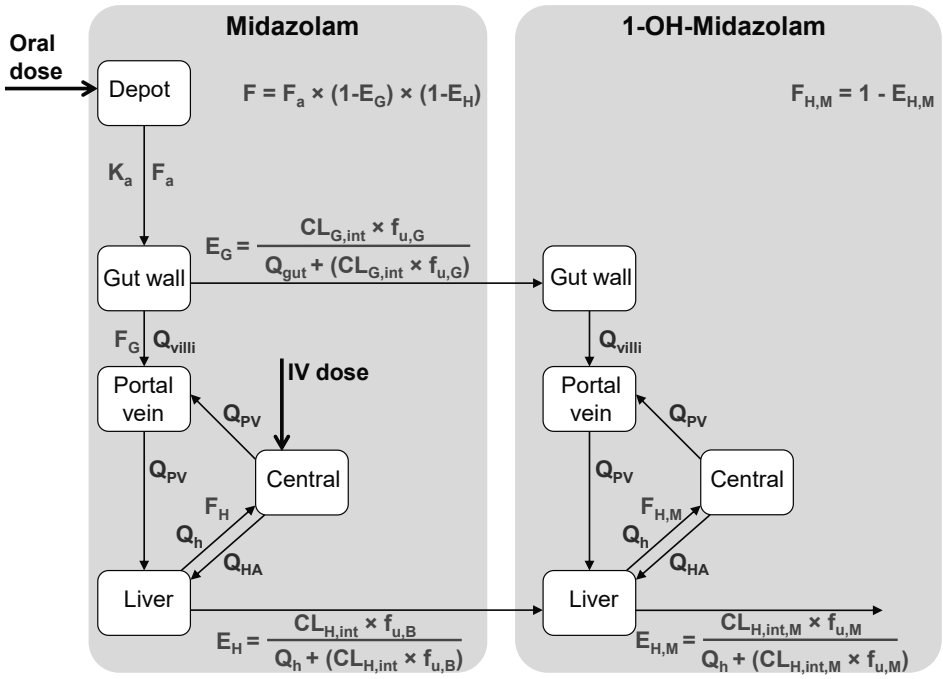



**Figure 1.** Schematic representation of the model for midazolam and the 1-OH-midazolam metabolite. E = extraction ratio, F = bioavailability in the gut wall (gut, G) and the liver (hepatic, H). $CL_{int}$ is the intrinsic clearance in the blood, $K_a$ indicates the absorption rate constant and the fraction unbound in blood and gut wall are described with $f_{u,B}$ and $f_{u,G}$, respectively. Blood flows are represented by Q; in the micro villi ($Q_{villi}$), portal vein ($Q_{PV}$), hepatic artery ($Q_{HA}$) and the hepatic blood flow (Qh). Parameters relating to the metabolite are indicated with subscript M. Intrinsic gut wall ($CL_{G,int}$) and intrinsic hepatic clearance($CL_{H,int}$ and $CL_{H,int,M}$), as well as volume of distribution (for midazolam and 1-OH-midazolam), values were estimated in the model. Total plasma clearance of midazolam was derived using equation 8, and the bioavailability in the gut wall ($F_g$), liver ($F_h$) and the total oral bioavailability ($F_{total}$) were derived based on equations 1, 2 and 5.

in which r is the intestinal radius of 1 cm (26) and h the intestinal length of 2.736 × (WT[g])$^{0..512}$ cm (27). The fraction unbound in the gut ($f_{u,G}$) for both midazolam and 1-OH-midazolam was assumed 1 (25). The absorption rate constant could not be estimated and was assumed to be 10 $h^{-1}$, which entails an expected maximum concentration around 12.5 minutes ($t_{max}$). A sensitivity analysis was performed with values for $k_a$ ranging from 4.16 – 25 $h^{-1}$, resulting in a $t_{max}$ between 5-30 minutes post-dose. The oral bioavailability was calculated with equation 5:

$$F_{total} = F_a \times F_g \times F_h \qquad \text{(Eq. 5)}$$

where $F_a$ is the fraction absorbed, which is assumed 1 for midazolam (10), $F_g$ is the gut wall bioavailability, equal to 1 minus $E_g$, and $F_h$ is the hepatic bioavailability and $F_h = 1 - E_h$.

The fraction unbound in blood for both midazolam and 1-OH-midazolam in blood was calculated based on the formula of McNamara and Alcorn (6):

$$f_{u,B,pediatric} = \frac{1}{1+\frac{(1-f_{u,B,adult}) \times [P]_{pediatric}}{[P]_{adult} \times f_{u,B,adult}}} \qquad \text{(Eq. 6)}$$

where $f_{u,pediatric}$ and $f_{u,adult}$ are the fraction unbound of the drug in blood for preterm neonates and adults, respectively and $[P]_{pediatric}$ and $[P]_{adult}$ are the plasma albumin concentrations in preterm neonates and adults, respectively. These albumin concentrations are calculated based on an age-based formula from Johnson *et al.* (5) (table I) and the fractions unbound of midazolam and 1-OH-midazolam in adults were reported in literature (28, 29). The fraction unbound in blood and hematocrit were used to calculate the blood:plasma ratios for midazolam and 1-OH-midazolam using the formula of Maharaj *et al.* (30):

$$B{:}P \text{ ratio} = 1 + [Hem \times (f_{u,B} \times K_p - 1)] \qquad \text{(Eq. 7)}$$

where B:P ratio is the blood:plasma ratio, Hem is the hematocrit in preterm neonates (45%) (31), $f_{u,B}$ is the fraction unbound in the blood and $K_p$ is the unbound partition coefficient of red blood cells (assumed to be constant between adults and children) (30).

Total plasma clearance by the liver was calculated based on (32):

$$CL_{plasma} = \frac{Q_h \times f_u \times CL_{h,int}}{Qh + (f_u \times CL_{h,int}/(B{:}P\ ratio))} \qquad \text{(Eq. 8)}$$

in which $Q_h$ is the hepatic blood flow, $f_u$ the fraction unbound in plasma and $CL_{h,int}$ the intrinsic hepatic clearance.

To evaluate the structural identifiability or our nonlinear model, we used the DAISY (Differential Algebra for Identifiability of Systems) software (33).

### *Statistical model*

Inter-individual variability was included in the model as a log-normal distribution:

$$\theta_i = \theta_{TV} \times e^{\eta_i} \quad \text{(Eq. 9)}$$

where $\theta_i$ is individual parameter estimate for individual *i*, $\theta_{TV}$ the typical value of the parameter in the studied population and $\eta_i$ is a random variable from a normal distribution with a mean of zero and estimated variance of $\omega^2$.

Residual unexplained variability was modelled using a combined error model. The *j*th observed concentration (Y) of the *i*th individual was modelled according to:

$$Y_{ij} = C_{pred,ij} \times (1+\varepsilon 1_{ij}) + \varepsilon 2_{ij} \quad \text{(Eq. 10)}$$

where $C_{pred,ij}$ is the *j*th predicted midazolam concentration of the *i*th individual, $\varepsilon 1_{ij}$ and $\varepsilon 2_{ij}$ are random variables from normal distributions with a mean of zero and estimated variance of $\sigma^2$, representing the proportional and additive component of the error model, respectively.

### *Covariate analysis*

A covariate analysis on the clearance and volume parameters was performed in which the following covariates were tested for statistical significance: body weight at birth, gestational age (GA), gender and mechanical respiratory support, and furthermore body weight, postmenstrual age (PMA) and postnatal age (PNA) per occasion (e.g. at the day of dose administration). There was no missing covariate information for any subject.

For categorical covariates, separate typical values ($\theta_{TV}$) for the two populations were estimated. Continuous covariates were tested using a linear (Eq. 11) or power (Eq. 12) function.

$$\theta_i = \theta_{TV} \times (1 + \theta_{cov} \times (COV - COV_{med}) \quad \text{(Eq. 11)}$$

$$\theta_i = \theta_{TV} \times \left(\frac{COV}{COVmed}\right)^{\theta cov} \quad \text{(Eq. 12)}$$

where $\theta_i$ is individual parameter estimate for individual *i*, $\theta_{TV}$ the typical value of the parameter in the studied population with a median value ($COV_{med}$) of the covariate (COV) and $\theta_{COV}$ the estimated slope or exponent for a linear or power function, respectively.

## Model evaluation

Discrimination between different structural models was made by comparison of the objective function value (OFV, i.e. -2 × log-likelihood). A decrease of 3.84 points in the OFV between nested models was considered statistically significant ($p<0.05$). Furthermore, goodness-of-fit plots (individual- and population-predicted versus

observed concentrations and conditional weighted residuals [CWRES] versus time and population predicted concentrations) of midazolam and 1-OH-midazolam were assessed. In addition, the confidence interval of the parameter estimates, and visual improvement of the individual plots were used to evaluate the models.

For inclusion of covariates, a decrease in OFV of 6.64 points ($p<0.01$) was considered statistically significant, while for the backward deletion a more stringent p value ($p<0.005$, $\Delta OFV>7.88$) was used. Furthermore, to retain a covariate in the model, the inter-individual variability (IIV) in the PK parameter should decrease and in a plot of the covariate versus the IIV in the PK parameter, the data points should be randomly scattered around zero.

The model was further internally evaluated using two different methods, a bootstrap analysis (n=200) and a normalized prediction error (NPDE) analysis (see Supplemental material).

### Sensitivity analysis

To evaluate the assumptions made in the model, a sensitivity analysis was performed using simulations in Berkeley Madonna (Berkeley Madonna Inc, version 8.3.18)(34). Parameter values for tissue volumes and blood flows as well as intestinal length and the fraction unbound in blood were increased and decreased by 50% and the impact on predicted midazolam concentrations was evaluated. Furthermore, the impact of the assumptions on the estimated PK parameters was assessed by re-estimating the model with the increased/decreased values for tissue volumes and blood flows as well as intestinal length and the fraction unbound in blood.

### Dose simulations

To illustrate the impact of first-pass metabolism on midazolam and 1-OH-midazolam exposure in preterm neonates, model-based simulations of concentration-time profiles were performed with our model. A dose of 0.1 mg/kg midazolam was simulated as oral administration or as a 30-minute intravenous infusion in 37 preterm neonates with the same patient characteristics as the individuals in our dataset.

## RESULTS

Using the physiological population PK model as depicted in figure 1, which was structurally identifiable according to the DAISY analysis (33), the pharmacokinetic data in preterm neonates were well described. Based on the available data, intrinsic CYP3A clearance in the gut wall and liver were estimated to be 0.0196 (relative

standard error (RSE) 178%) and 6.7 (RSE 10%) L/h, respectively (table II). Distribution volumes for midazolam and its metabolite in blood were estimated to be 3 (RSE 11%) and 2.7 (RSE 43%) L, respectively, and the addition of peripheral compartments for either midazolam or 1-OH-midazolam did not improve the model. No additional covariates could be identified for intrinsic clearance and volume of distribution. The model was graphically and numerically evaluated (table II, figure S1, S2) and generally the model parameters described the PK data of both the midazolam and 1-OH-midazolam well. The additive errors were fixed to very small numbers (table II). Goodness-of-fit plots (figure S1) showed that the model adequately describes the data, albeit with a small over-prediction for the low concentrations of midazolam. Also the prediction of the data was unbiased as shown in the NPDE analysis (figure S2), with slightly over-predicted variability in the metabolite concentrations.

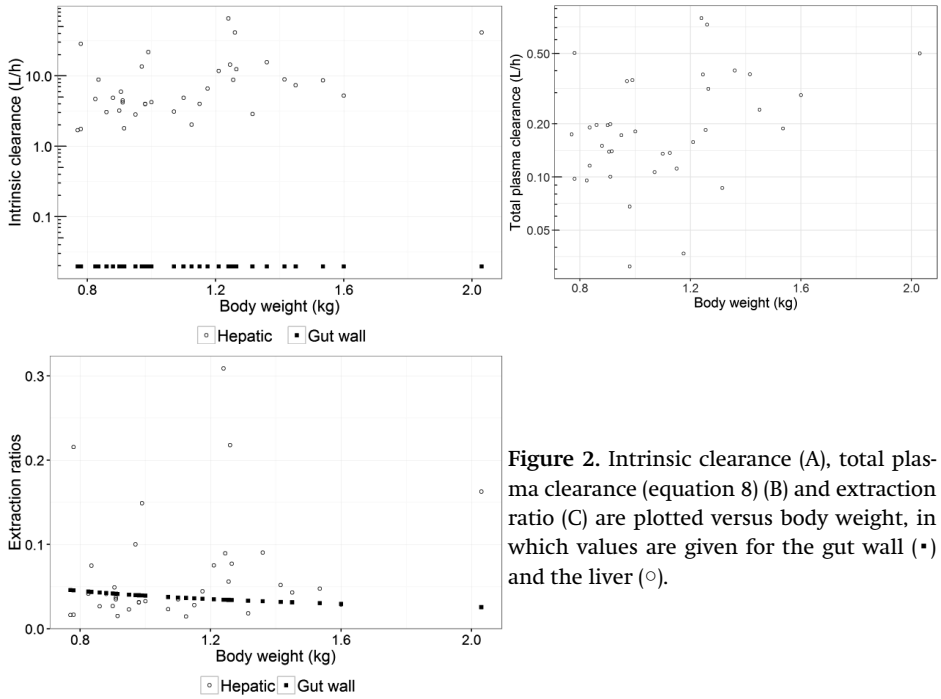



**Figure 2.** Intrinsic clearance (A), total plasma clearance (equation 8) (B) and extraction ratio (C) are plotted versus body weight, in which values are given for the gut wall (▪) and the liver (○).

Intrinsic hepatic clearance was much higher and also more variable than the intrinsic gut wall clearance (fig 2a). Figures 2 and 3 show the estimated and derived model parameters related to the intestinal and hepatic metabolism in preterm neonates versus bodyweight. The median total plasma clearance by the liver was 0.181 L/h (range 0.03-0.79 L/h)(fig. 2b). As both the intrinsic gut wall and hepatic clearance were found to be very low (fig. 2a), the extraction ratios were very low for both organs, with a median of 0.04 in the gut wall (range 0.026-0.046) and a similar

**Table II.** Parameter estimates and bootstrap results of the physiological population PK model

| Parameter definition | Parameter | Value (RSE%) [shrinkage %] | Bootstrap median* | Bootstrap 90% CI |
|---|---|---|---|---|
| **Midazolam** | | | | |
| Intrinsic hepatic clearance | $CL_{H,int}$ (L/h) | 6.7 (10%) | 6.6 | 5.0-8.7 |
| Intrinsic gut wall clearance | $CL_{G,int}$ (mL/h) | 19.6 (178%) | 14.0 | 0.2#-319 |
| Volume of distribution | V (L) | 3.0 (11%) | 3.0 | 2.4-3.7 |
| **1-OH-midazolam** | | | | |
| Intrinsic hepatic clearance | $CL_{H,int,M}$ (L/h) | 8.9 (22%) | 7.7 | 3.5-11.2 |
| Volume of distribution | $V_M$ (L) | 2.7 (43%) | 2.9 | 1.5-7.2 |
| **Inter individual variability ($\omega^2$)** | | | | |
| Intrinsic hepatic clearance | $\omega^2$ $CL_{H,int}$ | 0.887 (26%) [3%] | 0.851 | 0.551-1.16 |
| Intrinsic gut wall clearance | $\omega^2$ $CL_{G,int}$ | - | - | - |
| Volume of distribution | $\omega^2$ V | 0.603 (26%) [2%] | 0.603 | 0.311-0.857 |
| Intrinsic hepatic clearance 1-OH-midazolam | $\omega^2$ $CL_{H,int,M}$ | 0.832 (42%) [15%] | 0.709 | 0.201-1.65 |
| Volume of distribution 1-OH-midazolam | $\omega^2$ $V_M$ | 0.887 (48%) [8%] | 1.2 | 0.442-4.04 |
| **Residual variability ($\sigma^2$)** | | | | |
| Proportional error (Midazolam) | | 0.201 (26%) [10%] | 0.192 | 0.134-0.264 |
| Additional error (Midazolam) | | 0.0001 FIX | 0.0001 | - |
| Proportional error (1-OH-midazolam) | | 0.164 (91%) [33%] | 0.155 | 0.000#-0.242 |
| Additional error (1-OH-midazolam) | | 0.0001 FIX | 0.0001 | - |

RSE: relative standard error. CI: confidence interval. *Bootstrap results based on stratified bootstrap sampling for patients receiving an intravenous, an oral, or twice a dose administration. The median and 90% confidence interval are calculated based on 37.8% successful runs and runs with estimates near a boundary. #The 5% percentile reached the lower boundary of 0.2 mL/h and $0.1*10^{-4}$, for $CL_{G,int}$ and the proportional error for 1-OH-midazolam, respectively. Inter-individual and residual variability values are shown as variance estimates.

median of 0.04 (range 0.01-0.31) in the liver (fig. 2c). Based on the extraction ratio in the gut wall and liver, the fraction escaping gut wall metabolism ($F_g$) and the fraction escaping hepatic metabolism ($F_h$) can be calculated and the median values are both 0.96. Figure 3 also shows the total bioavailability for all preterm neonates in our study, as calculated based on the fraction absorbed ($F_a$), $F_g$ and $F_h$ according to Eq. 5. A very low first-pass metabolism was observed with 92% of midazolam entering the systemic circulation in a typical preterm neonate of 1.1 kg, but the overall range of percentage entering systemic circulation varies largely between 67 and 95%. Model-based simulations of plasma concentration-profiles show limited differences in median plasma concentrations of midazolam after oral and intravenous administration due to the high bioavailability of 92% (figure 4a), while

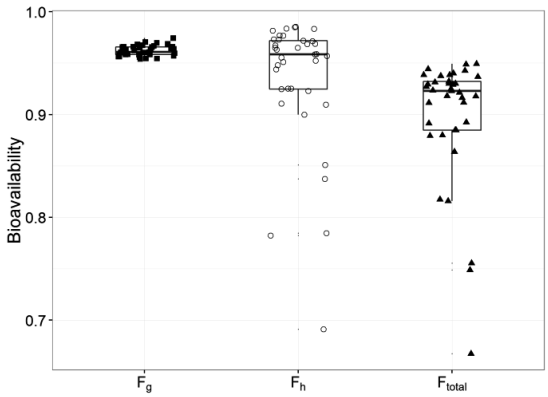



**Figure 3.** Bioavailability in the gut ($F_g$) and liver ($F_h$), and total bioavailability ($F_{total}$) in preterm neonates

the concentrations of 1-OH-midazolam after oral administration are higher for the first 4 hours post-dose compared to the 30-minute infusion, due to presystemic metabolism (figure 4b).

A sensitivity analysis showed that blood concentration predictions would change <1% for both peak and trough concentrations in case the values for tissue volumes and tissue blood flows were altered with ± 50%. Also, no significant change in parameter estimates was found when the parameters were re-estimated based on the same changes in tissue volumes, nor did different $k_a$ values impact estimated and derived clearance and bioavailability parameters. However, an increase of 50% in intestinal and hepatic blood flow resulted in an increase of 20-30% and 50% in the estimated intrinsic intestinal or hepatic clearance, respectively, and vice versa without profound changes in extraction ratio and bioavailability. Changes in intestinal length (which contributes to the flow term in the gut wall ($Q_{gut}$), that accounts for the permeability through the enterocyte ($CL_{perm}$) and the villous blood flow ($Q_{vi}$)) did not result in different blood concentrations (change <1%), although the re-estimated intrinsic clearance in the gut wall changed +18 or -32% for an increase or decrease in intestinal length, respectively. The change in fraction unbound in blood for either midazolam or 1-OH-midazolam was inversely correlated with the same fractional change in estimated hepatic intrinsic clearance.

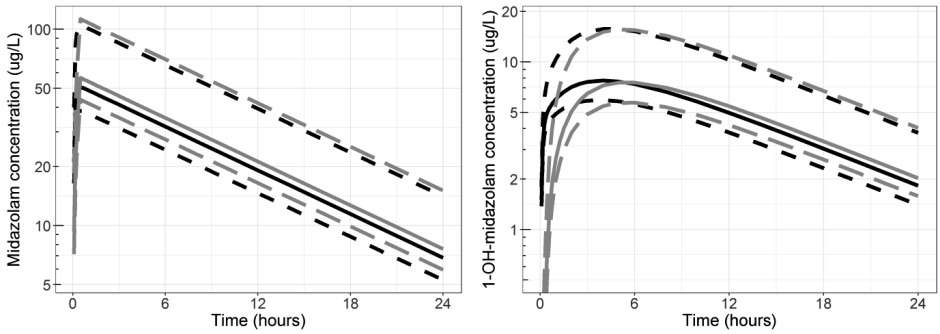



**Figure 4.** Model-based simulations of midazolam (A) and 1-OH-midazolam (B) PK profiles following a 0.1 mg/kg dose via an 30-minute infusion (grey lines) or orally (black lines). The solid lines represent the median plasma concentrations and the dashed lines show the minimal and maximal achieved concentrations of midazolam in the studied population.

## DISCUSSION

Using a physiological population PK model in which both physiological information and midazolam and metabolite concentrations after oral and intravenous administration were used, we were able to distinguish between intestinal and hepatic intrinsic clearance of midazolam in preterm neonates. The PK data used to estimate the CYP3A-mediated midazolam clearance came from a unique dataset with a cross-over design in which preterm neonates received both an oral and an intravenous dose, allowing to study both the first-pass and systemic metabolism. Our physiological population PK modelling approach, which has already been applied in healthy adults (22), was also able to describe the absorption and disposition of midazolam in preterm neonates. The results show that the CYP3A-mediated intrinsic gut clearance is much lower than the intrinsic hepatic clearance (table II, fig. 2a), while in healthy adult volunteers this difference is reported to be smaller (ratio of approximately 340 in preterm neonates versus 60 in adults) (22). While this indicates a difference in maturation of CYP3A activity in the gut wall and the liver in preterm neonates, both the intestinal and hepatic extraction ratio of midazolam in preterm neonates were very low (median of 0.04 each). This results in a very small first-pass effect leading to a high total bioavailability of 92.1% (fig. 3) and almost identical concentration-time profiles after intravenous and oral administration (fig. 4a) for the CYP3A-substrate midazolam in preterm neonates. For the metabolite however, an increased plasma concentration can be observed the first 4 hours after oral administration due to the presystemic formation of the metabolite in both the gut wall and liver (fig. 4b). In adults, much higher median extraction ratios of

0.59 and 0.34 have been reported for the gut wall and the liver, respectively (22), resulting in a lower total bioavailability of around 30% in adults.

The intrinsic gut wall clearance values we obtained in preterm neonates were found to be lower than the values reported in adults. Additionally, in preterm neonates the intrinsic gut wall clearance was much lower than the intrinsic hepatic clearance, and this difference was much larger in preterm neonates than in adults (22). This could be due to the immaturity of enterocytic CYP3A enzyme activity in this population (35,36). The activity in the gut wall has been reported to be lower with decreasing age (36), but also conflicting activity values have been reported (35). Besides the activity, the abundance of the CYP3A enzyme, reflected by a smaller number of milligrams of microsomal protein per gram of intestine (36), as well as the smaller intestinal surface area lead to a lower total intestinal CYP3A activity in preterm neonates compared to adults. The smaller surface area was calculated in our study based on intestinal length (70-157 cm for infants with a postconceptional age of 24-40 weeks without gastrointestinal malformations undergoing laparotomy (27), which is in agreement with other literature (37,38) and on the mean intestinal radius of 1 cm (26). A sensitivity analysis showed that with a decreased intestinal length, both the flow term that accounts for villous blood flow and permeability ($Q_{gut}$) and the gut wall clearance ($CL_{G,int}$) decreased, resulting in the same reported extraction ratio of 0.04. Furthermore, preterm infants have an underdeveloped intestinal barrier (15), and neonates with a GA < 34 weeks have a higher intestinal permeability (16), which could be due to differences in the intracellular structures that regulate the intestinal permeability (39). In our model, the permeability factor $CL_{perm}$ (25) accounts for the intestinal surface area and the permeability of the intestinal barrier in preterm neonates. Food in the GI tract may alter the GI physiology, including the motility patterns, intestinal transit time and the local blood flow (40), but was not accounted for in our model as the exact times of parenteral and enteral feeding were not recorded during the study.

The intrinsic hepatic clearance obtained in our study in preterm neonates was very low compared to reported values in healthy adults (6.7 L/h and 1620 L/h in preterm neonates and adults, respectively) (22). The neonatal liver is relatively immature shortly after birth and its functional capacity in bile synthesis, detoxification and metabolism increases during the early postnatal period (41). Fetal and neonatal livers have different bile acid synthetic pathways than adult livers, and the bile acid pool is reduced (41), limiting the probability of biliary excretion and enterohepatic recirculation of drugs in preterm neonates. The maturation of liver function is not a linear process, as the drug metabolizing enzyme expression changes non-linearly

during development (3). In the fetal liver, 30-60% of adult values in cytochrome P450 content is found and the total hepatic CYP content increases after birth (42). Of these CYP enzymes, the CYP3A family is the most abundant (8, 13, 43). The CYP3A isoforms show a different ontogeny profile, with CYP3A4 activity increasing in preterm neonates with increasing age, CYP3A5 activity appears to be stable from neonatal life to adulthood, while simultaneously CYP3A7 activity declines in neonates (43). Within the group of preterm neonates included in this study (19, 20), we could not identify a trend in hepatic intrinsic clearance with gestational age or postnatal age, which can be explained by the small age range of the studied population. Due to the lower intrinsic hepatic clearance, the hepatic extraction ratio is very low in preterm neonates compared to adults, resulting in a much higher hepatic bioavailability than expected based on adult values. This has been previously reported by Salem *et al.* who found that the hepatic extraction ratio of midazolam increased with age (44). They found that the ontogeny of hepatic enzyme abundance and to a lesser extent the smaller number of microsomal protein per gram of liver (44) contributed to the observed differences between preterm neonates and adults. Based on the hepatic intrinsic clearance, the hepatic blood flow, the fraction unbound in blood and the blood: plasma ratio, the total plasma clearance can be calculated (eq.8). The plasma clearance ranged from 0.03-0.79 L/h with a median value of 0.181 L/h (figure 2b). This is in agreement with other reported values of 3.9 mL/min (0.23 L/h) for preterm neonates with a mean gestational age (GA) of 32.1 ± 2.8 weeks (12) and higher than the reported values of 0.783 mL/min (0.05 L/h) and 0.104 L/h in very premature neonates with a mean GA of 27 (24-31) and 27.9 (25-30) weeks, respectively (45, 46).

The RSE percentage for the estimated intrinsic gut wall clearance value and high range of the 90% bootstrap CI of this parameter together with a high number of unsuccessful runs in the bootstrap and a high condition number suggest over-parameterization of the model. In a population modeling approach, this could warrant a re-evaluation of the structural model, however our structural model and a subset of parameter values are based on physiological knowledge and PBPK principles and only the values of the remaining subset of parameters were estimated from concentration-time data using population modeling principles. The high RSE% and 90% bootstrap CI can therefore be interpreted to mean that the data does not support a very precise estimate of intrinsic gut wall clearance.

For the structural model a few assumptions were included, that were evaluated in a sensitivity analysis. Plasma albumin concentrations were calculated based on a reported age-based formula by Johnson *et al.* (5) in term neonates, assuming the preterm neonates to have the same concentrations as a 1-day-old term neonate. In

addition, only plasma albumin concentrations were taken into account. Free fatty acids (FFA) concentrations are known to reduce protein binding of diazepam in neonates (47), and could result in a higher fraction unbound in blood for midazolam as well, but this was not taken into account, nor were other factors that could impact protein binding of midazolam. Our findings about the low gut wall and hepatic extraction leading to a small the first-pass effect and high bioavailability in preterm neonates are however not influenced by these assumptions. Even though the fraction unbound and the intrinsic hepatic clearance are related, a different fraction unbound would increase the intrinsic clearance proportionally, yielding no net changes in extraction ratio or bioavailability. Furthermore, tissue volumes and organ blood flows are not directly measurable in preterm neonates. Therefore, allometric scaling was applied to scale the organ blood flows from data in term neonates (7) to preterm neonates. The sensitivity analysis showed that changes in assumed organ blood flow are correlated with the estimated organ clearances: with an increased intestinal blood flow, the intrinsic intestinal clearance was estimated higher and the assumptions of the hepatic blood flow were found to correlate with the estimated intrinsic hepatic clearance. However, here also the extraction ratios and bioavailability derived from the estimated parameter values remained unaffected by changes in organ blood flows and would therefore not have an impact on our finding that the first-pass midazolam in preterm neonates is much smaller than in adults.

To conclude, the developed physiological population PK model was able to distinguish between CYP3A-mediated intestinal and hepatic metabolism of midazolam in preterm neonates. Intrinsic clearance in the gut wall was much lower than in the liver, but the median intestinal and hepatic bioavailability values were both very high. This indicates a very low first-pass effect by intestinal and hepatic CYP3A-mediated metabolism in preterm neonates compared to adults. Furthermore, the variability in bioavailability was very high, indicating that oral dosing may yield large differences in drug exposure within this population. Overall, the PK of midazolam and its primary metabolite 1-OH-midazolam were well-described by the model, and this physiological model may therefore be used to predict the first-pass effect and systemic metabolism of midazolam and other orally administered CYP3A substrates in preterm neonates based on the physiological and drug properties.

## ACKNOWLEDGEMENTS

CAJ Knibbe was supported by an NWO Vidi grant (Knibbe 2013).

## REFERENCES


1. Kearns GL. Impact of developmental pharmacology on pediatric study design: overcoming the challenges. J Allergy Clin Immunol. 2000;106(3 Suppl):S128-38.
2. O'Hara K, Wright IM, Schneider JJ, Jones AL, Martin JH. Pharmacokinetics in neonatal prescribing: evidence base, paradigms and the future. Br J Clin Pharmacol. 2015;80(6):1281-8.
3. Allegaert K, van den Anker JN, Naulaers G, de Hoon J. Determinants of drug metabolism in early neonatal life. Curr Clin Pharmacol. 2007;2(1):23-9.
4. Johnson PJ. Neonatal pharmacology--pharmacokinetics. Neonatal Netw. 2011;30(1):54-61.
5. Johnson TN, Rostami-Hodjegan A, Tucker GT. Prediction of the clearance of eleven drugs and associated variability in neonates, infants and children. Clin Pharmacokinet. 2006;45(9):931-56.
6. McNamara PJ, Alcorn J. Protein binding predictions in infants. AAPS PharmSci. 2002;4(1):E4.
7. Bjorkman S. Prediction of drug disposition in infants and children by means of physiologically based pharmacokinetic (PBPK) modelling: theophylline and midazolam as model drugs. Br J Clin Pharmacol. 2005;59(6):691-704.
8. de Wildt SN, Kearns GL, Leeder JS, van den Anker JN. Cytochrome P450 3A: ontogeny and drug disposition. Clin Pharmacokinet. 1999;37(6):485-505.
9. Thummel KE, Shen DD, Podoll TD, Kunze KL, Trager WF, Hartwell PS, et al. Use of midazolam as a human cytochrome P450 3A probe: I. In vitro-in vivo correlations in liver transplant patients. J Pharmacol Exp Ther. 1994;271(1):549-56.
10. Gorski JC, Hall SD, Jones DR, VandenBranden M, Wrighton SA. Regioselective biotransformation of midazolam by members of the human cytochrome P450 3A (CYP3A) subfamily. Biochem Pharmacol. 1994;47(9):1643-53.
11. Hall RW, Shbarou RM. Drugs of choice for sedation and analgesia in the neonatal ICU. Clin Perinatol. 2009;36(1):15-26.
12. Jacqz-Aigrain E, Daoud P, Burtin P, Maherzi S, Beaufils F. Pharmacokinetics of midazolam during continuous infusion in critically ill neonates. Eur J Clin Pharmacol. 1992;42(3):329-32.
13. Ince I, Knibbe CA, Danhof M, de Wildt SN. Developmental changes in the expression and function of cytochrome P450 3A isoforms: evidence from in vitro and in vivo investigations. Clin Pharmacokinet. 2013;52(5):333-45.
14. Debotton N, Dahan A. A mechanistic approach to understanding oral drug absorption in pediatrics: an overview of fundamentals. Drug Discov Today. 2014;19(9):1322-36.
15. Anderson RC DJ, Gopal PK, Bassett S, Ellis A, Roy NC The Role of Intestinal Barrier Function in Early Life in the Development of Colitis, Colitis, Dr Fukata (Ed.). 2012.
16. Weaver LT, Laker MF, Nelson R. Intestinal permeability in the newborn. Arch Dis Child. 1984;59(3):236-41.
17. Tsamandouras N, Rostami-Hodjegan A, Aarons L. Combining the 'bottom up' and 'top down' approaches in pharmacokinetic modelling: fitting PBPK models to observed clinical data. Br J Clin Pharmacol. 2015;79(1):48-55.
18. Rostami-Hodjegan A. Reverse Translation in PBPK and QSP: Going Backwards in Order to Go Forward With Confidence. Clin Pharmacol Ther. 2017.

19. de Wildt SN, Kearns GL, Hop WC, Murry DJ, Abdel-Rahman SM, van den Anker JN. Pharmacokinetics and metabolism of intravenous midazolam in preterm infants. Clin Pharmacol Ther. 2001;70(6):525-31.
20. de Wildt SN, Kearns GL, Hop WC, Murry DJ, Abdel-Rahman SM, van den Anker JN. Pharmacokinetics and metabolism of oral midazolam in preterm infants. Br J Clin Pharmacol. 2002;53(4):390-2.
21. Yang J, Kjellsson M, Rostami-Hodjegan A, Tucker GT. The effects of dose staggering on metabolic drug-drug interactions. Eur J Pharm Sci. 2003;20(2):223-32.
22. Frechen S, Junge L, Saari TI, Suleiman AA, Rokitta D, Neuvonen PJ, et al. A semiphysiological population pharmacokinetic model for dynamic inhibition of liver and gut wall cytochrome P450 3A by voriconazole. Clin Pharmacokinet. 2013;52(9):763-81.
23. Brill MJ, Valitalo PA, Darwich AS, van Ramshorst B, van Dongen HP, Rostami-Hodjegan A, et al. Semiphysiologically based pharmacokinetic model for midazolam and CYP3A mediated metabolite 1-OH-midazolam in morbidly obese and weight loss surgery patients. CPT Pharmacometrics Syst Pharmacol. 2016;5(1):20-30.
24. Aguirre-Reyes DF, Sotelo JA, Arab JP, Arrese M, Tejos R, Irarrazaval P, et al. Intrahepatic portal vein blood volume estimated by non-contrast magnetic resonance imaging for the assessment of portal hypertension. Magn Reson Imaging. 2015;33(8):970-7.
25. Yang J, Jamei M, Yeo KR, Tucker GT, Rostami-Hodjegan A. Prediction of intestinal first-pass drug metabolism. Curr Drug Metab. 2007;8(7):676-84.
26. Ives GC, Demehri FR, Sanchez R, Barrett M, Gadepalli S, Teitelbaum DH. Small Bowel Diameter in Short Bowel Syndrome as a Predictive Factor for Achieving Enteral Autonomy. J Pediatr. 2016;178:275-7 e1.
27. Struijs MC, Diamond IR, de Silva N, Wales PW. Establishing norms for intestinal length in children. J Pediatr Surg. 2009;44(5):933-8.
28. Ito K, Ogihara K, Kanamitsu S, Itoh T. Prediction of the in vivo interaction between midazolam and macrolides based on in vitro studies using human liver microsomes. Drug Metab Dispos. 2003;31(7):945-54.
29. Mandema JW, Tuk B, van Steveninck AL, Breimer DD, Cohen AF, Danhof M. Pharmacokinetic-pharmacodynamic modeling of the central nervous system effects of midazolam and its main metabolite alpha-hydroxymidazolam in healthy volunteers. Clin Pharmacol Ther. 1992;51(6):715-28.
30. Maharaj AR, Barrett JS, Edginton AN. A workflow example of PBPK modeling to support pediatric research and development: case study with lorazepam. AAPS J. 2013;15(2):455-64.
31. Irwin JJ, Kirchner JT. Anemia in children. Am Fam Physician. 2001;64(8):1379-86.
32. Yang J, Jamei M, Yeo KR, Rostami-Hodjegan A, Tucker GT. Misuse of the well-stirred model of hepatic drug clearance. Drug Metab Dispos. 2007;35(3):501-2.
33. Bellu G, Saccomani MP, Audoly S, D'Angio L. DAISY: a new software tool to test global identifiability of biological and physiological systems. Comput Methods Programs Biomed. 2007;88(1):52-61.
34. Krause A, Lowe PJ. Visualization and communication of pharmacometric models with berkeley madonna. CPT Pharmacometrics Syst Pharmacol. 2014;3:e116.

35. Fakhoury M, Litalien C, Medard Y, Cave H, Ezzahir N, Peuchmaur M, et al. Localization and mRNA expression of CYP3A and P-glycoprotein in human duodenum as a function of age. Drug Metab Dispos. 2005;33(11):1603-7.
36. Johnson TN, Tanner MS, Taylor CJ, Tucker GT. Enterocytic CYP3A4 in a paediatric population: developmental changes and the effect of coeliac disease and cystic fibrosis. Br J Clin Pharmacol. 2001;51(5):451-60.
37. Archie JG, Collins JS, Lebel RR. Quantitative standards for fetal and neonatal autopsy. Am J Clin Pathol. 2006;126(2):256-65.
38. Touloukian RJ, Smith GJ. Normal intestinal length in preterm infants. J Pediatr Surg. 1983;18(6):720-3.
39. Halpern MD, Denning PW. The role of intestinal epithelial barrier function in the development of NEC. Tissue Barriers. 2015;3(1-2):e1000707.
40. Abuhelwa AY, Williams DB, Upton RN, Foster DJ. Food, gastrointestinal pH, and models of oral drug absorption. Eur J Pharm Biopharm. 2017;112:234-48.
41. Grijalva J, Vakili K. Neonatal liver physiology. Semin Pediatr Surg. 2013;22(4):185-9.
42. Hines RN, McCarver DG. The ontogeny of human drug-metabolizing enzymes: phase I oxidative enzymes. J Pharmacol Exp Ther. 2002;300(2):355-60.
43. de Wildt SN. Profound changes in drug metabolism enzymes and possible effects on drug therapy in neonates and children. Expert Opin Drug Metab Toxicol. 2011;7(8):935-48.
44. Salem F, Abduljalil K, Kamiyama Y, Rostami-Hodjegan A. Considering Age Variation When Coining Drugs as High versus Low Hepatic Extraction Ratio. Drug Metab Dispos. 2016;44(7):1099-102.
45. Lee TC, Charles BG, Harte GJ, Gray PH, Steer PA, Flenady VJ. Population pharmacokinetic modeling in very premature infants receiving midazolam during mechanical ventilation: midazolam neonatal pharmacokinetics. Anesthesiology. 1999;90(2):451-7.
46. Harte GJ, Gray PH, Lee TC, Steer PA, Charles BG. Haemodynamic responses and population pharmacokinetics of midazolam following administration to ventilated, preterm neonates. J Paediatr Child Health. 1997;33(4):335-8.
47. Nau H, Luck W, Kuhnz W. Decreased serum protein binding of diazepam and its major metabolite in the neonate during the first postnatal week relate to increased free fatty acid levels. Br J Clin Pharmacol. 1984;17(1):92-8.
48. Basic anatomical and physiological data for use in radiological protection: reference values. A report of age- and gender-related differences in the anatomical and physiological characteristics of reference individuals. ICRP Publication 89. Ann ICRP. 2002;32(3-4):5-265.

# SUPPLEMENTAL MATERIAL (CHAPTER 5)

## Model evaluation

### *Methods: Model evaluation*

To evaluate model stability and parameter precision, a bootstrap analysis (n=200) was performed, based on repeatedly randomly sampling in the population, and the sampling was stratified for patients receiving an intravenous, an oral, or twice a dose administration. Moreover, a normalized prediction distribution error (NPDE) analysis was performed to evaluate the model, which takes into account the predictive distribution of each observation. For this purpose, 1000 midazolam concentrations were simulated for each observed concentration. The simulations were based on the parameter values including inter-individual and residual variability that were obtained for the original model (table II). Using the NPDE package in R (version 2.0)[Comets E, *et al.* Comput Methods Programs Biomed. 2008;90(2):154-66], these 1000 predicted concentrations were numerically and visually compared with the observed concentrations.

### *Results: Model evaluation*

The model was evaluated using goodness-of-fit plots (figure S1) and the plots show that both the midazolam and 1-OH-midazolam concentrations were described well by the model. Midazolam concentrations after both the IV and the oral administration were predicted without bias (open and closed circles, figure S1). For the metabolite, fewer observations were available after oral administration, but no trend in the goodness-of-fit plots could be observed, except for a small over-prediction for midazolam at low concentration.

The results from the bootstrap analysis showed signs of over-parametrization, but did yield similar mean values for clearances and distribution volumes (table II). It also confirmed the high relative standard error (RSE) in the model fit of the intrinsic gut wall clearance (table II), indicating large uncertainty for this parameter. This means that the true value lies between 0 and 0.7 L/h, however, the bootstrap analysis indicated a 90% confidence interval of 0.2-319 mL/h (table II) with a median value of 14.0 mL/h, which is similar to the estimated value of 19.6 mL/h.

The NPDE analysis showed no trends in the plots of normalized prediction distribution errors versus predicted concentrations or time after first dose (figure S2). For midazolam, the mean NPDE was not significantly different from zero ($p>0.05$), which indicates no systematic model misspecification, although the variability was slightly overestimated in our model. For 1-OH-midazolam, mean and variance were 0.14 ($p<0.05$) and 0.72 ($p<0.01$), respectively, indicating slight over-estimation of the variability in metabolite concentrations, but the plots showed a normal distribution of errors without any trends.

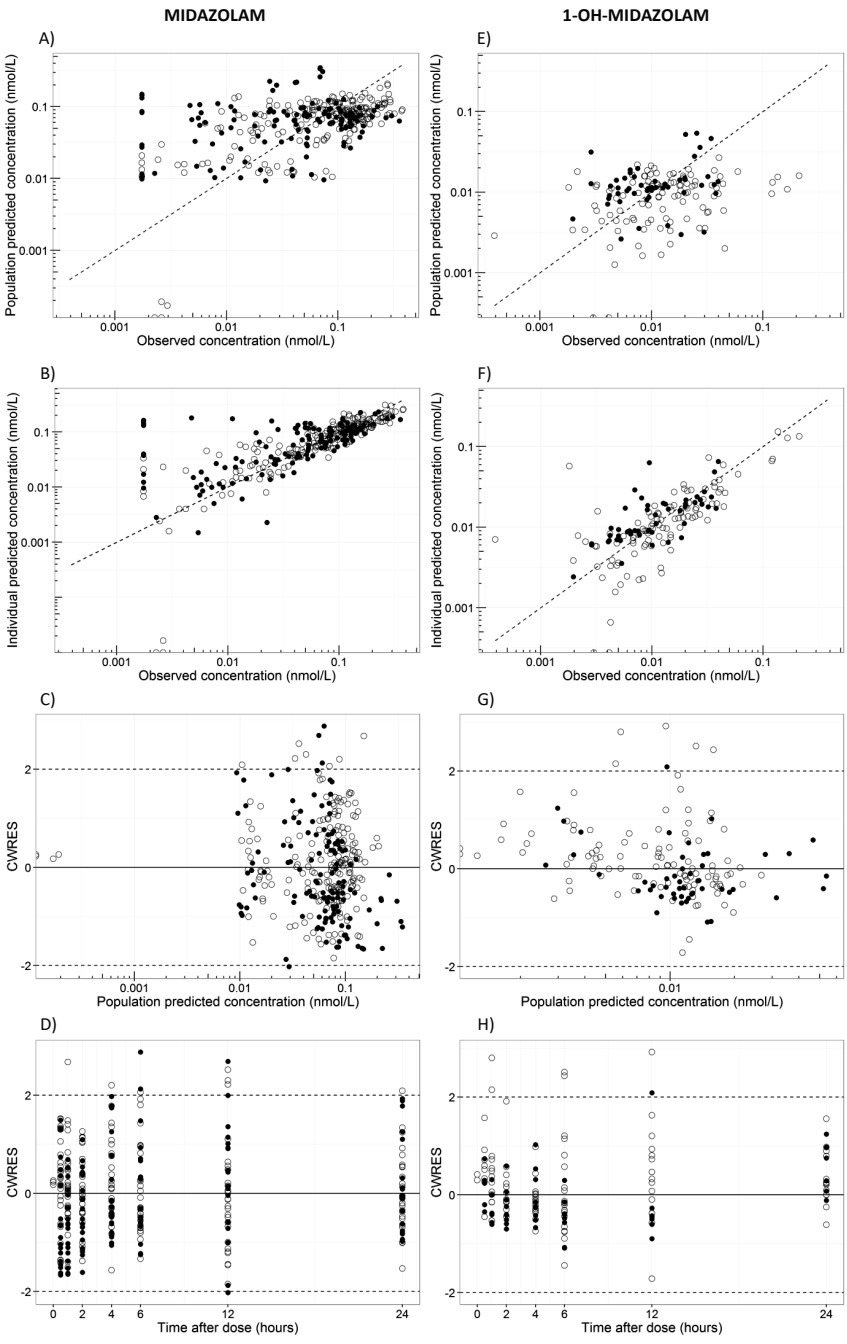



**Figure S1.** Goodness-of-fit plots for midazolam (**A-D**) and 1-OH-midazolam (**E-H**). First rows show the population (**A,E**) and individual (**B,F**) predicted concentrations versus the observed concentrations and the last two rows shows the conditionally weighted residuals (CWRES) versus population prediction (**C,G**) and versus time after dose (**D,H**). Open circles indicate concentrations after an IV administration, while closed circles represent concentrations after an oral administration.

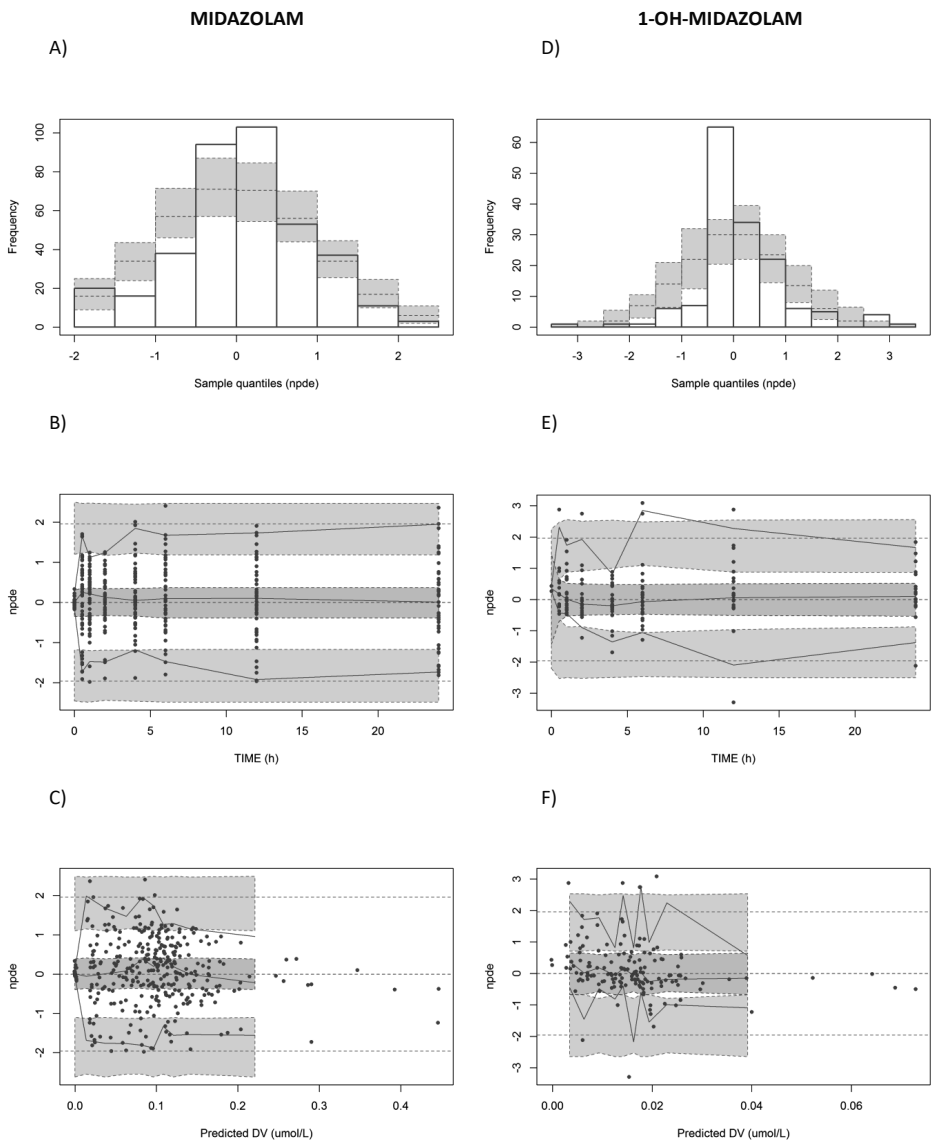



**Figure S2.** Normalized Prediction Distribution Error (NPDE) plots of the model for midazolam (**A-C**) and 1-OH-midazolam (**D-F**) concentrations. First row show the histograms of NPDEs (**A,D**), in which the white bars indicate the observed frequency of sample quantiles of the NPDEs, overlaid with the density of the standard normal distribution in blue bars. Second row shows the NPDE versus time (**B,E**) and third row shows the NPDE versus predicted concentration (**C,F**), in which the dots represent the NPDE for each observation, the lines indicate the mean (red) and the 90% percentiles (blue) of the NPDEs, and the shaded areas are the simulated 90% confidence intervals of the NPDE median (red) and 90% percentiles (blue).

## Model code

```
$PROBLEM Physiological popPK model midazolam in preterm neonates

$INPUT COMM SET ID TIME AMT RATE DURH DV MDV CMT IVPO AGEM PNA GA
PMA WT WTG BW ORGF CRP VENT SEX TAD EV
;UNITS:
;TIME hours, AMT umol, RATE umol/h, DV umol/L
;BLOOD concentrations rather than plasma conc (B:P ratio 0.568)

$DATA Neonates_20161021.csv IGNORE=#

$SUBROUTINES ADVAN6 TOL=6

$MODEL
COMP=(PODOSE)     ;1 midazolam in oral dosing depot
COMP=(GUTWALL)    ;2 midazolam in gut wall
COMP=(PV)         ;3 midazolam in portal vein
COMP=(LIVER)      ;4 midazolam in liver
COMP=(CENTRAL)    ;5 midazolam in central compartment
COMP=(MOHCENTR)   ;6 1-OH-midazolam in central compartment
COMP=(MOHGW)      ;7 1-OH-midazolam in gut wall
COMP=(MOHPV)      ;8 1-OH-midazolam in portal vein
COMP=(MOHLVR)     ;9 1-OH-midazolam in liver

$PK
;parent compound (midazolam)
V5= THETA(1)*EXP(ETA(1))    ;(L) central cmt
KA= THETA(2)                ;(h-1)
F1= 1  ;total oral bioavailability F = Fa * Fg * Fh with Fa=1

; intrinsic hepatic clearance
TVCL=THETA(3)               ;(L/h)
CL = TVCL * EXP(ETA(2))     ;
FUB= 0.04094                ; fraction unbound in blood

;intrinsic gut wall clearance
CLG= THETA(4)/1000         ;(L/h),TH(4)in mL/h for model stability
FUG= 1                      ; fraction unbound in gut wall
```

```
;organ blood flows, allometric scaling from term neonates
QH=  13.2*(WT/3.55)**0.75  ;(L/h)
QPV= 0.75*QH               ;(L/h) portal vein blood flow
QHA= 0.25*QH               ;(L/h) hepatic artery blood flow
QIN= 0.4*QH                ;(L/h) intestinal blood flow
QMU= 0.8*QIN               ;(L/h) mucosa blood flow
QVI= 0.6*QMU               ;(L/h) villous blood flow

;organ volumes, scaled from term neonates, and organ size
VH=  0.12*(WT/3.55)**1     ;(L) hepatic volume
VPV= 0.778*VH              ;(L) portal vein
VGW= 0.05*(WT/3.55)**1     ;(L) small intestine
INTL = 2.736* (WT*1000)**0.512       ;intestinal length (cm)
INTS = (2*3.141592*1*(1+INTL))/100   ;intestinal surface (dm2)
;INTS: calculation of cylindrical surface area of small intestine

;Permeability factor for 'Qgut' model
;CLperm = Peff,man (4.4E-4 cm/s)*intestinal surface area INTS
;units: INTS dm2, Peff 4.4E-4 cm/s -> /10 for dm -> *60*60 for
hours
CLPERM = 0.44/1000/10*60*60 * INTS   ;(L/h)

;'Qgut' model
QGUT = (QVI*CLPERM)/(QVI+CLPERM)

; Midazolam conversion into 1-OH-midazolam
; hepatic extraction
EH= (CL*FUB)/(QH+(CL*FUB))
FH= 1-EH
; gut wall extraction
EG= (CLG*FUG)/(QGUT+(CLG*FUG))
FG= 1-EG

; Primary metabolite (1-OH-midazolam) parameters
VMET=THETA(5)*EXP(ETA(3))      ;(L)
CLHM=THETA(6)*EXP(ETA(4))      ;(L/h)intrinsic hepatic clearance
FUBM=0.1394                    ;fraction unbound in blood
```

```
; Hepatic extraction of 1-OH-midazolam
EHM= (CLHM*FUBM)/(QH+(CLHM*FUBM))
FHM= 1-EHM

S5=V5     ; scaling for Central CMT midazolam
S6=VMET   ; scaling for Central CMT 1-OH-midazolam

;absorption rate constant
K12=KA

$DES
;1. Midazolam in oral dosing depot
DADT(1)= -K12*A(1)

;2. Midazolam in gut wall
DADT(2)=  K12*A(1)-FG*(QVI/VGW)*A(2)-EG*(QVI/VGW)*A(2)

;3. Midazolam in portal vein
DADT(3)=  FG*(QVI/VGW)*A(2) +(QPV/V5)*A(5)     -(QPV/VPV)*A(3)

;4. Midazolam in liver
DADT(4)= -FH*(QH/VH)*A(4)   +(QHA/V5)*A(5)     +(QPV/VPV)*A(3)
         -EH*(QH/VH)*A(4)

;5. Midazolam in central compartment
DADT(5)=  FH*(QH/VH)*A(4)-(QHA/V5)*A(5)-(QPV/V5)*A(5)

;6. 1-OH-midazolam in central compartment
DADT(6)= FHM*(QH/VH)*A(9)-(QHA/VMET)*A(6)-(QPV/VMET)*A(6)

;7. 1-OH-midazolam in gut wall
DADT(7)= -(QVI/VGW)*A(7)+EG*(QVI/VGW)*A(2)

;8. 1-OH-midazolam in portal vein
DADT(8)=  (QVI/VGW)*A(7) -(QPV/VPV)*A(8) +(QPV/VMET)*A(6)

;9. 1-OH-midazolam in liver
DADT(9)=-FHM*(QH/VH)*A(9)+(QHA/VMET)*A(6)
        -EHM*(QH/VH)*A(9)+(QPV/VPV)*A(8) + EH*(QH/VH)*A(4)
```

```
$ERROR
IF(CMT.EQ.5) Y=F*(1+ERR(1))+ERR(2) ;midazolam (parent)
IF(CMT.EQ.6) Y=F*(1+ERR(3))+ERR(4) ;1-OH-midazolam (metabolite)
IPRED = F

$THETA
;Midazolam
(0.01, 5.1)    ;Vcentral (L)           ;1
10 FIX         ;KA(/h)                 ;2
(0.1, 8.3)     ;CLh,intr (L/h)         ;3
(0.01, 50)     ;CLg,intr (mL/h)        ;4
;1-OH-midazolam
(0.01,5.2)     ;1OH-Vcentral (L)       ;5
(0.1,12.2)     ;1OH-CLh,intr (L/h)     ;6

$OMEGA BLOCK(4)
0.81  ;IIV V
0.01 0.75  ;IIV CLh,intr
0.01 0.01 0.7   ;IIV 1OH-V
0.01 0.01 0.01 0.65   ;IIV 1OH-CLh,intr

$SIGMA
0.1          ;Prop err midazolam
0.0001 FIX   ;Add. err midazolam
0.1          ;Prop err 1-OH-midazolam
0.0001 FIX   ;Add. err 1-OH-midazolam

$EST METHOD=1 INTER MAXEVAL=9999 NOABORT SIG=3 PRINT=5 POSTHOC
$COV PRINT=E

$TABLE SET ID TIME TAD CMT DV MDV EVID IPRED CWRES IVPO WT
ONEHEADER NOPRINT FILE=sdtab
$TABLE SET ID V5 KA F1 VPV TVCL CL FUB QH QPV QHA VH CLG FUG QIN
QMU QVI QGUT VGW EH FH EG FG VMET CLHM FUBM FUGM EHM FHM ETA(1)
ETA(2) ETA(3) ETA(4) CMT GA ORGF CRP WT SEX VENT PNA DURH WTG AGEM
PMA IVPO BW FIRSTONLY ONEHEADER NOPRINT FILE=patab
```

# Chapter 6

## Characterization of intestinal and hepatic CYP3A-mediated metabolism of midazolam in children using a physiological population pharmacokinetic modelling approach

Janneke M Brussee[1], Huixin Yu[1,2], Elke HJ Krekels[1], Semra Palić[1,3], Margreke JE Brill[4], Jeffrey S Barrett[5,6], Amin Rostami-Hodjegan[7,8], Saskia N de Wildt[9,10], Catherijne AJ Knibbe[1,11]

[1]Division of Systems Biomedicine and Pharmacology, Leiden Academic Centre for Drug Research (LACDR), Leiden University, Leiden, the Netherlands; [2]Current affiliation: Novartis, Basel, Switzerland; [3]Current affiliation: Netherlands Cancer Institute (NKI), Amsterdam, the Netherlands; [4]Department of Pharmaceutical Biosciences, Uppsala University, Uppsala, Sweden; [5]Translational Informatics, Sanofi, Bridgewater, NJ, USA; [6]Department of Pediatrics, Division of Clinical Pharmacology & Therapeutics, Children's Hospital of Philadelphia, Philadelphia, PA, USA; [7]Centre for Applied Pharmacokinetic Research, University of Manchester, Manchester, UK; [8]Simcyp Limited (A Certara Company), Sheffield, UK; [9]Intensive Care and Department of Pediatric Surgery, Erasmus MC - Sophia Children's Hospital, Rotterdam, the Netherlands; [10]Department of Pharmacology and Toxicology, Radboud University Medical Centre, Nijmegen, the Netherlands; [11]Department of Clinical Pharmacy, St. Antonius Hospital, Nieuwegein, the Netherlands

*Pharm. Res. 2018 Jul 30;35(9):182.*

## ABSTRACT

Changes in drug absorption and first-pass metabolism have been reported throughout the pediatric age range. Our aim is to characterize both intestinal and hepatic CYP3A-mediated metabolism of midazolam in children in order to predict first-pass and systemic metabolism of CYP3A substrates.

Pharmacokinetic (PK) data of midazolam and 1-OH-midazolam from 264 post-operative children 1-18 years of age after oral administration were analyzed using a physiological population PK modelling approach. In the model, consisting of physiological compartments representing the gastro-intestinal tract and liver, intrinsic intestinal and hepatic clearances were estimated to derive values for bioavailability and plasma clearance.

The whole-organ intrinsic clearance in the gut wall and liver were found to increase with body weight, with a 105 (95% confidence interval (CI): 5-405) times lower intrinsic gut wall clearance than the intrinsic hepatic clearance (i.e. 5.08 L/h (relative standard error (RSE) 10%) versus 527 L/h (RSE 7%) for a 16 kg individual, respectively). When expressed per gram of organ, intrinsic clearance increases with increasing body weight in the gut wall, but decreases in the liver, indicating that CYP3A-mediated intrinsic clearance and local bioavailability in the gut wall and liver do not change with age in parallel. The resulting total bioavailability was found to be age-independent with a median of 20.8% in children (95%CI: 3.8-50.0%).

In conclusion, the intrinsic CYP3A-mediated gut wall clearance is substantially lower than the intrinsic hepatic CYP3A-mediated clearance in children from 1-18 years of age, and contributes less to the overall first-pass metabolism compared to adults.

**Keywords**
CYP3A, extraction ratio, absorption, first-pass metabolism, gut wall, liver, pediatrics

## INTRODUCTION

Differences in drug absorption and first-pass metabolism have been reported in children compared to adults (1-3). These differences may for instance result from a smaller intestinal surface area in children (2) and altered permeability across age (1). In addition, besides gastric emptying time, intestinal transit time, the production of bile fluid (3) and organ blood flow to intestines and liver that may be altered in children (4), intestinal and hepatic drug metabolizing enzyme activity may be different from those in adults. For first-pass metabolism, the activity of both intestinal and hepatic enzymes is of relevance, while for systemic clearance the activity of hepatic enzymes is important with activity of intestinal enzymes probably being of negligible influence.

With cytochrome P450 (CYP) being an enzyme family involved in metabolism of many drugs (5), this study focuses on CYP3A enzymes, as they are abundant in both intestine and liver (6, 7). From the available *in vitro* and *in vivo* studies on the ontogeny of CYP3A in children (8-10), there is some evidence that the maturation and regulation of these enzymes in the gut wall and liver may differ (11). However, the translation of enzyme activity in gut wall and liver to intestinal and hepatic clearance is complex, because other parameters like organ blood flow, organ size and other physiological parameters need to be taken into account (4, 12). In order to distinguish between intestinal and hepatic clearance (and their maturation), a combination of mechanistic and empirical models can be useful, as was shown in adults before (13, 14). This hybrid of approaches seems necessary as for full physiologically-based PK models in children not all parameters are always available and/or identifiable, while empirical models may lack direct physiological interpretation. The latter is particularly problematic, because both hepatic and intestinal metabolism contribute to first-pass metabolism. As such, the combination of PBPK concepts with population modelling using PK data from children enables incorporation of prior knowledge of the system, while obtaining more insight into the system by parameter estimation based on reverse translation of the observed clinical data (15).

In this study, the aim is to characterize both intestinal and hepatic CYP3A-mediated metabolism of midazolam in children between 1 and 18 years of age. We will adopt the above described physiological population PK modelling approach, in which we account for known changes in the physiology of the gastrointestinal tract, and use the available PK data from the population, to estimate the whole-organ intrinsic intestinal and hepatic CYP3A-mediated midazolam clearance in children. For this

analysis, we had access to data from a clinical study in which the CYP3A substrate midazolam which is considered a probe drug for CYP3A (16), was administered to children pre-operatively, and in which both midazolam and the CYP3A-mediated metabolite (i.e. 1-OH-midazolam) concentrations were available.

# METHODS

## Data

In 873 plasma samples from 266 patients of the Children's Hospital of Philadelphia, PA, midazolam and 1-OH-midazolam concentrations were measured (17). The children received a median dose of 10 mg (range 3-15 mg) of midazolam as oral suspension pre-operatively. Subjects include children (150 boys/116 girls) between 1 and 18 years of age (median 7 years), with a median body weight of 27.2 kg (range 9.1-137.6 kg), who fit the criteria I or II of the American Society of Anesthesiologist's (ASA) classification, undergoing surgery. In 31 patients, midazolam and its primary metabolite were densely sampled around 0.25, 0.5, 1, 1.5, 2, 3, 4, 6, 8, 10 and 22 hours after dose administration with a median of 10 samples per patient (range 8-11), and in 235 patients, samples were sparsely collected for analysis at different time points post-dose (median 2, range 1-3 samples/patient) with most samples within the first four hours after dose administration (figure S1). Data from two 14-year old patients in the sparsely sampled group were excluded as their body weight was <12 kg. The patient groups who were in the dense and sparse sampled study were comparable in age and weight distribution (Table SI). Patient height and body surface area, required for some of the covariate relationships in the model, were derived from recorded age and body weight information (equations in supplemental material).

Blood concentrations (*B*) were estimated based on the measured plasma concentrations (*P*) using equation 1 (18):

$$B{:}P = 1 + [Hem \times (f_u \times K_p - 1)] \qquad \text{(Eq.1)}$$

In which Hem is the hematocrit based on population values reported in literature (19) ranging from 0.36 in 1- and 2-year-old infants up to 0.41-0.43 in adolescents of 12-18 years of age (table I), the $f_u$ is the fraction unbound in plasma and $K_p$ is the unbound partition coefficient of the red blood cells to plasma (assumed to be constant between adults and children) (18). The fraction unbound in plasma for both midazolam and 1-OH-midazolam were calculated based on the formula of McNamara and Alcorn (20):

$$f_{u,pediatric} = \frac{1}{1+\frac{(1-f_{u,adult}) \times [P]_{pediatric}}{[P]_{adult} \times f_{u,adult}}} \qquad \text{(Eq. 2)}$$

where $f_{u,pediatric}$ and $f_{u,adult}$ are the fraction unbound of the drug in plasma for children and adults respectively and $[P]_{pediatric}$ and $[P]_{adult}$ are the plasma albumin concentrations in children and adults respectively, assuming exclusive binding to albumin for midazolam and its metabolite. The fractions unbound of midazolam and 1-OH-midazolam in plasma in adults were reported in literature (21, 22). The albumin concentrations $[P]_{pediatric}$ are calculated based on the formula of Johnson *et al.* (12):

$$[P]_{pediatric}\,[g/L] = 1.1287 \times \ln(Age[yr]) + 33.746 \qquad \text{(Eq.3)}$$

Measurements below the lower limit of quantification were discarded according to the M6 method (23) (n=4 (0.5%) and n=5 (0.6%) of midazolam and 1-OH-midazolam measurements respectively).

## Model development

### *Structural model*

The physiological population PK analysis was performed using NONMEM version 7.3 (ICON, Globomax LLC, Ellicott, MD, USA) based on first-order conditional estimation with interaction, and for visualization of data Pirana 2.9.0, R (version 3.3.1), and R-studio (version 0.98.1078) were used. A physiological population pharmacokinetic (PK) model, earlier developed and applied by Yang *et al.* (24), Frechen *et al.* (13) and Brill *et al.* (14) to describe midazolam PK data in adults, was now applied to describe the midazolam PK data in children 1 – 18 years of age (figure 1). This model includes physiological compartments representing the gut wall, the portal vein and the liver, and also empirical central and peripheral compartments for midazolam and 1-OH-midazolam distribution, representing the blood circulation and fast equilibrating tissue, and peripheral slow equilibrating tissues (13, 24). Based on literature, central and peripheral volumes were linearly scaled based on body weight from a 76 kg healthy adult with volumes of 20.4 L/76kg, 55.2 L/76kg and 79.1 L/76kg for the central and two peripheral volumes for midazolam respectively and with a volume of 65.7 L/76kg for 1-OH-midazolam (13). The fraction midazolam metabolized into 1-OH-midazolam was assumed 100% (table II).

In the physiological compartments, tissue volumes and blood flows in children were based on literature data. The hepatic volume ($V_h$) was calculated based on body surface area (BSA, $m^2$) (25):

$$V_h\,[L] = 0.722 \times BSA^{1.176} \qquad \text{(Eq. 4)}$$

Volume of the portal vein was assumed to be equal to the reported value of 5.2 mL in adults (26). To calculate the volume of the intestines, a regression line was derived from data published by Björkman (4):

$$V_{in}\,[L] = 0.0467 \times Age[y] + 0.0901 \qquad \text{(Eq. 5)}$$

**Table I**. Parameter values for system specific and drug specific parameters included in the physiological population PK model

| Parameter name (unit) | Parameter symbol | Formula for calculation | Value | References |
|---|---|---|---|---|
| **Tissue volumes (L)** | | | | |
| Liver | $V_h$ | $0.722 \times BSA^{1.176}$ | - | (25) |
| Portal vein | $V_{pv}$ | - | 0.0052 | (26) |
| Small intestine | $V_{in}$ | $0.0467 \times age + 0.0901$ | - | (4) |
| **Tissue blood flows (L/h)** | | | | |
| Cardiac output | CO | $BSA \times (110 + 184.974 \times (e^{-0.0378 \times age} - e^{-0.24477 \times age}))$ | - | (27) |
| Hepatic blood flow | $Q_h$ | $0.28 \times CO$ ♀<br>$0.255 \times CO$ ♂ | - | (27) |
| Portal vein<br>Hepatic artery | $Q_{pv}$<br>$Q_{ha}$ | $0.75 \times Q_h$<br>$0.25 \times Q_h$ | - | (12, 52) |
| Small intestine<br>Mucosa<br>Microvilli | $Q_{in}$<br>$Q_{muc}$<br>$Q_{villi}$ | $0.4 \times Q_h$<br>$0.8 \times Q_{in}$<br>$0.6 \times Q_{muc}$ | - | (30, 49) |
| **Plasma proteins** | | | | |
| Plasma albumin concentration (g/L) | $P_{pediatric}$ $P_{adult}$ | $1.1287 \times \ln(age) + 33.746$ | -<br>37.7 | (12) |
| Hematocrit (%) | $Hem_{1\text{-}2y}$<br>$Hem_{3\text{-}6y}$<br>$Hem_{7\text{-}12y}$<br>$Hem_{12\text{-}18y,}$♀<br>$Hem_{12\text{-}18y,}$♂ | - | 0.36<br>0.37<br>0.40<br>0.41<br>0.43 | (19) |
| **Midazolam** | | | | |
| Fraction absorbed | $F_a$ | - | 1 | (29) |
| Absorption rate constant ($h^{-1}$) | $K_a$ | - | 4.16 | - |
| Blood: plasma ratio | B:P ratio | $1+ [Hem \times (f_u \times K_p - 1)]$ with $K_p = 1$ | - | (18) |
| Fraction unbound in gut | $F_{u,G}$ | - | 1 | - |
| Fraction unbound in plasma | $F_{u,plasma}$<br>$F_{u,adult}$ | $\frac{1}{1 + \frac{(1 - f_{u,adult}) \times [P]_{pediatric}}{[P]_{adult} \times f_{u,adult}}}$ | 0.0303 | (20)<br>(21) |
| Permeability through the enterocyte (L/h) | $CL_{perm}$ | $CL_{perm} = P_{eff,man} \times A$ with $P_{eff,man} = 4.4 \times 10^{-4}$ cm/s | - | (30) |
| Intestinal surface area ($dm^2$) | A | $2\pi r(r+h)$ with radius $r = ½ \times (0.016 \times BSA + 0.0159)$ and length $h = 2.56 \times BSA + 2.95$ | - | (12) |
| **1-OH-midazolam** | | | | |
| Blood: plasma ratio | B:P ratio | $B:P = 1+ [Hem \times (f_{u,M} \times K_p - 1)]$ with $K_p = 1$ | - | (18) |
| Fraction unbound in plasma | $F_{u,M,pediatric}$<br>$F_{u,M,adult}$ | $\frac{1}{1 + \frac{(1 - f_{u,M,adult}) \times [P]_{pediatric}}{[P]_{adult} \times f_{u,M,adult}}}$ | 0.106 | (20)<br>(22) |

Age is expressed in years. A is the intestinal surface area in $dm^2$. BSA is the body surface area in $m^2$. $P_{eff,man}$ is the effective intestinal permeability per unit surface area (dm/h). WT is body weight in kg. ♀ female, ♂ male.

To calculate organ weight, the organ volumes are multiplied by the organ density of 1040 g/L (4). To compare with adult values (figure 2), organ weight in adults is calculated assuming organ volumes of 1 L (13) and an organ density of 1040 g/L.

The hepatic blood flow ($Q_h$) was assumed to be a fixed percentage of the cardiac output (CO), which was calculated based on BSA (27):

$CO = BSA \times (110 + 184.974 \times (e^{-0.0378 \times age} - e^{-0.24477 \times age}))$ (Eq. 6)

Other tissue blood flows were assumed to be proportional to the hepatic blood flow (table I). The relationship between plasma protein binding, intestinal surface area, tissue volumes, and organ blood flows and body weight for the individual patients in this study are depicted in figure S2. For all physiological parameters in table I, population values were used without inter-individual variability or uncertainty.

The absorption rate constant ($k_a$) for midazolam could not be estimated, and was therefore fixed at 4.16 $h^{-1}$, yielding peak concentrations to be reached round 30 minutes ($t_{max}$), which is in agreement with the observed $t_{max}$ and other reported literature values (28). The oral bioavailability ($F_{total}$) was calculated using:

$F_{total} = F_a \times F_g \times F_h$ (Eq. 7)

in which $F_a$ is the fraction absorbed, which is assumed 1 for midazolam (29), $F_g$ is the gut wall bioavailability, equal to 1 minus the gut wall extraction ratio ($E_g$), and $F_h$ is the hepatic bioavailability, which is equal to 1 minus the hepatic extraction ratio ($E_h$). The hepatic extraction ratio of midazolam ($E_H$) and 1-OH-midazolam ($E_{H,M}$) were defined by the well-stirred model:

$$E_H = \frac{CL_{H,int} \times f_{u,B}}{Q_h + (CL_{H,int} \times f_{u,B})}$$ (Eq. 8)

where $CL_{H,int}$ is the estimated intrinsic hepatic clearance (whole-organ), $f_{u,B}$ is the fraction unbound in the blood and $Q_h$ is the hepatic blood flow. The gut wall extraction ratio is described using the Qgut model (30):

$$E_G = \frac{CL_{G,int} \times f_{u,G}}{Q_{gut} + (CL_{G,int} \times f_{u,G})}$$ (Eq. 9)

Where $CL_{G,int}$ is the estimated intrinsic gut wall clearance (whole-organ), $f_{u,G}$ is the fraction unbound in the gut, which was assumed to be 1, and $Q_{gut}$ is the effective blood flow at the gut wall (30) which is defined by:

$$Q_{gut} = \frac{Q_{villi} \times CL_{perm}}{Q_{villi} + CL_{perm}}$$ (Eq. 10)

In which $Q_{villi}$ is the villous blood flow and $CL_{perm}$ is the permeability through the enterocytes of the gut wall for the drug. This permeability factor depends on the effective intestinal permeability per unit surface area (30) (table I) and the intestinal surface area A described by equation 12, and can be calculated using equation 11.

$$CL_{perm} = P_{eff,man} \times A$$ (Eq. 11)

With With $A = 2\pi r(r + h)$ (Eq. 12)

where r is the intestinal radius in meters and h the intestinal length in meters, which are both calculated using a BSA-based formula (eq. 13 and 14) (12):

$$r = ½ \times (0.016 \times BSA + 0.0159) \quad \text{(Eq. 13)}$$

$$h = 2.56 \times BSA + 2.95 \quad \text{(Eq. 14)}$$

The total intestinal surface area was cut-off at a maximum value of the adult value of 0.66 $m^2$ (30) (figure S2). The total plasma clearance was calculated using equation 15:

$$CL_{plasma} = \frac{Qh \times CL_{H,int} \times f_u}{Q_h + (f_u \times CL_{H,int})/(B:P\ ratio)} \quad \text{(Eq. 15)}$$

Where $Q_h$ is the hepatic blood flow, $CL_{H,int}$ is the estimated intrinsic hepatic clearance, $f_u$ is the fraction unbound in plasma, and B:P ratio is the blood-to-plasma ratio of midazolam.

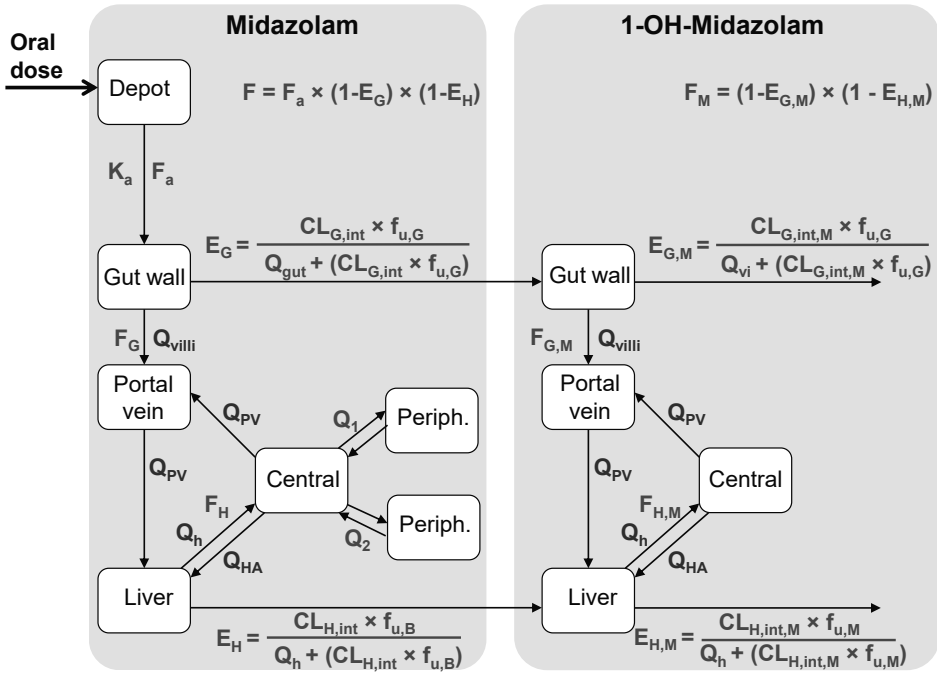



**Figure 1.** Schematic representation of the physiological population PK model for midazolam and the metabolite 1-OH-midazolam. The extraction of midazolam is defined by the well-stirred model in the liver and the '$Q_{gut}$' model in the gut wall. E = extraction ratio, F = bioavailability in the gut wall (gut, G) and the liver (hepatic, H). $CL_{int}$ is the whole-organ intrinsic clearance in the gut wall and liver, Ka indicates the absorption rate constant and the fraction unbound in blood and gut wall are described with $f_{u,B}$ and $f_{u,G}$ respectively. Blood flows are represented by Q; in the micro villi ($Q_{villi}$), portal vein ($Q_{PV}$), hepatic artery ($Q_{HA}$) and liver ($Q_h$). Distribution between central and peripheral (Periph.) compartments is estimated by inter-compartmental clearance $Q_1$ and $Q_2$ for the two peripheral compartments for midazolam. Parameters describing the metabolite are indicated with the subscript M.

*Statistical model*

Inter-individual variability in the estimated intrinsic clearance parameters for midazolam and 1-OH-midazolam was included in the model using the following equation:

$$CL_{int,i} = \theta_{TV} \times e^{\eta_i} \quad \text{(Eq. 16)}$$

In which $CL_{int,i}$ is the individual intrinsic clearance estimate for individual *i*, $\theta_{TV}$ is the typical value of the intrinsic clearance in the studied population and $\eta_i$ is a random variable for the *i*th individual form a normal distribution with a mean of zero and variance of $\omega^2$, yielding a log-normal distribution for the parameter value in the population. Inter-individual variability in the estimated intercompartmental clearance parameters ($Q_{cp1}$ and $Q_{cp2}$) for midazolam was included as well.

Residual unexplained variability was modelled using a combined proportional and additive error model for both midazolam and 1-OH-midazolam. The *j*th observed concentration Y of the *i*th individual was modelled according to:

$$Y_{ij} = C_{pred,ij} \times (1+\varepsilon 1_{ij}) + \varepsilon 2_{ij} \quad \text{(Eq. 17)}$$

where $C_{pred,ij}$ is the *j*th predicted midazolam concentration of the *i*th individual, $\varepsilon 1_{ij}$ and $\varepsilon 2_{ij}$ are random variables from a normal distribution with a mean of zero and variance of $\sigma^2$.

## Covariate analysis

A covariate analysis for the estimated parameters (whole-organ intrinsic clearance ($CL_{G,int}$, $CL_{H,int}$, $CL_{H,int,M}$) and intercompartmental clearance ($Q_{cp1}$, $Q_{cp2}$)) was performed in which the following covariates were tested for significance: age, body weight, height, body surface area, and sex. For sex, the typical value ($\theta_{TV}$) for girls was estimated relative to the value for boys. The remaining continuous covariates were tested using a power (Eq. 18) or linear (Eq.19) function.

$$P_i = \theta_{TV} \times \left(\frac{COV}{COVmed}\right)^{\theta_{COV}} \quad \text{(Eq. 18)}$$

$$P_i = \theta_{TV} \times (1 + \theta_{cov} \times (COV - COV_{med})) \quad \text{(Eq. 19)}$$

where $P_i$ is individual parameter estimate for individual *i*, $\theta_{TV}$ the typical value of the parameter in the studied population with a median value ($COV_{med}$) of the covariate (COV) and $\theta_{COV}$ the estimated exponent or slope for a power or linear function respectively.

## Model evaluation

Structural models were evaluated by comparison of the objective function values (OFV, i.e. -2×log-likelihood). A decrease of 3.84 in the OFV between nested models ($p<0.05$) was considered statistically significant. In addition, goodness-of-fit plots of

midazolam and 1-OH-midazolam were assessed, in which observed versus individual- and population-predicted concentrations and conditional weighted residuals (CWRES) versus time and population predicted concentrations are visualized. Moreover, the condition number, the confidence interval of the parameter estimates, and visual improvement of the individual plots were used to evaluate the models.

For inclusion of covariates, a drop in OFV by at least 6.64 points ($p<0.01$) was considered statistically significant, while for the backward deletion a more stringent p value ($p<0.005$, $\Delta OFV>7.88$) was used. Moreover, to retain a covariate in the model, the inter-individual variability in the PK parameter should decrease.

Two methods were applied to evaluate the final model internally. A bootstrap analysis (n=250) was performed to evaluate model stability and parameter precision (31). In addition, a normalized prediction distribution error (NPDE) analysis was performed using the NPDE package in R (32). For each observed concentration, 1000 midazolam concentrations were simulated based on the parameter values that were obtained for the original model (table II). The observed concentrations were compared to the range of 1000 predicted concentrations. The Wilcoxon signed rank test was used to assess the deviation of the observed mean value of the NPDE to the expected value of 0, and the Fisher variance test was used to assess the deviation of the observed variance from the expected value of 1.

### Sensitivity analysis

A sensitivity analysis was performed to evaluate the assumptions made in the model. For this, it was evaluated what the impact was of a 50% increase or decrease of the parameter values for intestinal length, the fraction unbound and tissue volumes and blood flows on predicted midazolam concentrations and on the estimated model parameters. Additionally, the impact of the assumed fraction absorbed ($F_a$) of 1 (29), on the estimated whole-organ intrinsic clearance in the gut wall and liver, and the derived total plasma clearance, was evaluated, as well as a 50% increase or decrease of volume of distribution of the primary metabolite, 1-OH-midazolam.

## RESULTS

In the model as shown in figure 1, the intrinsic gut wall clearance was 5.08 L/h (with a relative standard error (RSE) of 16%) and the intrinsic hepatic clearance was 527 L/h (RSE 7%) for a typical individual of 16 kg (table II). The increase in these whole-organ intrinsic clearance values, reflected by the inclusion of a power function (eq. 18) correlating body weight as covariate to intrinsic clearance with an exponent of 0.807 (RSE 10%) and 0.472 (RSE 16%) for intestinal and hepatic maturation

**Table II.** Parameter estimates of the final physiological population PK model

| Parameter definition | Parameter (unit) | Value (RSE%) [shrinkage %] | Bootstrap median | Bootstrap 90% CI | 70-kg individual |
|---|---|---|---|---|---|
| **Midazolam** | | | | | |
| Intrinsic hepatic clearance $CL_{H,int,i} = CL_{H,int,16kg} \times (WT/16)^{k1}$ | $CL_{H,int,16kg}$ (L/h) | 527.0 (7%) | 601.4 | 523.5-748.6 | 1057 |
| Exponent | k1 | 0.472 (16%) | 0.425 | 0.206-0.554 | 0.472 |
| Intrinsic gut wall clearance $CL_{G,int,i} = CL_{G,int,16kg} \times (WT/16)^{k2}$ | $CL_{G,int,16kg}$ (L/h) | 5.08 (10%) | 4.93 | 3.32-6.17 | 16.7 |
| Exponent | k2 | 0.807 (10%) | 0.881 | 0.622-1.27 | 0.807 |
| Volume of distribution (central) $V_{c,i} = V_{c,76kg} \times (WT/76)^{k3}$ | $V_{c,76kg}$ (L) | 20.4 fix | - | - | 18.8 |
| Volume of distribution (two peripheral compartments) $V_{p,i} = V_{p,76kg} \times (WT/76)^{k3}$ | $V_{p1,76kg}$ (L)<br>$V_{p2,76kg}$ (L) | 55.2 fix<br>79.1 fix | -<br>- | -<br>- | 50.8<br>72.9 |
| Exponent | k3 | 1 fix | - | - | 1 |
| Inter compartmental clearance $Q_{cp1,i} = Q_{cp1,16kg} \times (WT/16)^{k4}$ | $Q_{cp1}$ (L/h) | 14.9 (19%) | 14.9 | 8.9-25.9 | 57.9 |
| Exponent | k4 | 0.92 (21%) | 1.03 | 0.796-1.65 | 0.92 |
| Inter compartmental clearance ($2^{nd}$ peripheral compartment) | $Q_{cp2}$ (L/h) | 7.5 (10%) | 7.7 | 6.3-11.2 | 7.5 |
| **1-OH-midazolam (M)** | | | | | |
| Fraction midazolam metabolized into 1-OH-midazolam | $f_M$ | 1 fix | - | - | 1 |
| Intrinsic hepatic clearance $CL_{H,int,M,i} = CL_{H,int,M,16kg} \times (WT/16)^{k5}$ | $CL_{H,int,M,16kg}$ (L/h) | 235.0 (6%) | 236.2 | 219.6-269.6 | 614.2 |
| Exponent | k5 | 0.651 (9%) | 0.615 | 0.451-0.750 | 0.651 |
| Intrinsic gut wall clearance $CL_{G,int,M,i} = k6 \times CL_{G,int,i}$ | k6 | 18.4 (12%) | 19.2 | 10.6-198.2 | 18.4 |
| Volume of distribution $V_{M,i} = V_{M,76kg} \times (WT/76)^{k3}$ | $V_{M,76kg}$ (L) | 65.7 fix | - | - | 60.5 |
| **Inter individual variability** | | | | | |
| Intrinsic hepatic clearance | $\omega^2$ $CL_{H,int}$ | 0.25 (13%)[25%] | 0.24 | 0.16-0.32 | - |
| Intrinsic gut wall clearance | $\omega^2$ $CL_{G,int}$ | 1.20 (13%)[13%] | 1.25 | 1.04-1.56 | - |
| Inter compartmental clearance | $\omega^2$ $Q_{cp1}$ | 1.05 (35%)[42%] | 1.05 | 0.26-1.85 | - |
| | $\omega^2$ $Q_{cp2}$ | 1.06 (31%)[46%] | 1.06 | 0.68-1.79 | - |
| Intrinsic hepatic clearance 1-OH-midazolam (M) | $\omega^2$ $CL_{H,int,M}$ | 0.13 (18%)[31%] | 0.13 | 0.08-0.19 | - |
| **Residual variability** | | | | | |
| Proportional error (Midazolam) | | 0.166 ( 8%)[19%] | 0.169 | 0.150-0.199 | - |
| Additive error (Midazolam), nmol/L | | 0.001 fix | - | - | - |
| Proportional error (1-OH-midazolam) | | 0.292 (11%)[ 9%] | 0.271 | 0.225-0.309 | - |
| Additive error (1-OH-midazolam), nmol/L | | 0.528 (10%)[ 9%] | 0.454 | 0.130-0.826 | - |

RSE: relative standard error. CI: the $5^{th}$-$95^{th}$ percentiles are shown, indicating a 90% confidence interval. Bootstrap n=250. Inter-individual and residual variability values are shown as variance estimates. Intrinsic clearance values are reported for the whole organ.

respectively, appeared to be slightly larger in the gut wall than in the liver (table II). For intercompartmental clearance of midazolam to the first peripheral compartment (with $V_{p1}$ = 55.2 L), body weight was found as a covariate, while no covariate was identified for intercompartmental clearance to the second peripheral compartment (with $V_{p2}$ = 79.1 L). Lastly, a covariate was included in the model correlating weight to intrinsic hepatic clearance of the metabolite with an exponent of 0.651 (RSE 9%). Age, height, body surface area, and sex were not identified as covariates for the estimated parameters. The gut wall metabolism of the metabolite could not be estimated independently due to model instability, and was therefore estimated as a fraction of the gut wall metabolism of midazolam. The bootstrap results confirmed the model stability and the precision of parameter estimates of the model (table II).

Figure 2a illustrates the relation between body weight and whole-organ intrinsic clearance in the gut wall and the liver. As illustrated in this figure, the intrinsic hepatic clearance was estimated to be around 105 times higher than the intrinsic gut wall clearance for a typical individual of 16 kg, while this factor differed largely

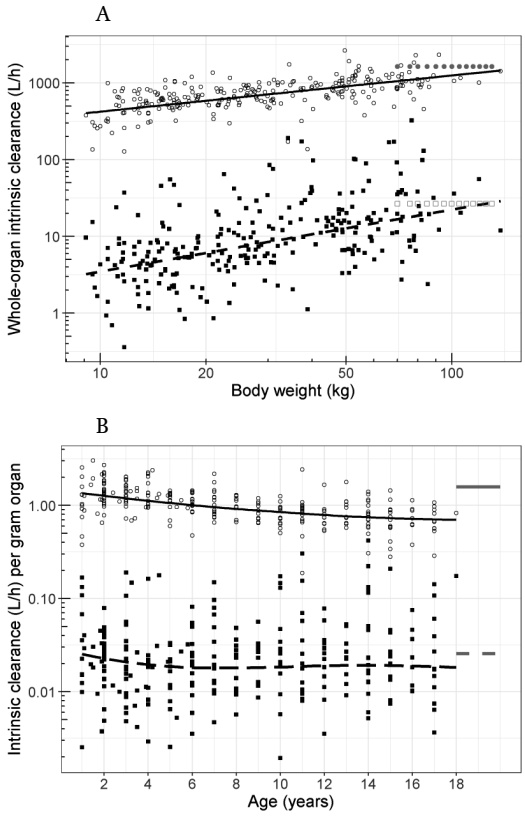



**Figure 2**. First-pass metabolism parameters in children. **A**) Intrinsic whole-organ intestinal (n) and hepatic (○) clearance versus body weight, both individually predicted (symbols) and the population predictions (lines) for children in our study. Also illustrated are the reported literature values of 26.7 and 1640 L/h for intestinal (o) and hepatic (•) clearance in adults, respectively (13). **B**) Intrinsic gut wall (n) and hepatic (○) clearance per gram of organ versus age for children in our study and for adults(–), both individually predicted (symbols) and a loess curve of the population predictions (lines) for children in our study.

between individuals (factor of 5-405, 95%CI). When the gut wall and hepatic intrinsic clearances are expressed per gram of organ, an inverse trend can be observed for hepatic intrinsic CYP3A activity per gram of organ. In figure 2b, the intrinsic clearance per gram of organ are plotted versus age, which shows a (slight) decrease in hepatic intrinsic CYP3A activity per gram of liver with age, while no change with age is observed for gut wall intrinsic CYP3A activity per gram of small intestine except for a small drop around the age of 4-5 years.

Using equation 15, the total plasma clearance was derived and plotted against body weight, showing that total plasma clearance also increases with body weight (figure 3). For comparison, in figure 2a, 2b and 3, literature values on whole-organ intrinsic and total plasma clearance in adults have been added (13).

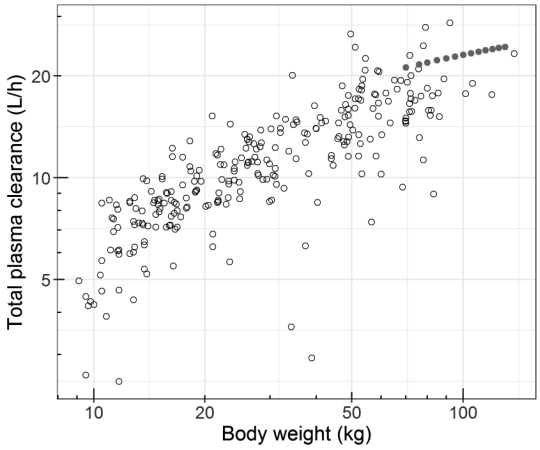



**Figure 3.** Total hepatic plasma clearance versus body weight for children in our study (○) and calculated plasma clearance in adults (•) based on the reported typical hepatic whole-organ intrinsic clearance of 1640 L/h, a hepatic blood flow increasing with body weight ($Q_h = 3.75 \cdot WT^{0.75}$), a fraction unbound of 0.0303 and a blood: plasma ratio of 0.66 (13) using equation 15.

Using the estimated whole-organ intrinsic clearance values, together with blood flow and fraction unbound, the extraction ratios $E_g$ and $E_h$ (eq. 8 and 9) and bioavailability values $F_g$ and $F_h$ (i.e. 1-$E_g$ or $E_h$, respectively) were derived. Figure 4 shows the results with gut wall bioavailability first slightly increasing and then decreasing with age, while the hepatic bioavailability showed an overall increase with age. More specifically, the hepatic bioavailability is increasing with body weight from a median of 58% (range 35-79%) to 73% (range 58-86%) from 1-2 year old to children 12-18 years of age ($p<0.001$, Wilcoxon-Mann-Whitney U-test) (figure 4). With respect to the gut wall bioavailability, the median of 37% (range 8-85%) in 1-2 year old children increases to 39% (range 6-82%) in children of 3-5 years of age, then to decrease to 34% (range 3-84%) and 29% (range 4-66%) in children of 6-12 and 12-18 years of age,

respectively. With total bioavailability being equal to $F_g$ times $F_h$ (eq. 7), figure 4 shows that no or only small changes in the total bioavailability for children up to 12 years of age can be expected. In adolescents, the gut wall, hepatic and total bioavailability proved not significantly different from the values observed in adults which were obtained from literature ($p>0.05$).

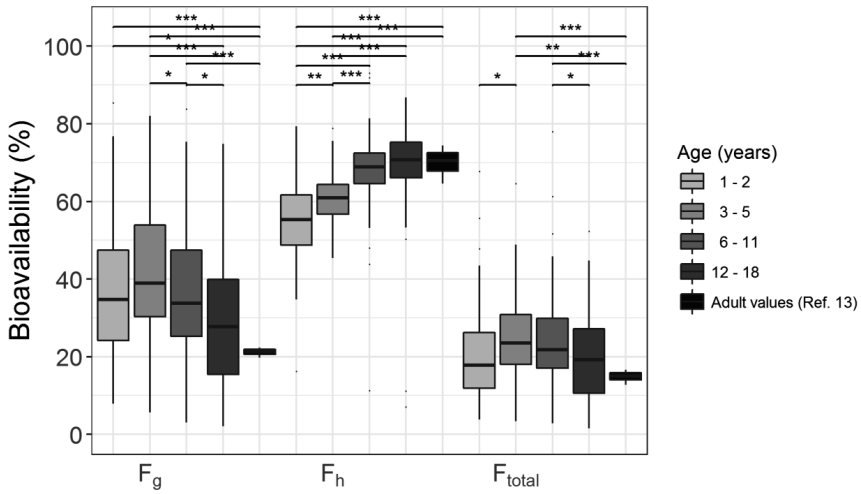



**Figure 4.** Bioavailability in in the gut wall ($F_g$), in the liver ($F_h$) and total bioavailability ($F_{total}$) for four different age categories: children of 1-2 years, 3-5 years, 6-11 years and 12-18 years of age (increasing dark grey) compared to adult values (13). A nonparametric test of group differences was performed using the independent 2-group Wilcoxon-Mann-Whitney Test, with *** indicating a p-value <0.001, ** for p<0.01, * for p<0.05 and 'NS' for p>0.05. Adult bioavailability values are calculated based on their reported typical whole-organ intrinsic hepatic clearance, hepatic blood flow for their body weight and the fraction unbound (see eq. 8 and 9) (13).

Figure S3 shows the goodness-of-fit plots of both midazolam and its primary metabolite. These plots for midazolam indicated no bias for midazolam in the individual and population concentration predictions versus the observed concentrations (figure S3 A,B) and no trend or bias in the conditionally weighted residuals versus the predicted concentrations or time after dose (figure S3 C,D). Also the presystemic formation of 1-OH-midazolam was well described by the model, as except for a small under prediction of the peak concentrations (figure S3 E), no bias in the goodness-of-fit plots for the metabolite was observed (figure S3 E-H). The normalized prediction distribution error (NPDE) results showed no bias in the concentration predictions for both midazolam and 1-OH-midazolam (figure S4), indicating no structural model misspecification. The variance of midazolam concentrations however was under-estimated in our model (Fisher variance test,

p<0.001), while the model adequately captures the variability for 1-OH-midazolam concentrations.
The sensitivity analysis (table SII) showed that changing volumes of the gut wall or liver by 50% does not considerably impact the predicted concentrations (<10%) nor our parameter estimates for whole-organ intrinsic clearance for gut wall and liver. With a 50% increase or decrease in hepatic blood flow, the whole-organ intrinsic hepatic clearance inversely changes with -14% and +49% respectively. A similar trend was found for intestinal blood flow and intestinal length (table SII). A change in fraction unbound in blood resulted in a change in whole-organ intrinsic hepatic clearance by the same factor. If the fraction midazolam that gets absorbed ($F_a$) is smaller than 100%, the median total bioavailability does not change considerably. While the hepatic bioavailability is not impacted, the gut wall bioavailability however increases by 4.1 and 18.7% for an $F_a$ of 0.90 and 0.80, respectively. A change in the volume of distribution of the primary metabolite leads to considerable changes in all clearance parameters. All results of the sensitivity analysis are summarized in the supplemental material (table SII).

## DISCUSSION

To characterize both intestinal and hepatic CYP3A-mediated metabolism of midazolam in children between 1 and 18 years of age, a physiological population PK model was developed (figure 1). The physiological population PK modelling approach we applied has been previously applied in healthy adults (13) and morbidly obese versus bariatric surgery patients (14), and this approach has now proven useful in distinguishing between metabolism by intestinal and hepatic CYP3A enzymes in children as well.

Using PK data from one of the few clinical studies in which children varying in age between 1 and 18 years old received midazolam orally (17), we showed that the whole-organ intrinsic clearance of gut wall and liver do not change in parallel (figure 2a). For all pediatric ages, the intrinsic hepatic clearance is higher than the intrinsic gut wall clearance, while the gut wall clearance appears to increase slightly faster than hepatic clearance (figure 2a). The estimated clearance values for the patients with the highest body weight (>16 years of age) are with 16.1 L/h and 1051 L/h in the same order of magnitude as the reported values of 26.7 L/h and 1640 L/h for intrinsic intestinal and hepatic clearance in adults respectively (13). As we used the whole-organ intrinsic clearance of midazolam as surrogate marker of total hepatic and intestinal CYP3A activity in this study, we found that the total intestinal CYP3A activity is lower than the hepatic CYP3A activity. However, when expressed

per gram of organ, no increase in intrinsic gut wall clearance per gram of organ can be observed, while the intrinsic hepatic clearance per gram of liver is highest in the youngest children and decreases with age (figure 2b).

The increase in whole-organ intrinsic clearance in the gut wall we report here can be mostly attributed to the organ growth and the increasing total weight of the enterocytes in children (33, 34), as per gram of gut wall no trend with increasing age (figure 2b) or body weight can be observed in children >2 year of age. The intrinsic intestinal CYP3A4 expression per gram of small intestine in children has been described to be slightly higher in children < 2 years of age, compared to 2-5 year old children, and then increases with age (33). This is in agreement with the small drop in gut wall intrinsic CYP3A activity per gram of small intestine we observe around the age of 4-5 years (figure 2b), and in combination with the other physiological changes this leads to a higher gut wall bioavailability in children 3-5 year of age compared to children 1-2 years of age, and a decrease in gut wall bioavailability with increasing age in children >3 years of age, which is in agreement with the trend observed in figure 4.

We report the whole-liver intrinsic hepatic CYP3A-mediated metabolism to increase with increasing body weight, which can be attributed to an increasing total liver weight (4). In literature, the amount of microsomal protein in the liver is believed to remain constant with age (35), while the CYP3A4 abundance per gram of microsomal protein (8, 36) has been reported to increase with age. Our results however show a slight decrease in intrinsic clearance per gram of liver throughout the pediatric age range, suggesting that the absolute abundance or activity of CYP3A4 per gram of liver slightly decreases with age in children 1-18 years of age.

The extraction ratios $E_g$ and $E_h$ can be derived from the estimated whole-organ intrinsic clearance, the organ blood flows and the fraction unbound (Eq. 8 and 9), and can be subsequently used to calculate the bioavailability (i.e. $F_g$ and $F_h$). The fraction escaping gut wall metabolism was found to be smaller (median $F_g$ 0.34, range 0.02-0.85) than the fraction escaping hepatic metabolism (median $F_h$ 0.66, range 0.35-0.93). These values for hepatic bioavailability are in agreement with previously reported values in adults (13, 37). The median hepatic bioavailability increases with body weight due to a smaller increase in whole-organ intrinsic hepatic clearance relative to the hepatic blood flow (figure 4), while an inverse, but smaller age-related trend in median intestinal bioavailability was found as the effective blood flow in the gut wall ($Q_{gut}$) increases less with age than the whole-organ intrinsic intestinal clearance.

In adults, the local bioavailability in the gut wall is much lower than in the liver with reported values for $F_g$ and $F_h$ around 0.2 and 0.7, respectively (13), and therefore in adults the extraction ratio in the gut wall is higher than in the liver, indicating that intestinal CYP3A enzymes play a large role in presystemic metabolism despite the low whole-organ intrinsic clearance. In children, the intrinsic gut wall CYP3A activity is lower than in adults (figure 2a), and together with a lower effective blood flow, this leads to a higher gut wall bioavailability compared to adults (figure 4). This indicates that the role of gut wall metabolism in presystemic metabolism is smaller in children compared to adults, and also gets smaller with decreasing age. This is compensated by the increased whole-organ intrinsic hepatic CYP3A-mediated intrinsic clearance (figure 2a), which together with the hepatic blood flow leads to lower hepatic bioavailability with decreasing age (figure 4), resulting in an age-independent total bioavailability $F_{total}$ with a median value of 20.8% (figure 4).

The parameters for clearance and total bioavailability are in agreement with literature. For clearance, the plasma clearance can be calculated based on the estimated intrinsic hepatic clearance, the fraction unbound, the hepatic blood flow and the blood-to-plasma ratio (equation 15). The derived total plasma clearance of 6.0 L/h in the youngest children of 1-2 years of age to 17.5 L/h in the older children ≥16 years of age (figure 3), is in agreement with literature values of 0.6 L/h/kg (0.56-0.68 L/h/kg) (28). For patients in the age range between 2 months and 3 years, median clearance values around 9 L/h have been reported in patients after major craniofacial surgery (38) and in patients with severe malaria (39), which is in agreement with our findings. Furthermore, it has been reported that disease severity impacts CYP3A-mediated clearance (40), and as the children in this study are relatively healthy (ASA criterion I or II), clearance is indeed a factor 2-4 higher than the reported midazolam clearance in critically ill children (40-43).

For bioavailability, the median total bioavailability of 20.8% (mean 22.7 ± 12.4%) across the pediatric age range is similar to the reported median value of 13.4% (13) or the reported mean ± SD of 34.3% ± 10% (37) in adults, but the observed variability in total bioavailability in the children in our study was very large, with values ranging from 1.5-77.9% A previous study in pediatric patients ranging in age from 6 months to 16 years, who had ASA physical status I-III, found similar values for bioavailability (28) and also found a large variability with the bioavailability ranging from 9-71% (28). This high variability has also been described in other studies (44, 45), and may be explained by the high unexplained variability in intestinal CYP3A activity, which may be due to e.g. the circadian rhythm (46), the (genetic) variability in CYP3A5 expression (47), and the different regulation of the gut (11) as a result of exposure to variable food and other environmental effects in different individuals throughout

their life (48). This implicates that oral administration will result in highly variable PK profiles and exposure of CYP3A substrates in children, which is relevant in the clinic setting as well as during drug development.

All parameters in the model could be estimated with good precision (RSE<30%, table II) and the model stability was evaluated by bootstrap (table II), which confirmed the precision of the parameter estimates. Furthermore, the goodness-of-fit plots showed that the concentrations of both midazolam and 1-OH-midazolam were well-predicted without bias (figure S3), indicating accurate model predictions for both the parent compound and the metabolite. Figure S4 shows the normalized prediction distribution errors versus predicted concentrations and versus time after first dose, which demonstrates accurate prediction of the midazolam and 1-OH-midazolam concentrations and variability, with only a small over-prediction of the variability of midazolam.

The model is based on accepted PBPK principles, and well-known equations and parameter values from the literature have been used. For unknown parameter values in the pediatric population, assumptions and scaling methods were applied and a sensitivity analysis was performed for these parameters (Table SII). For hepatic blood flow, the flow was assumed to be a fixed percentage of the cardiac output (25.5% in boys and 28% in girls) (27), which results in blood flow values in agreement with other literature values (49, 50). The sensitivity analysis indicated that if the hepatic or the intestinal blood flow would be 50% higher or lower, that peak concentrations would be impacted, but the derived values for extraction ratio and bioavailability were not impacted by this assumption. Moreover, actual blood flows will likely deviate less than 50% from the assumed flows. The assumed tissue volumes (figure S2 C) are in agreement with other literature values (51), and the sensitivity analysis indicated no impact of these assumptions on the results regarding the predicted plasma concentrations and the derived values for extraction ratio and bioavailability. Plasma protein binding to albumin has been accounted for in the model (eq. 2), while no protein binding to other plasma proteins was assumed, and the range of fraction bound was with 96.1-96.4% in agreement with the 97.0% protein binding reported in adults (figure S2 A). Furthermore, our sensitivity analysis indicated that assuming 50% increase or decrease in intestinal length, would lead to +9.3 or -37.2% change in whole-organ intrinsic gut wall clearance respectively, without affecting the estimated extraction ratio and bioavailability. This is because the intestinal length impacts the permeability factor of the gut wall and thereby the effective blood flow in the gut wall. Since the amount of drug reaching the systemic circulation is derived from the PK data and does not change, an increase in intestinal length is

compensated by a decrease in whole-organ intrinsic gut wall clearance so that the extraction ratio and bioavailability remain constant.

The absorption rate constant could not be estimated in our model, as sampling at early time points was limited and therefore we included an absorption rate constant of 4.16 $h^{-1}$, which means that maximum concentrations are reached around 30 minutes post-dose, which was close to the median observed $T_{max}$ and reported values in literature (28). As in this study only oral midazolam was administered, we could not estimate the volume of distribution for midazolam and its metabolite. We therefore linearly scaled the volumes of the central and peripheral compartments from a 76kg healthy adult (13) to children. The sensitivity analysis showed that the volume of distribution of the metabolite is impacting all estimated clearance parameters considerably (Table SII), but the assumed distribution volumes are in agreement with previously reported values for volume of distribution in children (28, 39). Moreover, since we could not estimate inter-individual variability (IIV) in volume of distribution, all inter-individual variability is in the model attributed to the intrinsic clearance parameters and the residual variability, both of which may therefore be inflated.

Furthermore, we assumed that all midazolam is metabolized by CYP3A into its primary metabolite, 1-OH-midazolam, and the volume and clearance values of the metabolite should therefore be considered as apparent values assuming a 100% formation. As these assumptions on volume of distribution and fraction metabolized are supported by literature (28, 39), the PK data of both midazolam and 1-OH-midazolam are well-described (figure S3, S4), and the intrinsic clearance values lead to total plasma clearance and bioavailability in range with previous published work (28, 38, 39), the intestinal and hepatic intrinsic clearance values are indeed well-estimated by the model and could therefore be used as surrogate marker for gut wall and hepatic CYP3A activity in children. As hepatic CYP3A4 is the most abundance cytochrome P450 enzyme and responsible for metabolism of a wide variety of therapeutics, the observed midazolam clearance as probe for CYP3A activity may have implications for other CYP3A substrates as well. It is also clinically relevant for patients receiving multiple CYP3A substrates or inhibitors/enhancers as different drug-drug interactions in children versus adults may be anticipated. However, as the variability in oral bioavailability is very high, a highly variable drug exposure may be anticipated when CYP3A substrates are orally administered.

To conclude, this is the first study in children 1 – 18 years of age to distinguish between pediatric intestinal and hepatic CYP3A-mediated metabolism using clinical data together with PBPK principles. The results show that the whole-organ intrinsic hepatic clearance appears much higher than the gut wall clearance, but also that

the difference between the whole-organ intrinsic clearances in children is smaller compared to adults. As a result, the intrinsic CYP3A-mediated gut wall clearance in children from 1-18 years of age contributes less to the overall first-pass metabolism compared to adults. Organ growth is the most important contributing factor to the increase in the whole-organ intrinsic CYP3A clearance in gut wall and liver with age, given the fact that the intestinal CYP3A activity per gram of organ remained relatively constant throughout childhood and the hepatic CYP3A activity per gram of liver even decreased slightly. While intestinal bioavailability decreased with age, the hepatic bioavailability increased with age, resulting in no change in total bioavailability in children with increasing age and body weight. This indicates an age-independent but highly variable first-pass effect by intestinal and hepatic CYP3A enzymes in children from 1-18 years of age.

## ACKNOWLEDGEMENTS

CAJ Knibbe was supported by an NWO Vidi grant (Knibbe 2013). The authors would like to thank Anthony Gebhart (LACDR, Leiden University) for the code review. Drs. Jeff Galinken and Peter Adamson were the PIs on the original study conducted at CHOP and the study was supported by NIH / NICHD, Pediatric Pharmacology Research Unit, Grant # HD037255-06.

## REFERENCES

1. Debotton N, Dahan A. A mechanistic approach to understanding oral drug absorption in pediatrics: an overview of fundamentals. Drug Discov Today. 2014;19(9):1322-36.
2. Bai JPF, Burckart GJ, Mulberg AE. Literature Review of Gastrointestinal Physiology in the Elderly, in Pediatric Patients, and in Patients with Gastrointestinal Diseases. J Pharm Sci. 2016;105(2):476-83.
3. Mooij MG, de Koning BA, Huijsman ML, de Wildt SN. Ontogeny of oral drug absorption processes in children. Expert Opin Drug Metab Toxicol. 2012;8(10):1293-303.
4. Bjorkman S. Prediction of drug disposition in infants and children by means of physiologically based pharmacokinetic (PBPK) modelling: theophylline and midazolam as model drugs. Br J Clin Pharmacol. 2005;59(6):691-704.
5. Danielson PB. The cytochrome P450 superfamily: biochemistry, evolution and drug metabolism in humans. Curr Drug Metab. 2002;3(6):561-97.
6. Paine MF, Hart HL, Ludington SS, Haining RL, Rettie AE, Zeldin DC. The human intestinal cytochrome P450 "pie". Drug Metab Dispos. 2006;34(5):880-6.
7. van Herwaarden AE, van Waterschoot RA, Schinkel AH. How important is intestinal cytochrome P450 3A metabolism? Trends Pharmacol Sci. 2009;30(5):223-7.

8. Hines RN, McCarver DG. The ontogeny of human drug-metabolizing enzymes: phase I oxidative enzymes. J Pharmacol Exp Ther. 2002;300(2):355-60.
9. Stevens JC, Hines RN, Gu C, Koukouritaki SB, Manro JR, Tandler PJ, et al. Developmental expression of the major human hepatic CYP3A enzymes. J Pharmacol Exp Ther. 2003;307(2):573-82.
10. de Wildt SN, Kearns GL, Leeder JS, van den Anker JN. Cytochrome P450 3A: ontogeny and drug disposition. Clin Pharmacokinet. 1999;37(6):485-505.
11. Bailey DG, Malcolm J, Arnold O, Spence JD. Grapefruit juice-drug interactions. Br J Clin Pharmacol. 1998;46(2):101-10.
12. Johnson TN, Rostami-Hodjegan A, Tucker GT. Prediction of the clearance of eleven drugs and associated variability in neonates, infants and children. Clin Pharmacokinet. 2006;45(9):931-56.
13. Frechen S, Junge L, Saari TI, Suleiman AA, Rokitta D, Neuvonen PJ, et al. A semiphysiological population pharmacokinetic model for dynamic inhibition of liver and gut wall cytochrome P450 3A by voriconazole. Clin Pharmacokinet. 2013;52(9):763-81.
14. Brill MJ, Valitalo PA, Darwich AS, van Ramshorst B, van Dongen HP, Rostami-Hodjegan A, et al. Semiphysiologically based pharmacokinetic model for midazolam and CYP3A mediated metabolite 1-OH-midazolam in morbidly obese and weight loss surgery patients. CPT Pharmacometrics Syst Pharmacol. 2016;5(1):20-30.
15. Rostami-Hodjegan A. Reverse Translation in PBPK and QSP: Going Backwards in Order to Go Forward With Confidence. Clin Pharmacol Ther. 2017.
16. Thummel KE, Shen DD, Podoll TD, Kunze KL, Trager WF, Hartwell PS, et al. Use of midazolam as a human cytochrome P450 3A probe: I. In vitro-in vivo correlations in liver transplant patients. J Pharmacol Exp Ther. 1994;271(1):549-56.
17. Gupta M, Edginton A, Willmann S, Adamson PC, Galinkin JL, Barrett JS. Model-based Approaches to Investigate Pharmacogenetic and Developmental Sources of Variation in the Pharmacokinetics of Midazolam after Oral administration in Children. 2006 [Available from: AAPS 2006. Abstract 003255. https://abstracts.aaps.org/Published/Browse.aspx]
18. Maharaj AR, Barrett JS, Edginton AN. A workflow example of PBPK modeling to support pediatric research and development: case study with lorazepam. AAPS J. 2013;15(2):455-64.
19. Irwin JJ, Kirchner JT. Anemia in children. Am Fam Physician. 2001;64(8):1379-86.
20. McNamara PJ, Alcorn J. Protein binding predictions in infants. AAPS PharmSci. 2002;4(1):E4.
21. Ito K, Ogihara K, Kanamitsu S, Itoh T. Prediction of the in vivo interaction between midazolam and macrolides based on in vitro studies using human liver microsomes. Drug Metab Dispos. 2003;31(7):945-54.
22. Mandema JW, Tuk B, van Steveninck AL, Breimer DD, Cohen AF, Danhof M. Pharmacokinetic-pharmacodynamic modeling of the central nervous system effects of midazolam and its main metabolite alpha-hydroxymidazolam in healthy volunteers. Clin Pharmacol Ther. 1992;51(6):715-28.
23. Beal SL. Ways to fit a PK model with some data below the quantification limit. J Pharmacokinet Pharmacodyn. 2001;28(5):481-504.
24. Yang J, Kjellsson M, Rostami-Hodjegan A, Tucker GT. The effects of dose staggering on metabolic drug-drug interactions. Eur J Pharm Sci. 2003;20(2):223-32.

25. Johnson TN, Tucker GT, Tanner MS, Rostami-Hodjegan A. Changes in liver volume from birth to adulthood: a meta-analysis. Liver Transpl. 2005;11(12):1481-93.
26. Arbeille P, Avan P, Treffel L, Zuj K, Normand H, Denise P. Jugular and Portal Vein Volume, Middle Cerebral Vein Velocity, and Intracranial Pressure in Dry Immersion. Aerosp Med Hum Perform. 2017;88(5):457-62.
27. Simcyp (R) Simulator version 15.1. Certara, Sheffield, United Kingdom. Available from: https://www.certara.com/software/physiologically-based-pharmacokinetic-modeling-and-simulation/simcyp-simulator/ [
28. Reed MD, Rodarte A, Blumer JL, Khoo KC, Akbari B, Pou S, et al. The single-dose pharmacokinetics of midazolam and its primary metabolite in pediatric patients after oral and intravenous administration. J Clin Pharmacol. 2001;41(12):1359-69.
29. Gorski JC, Hall SD, Jones DR, VandenBranden M, Wrighton SA. Regioselective biotransformation of midazolam by members of the human cytochrome P450 3A (CYP3A) subfamily. Biochem Pharmacol. 1994;47(9):1643-53.
30. Yang J, Jamei M, Yeo KR, Tucker GT, Rostami-Hodjegan A. Prediction of intestinal first-pass drug metabolism. Curr Drug Metab. 2007;8(7):676-84.
31. Yafune A, Ishiguro M. Bootstrap approach for constructing confidence intervals for population pharmacokinetic parameters. I: A use of bootstrap standard error. Stat Med. 1999;18(5):581-99.
32. Comets E, Brendel K, Mentre F. Computing normalised prediction distribution errors to evaluate nonlinear mixed-effect models: the npde add-on package for R. Comput Methods Programs Biomed. 2008;90(2):154-66.
33. Johnson TN, Tanner MS, Taylor CJ, Tucker GT. Enterocytic CYP3A4 in a paediatric population: developmental changes and the effect of coeliac disease and cystic fibrosis. Br J Clin Pharmacol. 2001;51(5):451-60.
34. Lu H, Rosenbaum S. Developmental pharmacokinetics in pediatric populations. J Pediatr Pharmacol Ther. 2014;19(4):262-76.
35. Barter ZE, Bayliss MK, Beaune PH, Boobis AR, Carlile DJ, Edwards RJ, et al. Scaling factors for the extrapolation of in vivo metabolic drug clearance from in vitro data: reaching a consensus on values of human microsomal protein and hepatocellularity per gram of liver. Curr Drug Metab. 2007;8(1):33-45.
36. Treluyer JM, Bowers G, Cazali N, Sonnier M, Rey E, Pons G, et al. Oxidative metabolism of amprenavir in the human liver. Effect of the CYP3A maturation. Drug Metab Dispos. 2003;31(3):275-81.
37. Lee JI, Chaves-Gnecco D, Amico JA, Kroboth PD, Wilson JW, Frye RF. Application of semisimultaneous midazolam administration for hepatic and intestinal cytochrome P450 3A phenotyping. Clin Pharmacol Ther. 2002;72(6):718-28.
38. Peeters MY, Prins SA, Knibbe CA, Dejongh J, Mathot RA, Warris C, et al. Pharmacokinetics and pharmacodynamics of midazolam and metabolites in nonventilated infants after craniofacial surgery. Anesthesiology. 2006;105(6):1135-46.
39. Muchohi SN, Kokwaro GO, Ogutu BR, Edwards G, Ward SA, Newton CR. Pharmacokinetics and clinical efficacy of midazolam in children with severe malaria and convulsions. Br J Clin Pharmacol. 2008;66(4):529-38.
40. Vet NJ, Brussee JM, de Hoog M, Mooij MG, Verlaat CW, Jerchel IS, et al. Inflammation and Organ Failure Severely Affect Midazolam Clearance in Critically Ill Children. Am J Respir Crit Care Med. 2016;194(1):58-66.

41. Brussee JM, Vet NJ, Krekels EHJ, Valkenburg AJ, Jacqz-Aigrain E, van Gerven JMA, et al. Predicting CYP3A-mediated midazolam metabolism in critically ill neonates, infants, children, and adults with inflammation and organ failure. Br J Clin Pharmacol. 2018 Feb;84(2):358-368.
42. de Wildt SN, de Hoog M, Vinks AA, van der Giesen E, van den Anker JN. Population pharmacokinetics and metabolism of midazolam in pediatric intensive care patients. Crit Care Med. 2003;31(7):1952-8.
43. Bienert A, Bartkowska-Sniatkowska A, Wiczling P, Rosada-Kurasinska J, Grzeskowiak M, Zaba C, et al. Assessing circadian rhythms during prolonged midazolam infusion in the pediatric intensive care unit (PICU) children. Pharmacol Rep. 2013;65(1):107-21.
44. Blumer JL. Clinical pharmacology of midazolam in infants and children. Clin Pharmacokinet. 1998;35(1):37-47.
45. Payne K, Mattheyse FJ, Liebenberg D, Dawes T. The pharmacokinetics of midazolam in paediatric patients. Eur J Clin Pharmacol. 1989;37(3):267-72.
46. van Rongen A, Kervezee L, Brill M, van Meir H, den Hartigh J, Guchelaar HJ, et al. Population Pharmacokinetic Model Characterizing 24-Hour Variation in the Pharmacokinetics of Oral and Intravenous Midazolam in Healthy Volunteers. CPT Pharmacometrics Syst Pharmacol. 2015;4(8):454-64.
47. Kirwan CJ, MacPhee IA, Lee T, Holt DW, Philips BJ. Acute kidney injury reduces the hepatic metabolism of midazolam in critically ill patients. Intensive Care Med. 2012;38(1):76-84.
48. Walter-Sack I, Klotz U. Influence of diet and nutritional status on drug metabolism. Clin Pharmacokinet. 1996;31(1):47-64.
49. Williams LR, Leggett RW. Reference values for resting blood flow to organs of man. Clin Phys Physiol Meas. 1989;10(3):187-217.
50. Price PS, Conolly RB, Chaisson CF, Gross EA, Young JS, Mathis ET, et al. Modeling interindividual variation in physiological factors used in PBPK models of humans. Crit Rev Toxicol. 2003;33(5):469-503.
51. Haddad S, Restieri C, Krishnan K. Characterization of age-related changes in body weight and organ weights from birth to adolescence in humans. J Toxicol Environ Health A. 2001;64(6):453-64.
52. Basic anatomical and physiological data for use in radiological protection: reference values. A report of age- and gender-related differences in the anatomical and physiological characteristics of reference individuals. ICRP Publication 89. Ann ICRP. 2002;32(3-4):5-265.

# SUPPLEMENTAL MATERIAL (CHAPTER 6)

## Supplemental methods

Calculation of height of children was based on age, using formulas from Simcyp® Physiologically-based Pharmacokinetic Modelling and Simulation software [1]. Equations S1 and S2 show the formula for height (HT) in cm based on age in years for boys and girls respectively:

$HT_{male} = 1.76179\times10^{-5}\times age^{7} - 1.19874\times10^{-3}\times age^{6} + 0.0323848\times age^{5} - 0.444112\times age^{4} + 3.2946\times age^{3} - 13.2191\times age^{2} + 33.75\times age + 52.62152$ (eq. S1).

$HT_{female} = -1.51027\times10^{-6}\times age^{8} + 1.21261\times10^{-4}\times age^{7} - 0.0040023\times age^{6} + 0.070179\times age^{5} - 0.708233\times age^{4} + 4.1872\times age^{3} - 14.3393\times age^{2} + 33.84778\times age + 51.535477$ (eq. S2)

The body surface area in $m^2$ was calculated using equations S3 [2] and S4 [3] for children lower than 15 kg and for children of 15 kg and heavier respectively:

$BSA_{<15kg}\ [m^2] = 0.007184 \times HT[cm]^{0.725} \times WT[kg]^{0.425}$ (eq. S3)

$BSA_{\geq15kg}\ [m^2] = 0.024265 \times HT[cm]^{0.3964} \times WT[kg]^{0.537}$ (eq. S4)

**Table SI.** Data characteristics

| | Densely sampled patients | Sparsely sampled patients | All patients |
|---|---|---|---|
| **No. of dosages** | 31 (1/pt) | 233 (1/pt) | 264 (1/pt) |
| **No. of samples** | 327 | 538 | 865 |
| **Samples/patient** | 10 (8-11) | 2 (1-3) | 2 (1-11) |
| **Age (years)** | 8 (1-17) | 7 (1-18) | 7 (1-18) |
| **Body weight (kg)** | 30.2 (9.5-83.2) | 26.8 (9.1-137.6) | 27.4 (9.1-137.6) |
| **Male/female (%)** | 15/16 (48/52%) | 133/100 (57/43%) | 148/116 (56/44%) |
| **Dose (mg)** | 12.5 (3-15) | 10 (3.5-10) | 10 (3-15) |

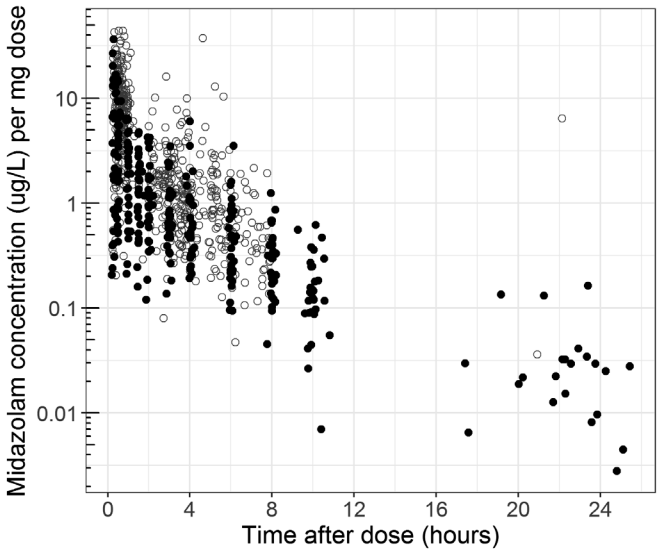



**Figure S1.** Dose-corrected midazolam concentrations in blood over time for patients who are densely sampled (•) and who are sparsely sampled (○).

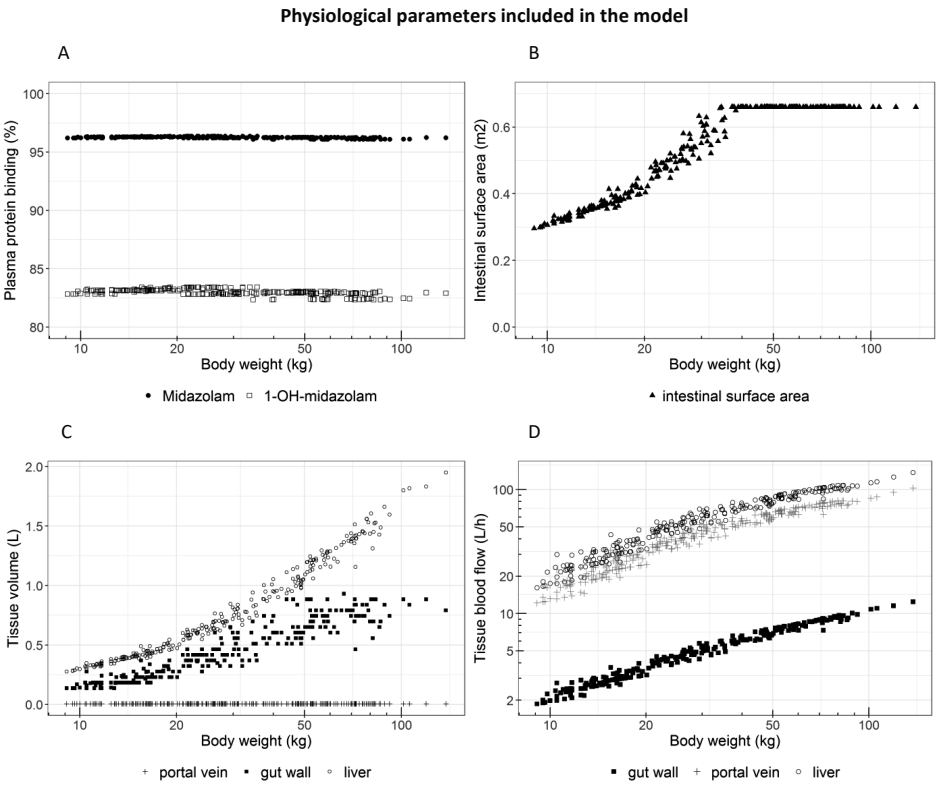
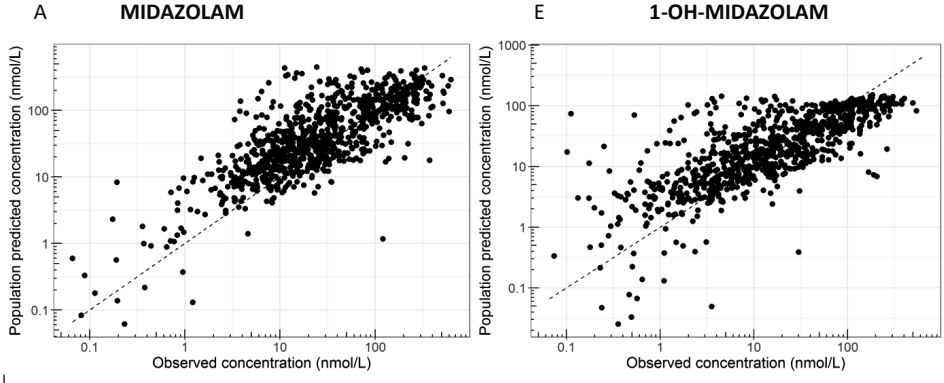



**Figure S2.** Visualization of relationships between body weight and parameters included in the physiological population PK model for the individuals in the study. For each individual, their actual age, sex, body weight and body surface area are used to calculate the physiological parameters using the formulas from table I, and therefore individuals of the same bodyweight can have different parameter values. **A**) Plasma protein binding for midazolam and 1-OH-midazolam. **B**) Intestinal surface area based on body surface area (eq. 12-14). **C**) Tissue volumes for the gut wall, and liver, which are based on body surface area and age, respectively (eq. 4-5) and the portal vein volume of 5.2 mL. **D**) Tissue blood flows for the gut wall, portal vein and liver, based on cardiac output (eq. 6) and sex. Liver blood flow is the sum of portal vein and hepatic artery flow, which contribute 75% and 25% to the total $Q_h$, respectively.



## Supplemental results

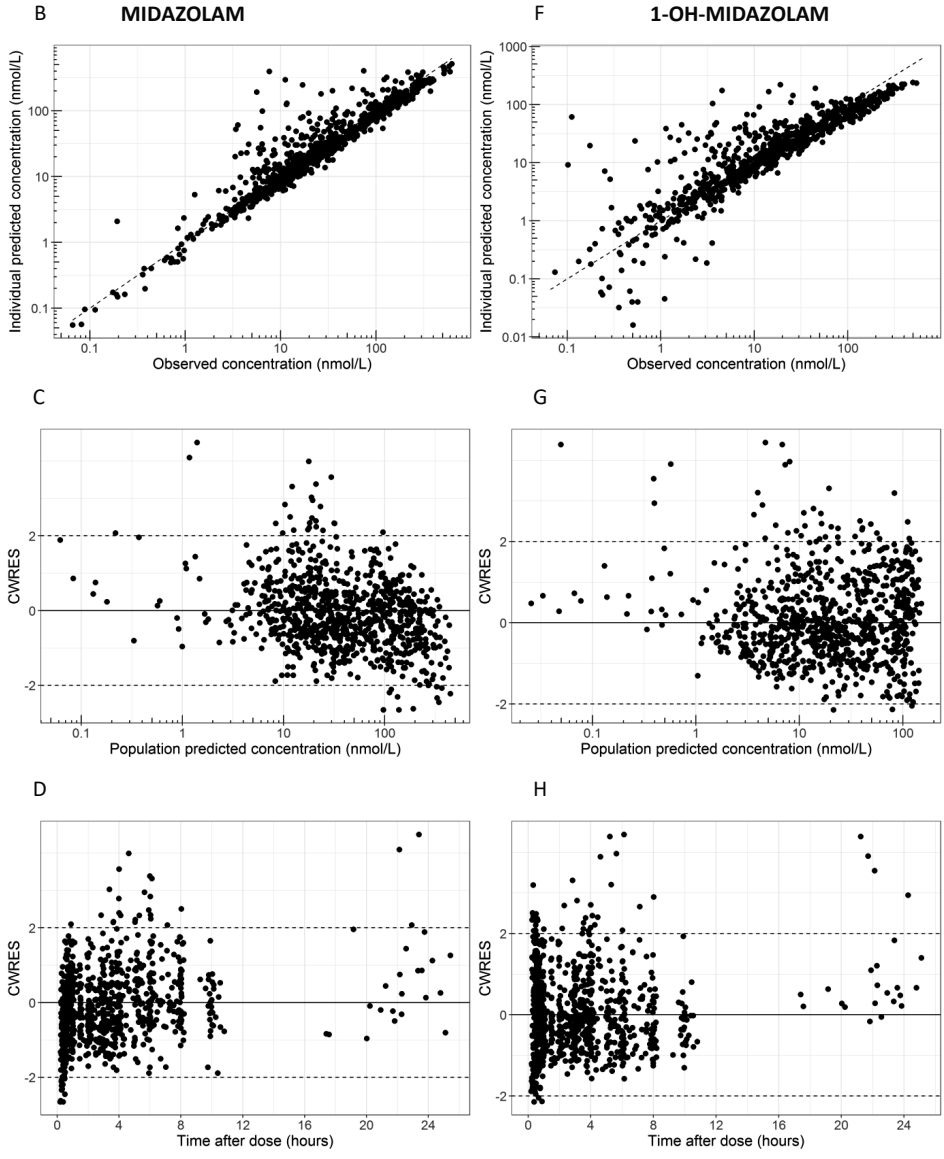



**Figure S3.** Goodness-of-fit plots for midazolam (A-D) and its primary metabolite 1-OH-midazolam (E-H). Plots include individual and population predicted concentration versus observed concentration (A,B,E,F) and conditionally weighted residuals (CWRES) versus predicted concentration (C,G) and versus time after dose (D,H).

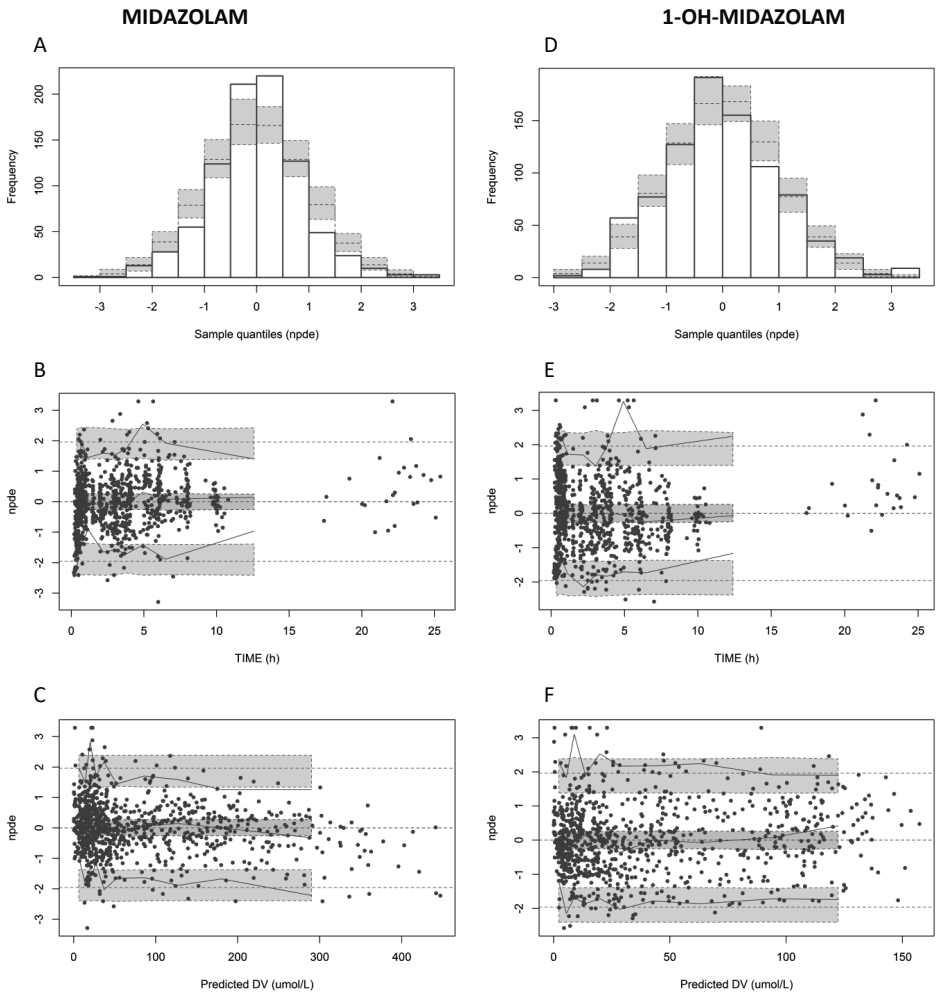



**Figure S4.** Visualization of the normalized prediction distribution error (NPDE) results for midazolam (**A-C**) and 1-OH-midazolam (**D-F**). First row show the histograms of NPDEs (**A,D**), with the white bars indicating the observed frequency of sample quantiles of the NPDEs, overlaid with the density of the standard normal distribution in blue bars. Second and third row show the NPDE versus time (**B,E**) and versus predicted concentration (**C,F**) respectively, in which the dots represent the NPDE for each observation, the lines indicate the mean (red) and the 95th percentiles (blue) of the NPDEs, and the shaded areas are the simulated 95% confidence intervals of the NPDE median (red) and 95th percentiles (blue).The mean NPDE for midazolam and 1-OH-midazolam were, with 0.003 and -0.004, respectively, not significantly different from 0 (Wilcoxon signed rank test, $p>0.1$), but the variance for midazolam of 0.76 ($p<0.001$) was significantly different from 1, while the variance for 1-OH-midazolam of 1.07 ($p>0.1$) was not significantly different from 1 (Fisher variance test).

**Table SII.** Results of the sensitivity analysis. The impact on the PK profile of midazolam was evaluated using model simulations, and the impact on the estimated whole-organ intrinsic clearance parameters was assessed based on re-estimation.

| | | Midazolam PK profile | Intrinsic clearance |
|---|---|---|---|
| **Tissue volumes** | $V_h$ +/-50% | x | $CL_{H,int}$ -5.5%/-17% & $CL_{G,int}$ -16%/+2.0% |
| | $V_{gw}$ +/-50% | x | $CL_{H,int}$ -1.5%/-7.0% & $CL_{G,int}$ -12%/-11% |
| **Organ blood flows** | $Q_h$ +/-50% | $C_{max}$ +15%/-40% | $CL_{H,int}$ -14%/+49% & $CL_{G,int}$ +4.7%/-67% |
| | $Q_{vi}$ +/-50% | $C_{max}$ +15%/-25% | $CL_{H,int}$ -11%/-0.6% & $CL_{G,int}$ +9.5%/-44% |
| **Intestinal length** | +/-50% | x | $CL_{H,int}$ -14%/-4.8% & $CL_{G,int}$ +9.3%/-37% |
| **Fraction unbound** | $F_{u,B,prediatric}$ = $F_{u,B,adult}$ | x | $CL_{H,int}$ -3.6% & $CL_{G,int}$ +17.2% |
| **Fraction absorbed** | $F_a$ (0.90)<br>$F_a$ (0.80) | Full PK profile -10%<br>full PK profile -20% | $CL_{H,int}$ -15% &$CL_{G,int}$ -3.2%<br>$CL_{int}$ -11% &$CL_{G,int}$ -20% |
| **Volume of distribution 1-OH-midazolam** | $V_m$ +/-50% | x | $CL_{H,int}$ +46%/-27% & $CL_{G,int}$ -41%/+93% & $CL_{H,int,M}$ +43%/-43% & $CL_{G,int,M}$ -55%/+1980% |

x: no impact was observed, $C_{max}$: peak concentrations. $CL_{int}$: whole-organ intrinsic clearance, H hepatic, G gut wall and M indicating the metabolite 1-OH-midazolam.

## REFERENCES SUPPLEMENTAL MATERIAL

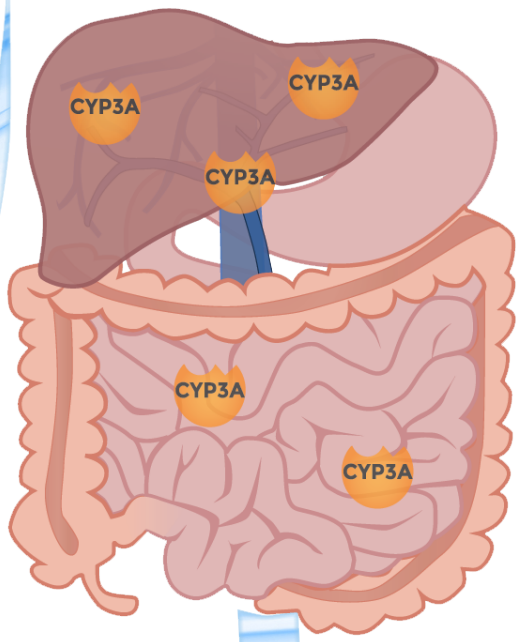

[1] Simcyp® Simulator version 15.1, Certara, Sheffield, United Kingdom, https://www.certara.com/ software/physiologically-based-pharmacokinetic-modeling-and-simulation/simcyp-simulator/

[2] Dubois D, Dubois EF. A formula to estimate the approximate surface area if height and weight be known. Archives of Internal Medicine, **1916**, 17: 863-871.

[3] Haycock GB, Schwartz GJ, Wisotsky DH. Geometric method for measuring body surface area: a height-weight formula validated in infants, children, and adults. J Pediatr. **1978** Jul;93(1):62-6.

# Section IV

## Midazolam as probe drug for other CYP3A substrates



# Chapter 7

## A pediatric covariate function for CYP3A-mediated midazolam clearance to scale clearance of selected CYP3A substrates in children

Janneke M Brussee[1], Elke HJ Krekels[1], Elisa AM Calvier[1], Semra Palić[1,2], Amin Rostami-Hodjegan[3,4], Meindert Danhof[1], Jeffrey S Barrett[5,6], Saskia N de Wildt[7,8], Catherijne AJ Knibbe[1,9]

[1]Division of Systems Biomedicine and Pharmacology, Leiden Academic Centre for Drug Research (LACDR), Leiden University, Leiden, the Netherlands; [2]Current affiliation: Dutch Cancer Institute (NKI), Amsterdam, the Netherlands; [3]Centre for Applied Pharmacokinetic Research, University of Manchester, Manchester, UK; [4]Simcyp Limited (A Certara Company), Sheffield, UK; [5]Translational Informatics, Sanofi, Bridgewater, NJ, USA; [6]Department of Pediatrics, Division of Clinical Pharmacology & Therapeutics, Children's Hospital of Philadelphia, Philadelphia, PA, USA; [7]Department of Pharmacology and Toxicology, Radboud University Medical Centre, Nijmegen, the Netherlands; [8]Intensive Care and Department of Pediatric Surgery, Erasmus MC - Sophia Children's Hospital, Rotterdam, the Netherlands; [9]Department of Clinical Pharmacy, St. Antonius Hospital, Nieuwegein, the Netherlands

*Manuscript in preparation*

## ABSTRACT

Recently a framework was presented to assess, based on drug properties, whether pediatric covariate models for clearance can be extrapolated between drugs sharing elimination pathways. Our aim is to evaluate when a pediatric covariate function for midazolam clearance can be used to scale clearance of other CYP3A substrates.

A population PK model including a covariate function for clearance was developed for midazolam in children aged 1-17 years. Commonly used CYP3A substrates were selected and using the framework, it was assessed whether the midazolam covariate function can accurately scale their clearance. For eight substrates, reported adult and pediatric clearance values were compared numerically and graphically with clearance values scaled using the midazolam covariate function. For sildenafil clearance values obtained with population PK modeling based on pediatric concentration-time data were compared to those obtained with the midazolam covariate function.

According to the framework, a covariate function for midazolam clearance will at least yield systematically accurate (absolute prediction error (PE) <30%) clearance scaling in children of all ages for CYP3A substrates with an extraction ratio of 0.35-0.65 or 0.05-0.55 for drugs binding <10% or >90% to albumin in adults, respectively. The results show that scaled clearance values for eight commonly used CYP3A substrates were reasonably accurate (PE <50%). Scaling of sildenafil clearance was accurate (PE <30%).

We defined for which CYP3A substrates a pediatric covariate function for midazolam clearance can accurately scale plasma clearance in children. This scaling approach is useful for CYP3A substrates with scarce or no available pediatric PK information.

**Keywords**
Pediatrics, clearance, CYP3A ontogeny, scaling function, population pharmacokinetics

# INTRODUCTION

To define the optimal first-in-child dose during drug development and to develop pediatric dose recommendations for clinical practice, accurate scaling of the plasma clearance of drugs is essential (1-3). This is of particular relevance as it would take many resources to perform dedicated pharmacokinetic (PK) studies for all drugs in all pediatric (sub)populations and as this is even unethical when other methods are possible. One proposed approach shares PK information of drugs eliminated by the same pathway by extrapolating covariate relationships for clearance between drugs (4). This has been successfully applied for scaling pediatric clearance for drugs glucuronidated by UGT2B7 and drugs eliminated by glomerular filtration (4-6).

Within this context, recently, a framework was presented for hepatically metabolized drugs identifying the conditions for which between-drug extrapolation is systematically accurate (7). This framework takes into account changes in physiological parameters with age, including changes in (hepatic) blood flow, plasma protein concentrations, hematocrit, liver size, the amount of microsomal protein per gram of liver, and the ontogeny of isoenzyme expression (the microsomal intrinsic clearance)(7). Based on this framework, it was shown that the accuracy of this scaling method depends on the fraction metabolized by the isoenzyme pathway for which plasma clearance is scaled, on the hepatic extraction ratio of both drugs in adults, on the type of binding plasma protein, and on the unbound drug fraction ($f_u$) in adults (7).

As many drugs are eliminated by the cytochrome P450 (CYP) 3A enzyme family (8, 9), a pediatric covariate function for CYP3A-mediated clearance may aid in scaling clearance of CYP3A substrates. Midazolam is an established probe drug for CYP3A-mediated clearance (10, 11) and has an intermediate extraction ratio (12). Our aim is to evaluate when a pediatric covariate function for midazolam clearance can be used to scale clearance of other CYP3A substrates in children, taking into account the recent insights of the developed framework (7).

# METHODS

## Overall approach

A population PK model for midazolam in children was developed based on concentration-time data, to establish a pediatric covariate function for midazolam clearance. Next, we selected a range of drugs that are CYP3A substrates that are

commonly prescribed in children, covering compounds prescribed for varying indications in different therapeutic areas, with oral or intravenous administration, and with different drug properties, i.e. alprazolam (13), atorvastatin (14), cisapride (15), domperidone (16), quinidine (17), sildenafil (18), simvastatin (19), solifenacin (20), sufentanil (21), sirolimus (22), tacrolimus (23), tamsulosin (24), and vincristine (25). Based on the drug properties of these CYP3A substrates, we used the framework of Calvier *et al.*(7) to define to which age the covariate function for midazolam can be used for accurate scaling of pediatric clearance of the CYP3A substrates from adult clearance values. For eight of the selected CYP3A substrates pediatric and adult clearance values were available in literature, allowing for the assessment of the accuracy of the scaling function by comparing pediatric clearance values that were scaled from adult clearance values using the covariate function for midazolam to the published literature clearance values in children. Furthermore, for sildenafil, concentration-time data were available from 156 children (26). Using these data, we developed two pediatric population PK models for sildenafil; one using the pediatric covariate function of midazolam clearance directly and one in which the covariate relationship for clearance was optimized using a data-driven analysis, after which the performance of both models, as well as the estimated and scaled clearance values, were compared.

**Table I.** Study and patient characteristics of the midazolam and sildenafil PK studies

| | Midazolam | Sildenafil |
|---|---|---|
| **Indication** | Pre-operatively | Pulmonary arterial hypertension |
| **Number of patients** | 31 | 156 |
| **Number of samples** | 327 | 591 |
| **Samples/patient*** | 10 (8-11) | 4 (1-4) |
| **Age (years)*** | 8 (1-17) | 10 (1-17) |
| **Body weight (kg)*** | 30.2 (9.5-83.2) | 28.0 (8.2-106.0) |
| **Male/female, n (%)** | 15/16 (48/52%) | 57/99 (37/63%) |
| **Dose (mg)*** | 12.5 (3-15) | 20 (10-80) |

*median (range)

## Midazolam population PK model

Midazolam PK data were available from 31 patients (15 male, 16 female) from the Children's Hospital of Philadelphia, PA (Table I), with a median age of 8 years of age (range 1-17 years) and a median body weight of 30.2 kg (range 9.5-83.2 kg) (27). Before participation, signed informed consent by the subject's parents or guardian, and assent were obtained. Children undergoing surgery were included if they met the criteria I or II of the American Society of Anesthesiologist's (ASA) classification. A median dose of 12.5 mg (range 3-15 mg) of midazolam was administered as oral

suspension (5 mg/mL, Roche Laboratories) to the patients pre-operatively. Blood was densely sampled for midazolam plasma concentrations around 0.25, 0.5, 1, 1.5, 2, 3, 4, 6, 8, 10 and 22 hours after dose administration, with a median of 10 samples per patient (range 8-11). Blood was centrifuged and plasma samples stored at <-20°C until midazolam plasma concentrations were determined using LC/MS (27).

A population PK model was developed using non-linear mixed effects modelling (NONMEM version 7.3, ICON, Globomax LLC, Ellicott, MD, USA; Perl-speaks-NONMEM (PsN) version 4.2.0, Uppsala, Sweden; and Pirana 2.9.0, Pirana Software & Consulting BV, Denekamp, the Netherlands) based on first-order conditional estimation with interaction. R (version 3.3.1) and R-studio (version 0.98.1078) were used for data visualization. Several structural models were considered, including 1, 2 and 3-compartmental models, and evaluated based on criteria for model stability, goodness-of-fit, and parameter precision, and on comparisons of the objective function values (OFV, -2 × log-likelihood), using a significance level of $p<0.05$. The absorption rate could not be estimated and was therefore fixed at 3.5 $h^{-1}$, which results in a $t_{max}$ around 0.5 hours post-dose, which is in agreement with known values.

Inter-individual variability in the estimated parameters for clearance and central volume of distribution was included in the model by the following equation:

$$P_i = \theta_{TV} \times e^{\eta_i} \qquad \text{(Eq. 1)}$$

In which $P_i$ is the individual parameter estimate for individual $i$, $\theta_{TV}$ is the typical value of the parameter in the studied population and $\eta_i$ is a random variable for the $i$th individual form a normal distribution with a mean of zero and variance of $\omega^2$, assuming a log-normal distribution for the parameter value in the population.

To describe residual unexplained variability, a proportional error model, an additive error model, and a combination of the proportional and additive error were considered. The $j$th observed concentration of the $i$th individual ($Y_{ij}$) was modeled according to:

$$Y_{ij} = C_{pred,ij} \times (1+\varepsilon 1_{ij}) + \varepsilon 2_{ij} \qquad \text{(Eq. 2)}$$

where $C_{pred,ij}$ is the $j$th predicted midazolam concentration of the $i$th individual, and $\varepsilon_{ij}$ is a random variable from a normal distribution with a mean of zero and variance of $\sigma^2$, with $\varepsilon 1$ the proportional error and $\varepsilon 2$ the additive error.

A systematic covariate analysis was performed for the estimated model parameters in which age, body weight, and sex were tested for statistical significance. For sex, the typical value ($\theta_{TV}$) for girls was estimated relative to the value for boys. The remaining continuous covariates body weight and age were tested using a power (Eq. 3) function:

$$P_i = \theta_{TV} \times \left(\frac{COV_i}{COVmed}\right)^{\theta_{COV}} \times e^{\eta_i} \qquad \text{(Eq. 3)}$$

where $P_i$ is individual parameter estimate for individual $i$ with a covariate value of $COV_i$, $\theta_{TV}$ is the parameter value for a typical individual with a median covariate value ($COV_{med}$), $\theta_{COV}$ is the estimated exponent and $\eta_i$ is a random variable as described above (eq. 1). For the forward inclusion of a covariate, a drop in OFV by at least 6.64 points ($p<0.01$) was considered statistically significant, while for the backward deletion a more stringent p value ($p<0.005$, $\Delta OFV>7.88$) was used. In addition, the inter-individual variability in the PK parameter or the residual variability should decrease for a covariate to be retained in the model.

To evaluate whether the model described the observed concentrations well, goodness-of-fit plots were assessed. These diagnostic plots include observed versus population- and individual-predicted concentrations and conditional weighted residuals (CWRES) versus population predicted concentrations and versus time. To evaluate model stability and parameter precision, a bootstrap analysis (n=250) was performed. Finally, a normalized prediction distribution error (NPDE) analysis was performed using the NPDE package in R (28), with n=1000 simulations to evaluate whether the model can accurately predict the concentration and captures the observed variability.

## Between-drug extrapolation potential of midazolam clearance to other CYP3A substrates

The previously published framework on between drug extrapolation of covariate functions (7) was used to assess, based on the drug properties of CYP3A substrates, whether between-drug extrapolation of the covariate relationship for midazolam would lead to accurate scaling of the pediatric clearance of the selected CYP3A substrates. For this, the relevant drug properties, i.e. the extraction ratio, the plasma protein to which the drug is binding, and the $f_u$ for midazolam and the selected drugs were obtained from literature. In this analysis, the selected drugs were assumed to exclusively bind to either human serum albumin (HSA) or $\alpha$1-acid glycoprotein (AAG), while midazolam was either assumed to bind to HSA (for comparison with HSA-binding drugs) or to AAG (for comparison with AAG-binding drugs).

Using the difference in extraction ratio and the $f_u$ between midazolam and the selected CYP3A-substrates that were considered within the results from the framework (7), it was assessed to what age clearance scaling with the covariate function of midazolam would certainly be accurate for the selected drugs. For this, we assumed CYP3A metabolism to be responsible for ≥75% of the total metabolism for both midazolam and all selected substrates. Based on the extraction ratio and $f_u$ from midazolam and the difference in these values that, according to the framework, are known to lead to systematically accurate scaling across the entire

pediatric age range, we also derived general criteria for accurate clearance scaling for CYP3A substrates using the covariate function for midazolam clearance.

## Comparison of scaled versus reported pediatric clearance values

For the selected CYP3A substrates for which both pediatric and adult clearance values were reported in literature, we applied the pediatric covariate function for midazolam clearance to the reported adult clearance values to scale to pediatric clearance values. For this we assumed that typical adults have a body weight of 70 kg. We graphically compared the scaled typical clearance values with the reported pediatric clearance values. Moreover, we calculated the prediction error (PE) for three typical subjects (an infant of 10 kg, a child of 20 kg, and an adolescent of 50 kg) based on literature values for pediatric clearance using equation 4:

$$PE = \frac{CL_{scaled} - CL_{ref}}{CL_{ref}} \times 100\% \qquad \text{(Eq. 4)}$$

with $CL_{scaled}$ the scaled clearance value and $CL_{ref}$ the reported pediatric clearance. An absolute PE of <30% was considered accurate, an absolute PE of 30-50% reasonably accurate, and an absolute PE of ≥50% inaccurate.

## Sildenafil population PK models

Sildenafil PK data from a previously published study (26) were made available by Pfizer Inc. In this study, sildenafil PK data were collected from 156 (57 male, 99 female) patients in a randomized, double-blind, placebo controlled, dose ranging, parallel group study of oral sildenafil for the treatment of children with pulmonary arterial hypertension (26, 29). Subjects included children ranging in age from 1-17 years (median 10 years), with a median body weight of 28.0 kg (range 8.2-106 kg) (Table I). A median of 4 samples per patient (range 1-4) were available, with a total of 591 measurements available for analysis. Samples were taken at steady-state at through and around 3, 6 and 8 hours post-dose. Patients were randomly assigned to a low, medium or high dose group (n=39, n=48 and n=69, respectively), and the dosages were weight-stratified, with a medium dose of 10, 20 and 40 mg and a high dose of 20, 40 and 80 mg for patients of 8-20 kg, 20-45 kg or >45 kg, respectively. The low dose was 10 mg for all patients >20kg, and patients with a body weight ≤20 kg received either a medium or high dose, as no drug effect was expected with a lower dose than 10 mg (26, 29). In the population PK analysis, the samples without recorded sampling times were excluded.

Based on these data, a 'reference model' was developed in the same manner as described for midazolam. The absorption rate constant could not be estimated and was therefore fixed at 1 $h^{-1}$, leading to a maximum concentration around 2 hours post-dose, which was before the first sample was taken.

The extrapolation potential of the covariate function for midazolam clearance was evaluated in a second population PK model referred to as the 'extrapolation model'. This model was kept the same as the reference model, except the clearance was not estimated, but scaled from an apparent CL/F value of 100 L/h for adults, which was derived from reported systemic clearance and oral bioavailability values of 41 L/h and 0.41, respectively (30), using the covariate function for midazolam clearance. We assumed the same bioavailability in adults and pediatric patients.

The reference and extrapolation model were evaluated in the same manner as the midazolam PK model (see under Midazolam population PK model).

Sildenafil clearance values from the sildenafil 'reference model' ($CL_{ref}$) and the sildenafil 'extrapolation model' ($CL_{scaled}$) were compared graphically. For a numerical comparison of both sildenafil models, typical clearance values for three typical subjects (an infant of 10 kg, a child of 20 kg, and an adolescent of 50 kg) were calculated, and a PE for clearance was calculated using equation 4.

# RESULTS

## Midazolam population PK model

For midazolam, a two-compartmental model with body weight included in an exponential covariate relationship on clearance, volumes of distribution, and

**Table II.** Model parameter estimates for the midazolam PK model and the bootstrap results based on n=250 resampling

| Parameter | | Model estimate (RSE) | Bootstrap median (90 CI) |
|---|---|---|---|
| Midazolam clearance† | $CL_{30.2\ kg}$ (L/h) | 102.6 (9%) | 101.4 (89.1-118.2) |
| $CL_i = CL_{30.2kg} * (WT_i/30.2)^{k1}$ | k1 | 0.874 (13%) | 0.901 (0.698-1.11) |
| Volume of distribution† | $V_{c30.2\ kg}$ (L) | 156 (25%) | 141 (76.5-210) |
| $V_{c,i} = V_{30.2\ kg} * (WT_i/30.2)^{k2}$ | k2 | 1.88 (17%) | 2.15 (1.43-3.30) |
| Peripheral volume† | $V_{p,30.2\ kg}$ (L) | 255 (14%) | 252 (197-338) |
| $V_{p.i} = V_{30.2\ kg} * (WT_i/30.2)^{k3}$ | k3 | 0.91 (23%) | 0.88 (0.60-1.21) |
| Intercompartmental clearance† | $Q_{30.2\ kg}$ (L/h) | 121.8 (21%) | 115.6 (73.7-163) |
| $Q_i = Q_{30.2\ kg} * (WT_i/30.2)^{k4}$ | k4 | 0.75 fix | 0.75 fix |
| Absorption rate constant | $k_a$ ($h^{-1}$) | 3.5 fix | 3.5 fix |
| IIV Clearance | $\omega^2$ CL | 0.158 (41%) | 0.145 (0.063-0.259) |
| IIV Volume of distribution | $\omega^2$ $V_c$ | 1.19 (27%) | 1.06 (0.64-1.71) |
| Proportional error | $\sigma^2$ | 0.283 (13%) | 0.272 (0.222-0.346) |

RSE is the relative standard error, and 90 CI is the 90% confidence interval representing the 5th and 95th percentiles. Inter-individual and residual variability values are shown as variance estimates.

†Parameters are apparent parameters, as only oral data was included.

inter-compartmental clearance, best described the data (table II, figure S1, S2). As midazolam was administered orally, apparent parameters for clearance and volume of distribution were obtained. For a typical individual of 30.2 kg, apparent clearance was 102.6 L/h, and the exponent in the exponential equation relating body weight and clearance, was found to be 0.874 (table II). As a result, this pediatric covariate function was used to scale CYP3A-mediated clearance in the between-drug extrapolation:

$$CL_{pediatric} = CL_{adult} \times \left(\frac{WT}{70}\right)^{0.874} \qquad \text{(Eq. 5)}$$

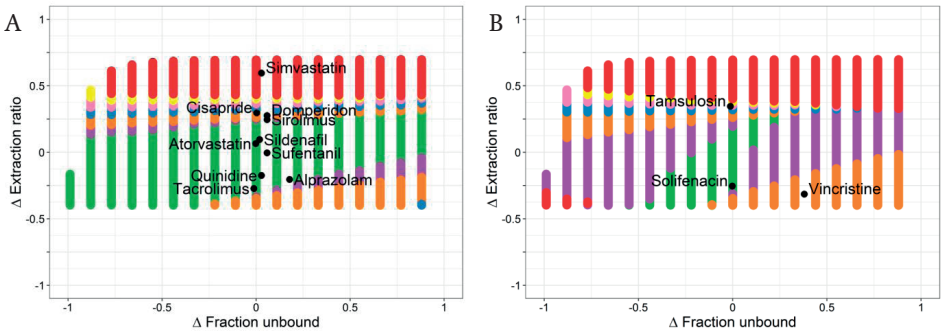



**Figure 1.** Prediction of the age down to which the pediatric covariate function for CYP3A-mediated midazolam clearance can be used to accurately scale clearance of CYP3A substrates with specific drug properties. Difference in extraction ratio between CYP3A substrates (test drugs) and midazolam (model drug) is plotted versus difference in fraction unbound ($f_u$) between these drugs. The color scheme was obtained from the published framework (7) and represent hypothetical model-test drug combinations that lead to systematically accurate scaling of clearance in children down to 1 day (green), 1 month (purple), 6 months (orange), 1 year (blue), 2 years (pink), and 5 years of age (yellow). Red indicates that scaling is not systematically accurate in children of 5 years and younger. The black data points represent the included test drugs and their parameter values relative to midazolam. Panel A shows drugs binding to albumin (HSA), while panel B shows drugs binding to α1-acid glycoprotein (AAG). Modified from Calvier *et al.* (7) (with permission).

## Between-drug extrapolation potential of midazolam clearance to other CYP3A substrates

The obtained drug properties of midazolam and the selected CYP3A substrates required for between-drug extrapolation of clearance are listed in Table SI (31-52). Figure 1 shows down to what age the clearance of the selected substrates can at least be extrapolated from adult values with the covariate relationships for midazolam clearance, based on the differences in extraction ratio and $f_u$ according to the framework that was previously reported (7). This figure shows that this method will accurately scale pediatric clearance values down to neonates of 1 day of age

for alprazolam, atorvastatin, quinidine, sildenafil, solifenacin, sufentanil, and tacrolimus, while for the other drugs clearance will be at least accurately scaled down to infants of 1 month (sirolimus), and 6 months of age (cisapride, domperidon, and vincristine). Tamsulosin clearance scaling will be accurate down to at least 2 years of age, while for simvastatin accurate scaling down to 5 years of age may not even be possible (figure 1).

From figure 1 it can also be derived that a pediatric covariate function for midazolam can be used to scale CYP3A-mediated clearance of HSA-bound substrates which are highly protein bound (>90%, $f_u \leq 0.1$) when the extraction ratio in adults that does not differ more than +0.20 or -0.30 from the extraction ratio of midazolam (assuming ≥75% metabolism by CYP3A enzymes for both drugs), resulting in required extraction ratio values between 0.05 and 0.55. In addition, for substrates with low protein binding (<10%, $f_u \geq 0.9$) the drug to which the covariate function is extrapolated should have an extraction ratio between 0.35 and 0.65. For AGP-bound drugs, fewer combinations of drug properties lead to accurate scaling based on a midazolam pediatric covariate function, with no scenarios for drugs with low protein binding ($f_u \geq 0.9$), but an extraction ratio of 0.4-0.6 or 0.1-0.5 in adults lead to accurate scaling for drugs that are 90% or ≥97.5% bound, respectively (figure 1).

## Comparison of scaled versus reported pediatric clearance values

Obtained pediatric and adult clearance values of CYP3A substrates are summarized in table SI (30, 33, 53-63). In figure 2, the scaled clearance values are shown together with the reported pediatric clearance values for the various substrates versus body weight. Table IV lists the calculated prediction errors for the three typical pediatric individuals. For most drugs, the scaled covariate relationships fall within the range of observed values, except for sirolimus and vincristine. The calculated PE values also show that scaled vincristine and sirolimus clearance values are inaccurate, although with a PE value of 64.3% and 58.3%, respectively, this inaccuracy is not extreme. The PE values for all other drugs are <50%, indicating accurate or reasonably accurate scaling of clearance in infants, children, and adolescents.

**Table III.** Model parameter estimates for the sildenafil 'reference model' versus the sildenafil 'extrapolation model', and the bootstrap results for both models based on n=250 resampling

| Parameter | | Reference model | | Extrapolation model | |
|---|---|---|---|---|---|
| | | **Model estimate (RSE)** | **Bootstrap (90 CI)** | **Model estimate (RSE)** | **Bootstrap (90 CI)** |
| Sildenafil clearance† $\mathbf{CL_i = CL_{70\ kg} * (WT_i/70)^{k1}}$ | $CL_{70\ kg}$ (L/h) | 113 (13%) | 112 (84.6-149) | 100 fix | 100 fix |
| | k1 | 1.08 (11%) | 1.05 (0.82-1.30) | 0.874 fix | 0.874 fix |
| Volume of distribution† $\mathbf{V_i = V_{28\ kg} * (WT_i/28)^{k2}}$ | $V_{28\ kg}$ (L) | 540 (33%) | 561 (311-1424) | 590 (29%) | 574 (389-1134) |
| | k2 | 3.18 (10%) | 3.17 (2.41-4.27) | 3.18 (10%) | 3.16 (2.49-4.01) |
| Absorption rate constant | $k_a$ ($h^{-1}$) | 1 fix | 1 fix | 1 fix | 1 fix |
| IIV Clearance | $\omega^2$ CL | 0.493 (14%) | 0.487 (0.363-0.631) | 0.510 (13%) | 0.512 (0.397-0.650) |
| Proportional error | $\sigma^2$ | 0.627 (7%) | 0.616 (0.538-0.703) | 0.651 (8%) | 0.646 (0.564-0.738) |

RSE is the relative standard error, and 90 CI is the 90% confidence interval representing the 5th and 95th percentiles. Inter-individual and residual variability values are shown as variance estimates.

†Parameters are apparent parameters, as only oral data was included.

## Sildenafil population PK models

The reference model and extrapolation model for sildenafil, described the sildenafil concentrations with a one-compartmental model. Table III presents model parameters and bootstrap values for both models and the goodness-of-fit plots and results from the NPDE analyses are presented in figure S3 and figure S4, respectively. These results show that descriptive and predictive properties of both models are similar.

In the reference model, apparent sildenafil clearance for a typical individual of 28 kg was found to be 41.9 L/h, and clearance increased exponentially with increasing body weight (exponent of 1.08 [RSE 11%]), leading to an apparent clearance of 113 L/h for a 70-kg individual. In the extrapolation model, apparent clearance was scaled using eq. 5, with a $CL_{adult}$ of 100 L/h for a 70-kg individual, leading to a scaled apparent clearance of 44.9 L/h for a 28-kg individual. As shown in a graphical comparison in figure 3A, both covariate relationships are very similar, with only a small difference in clearance values between the two models for children with the lowest body weight. Figure 3B shows that when individual clearance predictions by both models are plotted versus age, the loess functions for these relationships are also similar with small difference in the youngest age range. These small discrepancies may be

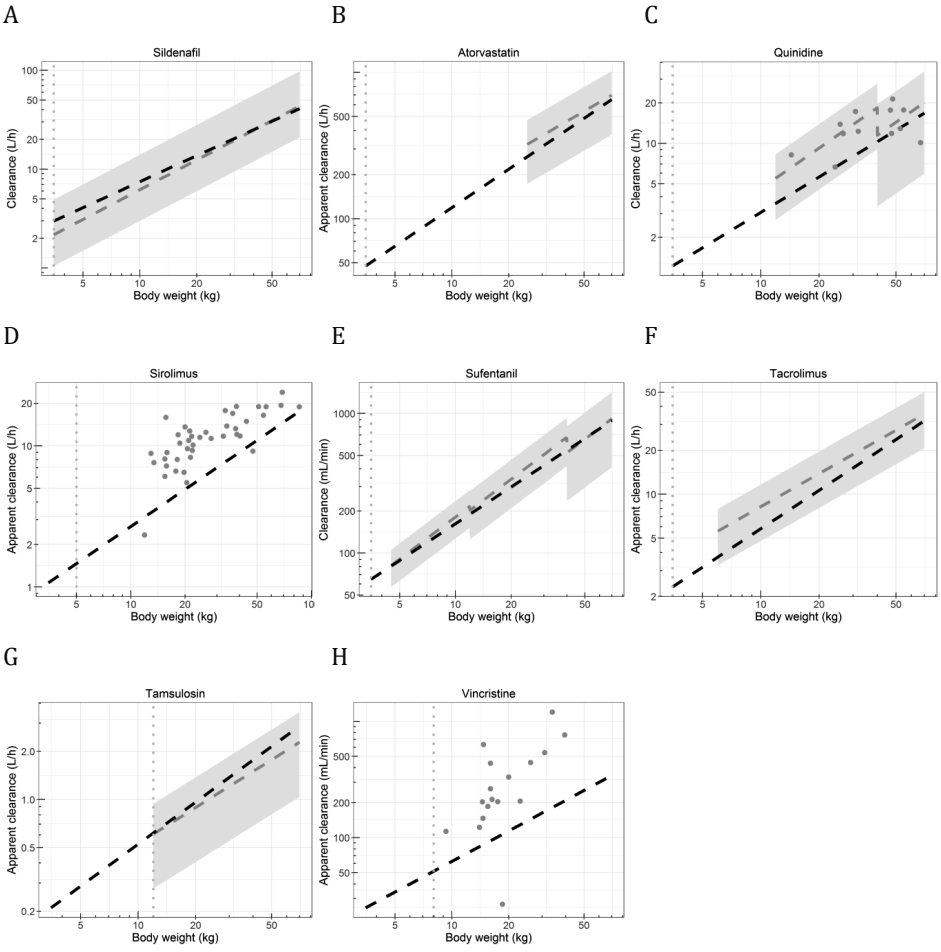



**Figure 2.** Scaled and reported clearance values versus body weight for various CYP3A substrates. Clearance (or apparent clearance) values are based on the between-drug extrapolation of the pediatric covariate function for CYP3A-mediated midazolam clearance and reported adult clearance values (**black**), and based on reported pediatric clearance values in literature (**grey**), for sildenafil (A), atorvastatin (B), quinidine (C), sirolimus (D), sufentanil (E), tacrolimus (F), tamsulosin (G) and vincristine (H). The vertical dotted line (grey) indicates the body weight down to which systemically accurate clearance scaling is predicted to be possible according to the framework (7). For the reported clearance values the following is depicted: A) Mean sildenafil clearance (line) with minimal and maximal reported values (grey area). B) Typical atorvastatin clearance (line) ± 46.3% (%CV, grey area). C) Mean quinidine clearance (line) ± 2 SD (grey area), and individual reported clearances (closed circles). D) Individual reported sirolimus clearances (closed circles). E) Mean sufentanil clearance (line) ± 2 SD (grey area). F) Typical tacrolimus clearance (line) ± 41.6% (%CV, with $CV = \sqrt{e^{\sigma^2} - 1}$, and $\sigma^2$ =0.16, grey area). G) Typical tamsulosin clearance (line) ± 54.4% (%CV, grey area). H) Individual reported vincristine clearances, corrected for body surface area (closed circles).

due to the small number of individuals in the youngest age group (1-2 years of age) in the population receiving midazolam used for establishing the pediatric covariate function.

The PE for clearance increases with decreasing age, with a PE of -5.2%, 14.6%, and 32.1%, in an adolescent, child, and infant, respectively, indicating that with decreasing age and body weight, the extrapolation model yields a larger overprediction of clearance. However, the scaled clearance values are within the range of observed clearance values, which show a high variability throughout the pediatric age range (figure 3B).

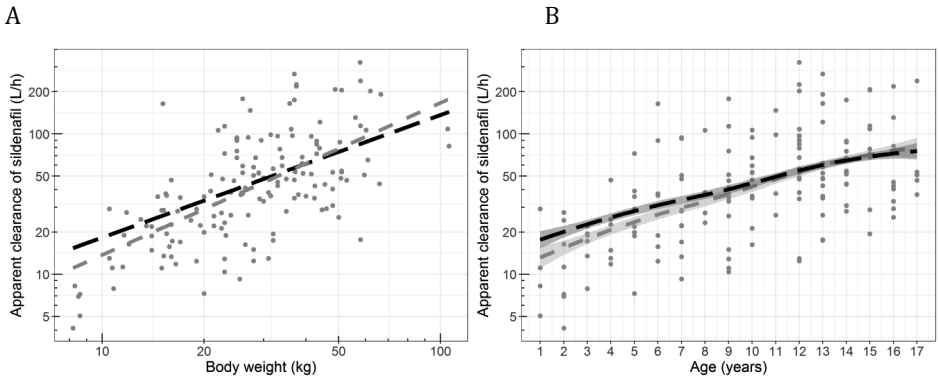



**Figure 3.** Sildenafil apparent clearance versus body weight (A) and versus age (B) for the sildenafil reference model (**grey**) and based on between-drug extrapolation of clearance (**black**) with points representing the individual predicted clearance by the reference model. In panel A the lines represent population predicted clearance values directly derived from the bodyweight-based covariate relationship, while in panel B the lines represent the loess function summarizing the population predicted clearance values with a 95% confidence interval (shaded area).

## DISCUSSION

Accurate scaling of plasma clearance is essential to establish optimal first-in-child doses during drug development and for the development of pediatric dose recommendations. As many drugs are metabolized by CYP3A enzymes and midazolam is a commonly accepted probe drug for CYP3A, we aimed to evaluate when a pediatric covariate function for CYP3A-mediated midazolam clearance can be used to scale pediatric clearance of CYP3A substrates given the recently reported guidance on between-drug extrapolation of covariate models.

Whether scaling of pediatric clearance of CYP3A substrates based on a covariate function from a pediatric population PK model for midazolam is accurate, depends

on the drug properties (7). We used a previously developed framework (7) to assess for which of the selected CYP3A substrates scaling with the pediatric covariate function from midazolam will lead to accurate clearance values (figure 1). The color code in this framework indicates down to which age scaling of clearance is expected to be systemically accurate based on differences in extraction ratio and $f_u$ of the test and model drug only. Each colored dot in this graph represents multiple drugs with differences in the remaining drug properties (i.e. blood-to-plasma partitioning and affinity to isoenzymes) and it should be noted that when the framework predicts that scaling of clearance is not systemically accurate for all drugs with the indicated combination of drug properties, there may still be drugs within the set of drugs represented by a data point for which this scaling is accurate. In those cases, it can however not be predicted *a priori* whether this will be the case for each of the individual drugs (7).

For the selected CYP3A substrates alprazolam, atorvastatin, cisapride, domperidone, quinidine, sildenafil, solifenacin, sufentanil, sirolimus, tacrolimus, and vincristine, scaling of clearance with the covariate function of midazolam is expected to be accurate down to children of at least 1 year of age and for some drugs even to neonates and infants (figure 1).

Several approaches and methods for scaling of clearance in children have been described in literature, including scaling of clearance using a bodyweight-based exponential function with exponents of e.g. 0.67, 0.75 or 1. In a systematic assessment of the applicability of bodyweight-based scaling with a fixed exponent of 0.75, it was found that this approach leads to increasingly inaccurate scaled values with decreasing age, reaching prediction errors of up to 278% in neonates (64). Extrapolation of pediatric covariate functions for drugs sharing elimination pathways were therefore considered as an alternative approach, and this method had already been successful in scaling pediatric clearance for UGT2B7 substrates and for drugs eliminated through glomerular filtration (4-6). A systematic assessment of this method provided the prerequisites for this scaling technique (7). In the current work we illustrate how the previously obtained knowledge can be applied. Moreover, we add CYP3A metabolism to the list of elimination pathways for which between-drug extrapolation of pediatric covariate relationships for clearance have been successfully applied.

Between-drug extrapolation of clearance on the basis of a pediatric covariate function for CYP3A-mediated midazolam clearance, indeed led to accurate or reasonably accurate scaling of pediatric clearance of most of the selected CYP3A

substrates in children (table IV, figure 2). This confirms that the pediatric covariate function for midazolam clearance can accurately scale pediatric clearance of CYP3A substrates down to at least one year of age for a large number of relevant substrates including sildenafil, atorvastatin, quinidine, sufentanil, tacrolimus and tamsulosin. In addition to reported clearance values, for sildenafil concentration-time data were available as well. With these data it was further confirmed that the between-drug extrapolation of the covariate relationship of midazolam clearance yields accurate clearance predictions.

**Table IV.** Prediction error (PE) of scaled clearance values using the pediatric covariate function for CYP3A-mediated midazolam clearance *versus* reported pediatric clearance values for three representative pediatric subjects of 10, 20 and 50 kg (eq. 4). Colors indicate an accurate prediction (<30%, green), a reasonably accurate prediction (30-50%, orange) and an inaccurate prediction (≥50%, red).

| | Infant (10 kg) | Child (20 kg) | Adolescent (50 kg) |
|---|---|---|---|
| Atorvastatin | -26.7% | -20.1% | -10.5% |
| Quinidine | -33.5% | -39.0% | -12.8% |
| Sildenafil | 20.7% | 10.6% | -1.4% |
| Sirolimus | x | -58.3% | -31.5% |
| Sufentanil | -10.3% | -12.0% | 1.1% |
| Tacrolimus | -44.6% | -39.6% | -32.3% |
| Tamsulosin | x | 8.1% | 21.2% |
| Vincristine | -64.3% | x | x |

x: No pediatric or adult clearance values reported in literature.

Contrary to what was expected based on the theoretical framework, scaled clearance values of sirolimus and vincristine were inaccurate compared to reported literature values (PE >50%, table IV). For sirolimus, this may be due to the known induction of hepatic CYP3A activity and possibly altered hepatic P-glycoprotein expression (65), which impacts its plasma clearance, which is not accounted for in the scaling method. The scaling of vincristine may be inaccurate, because it is predominantly metabolized by CYP3A5 (66), with a relative smaller contribution of CYP3A4-mediated metabolism compared to midazolam. Other factors that may affect the accuracy of our pathway-specific scaling approach, apart from the hepatic extraction ratio and $f_u$ in adults, include that the fraction eliminated by a certain pathway may be different from the ≥75% assumed here. It has for instance been shown that the age down to which clearance can accurately be scaled, increases when the contribution of CYP3A metabolism to the overall hepatic metabolism is decreasing (7). Additionally, the contribution of minor elimination pathways to overall drug clearance has been ignored in the current analysis. Moreover, scenarios

for the between-drug extrapolation of pediatric covariate functions for clearance of HSA-bound drugs to AAG-bound drugs have not been investigated; therefore we assumed midazolam to be AAG-bound when using its covariate function to scale the clearance of AAG-bound CYP3A substrates. The impact of this assumption would be largest in neonates and in the youngest children <1 year of age, as in these age groups the concentration of AAG is known to vary more with age than the concentration of HSA, due to the more rapid maturation of AAG-concentrations (67). Lastly, as in the sildenafil PK study not many samples were taken shortly after administration, absorption rate constants for sildenafil could not be estimated and were therefore fixed it at 1 $h^{-1}$, which is close to reported values for $k_a$ 0.34 $h^{-1}$ (68). A sensitivity analysis showed that fixing it at different values had no impact on the scaled clearance values.

In this analysis we only included midazolam PK data from children >1 year of age. Therefore, the pediatric covariate function for midazolam clearance we developed in this analysis cannot be used to scale clearance values of CYP3A substrates in children <1 year of age, as extrapolation of the covariate relationship to (premature) neonates and infants is anticipated to yield overprediction, due to the large impact of maturation in the first weeks and months of life (69). To be able to apply this covariate function to scale CYP3A-mediated clearance in neonates and young infants up to 1 year of age, the midazolam covariate function should be extended with children <1 year of age.

## CONCLUSION

This analysis showed that a pediatric covariate relationship describing how midazolam clearance changes throughout the pediatric age range can be used to scale adult clearance values for many other CYP3A substrates to pediatric clearance values. Specifically, it was found that this approach is applicable to accurately scale clearances of drugs that are mainly eliminated by CYP3A-mediated metabolism with for example high protein binding to HSA (>90%) and a low to intermediate extraction ratio of <0.55 in adults. Furthermore, clearances of CYP3A substrates with low binding to HSA (<10%) and an extraction ratio of 0.35-0.65 can be accurately scaled from adult values, while scaling of clearance of AGP-bound drugs is accurate for fewer combinations of drug properties. The ability to scale clearance of CYP3A substrates in children from adult clearance using a pediatric covariate function for CYP3A-mediated clearance will significantly enhance the development of dosing guidelines of CYP3A substrates for clinical practice and aid in determining the dose in first-in-child studies involving new CYP3A substrates. This may be especially useful for CYP3A substrates in which scarce or no pediatric PK information is available, for example for alprazolam, domperidone, and solifenacin.

## ACKNOWLEDGEMENTS

The authors would like to thank Pfizer Inc. for kindly sharing their data on sildenafil PK in children of 1-16 years of age. Drs. Jeff Galinken and Peter Adamson were the PIs on the original midazolam PK study conducted at CHOP, and the study was supported by NIH / NICHD, Pediatric Pharmacology Research Unit, Grant # HD037255-06. The authors would like to thank Bas Goulooze (LACDR, Leiden University) for reviewing all scripts involved in this analysis. CAJ Knibbe is supported by a NWO Vidi grant (Vidi Knibbe, June 2013).

## REFERENCES

1. EMA. EMA (EMA/CHMP/EWP/147013/2004 Committee for Medicinal Products for Human Use [CHMP]). Guideline on the role of pharmacokinetics in the development of medicinal products in the paediatric population. 2007.
2. FDA. General Clinical Pharmacology Considerations for Pediatric Studies for Drugs and Biological Products, Guidance for Industry, December 2014. Available from: https://www.fda.gov/downloads/Drugs/GuidanceComplianceRegulatoryInformation/Guidances/UCM425885.pdf.
3. Zisowsky J, Krause A, Dingemanse J. Drug Development for Pediatric Populations: Regulatory Aspects. Pharmaceutics. 2010;2(4):364-88.

4. Krekels EH, Neely M, Panoilia E, Tibboel D, Capparelli E, Danhof M, et al. From pediatric covariate model to semiphysiological function for maturation: part I-extrapolation of a covariate model from morphine to Zidovudine. CPT Pharmacometrics Syst Pharmacol. 2012;1:e9.
5. Zhao W, Biran V, Jacqz-Aigrain E. Amikacin maturation model as a marker of renal maturation to predict glomerular filtration rate and vancomycin clearance in neonates. Clin Pharmacokinet. 2013;52(12):1127-34.
6. De Cock RF, Allegaert K, Sherwin CM, Nielsen EI, de Hoog M, van den Anker JN, et al. A neonatal amikacin covariate model can be used to predict ontogeny of other drugs eliminated through glomerular filtration in neonates. Pharmaceutical research. 2014;31(3):754-67.
7. Calvier EAM, Krekels EHJ, Yu H, Valitalo PAJ, Johnson TN, Rostami-Hodjegan A, et al. Drugs Being Eliminated via the Same Pathway Will Not Always Require Similar Pediatric Dose Adjustments. CPT Pharmacometrics Syst Pharmacol. 2018.
8. Michaels S, Wang MZ. The revised human liver cytochrome P450 "Pie": absolute protein quantification of CYP4F and CYP3A enzymes using targeted quantitative proteomics. Drug Metab Dispos. 2014;42(8):1241-51.
9. Ince I, Knibbe CA, Danhof M, de Wildt SN. Developmental changes in the expression and function of cytochrome P450 3A isoforms: evidence from in vitro and in vivo investigations. Clin Pharmacokinet. 2013;52(5):333-45.
10. Gorski JC, Hall SD, Jones DR, VandenBranden M, Wrighton SA. Regioselective biotransformation of midazolam by members of the human cytochrome P450 3A (CYP3A) subfamily. Biochem Pharmacol. 1994;47(9):1643-53.
11. Thummel KE, Shen DD, Podoll TD, Kunze KL, Trager WF, Hartwell PS, et al. Use of midazolam as a human cytochrome P450 3A probe: I. In vitro-in vivo correlations in liver transplant patients. J Pharmacol Exp Ther. 1994;271(1):549-56.
12. Dundee JW, Collier PS, Carlisle RJ, Harper KW. Prolonged midazolam elimination half-life. Br J Clin Pharmacol. 1986;21(4):425-9.
13. von Moltke LL, Greenblatt DJ, Harmatz JS, Shader RI. Alprazolam metabolism in vitro: studies of human, monkey, mouse, and rat liver microsomes. Pharmacology. 1993;47(4):268-76.
14. Jacobsen W, Kuhn B, Soldner A, Kirchner G, Sewing KF, Kollman PA, et al. Lactonization is the critical first step in the disposition of the 3-hydroxy-3-methylglutaryl-CoA reductase inhibitor atorvastatin. Drug Metab Dispos. 2000;28(11):1369-78.
15. Bedford TA, Rowbotham DJ. Cisapride. Drug interactions of clinical significance. Drug Saf. 1996;15(3):167-75.
16. Simard C, Michaud V, Gibbs B, Masse R, Lessard E, Turgeon J. Identification of the cytochrome P450 enzymes involved in the metabolism of domperidone. Xenobiotica. 2004;34(11-12):1013-23.
17. Guengerich FP, Muller-Enoch D, Blair IA. Oxidation of quinidine by human liver cytochrome P-450. Mol Pharmacol. 1986;30(3):287-95.
18. Walker DK, Ackland MJ, James GC, Muirhead GJ, Rance DJ, Wastall P, et al. Pharmacokinetics and metabolism of sildenafil in mouse, rat, rabbit, dog and man. Xenobiotica. 1999;29(3):297-310.

19. Prueksaritanont T, Gorham LM, Ma B, Liu L, Yu X, Zhao JJ, et al. In vitro metabolism of simvastatin in humans [SBT]identification of metabolizing enzymes and effect of the drug on hepatic P450s. Drug Metab Dispos. 1997;25(10):1191-9.
20. Swart PJ, Krauwinkel WJ, Smulders RA, Smith NN. Pharmacokinetic effect of ketoconazole on solifenacin in healthy volunteers. Basic Clin Pharmacol Toxicol. 2006;99(1):33-6.
21. Tateishi T, Krivoruk Y, Ueng YF, Wood AJ, Guengerich FP, Wood M. Identification of human liver cytochrome P-450 3A4 as the enzyme responsible for fentanyl and sufentanil N-dealkylation. Anesth Analg. 1996;82(1):167-72.
22. Sattler M, Guengerich FP, Yun CH, Christians U, Sewing KF. Cytochrome P-450 3A enzymes are responsible for biotransformation of FK506 and rapamycin in man and rat. Drug Metab Dispos. 1992;20(5):753-61.
23. Vincent SH, Karanam BV, Painter SK, Chiu SH. In vitro metabolism of FK-506 in rat, rabbit, and human liver microsomes: identification of a major metabolite and of cytochrome P450 3A as the major enzymes responsible for its metabolism. Arch Biochem Biophys. 1992;294(2):454-60.
24. Kamimura H, Oishi S, Matsushima H, Watanabe T, Higuchi S, Hall M, et al. Identification of cytochrome P450 isozymes involved in metabolism of the alpha1-adrenoceptor blocker tamsulosin in human liver microsomes. Xenobiotica. 1998;28(10):909-22.
25. Zhou XJ, Zhou-Pan XR, Gauthier T, Placidi M, Maurel P, Rahmani R. Human liver microsomal cytochrome P450 3A isozymes mediated vindesine biotransformation. Metabolic drug interactions. Biochem Pharmacol. 1993;45(4):853-61.
26. Barst RJ, Ivy DD, Gaitan G, Szatmari A, Rudzinski A, Garcia AE, et al. A randomized, double-blind, placebo-controlled, dose-ranging study of oral sildenafil citrate in treatment-naive children with pulmonary arterial hypertension. Circulation. 2012;125(2):324-34.
27. Gupta M EA, Willmann S, Adamson PC, Galinkin JL, Barrett JS. Model-based Approaches to Investigate Pharmacogenetic and Developmental Sources of Variation in the Pharmacokinetics of Midazolam after Oral administration in Children. 2006 [Available from: AAPS 2006. Abstract 003255. https://abstracts.aaps.org/Published/Browse.aspx.
28. Comets E, Brendel K, Mentre F. Computing normalised prediction distribution errors to evaluate nonlinear mixed-effect models: the npde add-on package for R. Comput Methods Programs Biomed. 2008;90(2):154-66.
29. Pfizer. Study protocol 'A Randomized, Double-Blind, Placebo-Controlled Study of Sildenafil in Children With Pulmonary Arterial Hypertension'. https://clinicaltrials.gov/ct2/show/NCT00159913.
30. European Medicines Agency. Revatio Product Information. Accessed on 18th December 2017. Available from: http://www.ema.europa.eu/docs/en_GB/document_library/EPAR_-_Product_Information/human/000638/WC500055840.pdf
31. Frechen S, Junge L, Saari TI, Suleiman AA, Rokitta D, Neuvonen PJ, et al. A semiphysiological population pharmacokinetic model for dynamic inhibition of liver and gut wall cytochrome P450 3A by voriconazole. Clin Pharmacokinet. 2013;52(9):763-81.
32. Lown KS, Thummel KE, Benedict PE, Shen DD, Turgeon DK, Berent S, et al. The erythromycin breath test predicts the clearance of midazolam. Clin Pharmacol Ther. 1995;57(1):16-24.
33. DrugBank Canada, accessed July 17th 2017. Available from https://www.drugbank.ca.
34. Lennernas H. Clinical pharmacokinetics of atorvastatin. Clin Pharmacokinet. 2003;42(13):1141-60.

35. CVZ. College voor zorgverzekeringen Nederland; Farmacotherapeutisch Kompas (Dutch Pharmacotherapeutic Compass) 2013 [updated April 1, 2013. http://www.fk.cvz.nl/].
36. Rampe D, Roy ML, Dennis A, Brown AM. A mechanism for the proarrhythmic effects of cisapride (Propulsid): high affinity blockade of the human cardiac potassium channel HERG. FEBS Lett. 1997;417(1):28-32.
37. Heykants J, Hendriks R, Meuldermans W, Michiels M, Scheygrond H, Reyntjens H. On the pharmacokinetics of domperidone in animals and man. IV. The pharmacokinetics of intravenous domperidone and its bioavailability in man following intramuscular, oral and rectal administration. Eur J Drug Metab Pharmacokinet. 1981;6(1):61-70.
38. Simcyp (R) Simulator version 15.1. Certara, Sheffield, United Kingdom. Available from: https://www.certara.com/software/physiologically-based-pharmacokinetic-modeling-and-simulation/simcyp-simulator/ [
39. Bressler R, Bahl JJ. Principles of drug therapy for the elderly patient. Mayo Clin Proc. 2003;78(12):1564-77.
40. Zhao P, Zhang L, Grillo JA, Liu Q, Bullock JM, Moon YJ, et al. Applications of physiologically based pharmacokinetic (PBPK) modeling and simulation during regulatory review. Clin Pharmacol Ther. 2011;89(2):259-67.
41. Mehrotra N, Gupta M, Kovar A, Meibohm B. The role of pharmacokinetics and pharmacodynamics in phosphodiesterase-5 inhibitor therapy. Int J Impot Res. 2007;19(3):253-64.
42. Gruer PJ, Vega JM, Mercuri MF, Dobrinska MR, Tobert JA. Concomitant use of cytochrome P450 3A4 inhibitors and simvastatin. Am J Cardiol. 1999;84(7):811-5.
43. Benet LZ, Cummins CL, Wu CY. Unmasking the dynamic interplay between efflux transporters and metabolic enzymes. Int J Pharm. 2004;277(1-2):3-9.
44. Osmulski PA, Gaczynska M. Rapamycin allosterically inhibits the proteasome. Mol Pharmacol. 2013;84(1):104-13.
45. Doroshyenko O, Fuhr U. Clinical pharmacokinetics and pharmacodynamics of solifenacin. Clin Pharmacokinet. 2009;48(5):281-302.
46. Raucoules-Aime M, Kaidomar M, Levron JC, Le Moing JP, Goubaux B, Gugenheim J, et al. Hepatic disposition of alfentanil and sufentanil in patients undergoing orthotopic liver transplantation. Anesth Analg. 1997;84(5):1019-24.
47. Saari TI, Ihmsen H, Mell J, Frohlich K, Fechner J, Schuttler J, et al. Influence of intensive care treatment on the protein binding of sufentanil and hydromorphone during pain therapy in postoperative cardiac surgery patients. Br J Anaesth. 2014;113(4):677-87.
48. Tuteja S, Alloway RR, Johnson JA, Gaber AO. The effect of gut metabolism on tacrolimus bioavailability in renal transplant recipients. Transplantation. 2001;71(9):1303-7.
49. Piekoszewski W, Jusko WJ. Plasma protein binding of tacrolimus in humans. J Pharm Sci. 1993;82(3):340-1.
50. Matsushima H, Kamimura H, Soeishi Y, Watanabe T, Higuchi S, Tsunoo M. Pharmacokinetics and plasma protein binding of tamsulosin hydrochloride in rats, dogs, and humans. Drug Metab Dispos. 1998;26(3):240-5.
51. Dennison JB, Mohutsky MA, Barbuch RJ, Wrighton SA, Hall SD. Apparent high CYP3A5 expression is required for significant metabolism of vincristine by human cryopreserved hepatocytes. J Pharmacol Exp Ther. 2008;327(1):248-57.
52. Chan JD. Pharmacokinetic drug interactions of vinca alkaloids: summary of case reports. Pharmacotherapy. 1998;18(6):1304-7.

53. Knebel W, Gastonguay MR, Malhotra B, El-Tahtawy A, Jen F, Gandelman K. Population pharmacokinetics of atorvastatin and its active metabolites in children and adolescents with heterozygous familial hypercholesterolemia: selective use of informative prior distributions from adults. J Clin Pharmacol. 2013;53(5):505-16.
54. Dansirikul C, Morris RG, Tett SE, Duffull SB. A Bayesian approach for population pharmacokinetic modelling of sirolimus. Br J Clin Pharmacol. 2006;62(4):420-34.
55. Scholz J, Steinfath M, Schulz M. Clinical pharmacokinetics of alfentanil, fentanyl and sufentanil. An update. Clin Pharmacokinet. 1996;31(4):275-92.
56. Saeves I, Line PD, Bremer S, Vethe NT, Tveit RG, Meltevik TJ, et al. Tacrolimus exposure and mycophenolate pharmacokinetics and pharmacodynamics early after liver transplantation. Ther Drug Monit. 2014;36(1):46-53.
57. Tsuda Y, Tatami S, Yamamura N, Tadayasu Y, Sarashina A, Liesenfeld KH, et al. Population pharmacokinetics of tamsulosin hydrochloride in paediatric patients with neuropathic and non-neuropathic bladder. Br J Clin Pharmacol. 2010;70(1):88-101.
58. de Graaf SS, Bloemhof H, Vendrig DE, Uges DR. Vincristine disposition in children with acute lymphoblastic leukemia. Med Pediatr Oncol. 1995;24(4):235-40.
59. Hill KD, Sampson MR, Li JS, Tunks RD, Schulman SR, Cohen-Wolkowiez M. Pharmacokinetics of intravenous sildenafil in children with palliated single ventricle heart defects: effect of elevated hepatic pressures. Cardiol Young. 2016;26(2):354-62.
60. Szefler SJ, Pieroni DR, Gingell RL, Shen DD. Rapid elimination of quinidine in pediatric patients. Pediatrics. 1982;70(3):370-5.
61. Scott JR, Courter JD, Saldana SN, Widemann BC, Fisher M, Weiss B, et al. Population pharmacokinetics of sirolimus in pediatric patients with neurofibromatosis type 1. Ther Drug Monit. 2013;35(3):332-7.
62. Greeley WJ, de Bruijn NP, Davis DP. Sufentanil pharmacokinetics in pediatric cardiovascular patients. Anesth Analg. 1987;66(11):1067-72.
63. Jalil MH, Hawwa AF, McKiernan PJ, Shields MD, McElnay JC. Population pharmacokinetic and pharmacogenetic analysis of tacrolimus in paediatric liver transplant patients. Br J Clin Pharmacol. 2014;77(1):130-40.
64. Calvier EA, Krekels EH, Valitalo PA, Rostami-Hodjegan A, Tibboel D, Danhof M, et al. Allometric Scaling of Clearance in Paediatric Patients: When Does the Magic of 0.75 Fade? Clin Pharmacokinet. 2017;56(3):273-85.
65. Bai S, Stepkowski SM, Kahan BD, Brunner LJ. Metabolic interaction between cyclosporine and sirolimus. Transplantation. 2004;77(10):1507-12.
66. Dennison JB, Jones DR, Renbarger JL, Hall SD. Effect of CYP3A5 expression on vincristine metabolism with human liver microsomes. J Pharmacol Exp Ther. 2007;321(2):553-63.
67. McNamara PJ, Alcorn J. Protein binding predictions in infants. AAPS PharmSci. 2002;4(1):E4.
68. Olguin HJ, Martinez HO, Perez CF, Mendiola BR, Espinosa LR, Pacheco JLC, et al. Pharmacokinetics of sildenafil in children with pulmonary arterial hypertension. World J Pediatr. 2017;13(6):588-92.
69. Brussee JM, Vet NJ, Krekels EHJ, Valkenburg AJ, Jacqz-Aigrain E, van Gerven JMA, et al. Predicting CYP3A-mediated midazolam metabolism in critically ill neonates, infants, children, and adults with inflammation and organ failure. Br J Clin Pharmacol. 2017.
70. Brocks DR, Mehvar R. Stereoselectivity in the pharmacodynamics and pharmacokinetics of the chiral antimalarial drugs. Clin Pharmacokinet. 2003;42(15):1359-82.

# SUPPLEMENTAL MATERIAL (CHAPTER 7)

**Table SI.** Drug properties of selected CYP3A substrates

| Drug | $ER_{adult}$ | Ref | Protein binding | Ref | $F_{u,adult}$ | Ref | Reported $CL_{adult,70kg}$ | Ref | Reported $CL_{child}$ | Ref |
|---|---|---|---|---|---|---|---|---|---|---|
| **Midazolam** | 0.354 | (31) | HSA | (33) | 0.022 | (32) | - | | - | |
| **Alprazolam** | 0.15 | (33) | HSA | (33) | 0.20 | (33) | - | | - | |
| **Atorvastatin** | 0.42 | (34) | HSA | (34) | 0.02 | (33, 35) | 652 L/h[#] | (53) | $699 \cdot \left(\frac{WT}{70}\right)^{0.75}$ L/h[#] | (53) |
| **Cisapride** | 0.65 | (33) | HSA | (36) | 0.025 | (36) | - | | - | |
| **Domperidone** | 0.63 | (37) | HSA | (37) | 0.08 | (37) | - | | - | |
| **Quinidine** | 0.18 | (38) | HSA | (39) | 0.05* | (35) | 4 mL/min/kg | (33) | Individual values, 0.461 L/h/kg 0.287 L/h/kg[+] | (60) |
| **Sildenafil** | 0.45 | (40) | HSA | (41) | 0.04 | (41) | 41 L/h | (30) | 0.62 L/h/kg | (59) |
| **Simvastatin** | 0.95 | (42) | HSA | (34) | 0.05 | (33, 35) | - | | - | |
| **Sirolimus** | 0.60 | (43) | HSA | (44) | 0.08 | (35) | 0.210 L/h/kg[#] | (54) | Individual values | (61) |
| **Solifenacin** | 0.10 | (45) | AAG | (45) | 0.02 | (35, 45) | - | | - | |
| **Sufentanil** | 0.35 | (46) | HSA | (47) | 0.08 | (35) | 0.762 L/h/kg | (55) | 18.1 mL/min/kg 16.9 mL/min/kg 13.1 mL/min/kg[†] | (62) |
| **Tacrolimus** | 0.082 | (48) | HSA | (49) | 0.01 | (33, 35) | 31.8 L/h[‡#] | (56) | $12.9 \cdot \left(\frac{WT}{12.2}\right)^{0.75}$ L/h[#] | (63) |
| **Tamsulosin** | 0.70[^] | (50) | AAG | (50) | 0.01 | (35, 50) | 2.88 L/h | (57) | $2.28 \cdot \left(\frac{WT}{70}\right)^{0.75}$ L/h[#] | (57) |
| **Vincristine** | 0.04 | (51) | AAG | (52) | 0.402 | (52) | 0.293 L/h/kg | (58) | Individual values, 1.049 L/h/kg | (58) |

ER: extraction ratio. $F_u$: fraction unbound. Ref: reference.
HSA: human serum albumin. AAG: α1-acid glycoprotein
[#]Reported clearances are apparent clearances (CL/F).
*Brocks *et al.* describe a different value of $f_u$ of 0.23 (70), but both $f_u$ values (0.23 or 0.05) lead to the same conclusion down to which age accurate scaling is possible (down to ≤ 1 day of age).
[+]Quinidine clearance in children was reported for children 3.7-12 years and ≥12 years of age.
[†]Sufentanil clearance in children was reported for 3 different age groups of 1-24 months of age, 2-12 years of age, and 12-18 years of age, with assumed weight ranges (based on WHO guidelines) of 4.5-12, 12-40 and 40-70 kg respectively.
[‡]Tacrolimus clearance was derived from dose and exposure.
[^]Vincristine is reported to be a high extraction ratio drug. Therefore, the extraction ratio was assumed 0.7, but this may be higher.

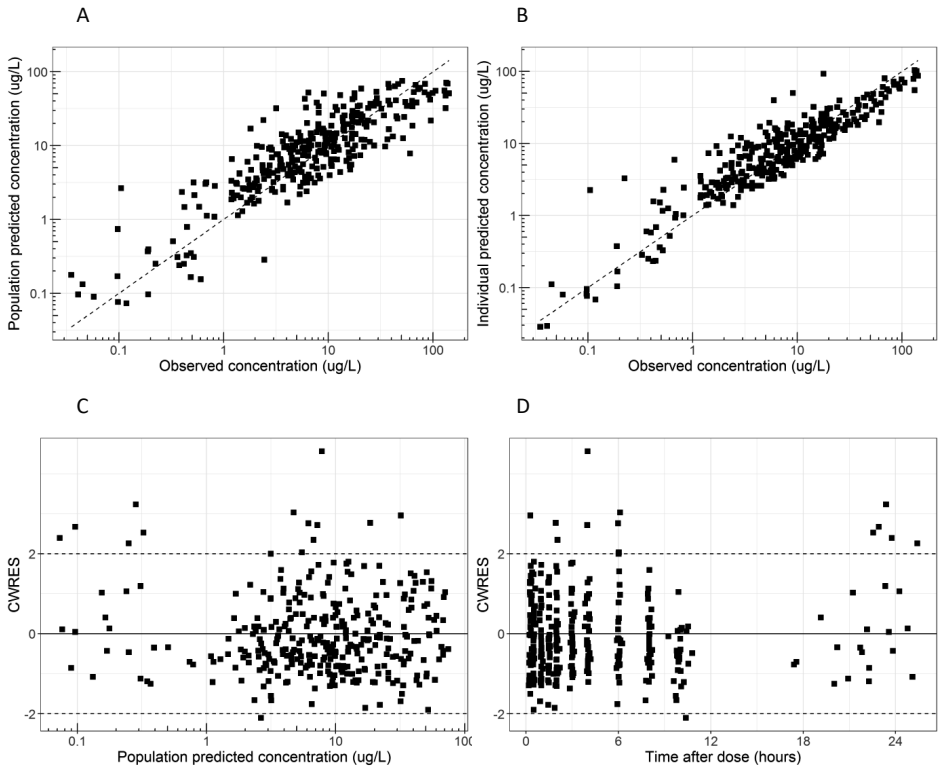



**Figure S1.** Goodness-of-fit plots for the pediatric population PK model of midazolam (model drug). Plots include individual and population predicted concentration versus observed concentration (A,B) and conditionally weighted residuals (CWRES) versus predicted concentration (C) and versus time after dose (D).

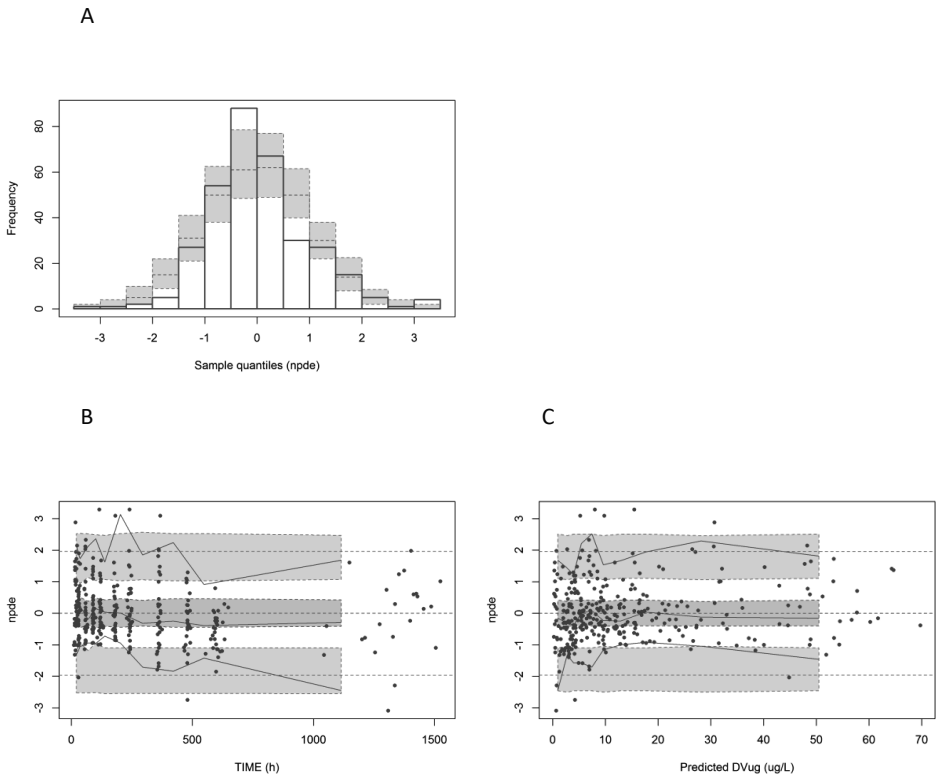
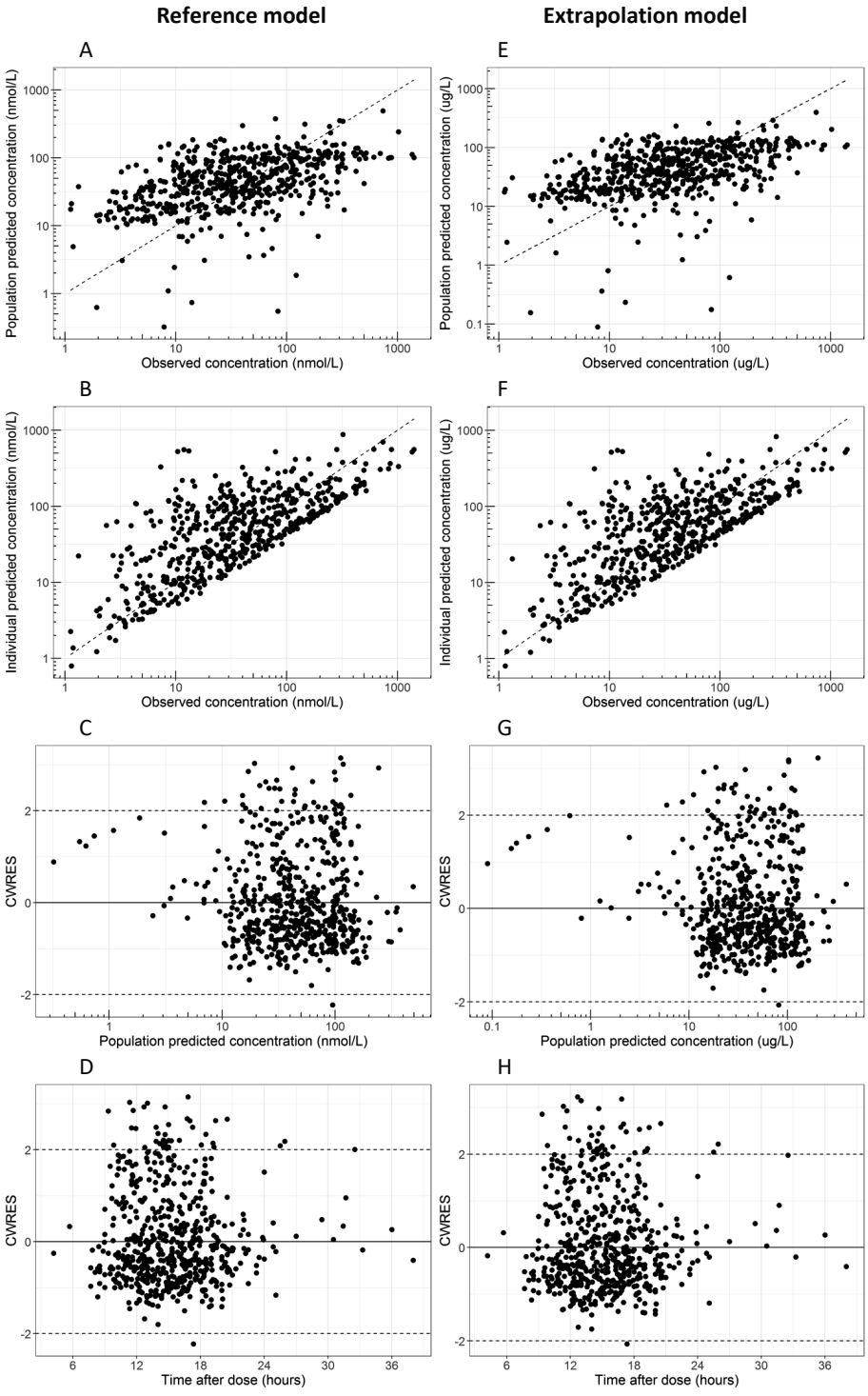



**Figure S2.** Visualization of the normalized prediction distribution error (NPDE) results for midazolam (E-G) showed that the mean NPDE of 0.016 was not significantly different from 0 ($p>0.1$, Wilcoxon signed rank test), and the variance for midazolam of 0.92 was not significantly different from 1 ($p>0.1$, Fisher variance test). A) Histogram of NPDEs, with the observed frequency of sample quantiles of the NPDEs (white bars), overlaid with the density of the standard normal distribution (blue bars). B) NPDE versus time, with the NPDE for each observation (dots), and the lines indicate the mean (red) and the 5$^{th}$ and 95$^{th}$ percentiles (blue) of the NPDEs, and the shaded areas are the simulated 95% confidence intervals of the NPDE median (red) and 5$^{th}$ and 95$^{th}$ percentiles (blue). C) NPDE versus predicted concentration, with dots and lines as described for panel B.

**Figure S3.** Goodness-of-fit plots for the two pediatric population PK models for the test drug (sildenafil). In the reference model clearance was estimated from the data (A-D) and in the extrapolation model the covariate model obtained with midazolam was used to describe the change in clearance in this population (E-H).


Reference model
Extrapolation model
A
E
B
F
C
G
D
H
Population predicted concentration (nmol/L)
Observed concentration (nmol/L)
Population predicted concentration (ug/L)
Observed concentration (ug/L)
Individual predicted concentration (nmol/L)
Individual predicted concentration (ug/L)
CWRES
Time after dose (hours)

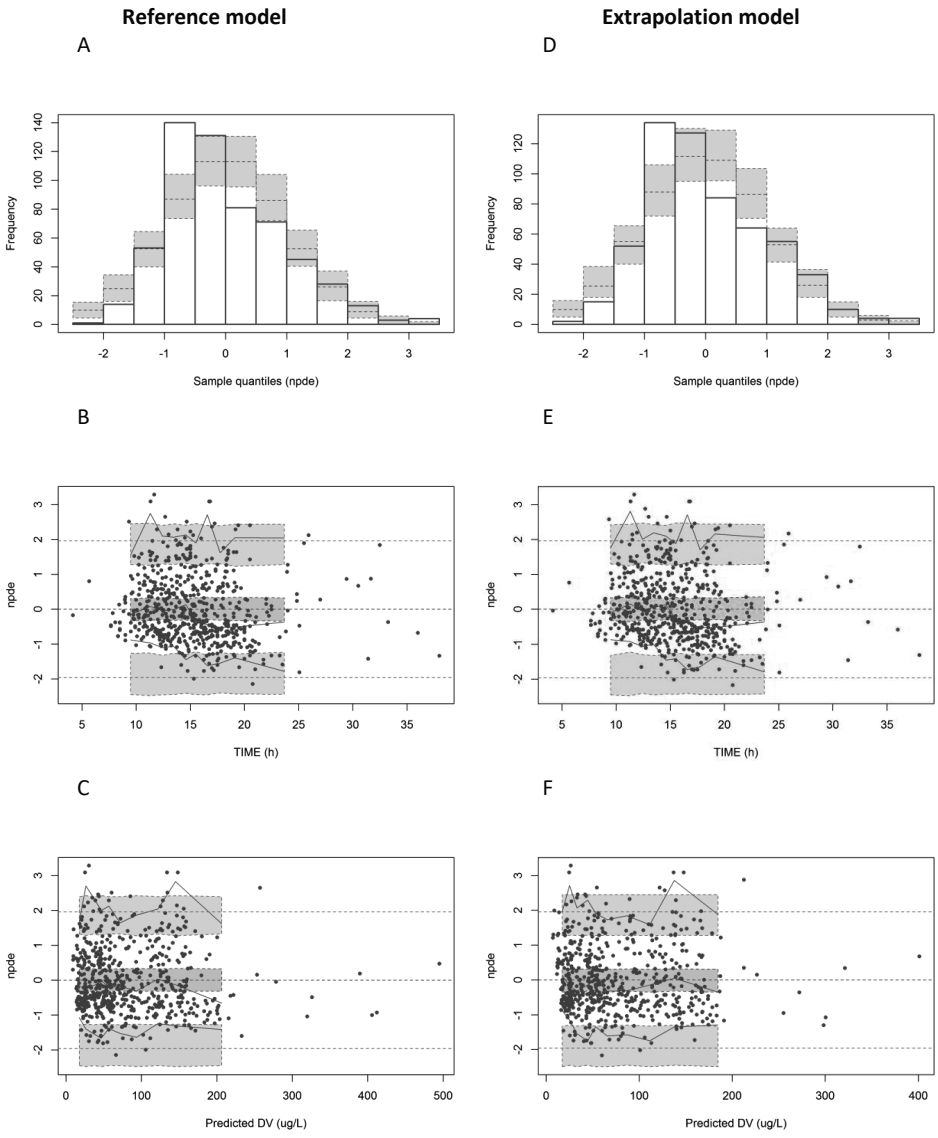
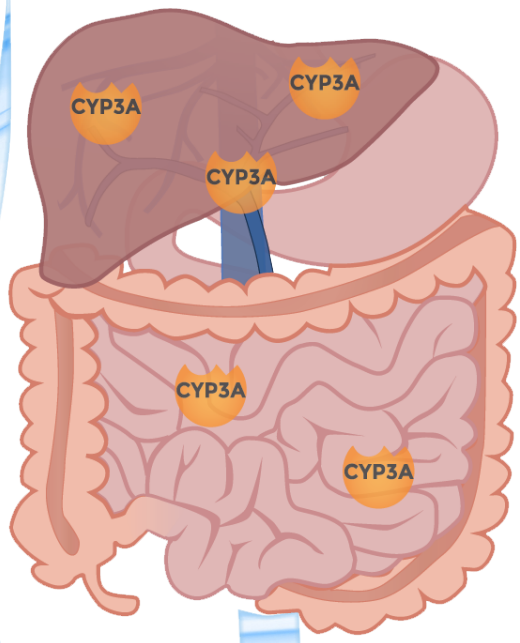



**Figure S4.** Visualization of the normalized prediction distribution error (NPDE) results for the sildenafil reference model (A-C) and the model based on between-drug extrapolation (D-F). The mean NPDE for the reference and extrapolated model were with 0.004 and 0.031, respectively, not significantly different from 0 ($p>0.1$, Wilcoxon signed rank test), and the variances were with 0.92 and 0.97, respectively, not significantly different from 1 ($p>0.1$, Fisher variance test). First row: Histogram of NPDEs, with the observed frequency of sample quantiles of the NPDEs (white bars), overlaid with the density of the standard normal distribution (blue bars). Second and third row: NPDE versus time and predicted concentration respectively, with the NPDE for each observation (dots), and the lines indicate the mean (red) and the 5$^{th}$ and 95$^{th}$ percentiles (blue) of the NPDEs, and the shaded areas are the simulated 95% confidence intervals of the NPDE median (red) and 5$^{th}$ and 95$^{th}$ percentiles (blue).

# Section V

## Summary, Conclusions, and Perspectives



# Chapter 8

## First-pass and systemic metabolism of cytochrome P450 3A substrates in neonates, infants, and children – Summary, Conclusions, and Perspectives

Growth and development affect the pharmacokinetics (PK) of drugs administered to neonates, infants, and children (1, 2). Among these developmental changes is the maturation of drug metabolizing enzyme expression and activity, which impacts the rate of metabolic clearance of drugs (3). As described in **Chapter 1**, the research described in this thesis focused on the metabolism by cytochrome P450 (CYP) 3A enzymes, using midazolam as probe drug (4). The overall aim of this thesis was to predict CYP3A-mediated plasma clearance in neonates, infants, and children, by development of pediatric (physiological) population PK models. Accurate prediction of plasma clearance of drugs is essential to provide rational support for pediatric doses in first-in-child studies during drug development and to develop pediatric dose recommendations for clinical practice.

For this purpose, we presented in **Section I** our view on preferred approaches to estimate drug clearance to establish individualized dosing regimens for drugs in the pediatric population. **Section II** described the CYP3A-mediated systemic metabolism in critically ill pediatric patients. Within the developed population PK model, body weight, critical illness, and inflammation were identified as covariates to explain part of the inter- and intra-individual variability within this population. This model was next evaluated for its predictive performance for clearance in similar (postoperative or critically ill) patients, and in other populations including preterm neonates and adults. **Section III** focused on methods to distinguish between first-pass and systemic CYP3A-mediated metabolism to elucidate the role of intestinal and hepatic CYP3A in neonates and children covering the whole pediatric age range. Lastly, **Section IV** discussed how information on CYP3A-mediated clearance of the probe drug midazolam in children can be used for scaling of clearance of other CYP3A substrates, and described when a pediatric covariate function for CYP3A-mediated midazolam clearance can be applied to scale plasma clearance of other commonly used CYP3A substrates (including sildenafil) in the pediatric population.

## I. Children in clinical trials: towards evidence-based pediatric pharmacotherapy using pharmacokinetic-pharmacodynamic modelling

**Chapter 2** presented our view on model-based pediatric drug development. It discussed the lack of dedicated pharmacokinetic-pharmacodynamic (PKPD) studies in children compared to adults, and that therefore pediatric doses for many CYP3A substrates and other drugs are often linearly or allometrically scaled from adult values. However, predicting plasma clearance in especially young children is complicated, as each hepatic isoenzyme has a different maturation profile, and therefore maturation functions reflecting these changes to scale plasma clearance in the pediatric population are needed for each hepatic elimination pathway. These

functions are not always available, but studying the clearance of the CYP3A-substrate midazolam (5) in children will increase our understanding of the CYP3A enzyme maturation patterns.

General pediatric PK models, or physiologically-based models when sufficient system-specific and drug-specific information are available, describing drug clearance should be developed in order to develop evidence-based dosing regimens in children, and these models should be thoroughly evaluated and validated with external data, as also illustrated for instance in Chapter 4.

A proper study design is pivotal in answering the research questions of pharmacological studies and therefore a multidisciplinary team including clinicians, clinical pharmacologists, and pharmacometricians should be involved in the study design to discuss e.g. what (covariate) data should be collected at which time points. The covariate relationships with clearance in the developed PK models can be used to individualize drug regimens provided the therapeutic window and/or target exposure is known for the varying degrees of critical illness. Based on simulations with the model, dosing recommendations can be proposed and the optimized dosing schedule should be evaluated in clinical practice. For this approach, properly designed clinical PKPD studies will remain the backbone of pediatric research to develop and confirm model-based pediatric dose recommendations for drugs in children.

## II. Systemic CYP3A-mediated metabolism in critically ill children

We previously observed large differences in the reported mean values of midazolam clearance in pediatric populations of similar ages. The most striking difference between these cohorts was the severity of illness, with healthier children showing higher midazolam clearance than critically ill children. We hypothesized that these differences could be due to severity of disease and/or inflammation.

In **Chapter 3** we described the systemic CYP3A-mediated clearance of midazolam in critically ill neonates, infants, and children after multiple intravenous administrations based on therapeutic need. Based on prospectively collected pharmacokinetic data from 83 patients between 0 and 17 years of age, a two-compartment PK model was developed that described the concentrations of midazolam well. In the model, body weight was found as most significant covariate for clearance, with an almost linear increase in clearance with increasing body weight. In line with our hypothesis, an increased concentration of the inflammatory marker C-reactive protein (CRP) was found to correlate to a decreased midazolam clearance, with a 51.2% lower clearance

when CRP increased from 10 to 100 mg/L. Disease severity was also related to midazolam clearance, as with an increased number of failing organs, e.g. from 1 to 2 or 3, the midazolam clearance decreased by e.g. 25.6% or 34.9%, respectively. As a result, CYP3A-mediated midazolam clearance is even up to 77.4% lower in patients with both increased CRP concentrations and an increased number of failing organs.

The decreased midazolam plasma clearance in critically ill children described in **Chapter 3**, may be due to decreased CYP3A enzyme activity when the inflammatory markers CRP and IL-6 concentrations increase (6-8), and multiple organ failure, in addition to inflammation, may lead to a further decreased midazolam clearance, although the underlying mechanisms of how cardiovascular, respiratory (9), hepatic, and renal failure (10) may affect the PK of midazolam are not well understood (6). This decreased midazolam clearance in critically ill children leads to increased plasma concentrations and exposure of midazolam in patients with inflammation, organ failure, or both (**Chapter 3**).

The developed population PK model was subsequently externally validated in **Chapter 4**, which evaluated the model's predictive performance in both critically ill children and other populations including preterm neonates receiving midazolam intravenously. The results showed that in critically ill term neonates, infants, children and adults, the model could adequately predict the midazolam clearance. Compared to reported values for midazolam clearance in literature, the clearance of the critically ill patients in our study was found to be generally lower, which may be due to their disease state, as most published clearance values come from PK studies in relatively healthy children (11-15).

In healthy adults, the observed and predicted clearance values were also higher compared to critically ill adults, which may also be explained by the fact that no inflammation and organ failure is present in this population. However, clearance was largely over-predicted in preterm neonates with a body weight below 3.5 kg and a gestational age of less than 37 weeks. This is most likely due to the fact that the model did not account for immaturity of CYP3A in preterm infants. In preterm neonates, we anticipate that the total CYP3A activity is much lower compared to term neonates and young infants, and also more immature than would be expected based on scaling based on body weight from term neonates (16-18). Hence, while the model developed in **Chapter 3** should not be used for extrapolations to very young neonates, this external validation in **Chapter 4** confirmed that the developed PK model could adequately predict pediatric CYP3A-mediated clearance in (pediatric) patients with varying levels of (critical) illness.

## III. First-pass CYP3A-mediated metabolism in children after oral drug administration

A previous study showed that the oral bioavailability of midazolam is much higher in preterm infants (19) than in adults. This observation suggests immature intestinal and/or hepatic CYP3A activity in preterm infants, resulting in higher systemic midazolam exposure. However, to our knowledge, the relative contribution of intestinal and hepatic CYP3A metabolism and their relative changes with age have not been determined before.

The presystemic CYP3A-mediated clearance can only be described based on oral PK data, and preferably in combination with intravenous PK data. In **Chapters 5 and 6** we explored the role of gut wall and hepatic CYP3A enzymes in presystemic clearance of midazolam in preterm neonates and children from 1-18 years of age, respectively. For this, a novel approach called physiological population PK modelling was applied, utilizing both information on the biological system (physiology of the gastro-intestinal tract and liver) and population PK modelling of data of midazolam and its primary metabolite, 1-OH-midazolam, from children of varying ages.

The intrinsic clearance in the gut wall and liver both appeared to increase with increasing body weight in children of 1-18 years of age. Figure 1A shows that the intrinsic intestinal and hepatic CYP3A-mediated clearances do not increase in parallel, and that the intrinsic gut wall clearance increases faster with age. The intrinsic gut wall clearance is lower than the intrinsic hepatic clearance throughout the pediatric and adult age range, and the relative contribution of CYP3A enzymes in gut wall and liver to the presystemic metabolism of CYP3A substrates differs with age. In preterm neonates, the ratio of intrinsic hepatic over gut wall clearance is much larger than in children and healthy adults, with a ratio of approximately 340 in preterm neonates (**Chapter 5**) versus 153 in young infant up to 2 years of age, 87 for a typical 27-kg child, 48 in adolescents ≥ 16 years-of-age (**Chapter 6**), compared to a ratio of 60 in adults (20). This indicates a smaller contribution of intrinsic gut wall clearance to the presystemic clearance with decreasing age.

When we consider the intrinsic clearance of midazolam a surrogate marker of total intestinal and hepatic activity of CYP3A enzymes, this indicates that at 1 year of age the hepatic CYP3A activity is already close to the adult values, in contrast to the total intestinal CYP3A activity which needs to increase more with age (**Chapter 6**). Comparing these results with preterm neonates, the intestinal and hepatic CYP3A activity in preterm neonates both appear to be very immature (**Chapter 5**)(figure 1A),

and because of this very low CYP3A activity, preterm neonates should be regarded as a different population than other children and adults.

It has been reported that both the CYP3A enzyme content of the enterocytes and the total size of the small intestine increases with age (1, 21, 22), and together, this may lead to a higher intrinsic CYP3A-mediated clearance in the gut wall in adolescents compared to neonates and infants. For hepatic CYP3A activity, our analysis in **Chapter 6** suggests that liver growth mostly contributes to the increase in hepatic CYP3A-mediated intrinsic clearance in children, while the CYP3A abundance and the amount of microsomal protein in the liver may remain relatively constant with age (17, 23, 24).

Plasma clearance is mostly dependent on intrinsic hepatic CYP3A clearance, and can be calculated based on the well-stirred model using hepatic intrinsic clearance together with the hepatic blood flow, protein binding and the blood: plasma ratio. We found that the plasma clearance increases from 0.03-0.79 (median 0.18) L/h in preterm neonates and 2.5-8.7 (median 6.0) L/h in children of 1-2 years of age to 9.0-24.6 (median 17.5) L/h in children ≥ 16 years of age (**Chapters 5 and 6**)(figure 1B).

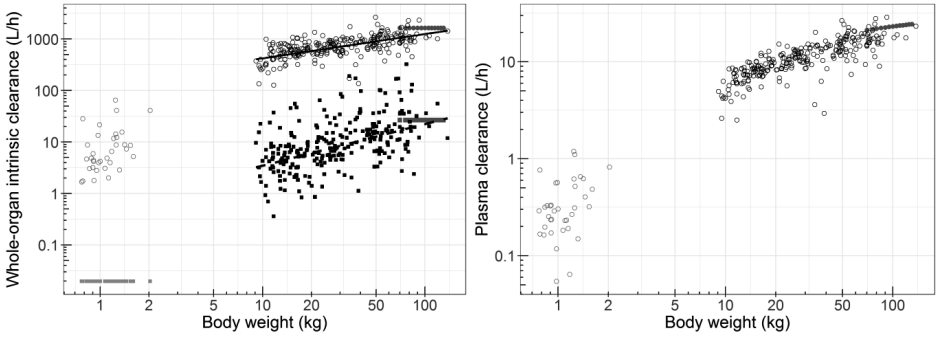



**Figure 1. A)** Whole-organ intrinsic clearance of midazolam in the gut wall (solid square) and the liver (open and solid circle) are plotted versus body weight, with values for preterm neonates (light grey solid squares and open circles)(Chapter 5) and children 1-18 years of age (black solid squares and open circles)(Chapter 6). Reported values from adults (20) of 26.7 (grey solid square) and 1640 L/h (grey solid circle), respectively, are shown as well. **B)** Total plasma clearance is shown versus body weight, with values for preterm neonates (light grey open circle)(Chapter 5), children 1-18 years of age (black open circle)(Chapter 6) and reported values for typical adults (grey closed circle)(20). Modified with permission from Brussee et al. (25).

**Chapter 5** also described that the intestinal and hepatic extraction ratio of midazolam were very low (median of 0.04 each), leading to extremely low presystemic clearance in preterm neonates. The total bioavailability is the product of the fraction absorbed

($F_a$), and the fractions escaping gut wall ($F_g$) and hepatic ($F_h$) metabolism, as per equation 1.

$F_{total} = F_a \times F_g \times F_h$ (eq. 1)

The resulting bioavailability of 92.3% is therefore very high, but highly variable in the population (90%CI: 75.4-94.5%)(figure 2) and this may lead to large differences in drug exposure and drug effect after oral dosing of CYP3A substrates in preterm neonates.

We also report a large variability in bioavailability around the median of 20.8% in children of 1-18 years of age (90%CI: 4.6-44.6%)(**Chapter 6**). As figure 2 shows, the fraction escaping hepatic metabolism (i.e. $F_h$) appears to increase significantly with age, while the fraction escaping gut wall metabolism (i.e. $F_g$) decreases with age, resulting in an age-independent total bioavailability of midazolam (i.e. $F_{total}$, which is calculated per eq. 1).

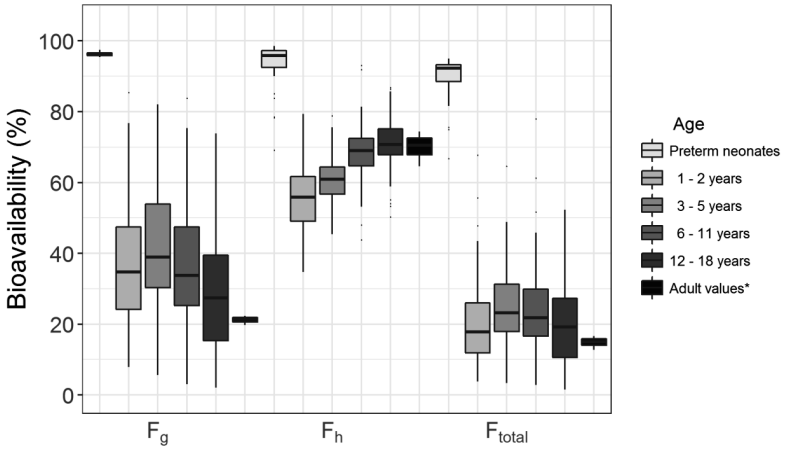



**Figure 2.** Midazolam bioavailability in the gut wall ($F_g$), in the liver ($F_h$) and total bioavailability ($F_{total}$) is much higher in preterm neonates (white)(Chapter 5), compared to children of four different age categories: 1-2 years, 3-5 years, 6-11 years, and 12-18 years of age (increasing grey scales)(Chapter 6) and compared to adult values (black)(20). *Adult bioavailability values are calculated based on their reported typical intrinsic hepatic clearance, hepatic blood flow for their body weight, the fraction unbound and blood: plasma ratio (20). Modified with permission from Brussee et al. (25).

## IV. Midazolam as probe drug for other CYP3A substrates

Midazolam is a widely accepted probe drug for CYP3A activity (4, 5), and midazolam clearance in neonates, infants, and children has been used to reflect the ontogeny of CYP3A in the pediatric population. Therefore, in **section IV** of this thesis, it was assessed when pediatric PK information from midazolam can be used to predict pediatric clearance of other CYP3A substrates.

As it would require many resources to study the PK of all drugs (including all CYP3A substrates) in the pediatric population, other approaches besides clinical studies have been proposed including full physiologically-based PK (PBPK) models to predict pediatric clearance values. While PBPK models require extensive system-specific and drug-specific information which may not always be available, it has been hypothesized that PK information of drugs sharing the same elimination pathway may be used to predict plasma clearance of drugs in children (26). This between-drug extrapolation of clearance has been applied successfully in predicting clearance for individual antibiotics eliminated by glomerular filtration in neonates with amikacin as model drug (27, 28). Additionally, the clearance of the UGT2B7-substrate zidovudine in children could be accurately scaled using a pediatric covariate function for UGT2B7-mediated drug glucuronidation from a morphine PK model (26).

While these data are very reassuring, the question emerges whether this also applies to CYP3A-mediated metabolism. Calvier *et al.* (29) explored this approach in a systematic way for all hepatic isoenzymes and reported on the basis of their developed framework that accurate between-drug extrapolation of clearance on the basis of a shared elimination pathway, depends not only on the fraction metabolized by the specific hepatic isoenzyme, but also on other properties of the test drug, including the drugs extraction ratio in adults (ER), the type of binding plasma protein, and the unbound fraction in adults ($f_u$).

In **Chapter 7**, this framework was applied to scale pediatric clearance of various commonly used CYP3A substrates from adult clearance values using a pediatric covariate function for CYP3A-mediated midazolam clearance. According to the framework of Calvier *et al.* (29), clearance of CYP3A substrates can be systematically accurately scaled using the pediatric covariate function for CYP3A-mediated clearance from a midazolam PK model if they have an extraction ratio of 0.35-0.65 or 0.05-0.55 and bind <10% or >90% to albumin in adults, respectively. Less combinations of drug properties of AGP-bound CYP3A substrates lead to accurate scaling based on a midazolam pediatric covariate function, with no scenarios for drugs with low protein binding ($f_u$ ≥0.9), but clearance of drugs that are 90% bound to AGP and have an extraction ratio of 0.4-0.6 in adults can be accurately scaled. For alprazolam, atorvastatin, quinidine, sildenafil, solifenacin, sufentanil and tacrolimus, this means that scaling of pediatric clearance using the pediatric covariate function of pediatric

PK model for midazolam will be systematically accurate down to one day of age, based on their drug properties.

For CYP3A substrates for which pediatric and adult clearance values were available in literature, we could confirm the accurate pediatric clearance predictions for atorvastatin, quinidine, sildenafil, sufentanil, tacrolimus, and tamsulosin, down to various ages, and as low as one year of age, as the scaled clearance values were in agreement with the reported pediatric clearance values (prediction error <50%) (**Chapter 7**). For sirolimus and vincristine, a larger prediction error was observed, which may possibly be due to the known induction of CYP3A activity by sirolimus (30) impacting its plasma clearance, and to the larger contribution of CYP3A5 in the metabolism of vincristine (31), with a relative smaller role for CYP3A4 compared to midazolam.

Furthermore, based on PK data from 156 children receiving sildenafil, **Chapter 7** showed that clearance of the CYP3A substrate sildenafil in children varying in age between 1 and 17 years was accurately scaled by the pediatric covariate function for CYP3A-mediated midazolam clearance, as no large differences were observed (prediction error <50%) compared to the estimated clearance values from a PK model for sildenafil.

Between-drug extrapolation of clearance from midazolam to drugs which are mainly metabolized by CYP3A (≥75% metabolized by that pathway), with the above described drug properties (i.e. an ER of 0.35-0.65 or 0.05-0.55 for <10% or >90% HSA-bound drugs in adults, respectively), can therefore be a valuable tool to predict CYP3A-mediated clearance in children, especially for CYP3A substrates with no or limited available pediatric PK information.

## Conclusions

**CYP3A-mediated plasma clearance of midazolam in term neonates, infants, and children increases non-linearly with increasing body weight, and is strongly reduced in pediatric patients with inflammation and organ failure.**

**Pediatric midazolam PK models may be used to predict midazolam clearance in term neonates, infants, and children, but preterm neonates should be regarded as a different population due to their immature CYP3A activity.**

**To distinguish between metabolism by CYP3A enzymes in the gut wall and liver, and to quantify the fractions escaping gut wall ($F_g$) and hepatic ($F_h$) metabolism, a physiological population PK modelling approach has proven useful.**

**The first-pass effect by intestinal and hepatic CYP3A-mediated metabolism in preterm neonates is extremely low compared to infants, children and adults.**

**The maturation of gut wall and hepatic CYP3A activity is not parallel. While the gut wall CYP3A activity is lower than the hepatic CYP3A activity in neonates, infants, children, and adults, it contributes more to first-pass metabolism with increasing age.**

**Between-drug extrapolation of clearance of midazolam to other CYP3A substrates is possible: a pediatric covariate function for CYP3A-mediated midazolam clearance can accurately scale the clearance of various commonly used CYP3A substrates that are ≥75% metabolized by CYP3A, with an ER<0.55 or 0.35-0.65 for low and highly albumin-bound drugs respectively, down to at least 1 year of age.**

## Perspectives

*Translation to the clinic: the impact of disease on midazolam PK and PD*

The developed PK model for midazolam in **Chapter 3** describes the CYP3A-mediated clearance in critically ill children and explains part of the inter-individual variability by taking into account the patient's body weight, their inflammation level (reflected by CRP concentrations) and organ failure. Based on these covariates for clearance, dosing recommendations can be derived when a therapeutic window or target concentration is known. For midazolam however, dosages are individually titrated to reach optimal sedation levels, and treatment starts with a maintenance dose between 0.05-0.2 mg/kg/h after a loading dose of 0.05-0.1 mg/kg (32, 33).

Based on the prediction of a lower clearance in critically ill patients (**Chapters 3 and 4**), also described in other patient populations (9, 10), this implies a lower dose would suffice to reach the same plasma concentration. However, studies have shown that interrupting or lowering the dose of midazolam in critically ill children does not improve the clinical outcome, which may suggest that higher midazolam plasma concentrations may be required to reach adequate sedation in children with inflammation and multiple organ failure (34). Also the contribution of the metabolites to the drug response is smaller in critically ill children, due to the decreased formation of the CYP3A-mediated metabolite 1-OH-midazolam, which is known to have half the activity of the parent drug (35), and the glucuronide metabolites who also have substantial pharmacological activity (36).

These results may be explained by differences in the PKPD or PD during inflammation. In rats, receptor binding to $GABA_A$ and $GABA_B$-receptors is known to be affected by inflammation (37, 38), and also human intestinal GABA receptors appear to be affected by inflammation (39). In contrast to the possibly higher concentrations of midazolam required for adequate sedation in critically ill children (34), a deeper level of sedation has been reported in critically ill adults receiving propofol, which acts at least partly via GABA receptors (40). However, whether GABA receptors in the brain, the site of action for midazolam, are affected by inflammation and disease severity in critically ill patients is unknown.

In addition, it is important that irrespective of disease state, differences in drug response of midazolam at different ages can be anticipated, due to a different number, density, distribution and ligand affinity of the GABA receptors (41, 42). The GABA receptors need to mature in the first years of life (43), as an increasing activity is observed with increasing age. Therefore, further studies are needed to determine

the best variable to optimize drug effect (e.g. peak or through concentration, steady-state concentration, or exposure), and to clarify the PD and the PKPD relationship of midazolam for varying levels of critical illness throughout the pediatric age range to come up with an optimized evidence-based dosing schedule for midazolam in neonates, infants, and children.

This dose optimization can for example be done by combining longitudinal PK measurements with time-to-event PD outcomes like the use of rescue medication for adequate sedation, and analyze these two types of data simultaneously (44). Repeated measurements of plasma concentrations (PK) and survival data (PD) are mostly analyzed separately or sequentially with different statistical methods, but together they have more informative value on the interplay between PK, PD, and the disease state (44). This is for example illustrated by Juul *et al.* in an analysis of postoperative analgesic requirements (45), and application of this joint modelling approach for sedation may improve pharmacotherapy in pediatric clinical practice as well.

*PD endpoints*

To evaluate and quantitatively measure drug effects, there is a need for validated, preferably non-invasive, biomarkers or PD endpoints in children that can be measured longitudinal to represent the dynamic changes of the system in healthy and diseased state (41). For midazolam, the COMFORT-B score can be used to assess sedation levels in children (46), but for many CYP3A substrates, the drug effect cannot be measured quantitatively. The emerging field of metabolomics may be useful for biomarker identification reflecting disease severity and/or drug effect in the pediatric population (47). Metabolomics applies a top-down systems biology approach (47, 48), in which a comprehensive analysis of compounds (metabolites) in body fluids is performed (48). In pediatrics, several matrices like urine, plasma and stool may be relevant for metabolomics analyses (47).

Because metabolomics is closer to the observed phenotype (e.g. disease, or treatment outcome) than for example genomics or proteomics, metabolic profiles are considered the most predictive for phenotypes (49), although standardization and validation of this new metabolomics methodology is still required (50, 51). Combining the fields of metabolomics, genomics, and proteomics, could be an even more powerful tool for the identification of biomarkers as early predictors of outcome (49).

The recent identification of several biomarkers for e.g. early detection and clinical diagnostics in the oncology field have shown that metabolomics has the potential

to be valuable in biomarker discovery (52-57), even though they cannot yet be used for clinical decision making, including diagnosis and monitoring of certain diseases and development of individualized pharmacotherapy (58). Identified biomarkers, after thorough validation, can be used for pediatric PKPD models in which drug exposure and PD biomarkers are related with clinical outcomes in neonates, infants, and children, and these models may provide rational support for pediatric dose finding to optimize pharmacotherapy in the pediatric population.

## Physiological approach

In **Chapters 5 and 6**, we used PK data from preterm neonates and children 1-18 years of age to study first-pass and systemic metabolism after oral administration of midazolam, ultimately to gain insight in the ontogeny of gut wall and hepatic CYP3A activity. The combination of physiologically-based PK modelling and the population approach enabled us to estimate the intrinsic clearance parameters in the gut wall and liver using both PBPK principles and the available PK data for midazolam in neonates and children. The gut wall and hepatic CYP3A ontogeny profiles based on midazolam PK data may be informative for other CYP3A substrates as well, as demonstrated in **Chapter 7**.

In PBPK modelling, patient-specific parameters related to anatomy, physiology, and pathophysiology are combined with drug-specific properties like physicochemical characteristics (59). The main advantages of this 'bottom-up' approach include the possibility to integrate preclinical *in vitro* and *in vivo* information with clinical information (60), and the use of these PBPK models can speed up the drug development process, while putting less of a burden on patients (61).

PBPK modelling is an example of the systems approach, and fits within the emerging field of systems pharmacology (62, 63), which combines systems biology with PKPD modelling and simulation. Systems pharmacology focuses on the understanding of the behavior of a system as a whole by quantitative analysis of dynamic interactions between a drug and a biological system (62, 63). In **Chapters 5 and 6**, we used a model with less complexity than a full PBPK model, as the main disadvantage of these complex models is that they require a lot of system- and drug-specific information.

In order to predict drug clearance in the pediatric population using a more complex PBPK model, more physiological information on e.g. the anatomy of neonates, infants, and children is needed (59). Different values for tissue blood flows as well as for tissue volumes and intestinal surface area have been assumed throughout

literature. Harmonization of these values, based on reliable measurements throughout the pediatric range from preterm neonates up to adolescents, is of the utmost importance to reduce uncertainty in clearance predictions by PBPK models in a clinical setting or during drug development. More consistent physiological information will also lead to a better understanding of the mechanistic basis for the absorption, distribution, metabolism and excretion of drugs in the pediatric population (59). For all pediatric ages, information on tissue blood flows, especially hepatic blood flow, is essential, as the sensitivity analyses in **Chapters 5 and 6** revealed that assumptions on these flow rates may impact conclusions on intrinsic clearance and local bioavailability. The challenge for the next years will be collecting especially the hepatic blood flow and other physiological information in neonates, infants, and children, and this is especially urgently needed for preterm neonates, as in this specific population the least physiological information is available (22).

## How to move forward for dosing of CYP3A substrates

To find the optimal first-in-child dose during drug development and to develop pediatric dose recommendations for clinical practice, accurate prediction of plasma clearance of drugs is essential. Based on the framework reported by Calvier *et al.* (29), we report in **Chapter 7** that, using midazolam as a probe drug, pediatric clearance of several CYP3A substrates could be accurately scaled down to 1 day of age from adult clearance values using the pediatric covariate function for CYP3A-mediated midazolam clearance. We anticipate that using this approach, clearance of other CYP3A substrates can be scaled in neonates, infants, and children (figure 3), provided they are either highly protein bound and have a low-intermediate extraction ratio or have an intermediate extraction ratio when low protein bound in adults.

As described in **Chapter 7**, the typical clearance ($CL_i$) of a CYP3A substrate administered to a pediatric subject $i$ >1 year of age with a body weight of $WT_i$ (in kg) can be described by:

$$CL_i = CL_{adult} \times \left(\frac{WT_i}{70}\right)^{0.874} \qquad \text{(eq. 2)}$$

In which $CL_{adult}$ is the reported adult clearance value, and in which both clearance values ($CL_i$ and $CL_{adult}$) are expressed in volume per time. This pediatric covariate function for CYP3A-mediated clearance derived from midazolam may be especially useful for the prediction of clearance of CYP3A substrate drugs with a small therapeutic window or CYP3A substrates with high toxicity like some anticancer agents (64). Accurate clearance predictions for these substrates in children can lead to optimal exposure and thereby ultimately limit the toxicity. Furthermore, it may be useful in dose-finding of drugs in neglected (tropical) diseases, as for example

very limited PK information is available for anthelmintic CYP3A substrates like ivermectin and praziquantel in children (65).

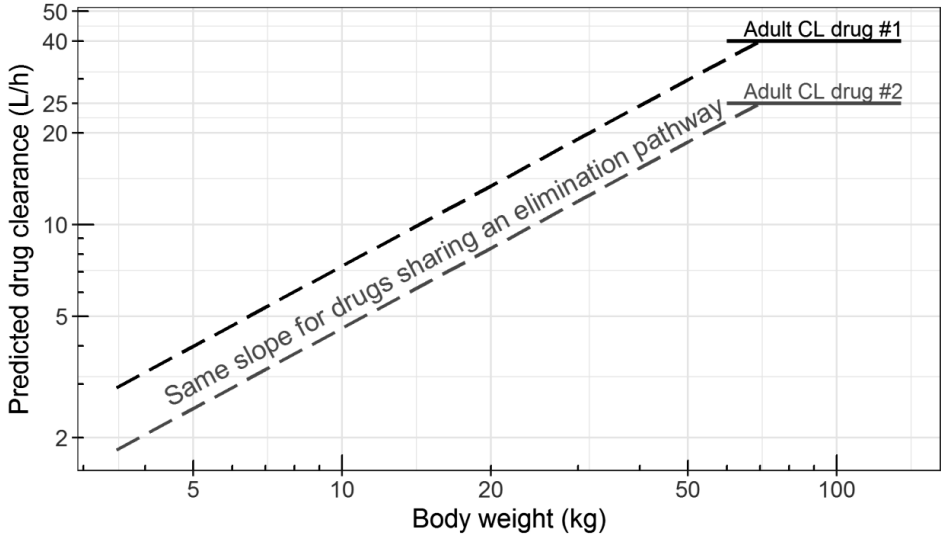



**Figure 3.** Example on how to scale pediatric clearance values from an adult clearance value. Using the framework developed by Calvier **et al.** (29), between-drug extrapolation of clearance can be assessed on the basis of drug properties (i.e. extraction ratio, type of plasma protein binding [e.g. HSA or AAG], fraction unbound, and elimination pathway). When accurate clearance predictions can be anticipated, the pediatric clearance of the new CYP3A substrates will follow the same pediatric covariate function as the model drug.
In this figure, the exponential function (Eq. 2) for CYP3A-mediated midazolam clearance is used to scale pediatric clearance of two hypothetical CYP3A substrates (#1 and #2, with an adult clearance of 40 and 25 L/h, respectively), which on a log-log scale shows as the same slope. The scaling of clearance should not be extrapolated beyond the studied population in which the pediatric covariate function is established, and also not to preterm neonates, which should be regarded as a different population due to their immature intestinal and hepatic CYP3A activity.

The use of pediatric covariate function for CYP3A-mediated clearance based on midazolam may significantly decrease the need for PK studies for each individual CYP3A substrate drug in the pediatric population, as information from one drug can be used to predict clearance of the next. This might also hold true for predictions of other pathways, with for example losartan, dextromethorphan, and omeprazole as probe drugs for CYP2C9, CYP2D6, and CYP2C19, respectively (66), as the same approach already has been shown to lead to accurate clearance predictions for e.g. UGT2B7-mediated drug metabolism and drug elimination by glomerular filtration in the pediatric population (26-28).

However, some limitations should be considered. In our analysis in **Chapter 7**, we assumed that the major elimination pathway is the same in children and adults, but the fraction metabolized by CYP3A activity may change with age for some drugs, and in that case this assumption may not hold true. For example for paracetamol, more sulfation and less glucuronidation is observed in neonates, infants and young children compared to children > 12 years of age and adults (67, 68). The ratio between the elimination pathways may change for some drugs (69), which may be resolved by taking into account the ontogeny of both pathways, rather than 1 major pathway. Moreover, for some drugs, the elimination route might change completely, for example caffeine is a CYP1A2-substrate in adults, while it is renally cleared in neonates (70). In addition, accurate clearance predictions may not be possible for all drugs across the entire pediatric age range, but only down to a certain age depending on its drug properties. Hence, more evaluations based on clinical data are needed, before this methodology can be applied for clearance predictions for all metabolic elimination pathways.

Despite these limitations for other pathways, the developed pediatric covariate function for CYP3A-mediated midazolam metabolism will aid in predicting pediatric clearance of various CYP3A substrates, and after evaluation, this function can be prospectively used for dose estimation of CYP3A substrates in the pediatric population.

## Conclusion

To conclude, children are not just small adults, and therefore dose estimation of CYP3A substrates needs to be different in neonates, infants, and children compared to adults. For optimal treatment with CYP3A substrates, accurate predictions of CYP3A-mediated clearance throughout the pediatric age range are necessary. We found that body weight should be used in the pediatric covariate function for CYP3A-mediated clearance, as it best reflects the growth and maturation, except for preterm neonates which should be regarded as a different population due to their immature intestinal and hepatic CYP3A activity. Also, the effect of disease severity on the pharmacokinetics of CYP3A substrates should be taken into account, as midazolam clearance is significantly lower in patients with inflammation and multiple failing organs.

We confirmed that when midazolam clearance in children is used to reflect CYP3A-mediated metabolism in children ranging in age from 1-18 years, pediatric plasma clearance of various commonly used CYP3A substrates with varying drug properties can be accurately scaled from adult values. For CYP3A substrates with different properties, for example with a high extraction ratio, the pediatric

covariate function for CYP3A-mediated midazolam clearance may not lead to accurate prediction of plasma clearance throughout the pediatric age range, but may only be able to predict in children above a certain age. As the pediatric covariate function for CYP3A-mediated clearance from a midazolam PK model can predict the clearance of various CYP3A substrates, between-drug extrapolation of clearance of drugs sharing a metabolic elimination pathway is found to be possible. This function from a midazolam PK model will significantly improve CYP3A-mediated clearance predictions in neonates, infants, and children, and after evaluation of these model-based clearance predictions in pediatric PKPD studies, dosing recommendations for midazolam and many other CYP3A substrates can be applied in clinical practice.

## REFERENCES


1. Lu H, Rosenbaum S. Developmental pharmacokinetics in pediatric populations. J Pediatr Pharmacol Ther. 2014;19(4):262-76.
2. Kearns GL, Abdel-Rahman SM, Alander SW, Blowey DL, Leeder JS, Kauffman RE. Developmental pharmacology--drug disposition, action, and therapy in infants and children. The New England journal of medicine. 2003;349(12):1157-67.
3. Alcorn J, McNamara PJ. Ontogeny of hepatic and renal systemic clearance pathways in infants: part II. Clin Pharmacokinet. 2002;41(13):1077-94.
4. Thummel KE, Shen DD, Podoll TD, Kunze KL, Trager WF, Hartwell PS, et al. Use of midazolam as a human cytochrome P450 3A probe: I. In vitro-in vivo correlations in liver transplant patients. J Pharmacol Exp Ther. 1994;271(1):549-56.
5. Gorski JC, Hall SD, Jones DR, VandenBranden M, Wrighton SA. Regioselective biotransformation of midazolam by members of the human cytochrome P450 3A (CYP3A) subfamily. Biochem Pharmacol. 1994;47(9):1643-53.
6. Carcillo JA, Doughty L, Kofos D, Frye RF, Kaplan SS, Sasser H, et al. Cytochrome P450 mediated-drug metabolism is reduced in children with sepsis-induced multiple organ failure. Intensive Care Med. 2003;29(6):980-4.
7. Aitken AE, Richardson TA, Morgan ET. Regulation of drug-metabolizing enzymes and transporters in inflammation. Annu Rev Pharmacol Toxicol. 2006;46:123-49.
8. Vet NJ, de Hoog M, Tibboel D, de Wildt SN. The effect of inflammation on drug metabolism: a focus on pediatrics. Drug Discov Today. 2011;16(9-10):435-42.
9. Taburet AM, Tollier C, Richard C. The effect of respiratory disorders on clinical pharmacokinetic variables. Clin Pharmacokinet. 1990;19(6):462-90.
10. Kirwan CJ, MacPhee IA, Lee T, Holt DW, Philips BJ. Acute kidney injury reduces the hepatic metabolism of midazolam in critically ill patients. Intensive Care Med. 2012;38(1):76-84.
11. Peeters MY, Prins SA, Knibbe CA, Dejongh J, Mathot RA, Warris C, et al. Pharmacokinetics and pharmacodynamics of midazolam and metabolites in nonventilated infants after craniofacial surgery. Anesthesiology. 2006;105(6):1135-46.

12. Muchohi SN, Kokwaro GO, Ogutu BR, Edwards G, Ward SA, Newton CR. Pharmacokinetics and clinical efficacy of midazolam in children with severe malaria and convulsions. Br J Clin Pharmacol. 2008;66(4):529-38.
13. Reed MD, Rodarte A, Blumer JL, Khoo KC, Akbari B, Pou S, et al. The single-dose pharmacokinetics of midazolam and its primary metabolite in pediatric patients after oral and intravenous administration. J Clin Pharmacol. 2001;41(12):1359-69.
14. Tolia V, Brennan S, Aravind MK, Kauffman RE. Pharmacokinetic and pharmacodynamic study of midazolam in children during esophagogastroduodenoscopy. J Pediatr. 1991;119(3):467-71.
15. Rey E, Delaunay L, Pons G, Murat I, Richard MO, Saint-Maurice C, et al. Pharmacokinetics of midazolam in children: comparative study of intranasal and intravenous administration. Eur J Clin Pharmacol. 1991;41(4):355-7.
16. Grijalva J, Vakili K. Neonatal liver physiology. Semin Pediatr Surg. 2013;22(4):185-9.
17. Hines RN, McCarver DG. The ontogeny of human drug-metabolizing enzymes: phase I oxidative enzymes. J Pharmacol Exp Ther. 2002;300(2):355-60.
18. Ince I, Knibbe CA, Danhof M, de Wildt SN. Developmental changes in the expression and function of cytochrome P450 3A isoforms: evidence from in vitro and in vivo investigations. Clin Pharmacokinet. 2013;52(5):333-45.
19. de Wildt SN, Kearns GL, Hop WC, Murry DJ, Abdel-Rahman SM, van den Anker JN. Pharmacokinetics and metabolism of oral midazolam in preterm infants. Br J Clin Pharmacol. 2002;53(4):390-2.
20. Frechen S, Junge L, Saari TI, Suleiman AA, Rokitta D, Neuvonen PJ, et al. A semiphysiological population pharmacokinetic model for dynamic inhibition of liver and gut wall cytochrome P450 3A by voriconazole. Clin Pharmacokinet. 2013;52(9):763-81.
21. Johnson TN, Tanner MS, Taylor CJ, Tucker GT. Enterocytic CYP3A4 in a paediatric population: developmental changes and the effect of coeliac disease and cystic fibrosis. Br J Clin Pharmacol. 2001;51(5):451-60.
22. Bjorkman S. Prediction of drug disposition in infants and children by means of physiologically based pharmacokinetic (PBPK) modelling: theophylline and midazolam as model drugs. Br J Clin Pharmacol. 2005;59(6):691-704.
23. Barter ZE, Bayliss MK, Beaune PH, Boobis AR, Carlile DJ, Edwards RJ, et al. Scaling factors for the extrapolation of in vivo metabolic drug clearance from in vitro data: reaching a consensus on values of human microsomal protein and hepatocellularity per gram of liver. Curr Drug Metab. 2007;8(1):33-45.
24. Treluyer JM, Bowers G, Cazali N, Sonnier M, Rey E, Pons G, et al. Oxidative metabolism of amprenavir in the human liver. Effect of the CYP3A maturation. Drug Metab Dispos. 2003;31(3):275-81.
25. Brussee JM, Yu H, Krekels EHJ, Palic S, Brill MJE, Barrett JS, et al. Characterization of Intestinal and Hepatic CYP3A-Mediated Metabolism of Midazolam in Children Using a Physiological Population Pharmacokinetic Modelling Approach. Pharm Res. 2018;35(9):182.
26. Krekels EH, Neely M, Panoilia E, Tibboel D, Capparelli E, Danhof M, et al. From pediatric covariate model to semiphysiological function for maturation: part I-extrapolation of a covariate model from morphine to Zidovudine. CPT Pharmacometrics Syst Pharmacol. 2012;1:e9.

27. Zhao W, Biran V, Jacqz-Aigrain E. Amikacin maturation model as a marker of renal maturation to predict glomerular filtration rate and vancomycin clearance in neonates. Clin Pharmacokinet. 2013;52(12):1127-34.
28. De Cock RF, Allegaert K, Sherwin CM, Nielsen EI, de Hoog M, van den Anker JN, et al. A neonatal amikacin covariate model can be used to predict ontogeny of other drugs eliminated through glomerular filtration in neonates. Pharmaceutical research. 2014;31(3):754-67.
29. Calvier EAM, Krekels EHJ, Yu H, Valitalo PAJ, Johnson TN, Rostami-Hodjegan A, et al. Drugs Being Eliminated via the Same Pathway Will Not Always Require Similar Pediatric Dose Adjustments. CPT Pharmacometrics Syst Pharmacol. 2018.
30. Bai S, Stepkowski SM, Kahan BD, Brunner LJ. Metabolic interaction between cyclosporine and sirolimus. Transplantation. 2004;77(10):1507-12.
31. Dennison JB, Jones DR, Renbarger JL, Hall SD. Effect of CYP3A5 expression on vincristine metabolism with human liver microsomes. J Pharmacol Exp Ther. 2007;321(2):553-63.
32. Vet NJ, de Wildt SN, Verlaat CW, Knibbe CA, Mooij MG, Hop WC, et al. Daily interruption of sedation in critically ill children: study protocol for a randomized controlled trial. Trials. 2014;15:55.
33. Kinderformularium, Accessed on February 20, 2018, Availabile from https://www.kinderformularium.nl/geneesmiddel/140/midazolam.
34. Vet NJ, de Wildt SN, Verlaat CW, Knibbe CA, Mooij MG, van Woensel JB, et al. A randomized controlled trial of daily sedation interruption in critically ill children. Intensive Care Med. 2016;42(2):233-44.
35. Johnson TN, Rostami-Hodjegan A, Goddard JM, Tanner MS, Tucker GT. Contribution of midazolam and its 1-hydroxy metabolite to preoperative sedation in children: a pharmacokinetic-pharmacodynamic analysis. Br J Anaesth. 2002;89(3):428-37.
36. Bauer TM, Ritz R, Haberthur C, Ha HR, Hunkeler W, Sleight AJ, et al. Prolonged sedation due to accumulation of conjugated metabolites of midazolam. Lancet. 1995;346(8968):145-7.
37. Castro-Lopes JM, Malcangio M, Pan BH, Bowery NG. Complex changes of GABAA and GABAB receptor binding in the spinal cord dorsal horn following peripheral inflammation or neurectomy. Brain Res. 1995;679(2):289-97.
38. Anseloni VC, Gold MS. Inflammation-induced shift in the valence of spinal GABA-A receptor-mediated modulation of nociception in the adult rat. J Pain. 2008;9(8):732-8.
39. Auteri M, Zizzo MG, Serio R. GABA and GABA receptors in the gastrointestinal tract: from motility to inflammation. Pharmacol Res. 2015;93:11-21.
40. Peeters MY, Bras LJ, DeJongh J, Wesselink RM, Aarts LP, Danhof M, et al. Disease severity is a major determinant for the pharmacodynamics of propofol in critically ill patients. Clin Pharmacol Ther. 2008;83(3):443-51.
41. Kearns GL, Artman M. Functional Biomarkers: an Approach to Bridge Pharmacokinetics and Pharmacodynamics in Pediatric Clinical Trials. Curr Pharm Des. 2015;21(39):5636-42.
42. Mulla H. Understanding developmental pharmacodynamics: importance for drug development and clinical practice. Paediatr Drugs. 2010;12(4):223-33.
43. Jansen LA, Peugh LD, Roden WH, Ojemann JG. Impaired maturation of cortical GABA(A) receptor expression in pediatric epilepsy. Epilepsia. 2010;51(8):1456-67.

44. Asar O, Ritchie J, Kalra PA, Diggle PJ. Joint modelling of repeated measurement and time-to-event data: an introductory tutorial. Int J Epidemiol. 2015;44(1):334-44.
45. Juul RV, Rasmussen S, Kreilgaard M, Christrup LL, Simonsson US, Lund TM. Repeated Time-to-event Analysis of Consecutive Analgesic Events in Postoperative Pain. Anesthesiology. 2015;123(6):1411-9.
46. Ista E, van Dijk M, Tibboel D, de Hoog M. Assessment of sedation levels in pediatric intensive care patients can be improved by using the COMFORT "behavior" scale. Pediatr Crit Care Med. 2005;6(1):58-63.
47. Moco S, Collino S, Rezzi S, Martin FP. Metabolomics perspectives in pediatric research. Pediatr Res. 2013;73(4 Pt 2):570-6.
48. Ramautar R, Berger R, van der Greef J, Hankemeier T. Human metabolomics: strategies to understand biology. Curr Opin Chem Biol. 2013;17(5):841-6.
49. Peng B, Li H, Peng XX. Functional metabolomics: from biomarker discovery to metabolome reprogramming. Protein Cell. 2015;6(9):628-37.
50. Fanos V, Barberini L, Antonucci R, Atzori L. Metabolomics in neonatology and pediatrics. Clin Biochem. 2011;44(7):452-4.
51. Fanos V, Antonucci R, Atzori L. Metabolomics in the developing infant. Curr Opin Pediatr. 2013;25(5):604-11.
52. Zhang A, Sun H, Yan G, Wang P, Han Y, Wang X. Metabolomics in diagnosis and biomarker discovery of colorectal cancer. Cancer Lett. 2014;345(1):17-20.
53. Gunther UL. Metabolomics Biomarkers for Breast Cancer. Pathobiology. 2015;82(3-4):153-65.
54. Suzuki M, Nishiumi S, Matsubara A, Azuma T, Yoshida M. Metabolome analysis for discovering biomarkers of gastroenterological cancer. J Chromatogr B Analyt Technol Biomed Life Sci. 2014;966:59-69.
55. Peng J, Chen YT, Chen CL, Li L. Development of a universal metabolome-standard method for long-term LC-MS metabolome profiling and its application for bladder cancer urine-metabolite-biomarker discovery. Anal Chem. 2014;86(13):6540-7.
56. Tosoian JJ, Ross AE, Sokoll LJ, Partin AW, Pavlovich CP. Urinary Biomarkers for Prostate Cancer. Urol Clin North Am. 2016;43(1):17-38.
57. Tumas J, Kvederaviciute K, Petrulionis M, Kurlinkus B, Rimkus A, Sakalauskaite G, et al. Metabolomics in pancreatic cancer biomarkers research. Med Oncol. 2016;33(12):133.
58. Monteiro MS, Carvalho M, Bastos ML, Guedes de Pinho P. Metabolomics analysis for biomarker discovery: advances and challenges. Curr Med Chem. 2013;20(2):257-71.
59. Barrett JS, Della Casa Alberighi O, Laer S, Meibohm B. Physiologically based pharmacokinetic (PBPK) modeling in children. Clin Pharmacol Ther. 2012;92(1):40-9.
60. Maharaj AR, Edginton AN. Physiologically based pharmacokinetic modeling and simulation in pediatric drug development. CPT Pharmacometrics Syst Pharmacol. 2014;3:e150.
61. Zhuang X, Lu C. PBPK modeling and simulation in drug research and development. Acta Pharm Sin B. 2016;6(5):430-40.
62. van der Graaf PH, Benson N. Systems pharmacology: bridging systems biology and pharmacokinetics-pharmacodynamics (PKPD) in drug discovery and development. Pharm Res. 2011;28(7):1460-4.
63. Vicini P, van der Graaf PH. Systems pharmacology for drug discovery and development: paradigm shift or flash in the pan? Clin Pharmacol Ther. 2013;93(5):379-81.

64. Coutant DE, Kulanthaivel P, Turner PK, Bell RL, Baldwin J, Wijayawardana SR, et al. Understanding Disease-Drug Interactions in Cancer Patients: Implications for Dosing Within the Therapeutic Window. Clin Pharmacol Ther. 2015;98(1):76-86.
65. Olliaro P, Delgado-Romero P, Keiser J. The little we know about the pharmacokinetics and pharmacodynamics of praziquantel (racemate and R-enantiomer). J Antimicrob Chemother. 2014;69(4):863-70.
66. Williams D, Tao X, Zhu L, Stonier M, Lutz JD, Masson E, et al. Use of a cocktail probe to assess potential drug interactions with cytochrome P450 after administration of belatacept, a costimulatory immunomodulator. Br J Clin Pharmacol. 2017;83(2):370-80.
67. Levy G, Khanna NN, Soda DM, Tsuzuki O, Stern L. Pharmacokinetics of acetaminophen in the human neonate: formation of acetaminophen glucuronide and sulfate in relation to plasma bilirubin concentration and D-glucaric acid excretion. Pediatrics. 1975;55(6):818-25.
68. Miller RP, Roberts RJ, Fischer LJ. Acetaminophen elimination kinetics in neonates, children, and adults. Clin Pharmacol Ther. 1976;19(3):284-94.
69. Salem F, Johnson TN, Barter ZE, Leeder JS, Rostami-Hodjegan A. Age related changes in fractional elimination pathways for drugs: assessing the impact of variable ontogeny on metabolic drug-drug interactions. J Clin Pharmacol. 2013;53(8):857-65.
70. Ginsberg G, Hattis D, Sonawane B. Incorporating pharmacokinetic differences between children and adults in assessing children's risks to environmental toxicants. Toxicol Appl Pharmacol. 2004;198(2):164-83.

# Chapter 9

## Presystemisch en systemisch metabolisme van geneesmiddelen door cytochroom P450 3A enzymen in kinderen – Nederlandse samenvatting

De farmacokinetiek (PK) van geneesmiddelen die worden toegediend aan neonaten, kinderen en adolescenten verschilt in kinderen ten opzichte van volwassenen door fysiologische verschillen als gevolg van groei en ontwikkeling (1, 2). Eén van deze ontwikkelingen is de rijping (maturatie) van metaboliserende enzymen, die invloed heeft op de metabole klaring van geneesmiddelen (3). Zoals beschreven in **Hoofdstuk 1**, richt het onderzoek in dit proefschrift zich op het metabolisme in kinderen door cytochroom P450 (CYP) 3A enzymen, waarbij midazolamklaring als surrogaat marker voor CYP3A activiteit is gebruikt (4). Het doel van dit proefschrift is het voorspellen van CYP3A-gemedieerde plasmaklaring van verschillende geneesmiddelen in neonaten, kinderen en adolescenten. Accurate voorspelling van plasmaklaring van geneesmiddelen is essentieel voor de wetenschappelijke onderbouwing van pediatrische doseringen voor een eerste klinische studie in kinderen en voor het ontwikkelen van doseeradviezen voor kinderen in de klinische praktijk.

Voor dit doel presenteren we in **Sectie I** onze visie op klinische studies in kinderen. Deze sectie beschrijft hoe op basis van PK eigenschappen van geneesmiddelen in kinderen geïndividualiseerde doseringsschema's in de pediatrische populatie kunnen worden ontwikkeld. **Sectie II** beschrijft het CYP3A-gemedieerde systemische metabolisme in kritisch zieke kinderen. Binnen het ontwikkelde populatie PK model zijn lichaamsgewicht, kritisch ziek-zijn en inflammatie geïdentificeerd als covariaten, welke een deel van de inter- en intra-individuele variabiliteit binnen deze populatie verklaren. De voorspellingen van dit model zijn vervolgens geëvalueerd in vergelijkbare (postoperatieve of kritisch zieke) patiënten en bij andere populaties waaronder preterme neonaten en gezonde en kritisch zieke volwassenen. **Sectie III** beschrijft methoden die onderscheid maken tussen presystemisch en systemisch CYP3A-gemedieerd metabolisme, om de rol van intestinale en hepatische CYP3A activiteit bij neonaten en kinderen met een grote leeftijdsspreiding te bestuderen. Tenslotte beschrijft **Sectie IV** hoe informatie over CYP3A-gemedieerde klaring van midazolam in kinderen kan worden gebruikt om plasmaklaring van andere CYP3A-substraten te schalen. De scenario's worden beschreven wanneer een pediatrische covariaatfunctie voor CYP3A-gemedieerde midazolamklaring kan worden toegepast voor het schalen van klaring van andere CYP3A-substraten bij pediatrische patiënten.

## Sectie I. Kinderen in klinische studies: wetenschappelijk-onderbouwde farmacotherapie in kinderen met behulp van farmacokinetische-farmacodynamische modellen

In **Hoofdstuk 2** wordt onze visie op modelgebaseerde geneesmiddelontwikkeling in kinderen besproken. Er zijn vergeleken met volwassenen weinig en soms zelfs geen farmacokinetische-farmacodynamische (PKPD) studies in kinderen gedaan en daarom

worden doseringen van CYP3A-substraten en andere geneesmiddelen in kinderen vaak lineair of allometrisch geschaald vanaf doseringen in volwassenen. Echter, het voorspellen van plasmaklaring in voornamelijk jonge kinderen is ingewikkelder dan dat, omdat veel fysiologische veranderingen plaatsvinden, onder andere in de darmoppervlakte, de grootte van de lever ten opzichte van lichaamsgewicht en de cardiac output. Bovendien heeft elk hepatisch isoenzym een ander maturatieprofiel en daarom zijn maturatiefuncties voor elke hepatische eliminatieroute nodig die deze veranderingen goed beschrijven en kunnen voorspellen. Deze functies zijn niet altijd bekend, maar het bestuderen van klaring van het CYP3A-substraat midazolam (5) in kinderen zal onze kennis van de maturatiepatronen van CYP3A-enzymen vergroten.

Pediatrische PK modellen die geneesmiddelklaring beschrijven moeten worden ontwikkeld om wetenschappelijk-onderbouwde doseringsschema's voor kinderen te kunnen ontwikkelen. Deze modellen moeten grondig worden geëvalueerd en gevalideerd met externe data, zoals in hoofdstuk 4.

Een goede studieopzet is extreem belangrijk om een onderzoeksvraag in een farmacologische studie te kunnen beantwoorden. Daarom zou een multidisciplinair team van artsen, klinisch farmacologen en farmacometristen betrokken moeten zijn bij het opzetten van de studie, om onder andere te bespreken welke (covariaat) gegevens moeten worden verzameld op welke tijdstippen. De covariaatrelaties met klaring in de ontwikkelde PK modellen kunnen vervolgens worden gebruikt voor het individualiseren van doseringsschema's, mits de effectieve en veilige concentratie bekend is voor patiënten met verschillende niveaus van (kritisch) ziek-zijn. Gebaseerd op simulaties met het model kunnen doseeradviezen worden gedaan. Tevens moet het geoptimaliseerde doseringsschema worden geëvalueerd in de klinische praktijk. Voor deze aanpak zullen goed opgezette klinische PKPD studies een centrale rol spelen bij het ontwikkelen en bevestigen van modelgebaseerde adviezen voor doseringsschema's in kinderen.

## Sectie II. Systemische CYP3A-gemedieerd metabolisme in kritisch zieke kinderen

In het verleden zijn grote verschillen waargenomen tussen de gerapporteerde gemiddelde waarden van midazolamklaring in pediatrische populaties van vergelijkbare leeftijden. Het belangrijkste verschil tussen deze cohorten is de mate van ziek-zijn, waar bij relatief gezonde kinderen een hogere midazolamklaring is gemeten dan in kritisch zieke kinderen. Onze hypothese is daarom dat deze

verschillen mogelijk kunnen worden verklaard door de mate van ziek-zijn en/of inflammatie.

In **Hoofdstuk 3** beschrijven we de systemische CYP3A-gemedieerde klaring van midazolam in kritisch zieke neonaten, kinderen en adolescenten na meerdere intraveneuze toedieningen getitreerd op therapeutisch effect. Gebaseerd op prospectief verzamelde PK data van 83 patiënten tussen de 0 en 17 jaar, is een twee-compartimenten PK model ontwikkeld dat de midazolamconcentraties goed beschrijft. Lichaamsgewicht is geïdentificeerd als meest significante covariaat voor klaring in het model, met een bijna lineaire toename in klaring met toenemend lichaamsgewicht. In overeenstemming met onze hypothese is een correlatie gevonden van verhoogde concentraties van de inflammatiemarker C-reactive protein (CRP) met verlaagde midazolamklaring, met een 51,2% lagere klaring als CRP toeneemt van 10 tot 100 mg/L. Orgaanfalen is ook gerelateerd aan midazolamklaring, namelijk zodra het aantal organen met orgaanfalen toeneemt van 1 naar bijvoorbeeld 2 of 3, dan daalt de klaring met respectievelijk 25,6% of 34,9%. Als gevolg hiervan kan de CYP3A-gemedieerde klaring van midazolam tot 77,4% lager zijn in patiënten met verhoogde CRP concentraties en een verhoogd aantal falende organen ten opzichte van gezondere patiënten.

De verlaagde midazolamklaring in kritisch zieke kinderen die wordt beschreven in **Hoofdstuk 3** is waarschijnlijk te wijten aan de verlaagde CYP3A activiteit bij verhoogde concentraties van de inflammatiemarkers CRP en interleukine-6 (6-8). Bovendien kan orgaanfalen, bovenop inflammatie, leiden tot een lagere midazolamklaring, al zijn de onderliggende mechanismes van hoe cardiovasculair, respiratoir (9), hepatisch en renaal falen (10) midazolam PK beïnvloeden nog onbekend (6). Deze verlaagde midazolamklaring in kritisch zieke kinderen leidt tot verhoogde midazolam plasmaconcentraties en -blootstelling in patiënten met inflammatie, orgaanfalen, of beide (**Hoofdstuk 3**).

Het ontwikkelde populatie PK model voor midazolam (**Hoofdstuk 3**) is vervolgens extern gevalideerd, zoals beschreven in **Hoofdstuk 4**, waar de voorspellende waarde van het model is geëvalueerd in zowel kritisch zieke en postoperatieve kinderen, als andere populaties zoals preterme neonaten en gezonde en kritisch zieke volwassenen. De resultaten laten zien dat het model de midazolamklaring adequaat kan voorspellen in kritisch zieke terme neonaten, kinderen en volwassenen. Vergeleken met de gerapporteerde waarden in de literatuur voor midazolamklaring, is de klaring in kritische zieke patiënten in onze studie over het algemeen lager, wat mogelijk te verklaren is door hun mate van ziek-zijn, omdat de meeste

gerapporteerde klaringswaarden uit studies met relatief gezonde kinderen komen (11-15).

In gezonde volwassenen wordt ook een hogere klaring voorspeld en waargenomen dan in de kritisch zieke volwassenen, dat kan worden verklaard door de afwezigheid van inflammatie en orgaanfalen in deze populatie. De voorspelde klaring wordt daarentegen sterk overschat in preterme neonaten met een lichaamsgewicht onder de 3,5 kg, die geboren zijn na een zwangerschapsduur korter dan 37 weken. Dit is waarschijnlijk te wijten aan het feit dat het model niet meeneemt dat in preterme neonaten CYP3A onrijp en onderontwikkeld is. De totale CYP3A activiteit is veel lager in preterme neonaten vergeleken met term geboren neonaten en zuigelingen en zelfs lager dan zou worden verwacht gebaseerd op schalen van lichaamsgewicht vanaf terme neonaten (16-18). Concluderend kan worden gezegd dat, hoewel het in **Hoofdstuk 3** ontwikkelde model niet kan worden toegepast voor extrapolatie naar preterme neonaten, de externe validatie in **Hoofdstuk 4** bevestigt dat het ontwikkelde PK model CYP3A-gemedieerde midazolamklaring kan voorspellen in (pediatrische) patiënten met verschillende mate van (kritisch) ziek-zijn.

## Sectie III. Presystemisch CYP3A-gemedieerd metabolisme in kinderen na orale toediening van geneesmiddelen

Een eerdere studie heeft laten zien dat de orale biobeschikbaarheid van midazolam een stuk hoger is in preterme neonaten (19) dan in volwassenen. Dit suggereert dat CYP3A activiteit in de darm en/of lever mogelijk onderontwikkeld is, wat leidt tot een hogere systemische blootstelling aan midazolam. De relatieve bijdrage van het intestinale en hepatisch CYP3A-gemedieerde metabolisme, en hun relatieve veranderingen in metabole activiteit op verschillende leeftijden zijn echter nog niet eerder bestudeerd *in vivo*.

De presystemische CYP3A-gemedieerde klaring kan alleen worden beschreven op basis van orale PK data in combinatie met intraveneuze PK data. In **Hoofdstuk 5 en 6** is de rol van CYP3A-enzymen in de darmwand en lever in de presystemische klaring van midazolam onderzocht in respectievelijk preterme neonaten en in kinderen van 1 tot en met 18 jaar. Hiervoor is een nieuwe aanpak gebruikt, namelijk fysiologisch populatie PK modelleren, waarbij we zowel informatie benutten over de fysiologie van het maag-darmkanaal en de lever, als populatie PK modelleren van data van zowel midazolam als de primaire metaboliet (1-OH-midazolam) in kinderen van variërende leeftijden.

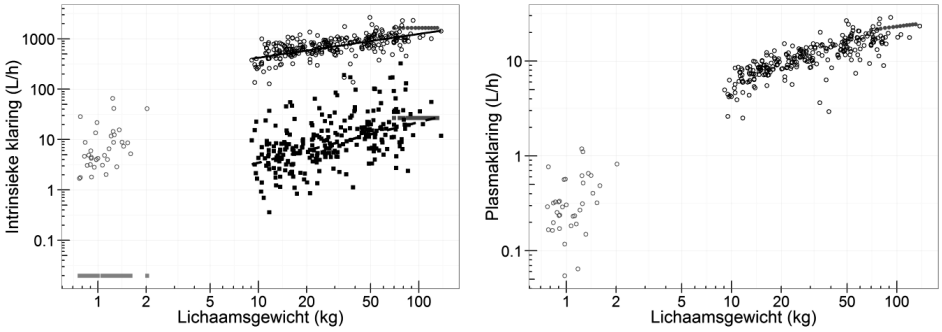
De intrinsieke klaring in de darmwand en lever lijken beide toe te nemen met toenemend lichaamsgewicht in kinderen van 1-18 jaar. Figuur 1A laat zien dat de intrinsieke intestinale en hepatische CYP3A-gemedieerde klaring niet parallel toenemen en dat de intrinsieke klaring in de darmwand sneller toeneemt met leeftijd. De intrinsieke intestinale klaring is lager dan de intrinsieke hepatische klaring voor kinderen en volwassenen van alle leeftijden en de relatieve bijdrage van CYP3A in de darmwand en lever aan het presystemische metabolisme van CYP3A-substraten verandert met leeftijd. In preterme neonaten is de ratio van intrinsieke hepatische versus intestinale klaring veel groter dan in kinderen en gezonde volwassenen, met een ratio van ongeveer 340 in preterme neonaten (**Hoofdstuk 5**) vergeleken met 153 in jonge kinderen tot 2 jaar, 87 voor een typisch individu van 27 kg, 48 in adolescenten ≥ 16 jaar (**Hoofdstuk 6**) en een ratio van 60 in volwassenen (20). Dit betekent dat de intrinsieke klaring in de darmwand een kleinere bijdrage levert aan de totale presystemische klaring met afnemende leeftijd.

Als we aannemen dat de intrinsieke klaring van midazolam een surrogaat marker is voor totale intestinale en hepatische activiteit van CYP3A-enzymen, duidt de veranderende ratio erop dat de hepatische activiteit in kinderen van 1 jaar en ouder al dicht bij de volwassen waarden ligt, in tegenstelling tot de totale intestinale CYP3A activiteit die nog ontwikkelt met leeftijd (**Hoofdstuk 6**). In preterme neonaten kan echter een erg lage intestinale en hepatische CYP3A activiteit worden waargenomen (**Hoofdstuk 5**), hetgeen wijst op een onderontwikkeld enzymsysteem.

In de literatuur is gerapporteerd dat zowel de CYP3A enzymaantallen die aanwezig zijn in de enterocyten, als het totale gewicht van de dunne darm toeneemt met leeftijd (1, 21, 22). Dit leidt samen tot een hogere intrinsieke CYP3A-gemedieerde klaring in de darmwand in adolescenten en volwassenen ten opzichte van neonaten en jonge kinderen. Betreffende de hepatische CYP3A activiteit, suggereren onze resultaten in **Hoofdstuk 6** dat levergroei het meest bijdraagt aan de toename in intrinsieke hepatische CYP3A-gemedieerde klaring in kinderen, terwijl de CYP3A enzymaantallen en de hoeveelheid microsomaal eiwit per gram lever relatief constant blijven met leeftijd (17, 23, 24).

Plasmaklaring is voornamelijk afhankelijk van de intrinsieke hepatische klaring en kan worden berekend gebaseerd op het *well-stirred model* dat de intrinsieke hepatische klaring samen met de doorbloeding (bloedstroom) in de lever, de eiwitbinding en de bloed:plasma ratio meeneemt. Uit onze resultaten kan worden afgeleid dat plasmaklaring toeneemt van 0,03-0,79 (mediaan 0,18) L/h in preterme neonaten

naar 2,5-8,7 (mediaan 6,0) L/h in 1-2 jaar oude kinderen tot 9,0-24,6 (mediaan 17,5) L/h in kinderen ≥ 16 jaar (**Hoofdstuk 5 en 6**) (figuur 1B).



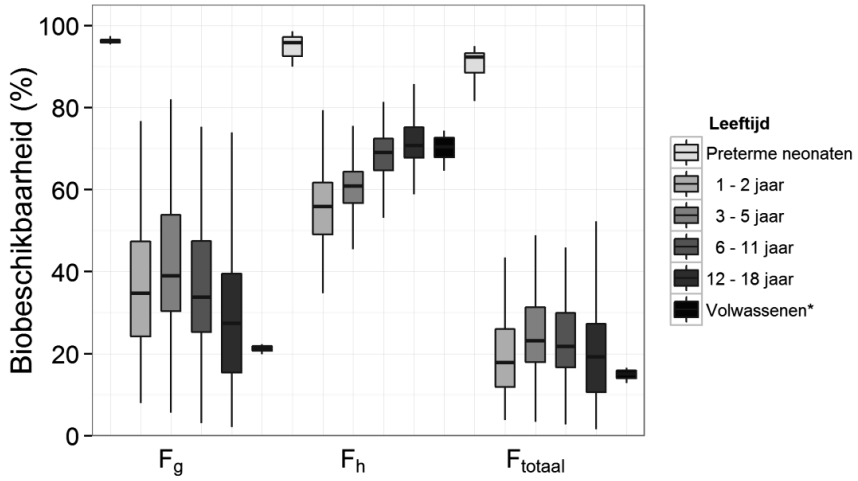

**Figuur 1. A)** Intrinsieke totale orgaan klaring van midazolam in de darmwand (vierkant) en de lever (cirkels) is weergegeven versus lichaamsgewicht, met waarden voor preterme neonaten (lichtgrijs) (**Hoofdstuk 5**) en kinderen van 1-18 jaar (zwart) (**Hoofdstuk 6**). Gerapporteerde waarden voor volwassenen (20) van respectievelijk 26,7 (grijze vierkanten) en 1640 L/h (grijze gesloten cirkels) zijn ook weergegeven. **B)** De totale plasmaklaring is weergegeven versus lichaamsgewicht, met waarden voor preterme neonaten (lichtgrijze open cirkel) (**Hoofdstuk 5**), kinderen van 1-18 jaar (zwarte open cirkel) (**Hoofdstuk 6**), en gerapporteerde waarden voor een typische volwassen populatie (grijze gesloten cirkel) (20). Aangepast van Brussee et al. met toestemming (25).

In **Hoofdstuk 5** wordt ook beschreven dat de extractieratio voor midazolam in de darm en lever erg laag zijn (mediaan voor elk 0,04), wat leidt tot een extreem lage presystemische klaring in preterme neonaten. De totale biobeschikbaarheid is het product van de fractie die wordt opgenomen ($F_a$) en de fracties die ontsnappen aan metabolisme in de darmwand ($F_g$) en de lever ($F_h$), weergegeven in vergelijking 1.

$$F_{totaal} = F_a \times F_g \times F_h \qquad [1]$$

De resulterende biobeschikbaarheid van 92,3% is daarom zeer hoog, maar is zeer variabel binnen de populatie (90%CI: 75,4-94,5%) (figuur 2). Dit kan leiden tot grote verschillen in blootstelling en geneesmiddeleffect na orale toediening van CYP3A-substraten in preterme neonaten.

We rapporteren ook een hoge variabiliteit in biobeschikbaarheid rond de mediaan van 20,8% in kinderen van 1-18 jaar (90%CI: 4,6-44,6%) (**Hoofdstuk 6**). Zoals figuur 2 laat zien, neemt de fractie die ontsnapt aan hepatisch metabolisme ($F_h$) toe met leeftijd, terwijl de fractie die ontsnapt aan metabolisme in de darmwand ($F_g$) afneemt met leeftijd, wat leidt tot een leeftijdsonafhankelijke totale biobeschikbaarheid van midazolam ($F_{totaal}$, berekend met vergelijking 1).




**Figuur 2.** De fractie die ontsnapt aan intestinaal (Fg) en hepatisch (Fh) metabolisme en de totale biobeschikbaarheid van midazolam ($F_{totaal}$) zijn significant hoger in preterme neonaten (lichtgrijs) (**Hoofdstuk 5**), vergeleken met kinderen in vier verschillende leeftijdscategorieën: 1-2 jaar, 3-5 jaar, 6-11 jaar en 12-18 jaar (toenemende grijsschaal) (**Hoofdstuk 6**) en vergeleken met waarden in volwassenen (zwart) (20).
*De biobeschikbaarheid in volwassenen is uitgerekend op basis van de gerapporteerde typische intrinsieke hepatische klaring, de hepatische bloedstroom toenemend met lichaamsgewicht, de ongebonden fractie en de bloed:plasma ratio (20). Aangepast van Brussee et al. met toestemming (25).

## Sectie IV. Midazolam als surrogaat geneesmiddel voor andere CYP3A-substraten

Midazolam is een bewezen CYP3A-substraat (4, 5) en midazolamklaring in kinderen wordt gebruikt om de maturatie van CYP3A in de pediatrische populatie te beschrijven. Daarom wordt in **Sectie IV** van dit proefschrift onderzocht of PK informatie afkomstig van midazolam kan worden gebruikt om klaring van andere CYP3A-substraten in kinderen te voorspellen.

Het zou te veel tijd en middelen kosten om de PK van alle CYP3A-substraten in kinderen in klinische studies te bestuderen. Daarom zijn andere benaderingen voorgesteld, zoals op fysiologie-gebaseerde PK (PBPK) modellen om klaring van enzymsubstraten in kinderen te voorspellen. Omdat voor deze PBPK modellen veel systeem- en geneesmiddelspecifieke informatie vereist zijn en deze informatie niet altijd beschikbaar is, is als alternatieve methode om klaring te schalen in kinderen voorgesteld om de PK informatie te gebruiken van geneesmiddelen die door dezelfde eliminatieroute worden afgebroken (26). Deze extrapolatie van het ene naar het andere geneesmiddel is al succesvol toegepast in het voorspellen van klaring van verscheidene antibiotica die door glomerulaire filtratie worden uitgescheiden in neonaten, met amikacine als surrogaat geneesmiddel (27, 28). Ook de klaring van

het UGT2B7-substraat zidovudine in kinderen is accuraat geschaald gebaseerd op een pediatrische covariaatfunctie voor UGT2B7-gemedieerde glucuronidatie afkomstig van een morfine PK model (26).

Hoewel dit een veelbelovende aanpak lijkt, roept dit de vraag op of dit ook toepasbaar is op het voorspellen van CYP3A-gemedieerde klaring. Calvier *et al.* (29) hebben deze aanpak op een systematische manier onderzocht voor alle hepatische isoenzymen. Gebaseerd op het ontwikkelde framework (29) blijkt dat accuraat schalen van klaring gebruikmakend van een covariaatfunctie ontwikkeld voor een geneesmiddel met dezelfde eliminatieroute, niet alleen afhankelijk is van de fractie van het metabolisme dat dit specifieke hepatische isoenzym op zich neemt, maar ook van andere eigenschappen van het surrogaat geneesmiddel en het nieuwe geneesmiddel, zoals de extractieratio in volwassenen (ER), het type plasmaeiwit waar het geneesmiddel aan bindt en de ongebonden fractie in volwassenen ($f_u$).

In **Hoofdstuk 7** wordt het hiervoor beschreven framework toegepast om, gebruikmakend van een pediatrische covariaatfunctie voor midazolamklaring, de klaring van verschillende veelgebruikte CYP3A-substraten in kinderen te schalen vanaf volwassen klaringswaarden. Volgens het framework (29) kan op basis van midazolam de klaring van CYP3A-substraten systematisch accuraat worden geschaald voor substraten met een extractieratio van 0,35-0,65 of 0,05-0,55 en die respectievelijk <10% of >90% gebonden zijn aan albumine. Voor CYP3A substraten die binden aan α-1-zuur-glycoproteïne (AGP) is van minder combinaties van geneesmiddeleigenschappen *a priori* duidelijk dat klaring accuraat kan worden geschaald. Voor alprazolam, atorvastatine, quinidine, sildenafil, solifenacine, sufentanil en tacrolimus betekent dit dat, op basis van de eigenschappen van deze geneesmiddelen, klaring accuraat kan worden geschaald vanaf volwassenen naar jongere kinderen tot en met term geboren kinderen van 1 dag oud door het toepassen van de pediatrische covariaatfunctie voor klaring van een PK model voor midazolam.

Voor CYP3A-substraten waarvoor klaringswaarden in kinderen en volwassenen beschikbaar zijn in de literatuur hebben we bevestigd dat de geschaalde klaringswaarden voor atorvastatine, quinidine, sildenafil, sufentail, tacrolimus en tamsulosine tot kinderen van 1 jaar en ouder accuraat zijn, aangezien de geschaalde klaringswaarden overeenkomen met de gerapporteerde klaringswaarden in kinderen (voorspellingsfout PE <50%) (**Hoofdstuk 7**). Voor sirolimus en vincristine hebben we grotere voorspellingsfouten gevonden, die kunnen worden verklaard door de inductie van CYP3A activiteit door sirolimus (30) dat de plasmaklaring beïnvloedt en

vanwege het grotere aandeel dat CYP3A5 heeft in het metabolisme van vincristine (31) en de kleinere rol voor CYP3A4 vergeleken met midazolam.

Bovendien beschrijft **Hoofdstuk 7,** op basis van PK data in 156 kinderen die sildenafil toegediend kregen, dat de klaring van dit CYP3A-substraat in kinderen van 1-17 jaar accuraat kan worden geschaald door de pediatrische covariaatfunctie voor CYP3A-gemedieerde midazolamklaring, aangezien er geen grote verschillen (PE <50%) zijn gevonden met de klaring die is geschat op basis van een populatie PK model. Het schalen van klaring kan niet worden geëxtrapoleerd buiten de populatie waarvoor de covariaatfunctie ontwikkeld is en ook niet in preterme neonaten vanwege de onderontwikkelde CYP3A activiteit waardoor de klaring in deze populatie afwijkt.

Extrapolatie van klaring van midazolam naar andere geneesmiddelen die voornamelijk door CYP3A worden gemetaboliseerd (≥75% metabolisme via deze route), met de hierboven beschreven eigenschappen (d.w.z. ER van 0,35-0,65 of 0,05-0,55 voor respectievelijk <10% of >90% eiwitbinding aan albumine in volwassenen), kan een waardevolle methode zijn om klaring van CYP3A-substraten in kinderen te voorspellen, vooral voor CYP3A-substraten waarvan geen of zeer weinig PK informatie in kinderen beschikbaar is.

## Conclusies

CYP3A-gemedieerde plasmaklaring van midazolam in terme neonaten en kinderen neemt non-lineair toe met toenemend lichaamsgewicht en is sterk verlaagd in kinderen met inflammatie en orgaanfalen.

Pediatrische midazolam PK modellen kunnen worden gebruikt voor het voorspellen van midazolamklaring in terme neonaten en kinderen, maar preterme neonaten hebben een veel lagere klaring vanwege de onderontwikkelde CYP3A activiteit.

Een fysiologische populatie PK modelleeranalyse is geschikt om onderscheid te maken tussen metabolisme door CYP3A-enzymen in de darmwand en de lever, en om de fracties die ontsnappen aan intestinaal ($F_g$) en hepatisch ($F_h$) metabolisme te kwantificeren.

Het presystemisch intestinaal en hepatisch CYP3A-gemedieerd metabolisme in preterme neonaten is zeer laag vergeleken met kinderen en volwassenen.

De maturatie van CYP3A activiteit in de darmwand en lever verloopt niet parallel. De CYP3A activiteit in de darmwand is lager dan de hepatische CYP3A activiteit in neonaten, kinderen en volwassenen, en draagt meer bij aan presystemisch metabolisme met toenemende leeftijd.

Extrapolatie van klaring van midazolam naar andere CYP3A-substraten is mogelijk: een pediatrische covariaatfunctie voor CYP3A-gemedieerde midazolamklaring kan de klaring van verschillende veelgebruikte CYP3A-substraten accuraat schalen tot 1 jaar, als ze ≥75% worden gemetaboliseerd door CYP3A, en een ER<0,55 of 0,35-0,65 hebben in volwassenen voor respectievelijk lage en hoge eiwitbinding.

## Perspectieven

*Vertaling naar de kliniek: de impact van ziekte op midazolam PK en PD*

Het ontwikkelde PK model voor midazolam in **Hoofdstuk 3** beschrijft de CYP3A-gemedieerde klaring in kritisch zieke kinderen en verklaart een deel van de interindividuele variabiliteit door rekening te houden met het lichaamsgewicht van de patiënt, het inflammatie niveau (weerspiegeld door CRP concentraties) en orgaanfalen. Gebaseerd op deze covariaten voor klaring kunnen doseeradviezen worden gedaan indien de effectieve concentratie of blootstelling bekend is, maar voor midazolam worden doseringen getitreerd op effect om optimale sedatie te bereiken. Deze behandeling start met een onderhoudsdosering van 0,05-0,2 mg/kg/uur na een oplaaddosering van 0,05-0,1 mg/kg (32, 33). Er dient echter wel rekening gehouden te worden met mogelijke doseringsaanpassingen voor kritisch zieke kinderen met inflammatie en orgaanfalen.

De voorspelde lagere klaring in kritisch zieke patiënten (**Hoofdstuk 3 en 4**), die ook beschreven is in andere patiëntpopulaties (9, 10), suggereert dat een lagere dosering voldoende moet zijn om dezelfde plasmaconcentratie te bereiken. Studies die de midazolamdosering in kritisch zieke kinderen onderbreken of verlagen laten echter zien dat dit geen verbetering is in de behandeling (34). Dit suggereert dat er wellicht een hogere plasmaconcentratie nodig is om adequate sedatie in kinderen met inflammatie en meervoudig orgaanfalen te bereiken. Ook de bijdrage van de metabolieten aan het therapeutisch effect in kritisch zieke patiënten is kleiner vanwege de verminderde vorming van de CYP3A-gemedieerde metaboliet 1-OH-midazolam, met ongeveer de helft van de activiteit als de moederstof (35), en de glucuronide metabolieten, die ook een substantieel farmacologisch effect hebben (36).

Deze resultaten kunnen wellicht worden verklaard door verschillen in de PKPD relatie, of de PD tijdens inflammatie. In ratten wordt de receptorbinding aan $GABA_A$- en $GABA_B$-receptoren beïnvloed door inflammatie (37, 38) en ook in de darmen in mensen lijken GABA-receptoren te worden beïnvloed door inflammatie (39). In tegenstelling tot de mogelijk hogere benodigde midazolamconcentraties in kritisch zieke kinderen wordt in kritisch zieke volwassenen een diepere sedatie gerapporteerd na toediening van propofol, dat tenminste deels werkt via GABA-receptoren (40). Of GABA-receptoren in de hersenen, waar midazolam zijn effect heeft, ook worden beïnvloed door inflammatie of mate van ziek-zijn in kritisch zieke patiënten is echter niet bekend.

Bovendien is het belangrijk dat, onafhankelijk van de mate van ziek-zijn, verschillen in therapeutisch effect van midazolam op verschillende leeftijden kunnen worden verwacht, vanwege verschillende aantallen, dichtheid, distributie en ligand affiniteit van GABA-receptoren (41, 42). De GABA-receptoren ontwikkelen zich nog in de eerste levensjaren (43), aangezien een toenemende activiteit wordt waargenomen met toenemende leeftijd. Daarom zijn verdere studies nodig om te bepalen wat de beste variabele is om geneesmiddeleffect op te optimaliseren (bijvoorbeeld piek- of dalconcentratie, *steady-state* concentratie of totale blootstelling) en om de PD en PKPD relatie van midazolam te bestuderen voor verschillende mate van ziek-zijn in kinderen van verschillende leeftijden, om uiteindelijk tot een optimaal en wetenschappelijk-onderbouwd doseringsschema te komen voor midazolam in neonaten, kinderen en adolescenten.

Deze optimalisatie van doseren kan bijvoorbeeld worden gedaan door de longitudinale PK metingen met *time-to-event* PD uitkomsten zoals het gebruik van *rescue* medicatie te combineren en deze twee datatypes tegelijk te analyseren (44). Herhaalde metingen van plasma concentraties van geneesmiddelen (PK) en *survivaldata* (PD) worden meestal apart of opeenvolgend geanalyseerd met verschillende statistische methoden, maar gecombineerd leveren ze meer informatie over de wisselwerking tussen PK, PD, en mate van ziek-zijn (44). Dit is bijvoorbeeld geïllustreerd door Juul *et al.* in een analyse van benodigde postoperatieve pijnstilling (45). De toepassing van deze gecombineerde modelgebaseerde aanpak voor sedatie kan farmacotherapie in kinderen in de klinische praktijk mogelijk ook verbeteren.

*PD eindpunten*

Om het therapeutisch effect van geneesmiddelen te evalueren en te kwantificeren zijn gevalideerde en bij voorkeur niet-invasieve biomarkers of PD eindpunten in kinderen nodig, die longitudinaal kunnen worden gemeten en de dynamische veranderingen in gezondheid en ziekte over tijd representeren (41). Voor midazolam kan de COMFORT-B score worden gebruikt om sedatieniveau in kinderen te kwantificeren (46), maar voor veel CYP3A-substraten kan het geneesmiddeleffect niet kwantitatief worden vastgesteld. Het opkomende vakgebied van metabolomics is een nuttige aanvulling bij het identificeren van biomarkers die de mate van ziek-zijn en/of de effecten van geneesmiddelen in kinderen kan reflecteren (47). Metabolomics is een systeembiologische methode (47, 48), waarbij een uitgebreide analyse van lichaamseigen stoffen (metabolieten) in lichaamsvloeistoffen plaatsvindt (48). In kinderen zijn verscheidene matrices zoals urine, plasma en ontlasting mogelijk relevant voor metabolomics analyses (47).

Aangezien metabolomics dichterbij het geobserveerde fenotype (bijv. ziekte of uitkomst van de behandeling) ligt dan bijvoorbeeld genomics of proteomics, worden metabolomicsprofielen beschouwd als het meest voorspellend voor klinische uitkomsten (49), hoewel standaardisatie en validatie van deze nieuwe metabolomics methodologie eerst vereist is (50, 51). Het combineren van metabolomics, genomics en proteomics kan wellicht nog meer bijdragen aan het identificeren van biomarkers als vroege voorspellers van uitkomst (49).

De recente identificatie van verscheidene biomarkers in de oncologie bewijzen dat metabolomics potentie heeft voor het ontdekken van biomarkers (52-57), al zijn er nog weinig gevalideerde biomarkers beschikbaar voor het nemen van beslissingen in de klinische praktijk, inclusief diagnose en monitoren van ziektes en behandelingseffecten, en het ontwikkelen van geïndividualiseerde farmacotherapie (58). Geïdentificeerde biomarkers kunnen na grondige evaluatie worden gebruikt in PKPD modellen, waarin blootstelling aan een geneesmiddel en PD biomarkers worden gerelateerd aan klinische uitkomsten in kinderen. Deze modellen kunnen dan rationele ondersteuning geven voor *dose-finding* studies in kinderen om farmacotherapie in kinderen te optimaliseren.

*Fysiologische benadering*

In **Hoofdstuk 5 en 6** hebben door het combineren van op fysiologie-gebaseerde PK modellen en de populatie aanpak de intrinsieke klaringsparameters kunnen schatten in de darmwand en de lever, gebruikmakend van PBPK principes en de beschikbare midazolam PK data in neonaten en kinderen. In PBPK modellen worden patiëntspecifieke parameters gerelateerd aan anatomie, fysiologie en pathofysiologie gecombineerd met geneesmiddelspecifieke eigenschappen zoals fysisch-chemische kenmerken (59). Eén van de grootste voordelen van deze aanpak is de mogelijkheid om preklinische *in vitro* en *in vivo* informatie met klinische informatie te combineren (60). Daarnaast kan het gebruik van deze PBPK modellen het ontwikkelen van geneesmiddelen versnellen met tevens minder last voor de patiënten (61).

PBPK modelleren is een voorbeeld van een systeemaanpak en past in het opkomende veld van de systeemfarmacologie (62, 63), die systeembiologie combineert met PKPD modelleren en simulatie. Systeemfarmacologie richt zich op het begrijpen van het systeem als een geheel door kwantitatief de dynamische interacties tussen geneesmiddel en biologisch systeem te analyseren (62, 63). In **Hoofdstuk 5 en 6** hebben we een minder complex model gebruikt dan een volledig PBPK model, omdat een groot nadeel van deze complexe modellen is dat ze veel systeem- en geneesmiddelspecifieke informatie nodig hebben.

Om klaring van geneesmiddelen in kinderen te voorspellen gebaseerd op een complex PBPK model, is meer fysiologische informatie over o.a. de anatomie van neonaten, kinderen en adolescenten nodig (59). In de literatuur worden verschillende aannames gedaan voor zowel de doorbloeding in de weefsels, als voor de orgaanvolumes en intestinale oppervlakte. Harmonisering van deze waarden gebaseerd op betrouwbare meetmethoden in kinderen van alle leeftijden, van preterme neonaten tot en met adolescenten, is daarom extreem belangrijk om de onzekerheid in de voorspellingen van klaring door PBPK modellen te verlagen. Consistentere fysiologische informatie zal ook leiden tot een beter begrip van de mechanismen van absorptie, distributie, metabolisme en excretie van geneesmiddelen in kinderen (59). Voor alle leeftijden is informatie over de doorbloeding in de weefsels en organen, met name de hepatische doorbloeding, essentieel, omdat de sensitiviteitsanalyses in **Hoofdstuk 5 en 6** laten zien dat de aannames over de snelheid van deze doorbloeding mogelijk invloed hebben op onze conclusies met betrekking tot intrinsieke klaring en lokale biobeschikbaarheid. De uitdaging voor de komende jaren is om de hepatische doorbloeding en andere fysiologische informatie in kinderen te verzamelen. Dit is vooral urgent in preterme neonaten, omdat van deze populatie de minste fysiologische informatie bekend is (22).

*Doseren van CYP3A-substraten in de toekomst*

Om de optimale *first-in-child* dosering tijdens de ontwikkeling van geneesmiddelen te vinden en om doseeradviezen te kunnen doen in kinderen, is het accuraat kunnen voorspellen van klaring van geneesmiddelen essentieel. Zoals beschreven in **Hoofdstuk 7**, wordt de typische klaring ($CL_i$) van een CYP3A-substraat in een individueel kind $i$ van 1 jaar of ouder met een lichaamsgewicht van $WT_i$ (in kg) beschreven door:

$$CL_i = CL_{volw} \times \left(\frac{WT_i}{70}\right)^{0,874} \quad [2]$$

waarbij $CL_{volw}$ de waarde voor klaring in volwassenen is en waarin beide klaringswaarden ($CL_i$ en $CL_{volw}$) worden uitgedrukt in volume per tijd. Deze pediatrische covariaatfunctie voor CYP3A-gemedieerde klaring is extra nuttig voor het voorspellen van klaring van CYP3A-substraten met een smal bereik voor therapeutisch effect en CYP3A-substraten met hoge toxiciteit zoals sommige oncologische middelen (64). Accurate voorspellingen van klaring van deze substraten leveren optimale voorspellingen van de blootstelling en daarmee kan uiteindelijk de toxiciteit beperkt worden. Bovendien kan deze aanpak nuttig zijn voor *dose-finding* studies in verwaarloosde (tropische) ziektes, omdat er bijvoorbeeld erg weinig PK informatie in kinderen bekend is over anthelminthica die door CYP3A worden gemetaboliseerd zoals ivermectine en praziquantel (65).

Het gebruik van de pediatrische covariaatfunctie voor CYP3A-gemedieerde klaring gebaseerd op midazolam kan de noodzaak voor PK studies voor elk CYP3A-substraat in kinderen significant verminderen, omdat informatie van het ene geneesmiddel kan worden gebruikt voor het volgende. Dit is wellicht ook mogelijk bij het voorspellen van klaring via andere eliminatieroutes, met bijvoorbeeld losartan, dextromethorphan en omeprazol als surrogaat geneesmiddelen voor respectievelijk CYP2C9, CYP2D6 en CYP2C19 (66), aangezien deze methode al succesvol is gebleken voor onder andere UGT2B7-gemedieerd metabolisme en eliminatie via glomerulaire filtratie in kinderen (26-28).

Enkele limitaties moeten echter in beschouwing worden genomen. In onze analyse in **Hoofdstuk 7** hebben we aangenomen dat de grootste eliminatieroute hetzelfde is in kinderen en volwassenen, hoewel de fractie van het metabolisme door CYP3A mogelijk verandert met leeftijd. Bijvoorbeeld voor paracetamol wordt meer sulfatering en minder glucuronidatie waargenomen in neonaten en jongere kinderen vergeleken met kinderen van 12 jaar en ouder en volwassenen (67, 68). De ratio tussen eliminatieroutes verandert mogelijk voor sommige geneesmiddelen (69) waarvoor kan worden gecorrigeerd als met beide (of meerdere) routes rekening wordt gehouden, in plaats van alleen de voornaamste route. Bovendien zou voor sommige geneesmiddelen de eliminatieroute volledig kunnen veranderen, zoals cafeïne dat een CYP1A2-substraat in volwassenen terwijl dit renaal wordt geklaard in neonaten (70). Daarnaast zal het niet voor alle geneesmiddelen mogelijk zijn om in alle leeftijdscategorieën klaring accuraat te voorspellen, maar afhankelijk van de eigenschappen van het geneesmiddel alleen tot een bepaalde leeftijd. Daarom blijft evaluatie op basis van klinische data nodig voordat de methodologie kan worden toegepast voor het voorspellen van klaring voor alle metabole eliminatieroutes.

Ondanks deze limitaties voor andere eliminatieroutes zal de ontwikkelde pediatrische covariaatfunctie voor CYP3A-gemedieerd midazolam metabolisme informatief zijn voor het voorspellen van klaring van verschillende CYP3A-substraten. Na evaluatie kan deze functie ook prospectief worden gebruikt voor het schatten van doseringen van CYP3A-substraten in kinderen.

## Conclusie

Voor een optimale behandeling met CYP3A-substraten zijn accurate voorspellingen van CYP3A-gemedieerde klaring voor kinderen van alle leeftijden noodzakelijk. We hebben gevonden dat lichaamsgewicht en mate van ziek-zijn kunnen worden gebruikt in een pediatrische covariaatfunctie voor CYP3A-gemedieerde klaring, om

de interindividuele midazolamklaring in terme neonaten, kinderen en adolescenten zo goed mogelijk te beschrijven. Een uitzondering vormen preterme neonaten voor wie met name hun onderontwikkelde intestinale en hepatische CYP3A activiteit ook van belang is. Bovendien hebben we bevestigd dat wanneer midazolamklaring in kinderen van 1-18 jaar wordt gebruikt om CYP3A-gemedieerd metabolisme in kinderen te representeren, de klaring van verscheidene veelgebruikte CYP3A-substraten met verschillende eigenschappen accuraat geschaald kunnen worden vanaf klaringswaarden in volwassenen. Met deze covariaatfunctie zal het voorspellen van CYP3A-gemedieerde klaring in neonaten, kinderen en adolescenten significant verbeteren en, na evaluatie van deze modelgebaseerde voorspellingen van klaring in pediatrische PKPD studies, kunnen de doseeradviezen voor midazolam en andere CYP3A-substraten worden toegepast in de klinische praktijk.

## REFERENTIES


1. Lu H, Rosenbaum S. Developmental pharmacokinetics in pediatric populations. J Pediatr Pharmacol Ther. 2014;19(4):262-76.
2. Kearns GL, Abdel-Rahman SM, Alander SW, Blowey DL, Leeder JS, Kauffman RE. Developmental pharmacology–drug disposition, action, and therapy in infants and children. The New England journal of medicine. 2003;349(12):1157-67.
3. Alcorn J, McNamara PJ. Ontogeny of hepatic and renal systemic clearance pathways in infants: part II. Clin Pharmacokinet. 2002;41(13):1077-94.
4. Thummel KE, Shen DD, Podoll TD, Kunze KL, Trager WF, Hartwell PS, et al. Use of midazolam as a human cytochrome P450 3A probe: I. In vitro-in vivo correlations in liver transplant patients. J Pharmacol Exp Ther. 1994;271(1):549-56.
5. Gorski JC, Hall SD, Jones DR, VandenBranden M, Wrighton SA. Regioselective biotransformation of midazolam by members of the human cytochrome P450 3A (CYP3A) subfamily. Biochem Pharmacol. 1994;47(9):1643-53.
6. Carcillo JA, Doughty L, Kofos D, Frye RF, Kaplan SS, Sasser H, et al. Cytochrome P450 mediated-drug metabolism is reduced in children with sepsis-induced multiple organ failure. Intensive Care Med. 2003;29(6):980-4.
7. Aitken AE, Richardson TA, Morgan ET. Regulation of drug-metabolizing enzymes and transporters in inflammation. Annu Rev Pharmacol Toxicol. 2006;46:123-49.
8. Vet NJ, de Hoog M, Tibboel D, de Wildt SN. The effect of inflammation on drug metabolism: a focus on pediatrics. Drug Discov Today. 2011;16(9-10):435-42.
9. Taburet AM, Tollier C, Richard C. The effect of respiratory disorders on clinical pharmacokinetic variables. Clin Pharmacokinet. 1990;19(6):462-90.
10. Kirwan CJ, MacPhee IA, Lee T, Holt DW, Philips BJ. Acute kidney injury reduces the hepatic metabolism of midazolam in critically ill patients. Intensive Care Med. 2012;38(1):76-84.

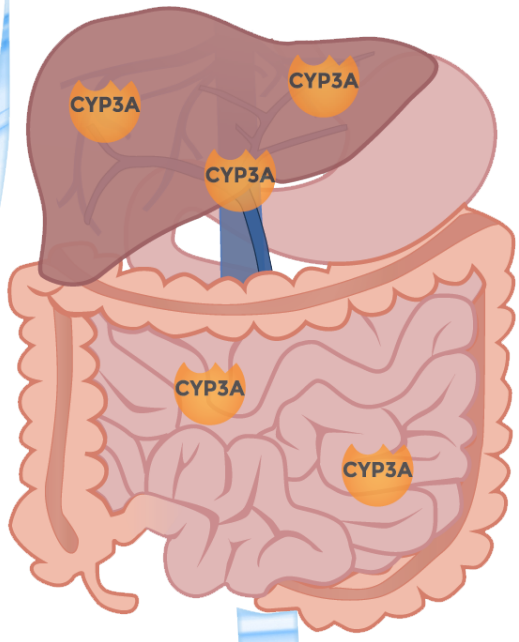
11. Peeters MY, Prins SA, Knibbe CA, Dejongh J, Mathot RA, Warris C, et al. Pharmacokinetics and pharmacodynamics of midazolam and metabolites in nonventilated infants after craniofacial surgery. Anesthesiology. 2006;105(6):1135-46.
12. Muchohi SN, Kokwaro GO, Ogutu BR, Edwards G, Ward SA, Newton CR. Pharmacokinetics and clinical efficacy of midazolam in children with severe malaria and convulsions. Br J Clin Pharmacol. 2008;66(4):529-38.
13. Reed MD, Rodarte A, Blumer JL, Khoo KC, Akbari B, Pou S, et al. The single-dose pharmacokinetics of midazolam and its primary metabolite in pediatric patients after oral and intravenous administration. J Clin Pharmacol. 2001;41(12):1359-69.
14. Tolia V, Brennan S, Aravind MK, Kauffman RE. Pharmacokinetic and pharmacodynamic study of midazolam in children during esophagogastroduodenoscopy. J Pediatr. 1991;119(3):467-71.
15. Rey E, Delaunay L, Pons G, Murat I, Richard MO, Saint-Maurice C, et al. Pharmacokinetics of midazolam in children: comparative study of intranasal and intravenous administration. Eur J Clin Pharmacol. 1991;41(4):355-7.
16. Grijalva J, Vakili K. Neonatal liver physiology. Semin Pediatr Surg. 2013;22(4):185-9.
17. Hines RN, McCarver DG. The ontogeny of human drug-metabolizing enzymes: phase I oxidative enzymes. J Pharmacol Exp Ther. 2002;300(2):355-60.
18. Ince I, Knibbe CA, Danhof M, de Wildt SN. Developmental changes in the expression and function of cytochrome P450 3A isoforms: evidence from in vitro and in vivo investigations. Clin Pharmacokinet. 2013;52(5):333-45.
19. de Wildt SN, Kearns GL, Hop WC, Murry DJ, Abdel-Rahman SM, van den Anker JN. Pharmacokinetics and metabolism of oral midazolam in preterm infants. Br J Clin Pharmacol. 2002;53(4):390-2.
20. Frechen S, Junge L, Saari TI, Suleiman AA, Rokitta D, Neuvonen PJ, et al. A semiphysiological population pharmacokinetic model for dynamic inhibition of liver and gut wall cytochrome P450 3A by voriconazole. Clin Pharmacokinet. 2013;52(9):763-81.
21. Johnson TN, Tanner MS, Taylor CJ, Tucker GT. Enterocytic CYP3A4 in a paediatric population: developmental changes and the effect of coeliac disease and cystic fibrosis. Br J Clin Pharmacol. 2001;51(5):451-60.
22. Bjorkman S. Prediction of drug disposition in infants and children by means of physiologically based pharmacokinetic (PBPK) modelling: theophylline and midazolam as model drugs. Br J Clin Pharmacol. 2005;59(6):691-704.
23. Barter ZE, Bayliss MK, Beaune PH, Boobis AR, Carlile DJ, Edwards RJ, et al. Scaling factors for the extrapolation of in vivo metabolic drug clearance from in vitro data: reaching a consensus on values of human microsomal protein and hepatocellularity per gram of liver. Curr Drug Metab. 2007;8(1):33-45.
24. Treluyer JM, Bowers G, Cazali N, Sonnier M, Rey E, Pons G, et al. Oxidative metabolism of amprenavir in the human liver. Effect of the CYP3A maturation. Drug Metab Dispos. 2003;31(3):275-81.
25. Brussee JM, Yu H, Krekels EHJ, Palic S, Brill MJE, Barrett JS, et al. Characterization of Intestinal and Hepatic CYP3A-Mediated Metabolism of Midazolam in Children Using a Physiological Population Pharmacokinetic Modelling Approach. Pharm Res. 2018;35(9):182.

26. Krekels EH, Neely M, Panoilia E, Tibboel D, Capparelli E, Danhof M, et al. From pediatric covariate model to semiphysiological function for maturation: part I-extrapolation of a covariate model from morphine to Zidovudine. CPT Pharmacometrics Syst Pharmacol. 2012;1:e9.
27. Zhao W, Biran V, Jacqz-Aigrain E. Amikacin maturation model as a marker of renal maturation to predict glomerular filtration rate and vancomycin clearance in neonates. Clin Pharmacokinet. 2013;52(12):1127-34.
28. De Cock RF, Allegaert K, Sherwin CM, Nielsen EI, de Hoog M, van den Anker JN, et al. A neonatal amikacin covariate model can be used to predict ontogeny of other drugs eliminated through glomerular filtration in neonates. Pharmaceutical research. 2014;31(3):754-67.
29. Calvier EAM, Krekels EHJ, Yu H, Valitalo PAJ, Johnson TN, Rostami-Hodjegan A, et al. Drugs Being Eliminated via the Same Pathway Will Not Always Require Similar Pediatric Dose Adjustments. CPT Pharmacometrics Syst Pharmacol. 2018.
30. Bai S, Stepkowski SM, Kahan BD, Brunner LJ. Metabolic interaction between cyclosporine and sirolimus. Transplantation. 2004;77(10):1507-12.
31. Dennison JB, Jones DR, Renbarger JL, Hall SD. Effect of CYP3A5 expression on vincristine metabolism with human liver microsomes. J Pharmacol Exp Ther. 2007;321(2):553-63.
32. Vet NJ, de Wildt SN, Verlaat CW, Knibbe CA, Mooij MG, Hop WC, et al. Daily interruption of sedation in critically ill children: study protocol for a randomized controlled trial. Trials. 2014;15:55.
33. Kinderformularium, Accessed on February 20, 2018, Availabile from https://www.kinderformularium.nl/geneesmiddel/140/midazolam.
34. Vet NJ, de Wildt SN, Verlaat CW, Knibbe CA, Mooij MG, van Woensel JB, et al. A randomized controlled trial of daily sedation interruption in critically ill children. Intensive Care Med. 2016;42(2):233-44.
35. Johnson TN, Rostami-Hodjegan A, Goddard JM, Tanner MS, Tucker GT. Contribution of midazolam and its 1-hydroxy metabolite to preoperative sedation in children: a pharmacokinetic-pharmacodynamic analysis. Br J Anaesth. 2002;89(3):428-37.
36. Bauer TM, Ritz R, Haberthur C, Ha HR, Hunkeler W, Sleight AJ, et al. Prolonged sedation due to accumulation of conjugated metabolites of midazolam. Lancet. 1995;346(8968):145-7.
37. Castro-Lopes JM, Malcangio M, Pan BH, Bowery NG. Complex changes of GABAA and GABAB receptor binding in the spinal cord dorsal horn following peripheral inflammation or neurectomy. Brain Res. 1995;679(2):289-97.
38. Anseloni VC, Gold MS. Inflammation-induced shift in the valence of spinal GABA-A receptor-mediated modulation of nociception in the adult rat. J Pain. 2008;9(8):732-8.
39. Auteri M, Zizzo MG, Serio R. GABA and GABA receptors in the gastrointestinal tract: from motility to inflammation. Pharmacol Res. 2015;93:11-21.
40. Peeters MY, Bras LJ, DeJongh J, Wesselink RM, Aarts LP, Danhof M, et al. Disease severity is a major determinant for the pharmacodynamics of propofol in critically ill patients. Clin Pharmacol Ther. 2008;83(3):443-51.
41. Kearns GL, Artman M. Functional Biomarkers: an Approach to Bridge Pharmacokinetics and Pharmacodynamics in Pediatric Clinical Trials. Curr Pharm Des. 2015;21(39):5636-42.

42. Mulla H. Understanding developmental pharmacodynamics: importance for drug development and clinical practice. Paediatr Drugs. 2010;12(4):223-33.
43. Jansen LA, Peugh LD, Roden WH, Ojemann JG. Impaired maturation of cortical GABA(A) receptor expression in pediatric epilepsy. Epilepsia. 2010;51(8):1456-67.
44. Asar O, Ritchie J, Kalra PA, Diggle PJ. Joint modelling of repeated measurement and time-to-event data: an introductory tutorial. Int J Epidemiol. 2015;44(1):334-44.
45. Juul RV, Rasmussen S, Kreilgaard M, Christrup LL, Simonsson US, Lund TM. Repeated Time-to-event Analysis of Consecutive Analgesic Events in Postoperative Pain. Anesthesiology. 2015;123(6):1411-9.
46. Ista E, van Dijk M, Tibboel D, de Hoog M. Assessment of sedation levels in pediatric intensive care patients can be improved by using the COMFORT "behavior" scale. Pediatr Crit Care Med. 2005;6(1):58-63.
47. Moco S, Collino S, Rezzi S, Martin FP. Metabolomics perspectives in pediatric research. Pediatr Res. 2013;73(4 Pt 2):570-6.
48. Ramautar R, Berger R, van der Greef J, Hankemeier T. Human metabolomics: strategies to understand biology. Curr Opin Chem Biol. 2013;17(5):841-6.
49. Peng B, Li H, Peng XX. Functional metabolomics: from biomarker discovery to metabolome reprogramming. Protein Cell. 2015;6(9):628-37.
50. Fanos V, Barberini L, Antonucci R, Atzori L. Metabolomics in neonatology and pediatrics. Clin Biochem. 2011;44(7):452-4.
51. Fanos V, Antonucci R, Atzori L. Metabolomics in the developing infant. Curr Opin Pediatr. 2013;25(5):604-11.
52. Zhang A, Sun H, Yan G, Wang P, Han Y, Wang X. Metabolomics in diagnosis and biomarker discovery of colorectal cancer. Cancer Lett. 2014;345(1):17-20.
53. Gunther UL. Metabolomics Biomarkers for Breast Cancer. Pathobiology. 2015;82(3-4):153-65.
54. Suzuki M, Nishiumi S, Matsubara A, Azuma T, Yoshida M. Metabolome analysis for discovering biomarkers of gastroenterological cancer. J Chromatogr B Analyt Technol Biomed Life Sci. 2014;966:59-69.
55. Peng J, Chen YT, Chen CL, Li L. Development of a universal metabolome-standard method for long-term LC-MS metabolome profiling and its application for bladder cancer urine-metabolite-biomarker discovery. Anal Chem. 2014;86(13):6540-7.
56. Tosoian JJ, Ross AE, Sokoll LJ, Partin AW, Pavlovich CP. Urinary Biomarkers for Prostate Cancer. Urol Clin North Am. 2016;43(1):17-38.
57. Tumas J, Kvederaviciute K, Petrulionis M, Kurlinkus B, Rimkus A, Sakalauskaite G, et al. Metabolomics in pancreatic cancer biomarkers research. Med Oncol. 2016;33(12):133.
58. Monteiro MS, Carvalho M, Bastos ML, Guedes de Pinho P. Metabolomics analysis for biomarker discovery: advances and challenges. Curr Med Chem. 2013;20(2):257-71.
59. Barrett JS, Della Casa Alberighi O, Laer S, Meibohm B. Physiologically based pharmacokinetic (PBPK) modeling in children. Clin Pharmacol Ther. 2012;92(1):40-9.
60. Maharaj AR, Edginton AN. Physiologically based pharmacokinetic modeling and simulation in pediatric drug development. CPT Pharmacometrics Syst Pharmacol. 2014;3:e150.
61. Zhuang X, Lu C. PBPK modeling and simulation in drug research and development. Acta Pharm Sin B. 2016;6(5):430-40.

62. van der Graaf PH, Benson N. Systems pharmacology: bridging systems biology and pharmacokinetics-pharmacodynamics (PKPD) in drug discovery and development. Pharm Res. 2011;28(7):1460-4.
63. Vicini P, van der Graaf PH. Systems pharmacology for drug discovery and development: paradigm shift or flash in the pan? Clin Pharmacol Ther. 2013;93(5):379-81.
64. Coutant DE, Kulanthaivel P, Turner PK, Bell RL, Baldwin J, Wijayawardana SR, et al. Understanding Disease-Drug Interactions in Cancer Patients: Implications for Dosing Within the Therapeutic Window. Clin Pharmacol Ther. 2015;98(1):76-86.
65. Olliaro P, Delgado-Romero P, Keiser J. The little we know about the pharmacokinetics and pharmacodynamics of praziquantel (racemate and R-enantiomer). J Antimicrob Chemother. 2014;69(4):863-70.
66. Williams D, Tao X, Zhu L, Stonier M, Lutz JD, Masson E, et al. Use of a cocktail probe to assess potential drug interactions with cytochrome P450 after administration of belatacept, a costimulatory immunomodulator. Br J Clin Pharmacol. 2017;83(2):370-80.
67. Levy G, Khanna NN, Soda DM, Tsuzuki O, Stern L. Pharmacokinetics of acetaminophen in the human neonate: formation of acetaminophen glucuronide and sulfate in relation to plasma bilirubin concentration and D-glucaric acid excretion. Pediatrics. 1975;55(6):818-25.
68. Miller RP, Roberts RJ, Fischer LJ. Acetaminophen elimination kinetics in neonates, children, and adults. Clin Pharmacol Ther. 1976;19(3):284-94.
69. Salem F, Johnson TN, Barter ZE, Leeder JS, Rostami-Hodjegan A. Age related changes in fractional elimination pathways for drugs: assessing the impact of variable ontogeny on metabolic drug-drug interactions. J Clin Pharmacol. 2013;53(8):857-65.
70. Ginsberg G, Hattis D, Sonawane B. Incorporating pharmacokinetic differences between children and adults in assessing children's risks to environmental toxicants. Toxicol Appl Pharmacol. 2004;198(2):164-83.

# Appendices



# APPENDIX I

## Curriculum vitae

Jantine Brussee was born on October 22nd, 1989 in Oegstgeest, the Netherlands. After her graduation in 2007 from the Andreas College in Katwijk ZH, she studied Bio-Pharmaceutical Sciences at Leiden University. She graduated for her barchelor's degree in 2011 and her master's degree in the Pharmacology track in 2013. She joined the Otago Pharmacometrics Group from the University of Otago in Dunedin, New Zealand for a six-month research internship in 2013. Later that year, she started as a PhD candidate at the Division of Systems Biomedicine and Pharmacology of the Leiden Academic Centre for Drug Research (LACDR) under supervision of professor dr. Catherijne A.J. Knibbe (LACDR), professor dr. Saskia N. de Wildt (Radboud UMC, Nijmegen) and dr. Elke H.J. Krekels (LACDR), resulting in this thesis. Since June 2018, Jantine has a joint post-doctoral research position at the Swiss Tropical and Public Health Institute and the University Children's Hospital in Basel.

# APPENDIX II

## List of publications

Brussee JM, Krekels EHJ, Calvier EAM, Palić S, Rostami-Hodjegan A, Danhof M, Barrett JS, De Wildt SN, Knibbe CAJ. A pediatric covariate function for CYP3A-mediated clearance can scale clearance of selected CYP3A substrates in children. **2018**. *Manuscript in preparation*

Brussee JM, Yu H, Krekels EHJ, Palić S, Brill MJE, Barrett JS, Rostami-Hodjegan A, de Wildt SN, Knibbe CAJ. Characterization of intestinal and hepatic CYP3A-mediated metabolism of midazolam in children using a physiological population pharmacokinetic modelling approach. Pharm Res. **2018**. Jul 30;35(9):182

Brussee JM, Yu H, Krekels EHJ, de Roos B, Brill MJE, van den Anker JN, Rostami-Hodjegan A, de Wildt SN, Knibbe CAJ. First-Pass CYP3A-Mediated Metabolism of Midazolam in the Gut Wall and Liver in Preterm Neonates. CPT Pharmacometrics Syst Pharmacol. **2018** Jun;7(6):374-383.

Brussee JM, Vet NJ, Krekels EHJ, Valkenburg AJ, Jacqz-Aigrain E, van Gerven JMA, Swart EL, van den Anker JN, Tibboel D, de Hoog M, de Wildt SN, Knibbe CAJ. Predicting CYP3A-mediated midazolam metabolism in critically ill neonates, infants, children, and adults with inflammation and organ failure. Br J Clin Pharmacol. **2018** Feb;84(2):358-368.

Brussee JM, Calvier EA, Krekels EH, Välitalo PA, Tibboel D, Allegaert K, Knibbe CA. Children in clinical trials: towards evidence-based pediatric pharmacotherapy using pharmacokinetic-pharmacodynamic modeling. Expert Rev Clin Pharmacol. **2016** Sep;9(9):1235-44.

Vet NJ, Brussee JM, de Hoog M, Mooij MG, Verlaat CW, Jerchel IS, van Schaik RH, Koch BC, Tibboel D, Knibbe CA, de Wildt SN; SKIC (Dutch collaborative PICU research network). Inflammation and Organ Failure Severely Affect Midazolam Clearance in Critically Ill Children. Am J Respir Crit Care Med. **2016** Jul 1;194(1):58-66.

Brussee JM, Yeo TW, Lampah DA, Anstey NM, Duffull SB. Pharmacokinetic-Pharmacodynamic Model for the Effect of l-Arginine on Endothelial Function in Patients with Moderately Severe Falciparum Malaria. Antimicrob Agents Chemother. **2015** Oct 19;60(1):198-205.

De Cock RF, Allegaert K, Brussee JM, Sherwin CM, Mulla H, de Hoog M, van den Anker JN, Danhof M, Knibbe CA. Simultaneous pharmacokinetic modeling of gentamicin, tobramycin and vancomycin clearance from neonates to adults: towards a semi-physiological function for maturation in glomerular filtration. Pharm Res. **2014** Oct;31(10):2643-54.

# APPENDIX III

## Nawoord / Acknowledgements

Dit proefschrift is tot stand gekomen dankzij vele mensen. Allereerst, wil ik Catherijne Knibbe, Saskia de Wildt en Elke Krekels bedanken. Catherijne, jouw onuitputtelijke enthousiasme en positieve energie werken aanstekelijk, ik heb ontzettend veel van je geleerd en ik heb alle (wetenschappelijke) gesprekken die we hebben gevoerd erg gewaardeerd. Saskia, met jouw klinische blik bleef je me kritisch bevragen en dat hield me scherp en doelgericht. Ik ben je erg dankbaar dat je jouw kennis over CYP3A-enzymen en je klinische ervaring hebt willen delen. Elke, bedankt voor ons wekelijkse overleg, waarin je alle tijd nam om alles te bespreken en geen blad voor de mond nam. Jouw kritische blik en hulp bij het (her)schrijven van manuscripten hebben geresulteerd in dit proefschrift, waar ik erg trots op ben.

Meindert Danhof wil ik bedanken voor de kans om bij het LACDR te promoveren, en voor de inbreng in verschillende projecten. Ook dank aan Peter Lindenburg voor alle support. Ik wil graag alle collega's van de division of Systems Biomedicine and Pharmacology bedanken, in het bijzonder Wilbert, Willem, Elisa, Sinziana, Rick, Michiel, Rob, Sven, Bas en Paola. Margreke en Anne bedankt voor de discussies over midazolam PK in verschillende populaties, and thanks to Pyry, Huixin, and Swantje for your valuable input and feedback.

Graag wil ik het team uit het Erasmus MC-Sophia Kinderziekenhuis bedanken voor de samenwerking, in het bijzonder Nienke Vet. Ik heb veel van je geleerd en van de fijne samenwerking genoten.

Furthermore, I would like to thank all coauthors for their ideas, comments and suggestions, and/or for sharing data: Dick Tibboel, Karel Allegaert, Matthijs de Hoog, Miriam Mooij, Carin Verlaat, Isabel Jerchel, Ron van Schaik, Birgit Koch, Bram Valkenburg, Evelyne Jacqz-Aigrain, Joop van Gerven, John van den Anker, Margreke Brill, Amin Rostami-Hodjegan and Jeff Barrett. I am also grateful to Pfizer Inc. for sharing their data with us.

Verder wil ik stagestudenten Berend de Roos, Semra Palić en Jelmer Meijer bedanken voor hun bijdragen aan onderzoek in dit proefschrift, en Emma Kruijt, Suzanne Kappetein, Iris Vennis en Janna Hoogduin (bachelorstages). Graag wil ik Roosmarijn De Cock en Rob Voskuyl bedanken voor mijn eerste kennismaking met farmacologie en pharmacometrics: ik ben jullie hier zeer dankbaar voor!

Tot slot wil ik graag mijn familie en vrienden bedanken voor de hulp en steun die ik de afgelopen jaren heb ontvangen, en in het bijzonder natuurlijk Freek.
Lieve allemaal, woorden schieten hier tekort, bedankt voor alles!